

FOR OFFICIAL USE ONLY

JPRS L/9123

3 June 1980

Translation

STRUCTURAL DESIGN OF CIVIL DEFENSE SHELTERS

By

M.D. Bodanskiy, L.M. Gorshkov et al.

FBIS FOREIGN BROADCAST INFORMATION SERVICE

FOR OFFICIAL USE ONLY

NOTE

JPRS publications contain information primarily from foreign newspapers, periodicals and books, but also from news agency transmissions and broadcasts. Materials from foreign-language sources are translated; those from English-language sources are transcribed or reprinted, with the original phrasing and other characteristics retained.

Headlines, editorial reports, and material enclosed in brackets [] are supplied by JPRS. Processing indicators such as [Text] or [Excerpt] in the first line of each item, or following the last line of a brief, indicate how the original information was processed. Where no processing indicator is given, the information was summarized or extracted.

Unfamiliar names rendered phonetically or transliterated are enclosed in parentheses. Words or names preceded by a question mark and enclosed in parentheses were not clear in the original but have been supplied as appropriate in context. Other unattributed parenthetical notes within the body of an item originate with the source. Times within items are as given by source.

The contents of this publication in no way represent the policies, views or attitudes of the U.S. Government.

For further information on report content
call (703) 351-2938 (economic); 3468
(political, sociological, military); 2726
(life sciences); 2725 (physical sciences).

COPYRIGHT LAWS AND REGULATIONS GOVERNING OWNERSHIP OF
MATERIALS REPRODUCED HEREIN REQUIRE THAT DISSEMINATION
OF THIS PUBLICATION BE RESTRICTED FOR OFFICIAL USE ONLY.

FOR OFFICIAL USE ONLY

JPRS L/9123

3 June 1980

STRUCTURAL DESIGN OF CIVIL DEFENSE SHELTERS

Moscow RASCHET KONSTRUKTSIY UBEZHISHCH in Russian 1974 signed to press 14 Feb 74 pp 1-208

Book by M.D. Bodanskiy, L.M. Gorshkov et al., Stroyizdat Publishers, 24,000 copies

CONTENTS

Foreword.....	2
CHAPTER I. CIVIL DEFENSE SHELTERS	
1. Classification of Shelters.....	4
2. Planning Solutions and Structural Designs of Shelters.....	10
CHAPTER II. DYNAMIC LOADS ON THE STRUCTURAL ELEMENTS OF CIVIL DEFENSE SHELTERS	
1. Parameters of the Air Shock Wave.....	29
2. Loads on the Structure from an Air Shock Wave of a Nuclear Blast.....	37
3. Loans on the Structures from Gas-Air Mixture Blasts	44
CHAPTER III. CALCULATION OF REINFORCED CONCRETE FLOORS, CEILINGS AND WALLS ON THE EFFECT OF AIR SHOCK WAVES	
1. General Principles.....	56
2. Calculation of the Structural Elements in the Elastic Stage.....	57
3. Dynamic Strength of Reinforcing Steel and Concrete.	63
4. Characteristic Limited States of Bent Structural Elements.....	68
5. Calculation of a Hinge-Supported Beam in the Plastic Stage.....	71
6. Calculation of a Beam with Clamped Ends in the Plastic Stage.....	86

- a -

[II- USSR - FOUO]
[III - USSR - 4 FOUO]

FOR OFFICIAL USE ONLY

FOR OFFICIAL USE ONLY

7.	Calculation of a Beam With One Clamped End and the Other Hinged End in the Plastic Stage.....	96
8.	Calculation of Continuous Beams.....	106
9.	Calculation of Rectangular Slabs.....	109
10.	Example Calculations.....	117
CHAPTER IV. CALCULATION OF THE STRUCTURAL DESIGNS OF CEILINGS AND FLOORS UNDER THE EFFECT OF COMPRESSION WAVES IN THE GROUND		
1.	Basic Prerequisites.....	128
2.	Loading Wave Propagation.....	131
3.	Process of Lowering the Pressure (Unloading).....	135
4.	Compression Wave Reflection From a Stationary Barrier.....	143
5.	Interaction of Compression Waves in the Ground With Flexible Structures.....	146
CHAPTER V. CALCULATION OF ROCK WALLS AND COLUMNS FOR THE EFFECT OF SHOCK WAVE LOADS		
1.	Loads.....	152
2.	Characteristic of the Limiting States.....	153
3.	Calculation of Outside Stone Walls.....	156
4.	Calculation of Columns and Inside Walls.....	163
CHAPTER VI. CALCULATION OF THE ENCLOSING STRUCTURES FOR THE THERMAL EFFECTS OF MASS FIRES		
1.	Calculation Thermal Effects.....	171
2.	Protection of the Enclosing Structures of Shelters From Heating.....	175
3.	Designing Enclosing Structures of Shelters for Heating During Fires.....	176
4.	Effect of Heating on the Bearing Capacity of the Ceilings and Floors and Seal of the Structure.....	184
5.	Example Calculations.....	186
BIBLIOGRAPHY.....		190

- b -

FOR OFFICIAL USE ONLY

FOR OFFICIAL USE ONLY

PUBLICATION DATA

English title : STRUCTURAL DESIGN OF CIVIL DEFENSE
SHELTERS

Russian title : RASCHET KONSTRUKTSIY UBEZHISHCH

Author (s) : M. D. Bodanskiy, L. M. Gorshkov, et al.

Editor (s) :

Publishing House : Stroyizdat

Place of Publication : Moscow

Date of Publication : 1974

Signed to press : 14 Feb 74

Copies : 24,000

COPYRIGHT : Stroyizdat, 1974

- c -

FOR OFFICIAL USE ONLY

FOR OFFICIAL USE ONLY

UDC 699.852.001.24

STRUCTURAL DESIGN OF CIVIL DEFENSE SHELTERS

Moscow RASCHET KONSTRUKTSIY UBEZHISHCH in Russian 1974 pp 1-208

[Article by M. D. Bodanskiy, L. M. Gorshkov, V. I. Morozov, B. S. Rastorguyev]

[Text] A discussion is presented of the calculation of the supporting structures of civil defense shelters against the effect of the shock waves from nuclear blasts, the explosion of gas-air mixtures and heating during fires. A study is made of the methods of dynamic calculation of flexible reinforced concrete structures in the elastic and plastic stages under various supporting conditions; the extracentric compressed elements -- brick walls considering the opening of horizontal cracks; inside columns and walls considering their joint operation with the ceilings and floors and with the dirt foundation.

There are 12 tables, 69 illustrations and 74 references.

FOR OFFICIAL USE ONLY

FOR OFFICIAL USE ONLY

FOREWORD

One of the primary goals of civil defense is the timely design and construction of structures to protect the population against weapons of mass destruction.

Among such structures a special role is played by the civil defense shelters, a special role is played by the civil defense shelters, the construction of which requires defined material expenditures and time. The structural designs of the shelters and their internal equipment must be calculated and designed so as to protect people from the destructive factors of a nuclear blast in the zone of total destruction of buildings, against high temperatures and smoke in the case of mass fires and also against the effect of chemical and bacteriological weapons.

The problems of calculating the structural designs of shelters for dynamic loads occurring under the effect of a nuclear blast shock wave have been discussed inadequately in the literature and are little known to construction engineers, planners and designers. At the same time, the methods and the calculation of protection against the radiation of radioactive fallout and primary radiation of a nuclear blast are the subject of a broad literature [14, 17, 21, 28, 38, 39, 46]; therefore they will not be investigated here.

The primary goal of calculating the structural elements of shelters loaded from a shock wave, the magnitudes of which are tens and hundreds of times more than the loads normalized in industrial and civil construction, is the establishment of the dimensions (cross section), guaranteeing the same presence of people in the shelter under the effect of modern methods of mass destruction. A characteristic feature of the calculation is the specific situation which is rare in the ordinary designing of industrial and civil structures: the structural elements of shelters are designed for shock wave load, which will occur once or twice during its entire service life. This makes it possible to approach the selection of the methods of calculating the structural designs with less rigid requirements, the basic one of which consisted in the fact that the structural element must withstand the load without collapsing [48]. Here it is possible to permit significant residual deformations in the shelter structures accompanied by the opening of cracks and large deflections.

FOR OFFICIAL USE ONLY

FOR OFFICIAL USE ONLY

The calculation of structures considering the effect of the changes in their geometric diagrams in the process of deformation and the consideration of the working of the material of the structure beyond the elastic strings that will permit lowering of the expenditures on the construction and the provision of protection for a larger number of people.

Based on the mentioned prerequisites, in this paper the specific nature of the design of shelters is reflected, the procedure is given for determining the dynamic loads from the explosion of gas-air mixtures and a nuclear blast. A discussion is presented of the methods of calculating the basic bearing structures (elements of reinforced concrete floors and ceilings, columns, walls and foundations) on the effect of the dynamic loads and also on the heating during fires. These methods can find application also for calculation of the structural designs of civil and industrial structures for the effect of dynamic loads in emergencies.

Chapter I was written by L. M. Gorshkov, Chapter II was written by V. I. Morozov; Chapters III and IV were written by B. S. Rastorguyev with the participation of V. I. Morozov, Chapter V was written jointly by V. I. Morozov and B. S. Rastorguyev, Chapter VI and the characteristics of the mass fires in Chapter I were written by M. D. Bodanskiy.

The authors hope that the book will be useful to a broad class of scientific workers and engineers engaged in designing shelters and specialists working in the field of dynamic structural design calculations.

The authors express deep appreciation to doctor of technical sciences, professor N. N. Popov for advice and suggestions which were taken into account when preparing the manuscript for publication; the authors also express their heartfelt thanks to candidates of technical sciences V. I. Ganushkin and A. I. Kostin for their work in reviewing the manuscript.

FOR OFFICIAL USE ONLY

FOR OFFICIAL USE ONLY

CHAPTER I. CIVIL DEFENSE SHELTERS

1. Classification of Shelters

Civil defense shelters are designed to protect the population against means of mass injury. The requirements on such structures are defined beginning with evaluation of the destructive factors of a nuclear blast and also evaluation of the injurious effect of poisons and bacterial means [1, 2, 23]. For the bearing structures of the shelters, the requirements arising from the destructive factors of a nuclear blast are defining.

General Characteristic of the Destructive Factors in a Nuclear Blast

A nuclear blast in a populated area causes destruction, fires and radioactive casualties. The nature of the destruction of the buildings and structures by the shock wave of a nuclear blast and injuries to people is presented in Table 1. When compiling the table it is considered that a shock wave also affects people indirectly -- injuries from fragments of destroyed buildings and structures, pieces of glass. The injuries from a shock wave are observed at pressures of 0.03 kg/cm² and more.

The mass destruction of above-ground buildings and structures in cities can be accompanied by blocking of the streets with pieces of walls, metal, reinforced concrete and wooden beams, brick and other materials which leads to the formation of one-sided or two-sided obstruction of the streets. With a shock wave pressure of more than 1.2 kg/cm², as a rule, solid obstructions are formed over the entire built-up area. The characteristics of the obstructions (composition, height, distance the main part of the fragments are scattered) are presented in references [14, 64].

An unavoidable consequence of nuclear blast is the fires caused both by the direct effect of the light emission on open combustible structural elements and materials and by the destruction of furnaces, industrial heating units, damage to the gas mains, electrical networks, and so on. The conditions for spreading of a fire in buildings after damage of the bearing structures by the shock wave and destruction of windows and doors will be ideal [21]. The control of fires is complicated if the water lines are out of order.

FOR OFFICIAL USE ONLY

FOR OFFICIAL USE ONLY

Table 1

Destructive Effect of the Shock Wave of a Nuclear Blast [14]

Nature of destruction	Pressure at the shock wave front in kg/cm ²	Killing radius for a ground blast of 1 million tons in km
Destruction of glazing	0.03	31
Destruction of the roofs of buildings, partitions, ceilings and floors on wooden beams	0.18-0.1	7-11.5
Destruction of wooden buildings	0.2 -0.14	7-10
Contusions and slight injuries to people	0.4 -0.2	4.5-7
Destruction of stone buildings	0.45-0.35	4.5-5
Medium serious injuries of people	0.5-0.4	4-4.5
Serious injuries of people	1 -0.5	2.8-4
Destruction of industrial-type buildings	1 -0.8	2.8-3.2
Destruction of strip foundations of residential buildings	4	1.5
Destruction of underground reinforced concrete pipe 1.5 meters in diameter with a wall thickness of 0.2 meters	15-12	0.8-1

During World War II, mass fires were one of the primary causes of the destruction of buildings and loss of life. It has been documented that out of the total amount of destruction in large populated areas subjected to air attacks, up to 80% was caused by fires [69, 73]. After an air burst of a 20 megaton nuclear bomb as a result of the combined effect of a shock wave and light emission the mass fires would occur at distances of up to 30 km from the blast epicenter [49].

Depending on the density of building and atmospheric conditions, various types of fires can occur in the city. The individual fires, solid fires, storm fires and versions of them -- cyclone fires, fires in obstructions -- are distinguished.

It is known [21] that the probability of the spread of fires with less than 20% density of building is very low. This is explained by significant spacing between the buildings which prevents the combination and mutual effect of the temperature fields of adjacent individual fires. Under these conditions even when all of the buildings are burning simultaneously in an area with the indicated building density each fire develops independently. Such mass fires are called individual. With an increase in the building density and corresponding decrease in the spacing between buildings, individual fires begin to have a mutual effect by the

FOR OFFICIAL USE ONLY

FOR OFFICIAL USE ONLY

radiation fields. These are solid fires. If the buildings are closer together, the thermal fields of individual fires merge in general (storm fires).

The first of these fires came to be called solid fires as a result of the fact that over the entire area encompassed by the fire, as a result of the interaction of the radiation fields of the burning objects, approximately the same temperature regime is established, and the second group of fires are so-called because in their presence merging of the flame of all of the burning objects in the investigated area is possible, and the wind velocities reach storm values.

In some cases during the occurrence of a storm fire in a section, the dimensions of which exceed 1x1 km, its growth into a fire storm or a fire cyclone, as it is called, is possible.

The fire cyclone is characterized by extremely intense burning of various combustible materials with the occurrence of powerful centripetal air flows and also the formation of a column of heated air and combustion products rising to an altitude of up to 4000 meters. The fire cyclone usually does not go beyond the limits of the region where it occurred. The velocity of the air flows directed toward the center of the cyclone fire reaches 35 m/sec or more, and the air temperature in the cyclone range approaches 1000°C. Four to 5 hours after the occurrence of a cyclone fire the region where it occurred is converted to a heap of incandescent structures and destroyed elements of buildings.

In addition to the enumerated types of mass fires which must be expected in an area where the pressure at the shock wave front does not exceed 0.2 to 0.5 kg/cm², at the limits of the zone with greater pressures fires in the obstruction are possible which are distinguished from the mass fires of other types by the great duration and relatively low air temperatures. The classification of the mass fires with respect to expected atmospheric conditions developing within the built-up areas of cities is presented in Table 2.

Table 2
Classification of Mass Fires by the Outside Air Parameters

Fire category	Type of fire	Maximum air temperature in °C	Probable maximum concentrations in %			Duration of the fire in hours
			CO	CO ₂	O ₂	
I	Storm	600-800	1.2	4.8	12.5	to 4
II	Solid	500-600	0.5	2.4	16.5	6-8
III	Individual	to 200	0.3	1.4	18.5	6-8
IV	In obstructions	to 40	0.2	0.8	20	to 24

FOR OFFICIAL USE ONLY

In order to discover the parts of the built-up areas of cities in danger from the point of view of the occurrence of one type of mass fire or another, it is possible in the first approximation to use the simplest procedure for estimating fire hazard in reference [14].

Here it is necessary to consider that the territory of category III of fire hazard, the dimensions of which are less than 200x200 meters, located within the boundaries of the calculated section of category I (II), is all evaluated by the category of the last-mentioned section, and for dimensions of greater than 200x200 meters with respect to category I (II) only the 100-meter strip around its perimeter is evaluated. This correction takes into account the calculated spread of the increased temperatures and concentrations of the products of combustion to a distance of up to 100 meters from the burning buildings located in the sections of higher category of their hazard by comparison with the investigated territory.

People can receive burns from the light emission during a nuclear blast. In the case of a ground burst of 1 million tons in clear weather the exposed parts of the skin will receive first degree burns at a distance of 9-12 km from the radiation source, second degree burns at a distance of 7-9 km, and third degree burns at a distance of 5-7 km. People in buildings can escape burns from light emission, but suffer from fragments of the destroyed buildings and also from other injurious factors of the nuclear blast: penetrating radiation and radioactive contamination.

Along with the shock wave and light emission the penetrating radiation is one of the decisive factors when determining the requirements on shelters.

Penetrating radiation which acts up to 15 seconds after the time of the blast consists basically of gamma radiation and a neutron flux. The gamma radiation is the most dangerous in view of its high penetrating capacity, large radius of effect and capacity to disperse in the air. In the case of a 1-million ton ground burst the gamma radiation dosage will be as follows [14]:

At a distance of 4 km (pressure 0.5 kg/cm ²)	4 roentgens
At a distance of 2.8 km (pressure 1 kg/cm ²)	80 "
At a distance of 2.26 km (pressure of 1.5 kg/cm ²)	1000 "
At a distance of 2 km (pressure of 2 kg/cm ²)	4000 "
At a distance of 1.78 km (pressure of 2.5 kg/cm ²)	10000 "

As a result of fallout of the radioactive particles on the ground from the cloud of a nuclear blast over large territories, radioactive contamination takes place. Thus, for example, for a 1-million ton blast at the edge of a large city on the windward side with a wind velocity of 24 km/hour, the part of the area of the city covered by the zone with a contamination level at the outer boundary of 10 roentgens/hour, 1 hour after the blast will be 60 to 70% of the entire area of the city; with a level of contamination of 100 roentgens/hour, 40-50%, and with a contamination level of 300 roentgens/hour, 30-40%.

FOR OFFICIAL USE ONLY

FOR OFFICIAL USE ONLY

If the city is covered by a radioactive cloud from adjacent blasts, the degree of radioactive contamination of the territory increases by several times. The radioactive contamination of the area which is dangerous to people can occur at a distance of hundreds of kilometers from the center of the nuclear blast. The gamma radiation from the radioactive fallout causing general external irradiation is of primary danger to man. The radioactive particles can get into the organism through the respiratory organs, together with water and food, causing internal irradiation. Taking the simplest measures of protection of the respiratory organs from dust and observing sanitary-hygienic requirements when eating, it is possible to exclude or significantly decrease the incidence of radioactive materials in the organism.

There are no effective measures of protection against external irradiation except a shelter. Therefore, irradiation presents the primary danger, and protection from it is the main problem in areas of radioactive contamination.

The protective properties of buildings and structures with respect to gamma radiation are characterized by the radiation attenuation factor which indicates how many times the irradiation dosage of man is diminished in the building (structure) by comparison with the irradiation dosage in the open. The admissible dosage of the total single external irradiation, considering its quickest aftereffects, must not exceed 25 to 75 roentgens.

A more detailed characteristic of the injurious factors of a nuclear blast can be found in references [10, 14, 21, 25, 39, 49].

In the set of destructive factors connected with the effect of modern means of destruction, it is necessary also to consider the so-called secondary destructive factors which are a consequence of the effect of the shock wave and light emission of the nuclear blast. These include destruction of reservoirs and various process units with easily inflammable, combustible, explosive and poisonous liquids and gases, as a result of which destruction of the surrounding buildings and structures, intense fires, and so on occur.

Requirements on Shelters

Considering the discussed peculiarities of the effect of the destructive factors of a nuclear blast, it is possible to formulate the following basic requirements on civil defense shelters.

In the cities which can become the target of a nuclear attack, it is necessary to protect people from all of the destructive factors of a nuclear blast. The shelters in these cities must have emergency exits for independent exit of people to the ground service in case of destruction of above-ground buildings and structures and the formation of obstructions. The enclosing structures of shelters must have the required

FOR OFFICIAL USE ONLY

FOR OFFICIAL USE ONLY

thermal resistances, preventing heating of the inside surfaces during fires. In built-in shelters the ceiling must not be punctured by individual falling fragments when the buildings are destroyed.

In rural populated areas and small cities which are not the target of nuclear attack, basically protection from radioactive contamination must be provided. However, near the limits of cities which can become the target of a nuclear attack, the shelters must also withstand the effect of the shock wave (of corresponding less intensity), and in individual cases, the secondary destructive factors (for example, protection against poisons which can spread in the direction of the prevailing wind far beyond the city limits after the containers are destroyed in the city). One of the most important requirements on civil defense shelters is the possibility of filling them with people in a short time measured in minutes. For shelters outside the cities which can become the target of a nuclear attack, this time can be greater and will depend on the distance to the city and the propagation rate of the radioactive cloud.

The civil defense structures must insure effective protection, that is, essentially diminish the possible losses of population under wartime conditions with the application of weapons of mass destruction; at the same time the construction of these structures must not cause significant additional expenditures. The basic increase in cost of the buildings and structures adaptable as shelters is connected with providing the required strength of the closing structures designed for the impact of the shock wave.

Classification of Shelters

The civil defense shelters are divided into regular shelters and radiation-proof shelters. The regular shelters are designed to protect people against the damaging effects of a nuclear blast and also poisons and bacterial means. The radiation-proof shelters are designed to protect people against radioactive contamination (radioactive radiation, the incidence of radioactive particles on the surface of human skin and also through the respiratory organs).

The shelters are classified with respect to protective properties, location and erection time.

With respect to protective properties the regular shelters are divided into five classes [23], depending on the calculated pressure of the air shock wave of the nuclear blast.

The radiation-proof shelters are divided into three groups with respect to degree of attenuation of radioactive radiation.

With respect to location the shelters can be built in (in the buried part of buildings) or separately standing (located outside buildings).

FOR OFFICIAL USE ONLY

FOR OFFICIAL USE ONLY

The separately standing shelters are divided into trench shelters and underground shelters. The covering of the trench-type structures is located, as a rule, at ground level. The structures of the underground type are at significant depths and are protected by the natural thickness of the ground.

The shelters are erected in advance, with the application of permanent incombustible material, structural elements and internal equipment of industrial manufacture.

When it is necessary to erect them in short time, local building materials (including wood) and internal equipment manufactured by the population and local industry are used to build the shelters.

The shelters (specially the regular shelters) are located near the places where the people work and live in view of the limited time to take shelter after the air alarm signal is given.

The most acceptable are the built-in shelters which can be filled with people in the shortest time. The distance from a separately standing shelter to the exit from a building must not exceed the gathering radius, the procedure for determination of which is presented in reference [14].

The separately standing shelters are located insofar as possible so that one of the entrances will be removed from the nearest building by a distance no less than the height of this building and can serve as emergency exit. If this solution is impossible, a special emergency exit is provided.

2. Planning Solutions and Structural Designs of Shelters

Planning Solutions

The space-planning and structural designs of shelters are determined by the requirements of protection against weapons of mass destruction and the conditions of their operation and maintenance in peacetime in the national economy. This combination of functions in one shelter is advantageously economic and promotes more intense accumulation of the shelter pool. During peacetime the shelters can be used as domestic and production facilities which do not require natural lighting, garages for cars, commercial and public eating enterprises, warehouses and other facilities. The space-planning solutions of such facilities must correspond most completely to their purpose, insure the required sanitary-hygienic conditions for the people working in them, and be economical and simple to the maximum with respect to composition. The shelters must be designed considering the erection of them by industrial methods coordinated with the structural elements of the buildings and with the enclosing construction.

FOR OFFICIAL USE ONLY

FOR OFFICIAL USE ONLY

In the shelters (Fig 1, 2) provision is made for basic (facilities for sheltering people, lock-type entries) and auxiliary facilities (filter-ventilation chambers, sanitary facilities, diesel electric power plants). The height of the facilities is taken in accordance with the requirements of their use in peacetime, but no less than 2.2 meters from the level of the floor to the bottom of the protruding structures of the ceiling. In a facility for sheltering people provision must be made for places to sit or lie down.

At one of the entrances to the shelter a lock chamber is built (single-chamber or double-chamber depending on the capacity of the shelter), the purpose of which is to prevent the danger of shock wave injury of the people in the shelter when the doors are opened. Therefore the outside and inside sealed protective doors of the lock chambers must have blocking to exclude simultaneous opening of them. After the shelter is filled it is expedient to use the lock chambers for people in the sitting position.

The dimensions of the filter-ventilation chamber (FVK) and the facility for the diesel electric power plant (DES) must be determined from the condition of the minimum required space for the equipment.

In view of the great variety of versions of the use of the shelters in peacetime it is expedient to standardize their space-planning solutions with the application of standard spans and standard column network. Considering the significant calculated load on the enclosing structures of the shelters, it is necessary to limit the size of the spans and the spacing of the columns. The ceiling span is usually taken equal to 6 m, and the column spacing, 6, 4.5 or 3 meters.

The inside longitudinal bearing walls are used comparatively rarely, for in this case the operation and maintenance of the facilities in peacetime are complicated. However, in cases where this solution is possible, it must be widely used as a result of the following advantages: a decrease in height of the facility, reduction of the types of prefabricated covering elements from 3 (slab, beam, column) to 1 (slab), a decrease in depth of the pit (replacement of the column foundations with strip foundations), simplicity of erection.

For shelters located in the basements of one-story production buildings or for separately standing shelters, a column grid can be used distinguished from the standard one inasmuch as it is not connected with the structural elements of the above-ground part of the building. Some decrease in the column grid, for example, from 6x6 to 4x4 meters, will permit a reduction in the consumption of materials without having a significant negative effect on the possibilities for use of the facilities in peacetime.

FOR OFFICIAL USE ONLY

FOR OFFICIAL USE ONLY

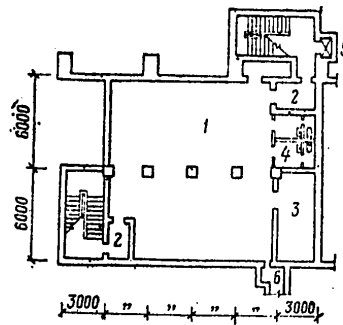


Figure 1. Planning a storage-shelter for 150-200 people in a basement.
1 -- facility for sheltering people; 2 -- lock chamber;
3 -- filter-fan chamber; 4 -- sanitary facility; 5 -- elevator;
6 -- emergency exit

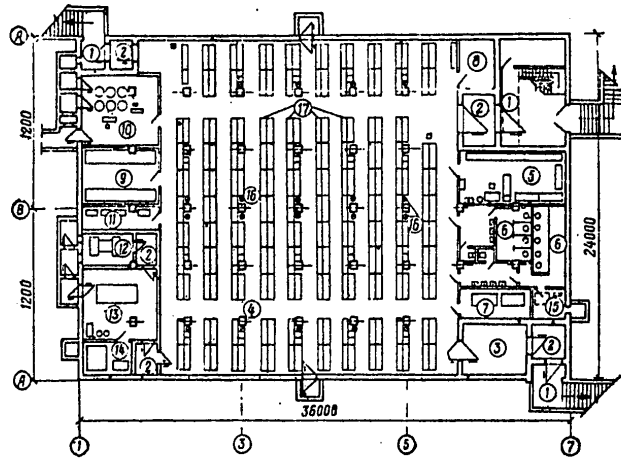


Figure 2. Planning a high-capacity shelter in the basement of a one-story industrial building with a column grid of 4x4 meters.
1 -- prelock; 2 -- lock chamber; 3 -- lock; 4 -- facility for sheltering people; 5 -- medical room; 6 -- sanitary facility; 7 -- water tank; 8 -- housekeeping storage; 9 -- produce storage; 10 -- ventilation chamber; 11 -- electric panel; 12 -- cooling unit of the diesel electric power plant (DES); 13 -- DES; 14 -- fuel and lubricant storage; 15 -- food waste storage; 16 -- drinking water; 17 -- benches and bunks

FOR OFFICIAL USE ONLY

FOR OFFICIAL USE ONLY

Fig 2 shows the planning of a shelter in the basement of a one-story building with a 24-meter span. In peacetime the basement is used as a storage for the materials of an industrial enterprise. The shelter is designed for 1000 people. There are three entrances in the shelter: two with doors 120x200 cm and one with gates 180x240 cm. Loads which are lowered from the first floor by a bridge crane are sent through the gates. The loads are transported within the storage by electric cars. The capacity of the shelter can be increased with placement of the people in the storage facilities and in the medical room which do not enter into the standardized list of mandatory facilities.

If with respect to the conditions of operation and maintenance of the shelters in peacetime it is necessary to have a large-span facility without inside walls and columns, then for separately standing shelters it is expedient to use the arch enclosures (see Fig 3). In this case the entrances and auxiliary facilities are placed at the ends which are made of flat structural elements.

For operation and maintenance in peacetime, an unloading and loading platform, the loads to which are supplied by elevator, is provided in front of the entrance to the storage.

When using the shelters in peacetime as transport structures (parking trucks, electric cars) an inclined ramp is built for entrance of the transport units, the length of which reaches 35 to 40 meters. This complicates the choice of the construction site under conditions of dense building up of the territory. With a small number of transport means instead of an inclined ramp it is expedient to design a vertical lift.

The space-planning solutions of shelters in residential and public buildings also have a number of peculiarities connected with the insurance of the required conditions of operation and maintenance of basement facilities and the buildings themselves during peacetime. The presence in the residential buildings of frequently occurring vertical stands of the sewerage, heating, water and gas supply systems complicates the operation of the basement facilities and sealing of the shelters.

Three versions of the placement of the pipes of the internal equipment systems below floor level of the first floor of the residential buildings are possible: the first -- passage of the pipes through the basement in steel tubes (for the sewerage risers) or reinforced concrete boxes; second -- the construction of a special engineering floor for the pipes; third -- passage of the pipes in the ceiling above the basement (in channels under the floor).

The first version is preferable with respect to cost. By comparison with it for five-story large-panel residential buildings the second version is 5% more expensive, and the third is 6% more expensive. However, the second version has significant advantages: it insures a good interior of the basement; it excludes the laying of the main lines through the

FOR OFFICIAL USE ONLY

FOR OFFICIAL USE ONLY

basement and the installation of sewerage risers; it permits the laying of the intrablock communications through the building; it provides for convenience of operation of the internal equipment systems of the building. In higher-rise buildings the construction of the engineering floor is cheaper. The third version is the worst with respect to all indexes.

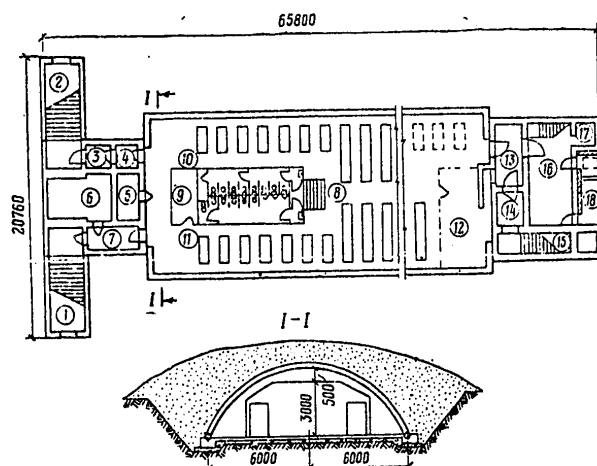


Figure 3. Arch type shelter:
 1, 2 -- entrances; 3 -- prelock; 4, 7 -- lock chamber; 5 -- electric panel; 6 -- diesel electric power plant; 8 -- facility for sheltering people; 9 -- sanitation facility; 10, 11 -- benches and bunks; 12 -- filter-ventilation chamber; 13, 15 -- lock chamber; 16 -- unloading area; 17 -- facility for entrance of engineering communications; 18 -- freight elevator

In public buildings the internal equipment system risers are arranged more compactly than in the residential buildings. Therefore it is possible to run the pipes through the basement at defined locations, setting aside small areas for this if necessary insulated from the shelter facility by a sealed-protective or sealed door.

Structural Designs of Shelters

The facilities adaptable for built-in shelters occupy the greater part of the building, and therefore the volume of the enclosing structures designed to take the shock wave impact is relatively small with respect to the volume of the entire building. For the enclosing structures of shelters, it is possible to use standard reinforced concrete structural elements which are widely used in industrial and civil construction. These include

FOR OFFICIAL USE ONLY

FOR OFFICIAL USE ONLY

the II-20 series structural elements for production buildings with a column grid of 6x6 and 9x6 meters designed for loads from 500 to 2500 kg/m², II-04 series for loads to 400 kg/m², and so on.

The bearing capacity of the ceiling of the shelter required by calculation of the shock wave impact can be attained by installing an auxiliary longitudinal and transverse reinforcing in intervals specially left when installing the ceiling (20-40 cm) between the prefabricated elements, increasing the working height of the ceiling by laying standard elements of the monolithic concrete layer above (see Fig 4). The amount of operating reinforcing is determined from the condition of the working of the same prefabricated monolithic cross section as monolithic. The joint working of the prefabricated monolithic concrete in the slabs is provided for by the forces of adhesion, and in the collar beams, projections of transverse reinforcing can also be provided.

The prefabricated monolithic structural elements are widely used in building shelters as a result of the following basic advantages:

The possibility of construction by industrial methods;

Increasing the spatial stability of the structure as a result of insuring the required rigidity of the corner structures by making them monolithic;

Simplicity of creation (joining of the assemblies without welding with subsequent monolithing) of continuous prefabricated elements on intermediate supports and the possibilities of changing the reinforcing in the supports;

Improvement of the seal of the joints of the prefabricated elements as a result of monolithing them;

Decreasing the weight of the prefabricated elements when they are made in complete profile.

The prefabricated-monolithic structural elements can be of three types:

From prefabricated elements with monolithic seams and intervals between elements;

From prefabricated elements of incomplete profile with respect to height with reinforcing protruding to the outside supplemented with finish concreting on sites to the total calculated height;

From basic supporting prefabricated elements and individual sections executed from monolithic reinforced concrete in the suspended form with general monolithic and finish concreting of the prefabricated elements to the full profile.

FOR OFFICIAL USE ONLY

FOR OFFICIAL USE ONLY

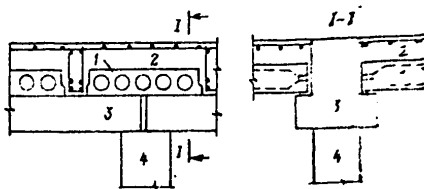


Figure 4. Structural design of the ceiling of structures with the application of standard prefabricated elements.
 1 -- II-03 series slabs; 2 -- monolithic reinforced concrete;
 3 -- prefabricated collar beams (nonstandard); 4 -- prefabricated column (nonstandard)

In Table 3 the nomenclature for the first type structural elements is presented. This set of structures permits the design of shelters (see Fig 5) built into the one-story industrial buildings. The monolithic concrete (15-20% of the total amount of concrete) is used for monolithing the seams, the construction of a reinforced coupler (5 cm) above the slabs, in the framing above the wall panels, in the corner sections of the walls and foundations, for the longitudinal beams built between the prefabricated beams.

The number of types and sizes of the prefabricated elements is reduced as a result of using concrete and steel of different types and different percentage of reinforcing. The same form is used here. For 32 marks and 18 types and sizes of elements only 10 types of forms are required.

The deficiencies of these structural designs include the following: increased consumption of concrete (1.46 m³ per m²) and steel (181 kg per m²) as a result of separate working of the elements (by the beam system with hinged supports), significant height of the ceiling (135 cm) as a result of floor by floor coupling of the beams and slabs, large volume of welding operations on site joining the laid parts of the elements. The coupling of the beams and slabs is possible within the height limits of the beam (Fig 6). However, the above-indicated deficiencies are also characteristic of this version of construction.

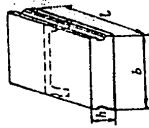

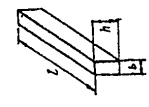
In practice the fully prefabricated structural design (10% monolithic concrete) is the construction of a shelter from T-beams (Fig 7) resting on columns in mutually perpendicular directions, and from square flat slabs laid on the webs of the beam. The continuous nature of the T-beams and their rigid coupling to the columns are achieved by connecting the projections of the reinforcing, installing additional reinforcing at the joints and monolithing with concrete. The joints of the auxiliary reinforcing to the projections are made dovetailed without welding. The deficiency of this structural solution is the great mass of the T-beams, reaching 15 tons, and the necessity for the application of a crane (type SKG-50) rarely used in construction for installation of them. The advantages are in the higher degree of plant readiness of the structural

16

FOR OFFICIAL USE ONLY

FOR OFFICIAL USE ONLY

Table 3. Nomenclature of Prefabricated Reinforced Concrete Structural Elements for Shelters

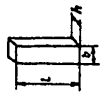
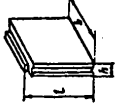
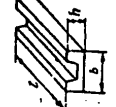
Элементы (1)	Схемы (2)	Марка элемента (3)	Размеры в мм (4)			Марка бетона (5)	Объем бетона в м ³ (6)	Масса элемента в т (7)
			l	b	h			
Плиты ребристые (8)		ПР-1 (9)	4420	1480	400	200	1.24	3.1
		ПР-2			400	200	1.24	3.1
		ПР-3			500	300	1.38	3.5
		ПР-4			500	300	1.38	3.5
		ПР-5	5920		450	200	2.05	5.1
		ПР-6			450	300	2.05	5.1
		ПР-7			550	300	2.24	5.6
		ПР-8			550	400	2.24	5.6
		ПР-9			550	300	2.63	6.6
Плоские плиты (10)		П-1	2920	1480	300	200	1.26	3.2
		П-2 (11)				300		
Балки (12)		Б-1	2900	400	800	300	0.93	2.3
		Б-2	4400			300	1.41	3.5
		Б-3 (13)	4400			300	1.41	3.5
		Б-4	4400			300	1.41	3.5
		Б-5	4400			400	1.41	3.5
		Б-6	5900			300	1.89	4.7
		Б-7	5900			400	1.89	4.7
		Б-8	5900			400	1.89	4.7

- Key:
1. Elements
 2. Sketch
 3. Type of element
 4. Dimensions in mm
 5. Concrete mark
 6. Concrete volume in m³
 7. Element mass in tons
 8. Ribbed slabs
 9. PR ...
 10. Flat slabs
 11. P ...
 12. Beams
 13. B ...

FOR OFFICIAL USE ONLY

FOR OFFICIAL USE ONLY

[Table 3, continued]

(1) Элементы	(2) Эскиз	(3) Марка Элемента	(4) Размеры в мм			(5) Марка бетона	(6) Объем бетона м ³	(7) Масса элемента в т
			l	b	h			
Колонны (14)		K-1 K-2 K-3 K-4	3500	500	600	200	1.05	2.6
				500			2.3	
				1000			1.05	
				1000			2.1	
Стеновые панели (15)		СП-1 СП-2 (16) СП-3 СП-4 СП-5	3900	1480	400	200	2.3	5.7
				3900			5.7	
				3100			4.6	
				3100			4.6	
				2700			3.0	
Фундаменты (17)		Ф-1 (18) Ф-2 Ф-3 Ф-4	5950	1200	500	200	2.63	6.6
				4450			4.9	
				2950			3.3	
				2950			1.1	

Key:

1. Elements
2. Sketch
3. Type of element
4. Dimensions in mm
5. Concrete mark
6. Concrete volume in m³
7. Element mass in tons

14. Columns
15. Wall panels
16. SP ...
17. Foundation
18. F ...

FOR OFFICIAL USE ONLY

FOR OFFICIAL USE ONLY

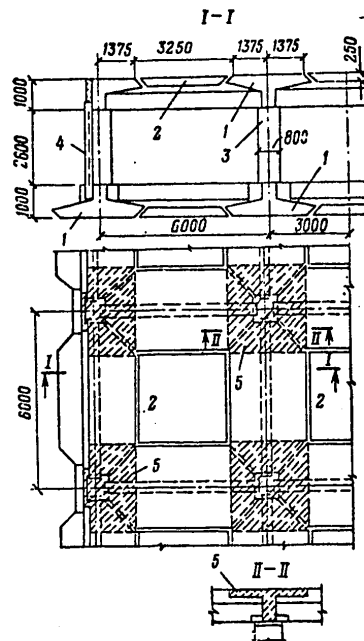


Figure 7. Structural diagram of a built-in shelter with ceiling made of continuous T-beams.
 1 -- T-beam; 2 -- square flat slab; 3 -- column; 4 -- wall panel; 5 -- monolithing sections

The prefabricated-monolithic structural elements with elements of incomplete profile with respect to height, especially the beamless ones, have high technical-economic indexes. They consist (see Fig 9) of prefabricated flat slabs (400x180 and 220x180 cm, 8-10 cm thick), laid on prefabricated column capitals (240 cm wide and 60 cm high) and a layer of monolithic reinforced concrete, the thickness of which depends on the degree of protection of the shelter. The capitals are executed in the form of a hollow truncated tetrahedral pyramid installed on a steel mounting table fastened at the upper level of the column. The reinforcing projections from the column run through an opening in the capitals. In the middle spans flat slabs are laid, and in the edge spans, slabs with one gentle rib by which they rest on the wall panels. All of the lower working reinforcing is in the slabs. The upper reinforcing above the support in the form of welded gratings is laid in the monolithic layer of the ceiling. Columns 50x50 cm are made in the foundation sleeves. The column grid 4x4 meters permits the application of this structural

FOR OFFICIAL USE ONLY

FOR OFFICIAL USE ONLY

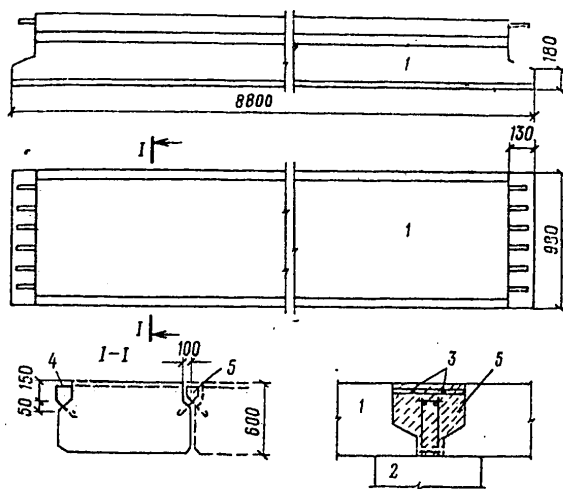


Figure 8. Continuous prefabricated slab with a 9-meter span. 1 -- slab; 2 -- support; 3 -- welded joint of the working reinforcing; 4 -- loops of the projections into the monolithing seam; 5 -- monolithing zone

solution for shelters built into one-story buildings and standing separately. The consumption of materials per m^2 of basement will be $0.8 m^3$ of concrete and 30 kg of steel.

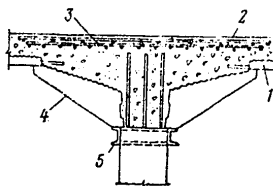


Figure 9. Prefabricated monolithic beamless shelter ceiling assembly. 1 -- prefabricated flat slab; 2 -- monolithic reinforced concrete; 3 -- fittings above the support; 4 -- prefabricated capitals; 5 -- mounting table

FOR OFFICIAL USE ONLY

FOR OFFICIAL USE ONLY

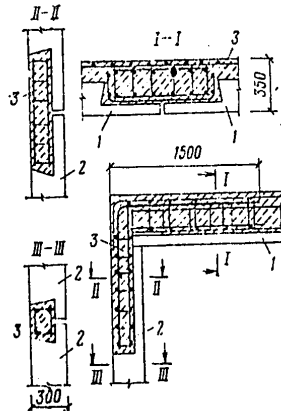


Figure 10. Assembly for joining wall panels to the prefabricated monolithic beam ceiling of a shelter.
 1 -- slab of the inverted I type; 2 -- wall panel; 3 -- monolithic reinforced concrete

The deficiencies of the prefabricated monolithic beamless ceilings can include the complexity of the form for manufacturing the capitals and significant weight of them with an increase in the column grid to 6x6 m.

The beam ceiling (Fig 10) has simpler structural elements. It consists of continuous beams laid on the columns and supported on the beams of the prefabricated slabs of the inverted I type (dimensions 600x300 cm, 30 cm thick). After installing the support reinforcing of the beams and monolithing to the calculated mark the slabs become continuous. All of the stressed span reinforcing is placed in the prefabricated slabs. As a result of the joining of the beam and the slab at the height limits of the beam the height of the ceiling does not exceed 80 cm. The basement walls are made of prefabricated panels (600 cm wide, height equal to the height of the basement, thickness 30 cm). The panels are of rectangular cross section (weighing up to 12 tons) with grooves for rigid connection of the wall to the ceiling by installing additional reinforcing in them and monolithing the joint. The weight of the main ceiling elements (slabs, beams, columns) is approximately the same and is 5 to 7 tons. The consumption of materials per m² of the basement is as follows: 0.8 m³ of concrete, 55 kg of steel. The amount of monolithic (construction) concrete is about 32% of the total consumption.

The advantages of the investigated structural solution must include the low structural height of the ceiling and the fact that all of the beams are arranged in one direction and protrude a total of 35 cm into the basement. The deficiency is the complex structural design of the wall panels (as a result of the presence of grooves) and significant weight

FOR OFFICIAL USE ONLY

FOR OFFICIAL USE ONLY

of them greatly exceeding the weight of the ceiling elements, which is disadvantageous from the point of view of selecting the crane equipment.

Decreasing the material consumption and weight of the prefabricated elements is the most important goal of improving the structural design of the shelters. The application of curvilinear prefabricated monolithic elements, in particular, the arches of the curved outline, permits a significant decrease in thickness of the shelter ceiling (to 16 cm for a span of 330 cm and rise of 60 cm). However, the frequent arrangement of the bearing walls on which the arches are supported (or the corresponding small column grid) leads to an increase in the concrete consumption and limits the possibility of using the facilities in peacetime. In addition, the technological process equipment has still not been created for mechanizing the forming of the curvilinear panels. The labor intensiveness of installing the cylindrical shells is 1.5 to 2.5 times higher than the standard flat structural elements.

An efficient form of enclosing structures for shelters providing for the most advantageous use of the bearing capacity of concrete under compression and the possibility of considering the plastic properties of the foundation soil can be considered to be the arch construction (see Fig 3). The curvature of the arch, the structural design of the hinges and the shape of the embankment of a separately standing structure can be selected so that the possibility of the occurrence of bending moments in the arch elements is excluded.

The structural designs in the form of a sphere, the cupola and so on are sometimes used abroad for the small-capacity shelters (family shelters, individual shelters).

A successful structural design of shelters made of monolithic reinforced concrete is the beamless ceiling (see Fig 11).

With a column grid of 6x6 meters the slab thickness of the ceiling varies from 250 to 450 mm depending on the load, the column cross section -- from 500x500 to 1000x1000 mm, the column capital size with respect to a height of 600 mm and the slope of the faces at 45°. For convenience of concreting it is expedient to design the walls flat (without pilasters) with continuous brackets next to the walls. In dry ground the foundations under the columns are columnar, and under the outside walls, strip. In the water-saturated soils the slab of a continuous foundation is designed as an inverted beamless ceiling.

In the case of dry ground the shelter walls can be made from prefabricated concrete modules (see Fig 12). In order to improve the working of the walls under the joint effect of vertical and horizontal loads, it is necessary to place the beams along the structure, which insures uniform loading of the walls from the ceiling. The unweighted walls work on bending and require reinforcement. The walls made of prefabricated concrete blocks usually are reinforced by a monolithic reinforced concrete

FOR OFFICIAL USE ONLY

FOR OFFICIAL USE ONLY

wall on the inside or the installation of monolithic columns at the breaks between the blocks which are laid in this case without tying.

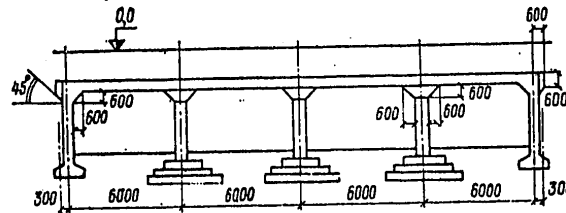


Figure 11. Monolithic beamless ceiling of a shelter

The structural design of shelter walls made of prefabricated concrete modules cannot be recognized as efficient with respect to concrete consumption, but it has become widespread as a result of the simplicity of erection and ubiquitous manufacture of these modules.

The foundations under the shelter walls are strip made of standard prefabricated reinforced concrete foundation modules or monoliths; under the columns they are columned or stripped (with a column spacing of less than 6 meters), prefabricated or more frequently monolithic. The standard foundation modules, as a rule, have sufficient thickness from the condition of working under impact, but in some cases they require reinforcement calculated for bending. Under the effect of a shock wave on the structure the foundations undergo significant settling (to several centimeters). In addition, the structure moves in the horizontal direction from the unequalled loads acting on the front and rear.

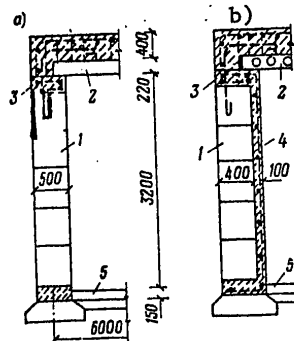


Figure 12. Outside walls of shelters made of prefabricated concrete modules.

a -- weighted ceiling; b -- unweighted ceiling; 1 -- concrete module; 2 -- prefabricated hollow slab; 3 -- monolithic reinforced concrete strip; 4 -- monolithic reinforced concrete wall; 5 -- concrete preparation

FOR OFFICIAL USE ONLY

FOR OFFICIAL USE ONLY

Thus, the structure and its individual parts are involved in complex movement in space under the effect of a shock wave, they are loaded and unloaded unsimultaneously.

In order to provide for general spatial stability of the shelters, it is necessary to take some structural measures: rigid building of the columns and wall panels into the foundation; coupling of the wall and ceiling elements and also all of the prefabricated reinforced concrete elements to each other; reinforcing the corners and the joints of the walls made of concrete modules; clamping of the ceiling slabs in the walls; the construction of monolithic reinforced concrete strips around the perimeter of the outside walls and across the structure above the columns in the prefabricated ceilings and floors; insurance of monolithic nature of the prefabricated ceilings and floors.

In order to avoid the transmission of additional forces to the structural elements of the built-in shelters when the above-ground part of the buildings is destroyed, it is necessary to connect the columns of the building rigidly to the shelter ceiling.

The structural elements of the shelters are designed for high-intensity loading, and improvement of the technical-economic indexes of the structural designs is a complex problem. One of the ways to improve the structural designs of the shelters can be the application of prefabricated monolithic pre-stressed reinforced concrete structural elements which are highly efficient with respect to material consumption.

Significant cost benefit can be obtained by considering the increase in strength of the concrete with time. For example, in 2 years the relative ultimate compressive strength of concrete will increase by 1.75 to 2 times by comparison with the trademark strength after 25 days used in the design calculations.

Technical-Economic Indexes of Shelters

In order to discover the optimal designs for shelters it is necessary to establish a method of determining the technical-economic indexes.

When designing buried structures adaptable for shelters, it is necessary to reinforce the structural elements, and provide special internal equipment. This gives rise to additional expenditures. At the same time the structures and their internal equipment also are operated and maintained in peacetime.

It would be possible to establish the additional expenditures on shelters by comparing two design solutions: the design of an ordinary buried structure (for example, a garage) and the design of a buried garage-shelter. However, for this purpose in each case it would be necessary to make two designs, which is unrealistic. A more accessible method is determination of the additional expenditures and the difference between

FOR OFFICIAL USE ONLY

FOR OFFICIAL USE ONLY

the estimated cost of the facilities adaptable to shelters and the average cost of the ordinary buried facilities (basements).

Here it is necessary primarily to decide whether the objects are comparable.

The first condition of comparableness of the objects is unity of purpose. It is possible to compare underground garage-shelters, but it is impossible to compare a garage-shelter and an underground storage-shelter. The second condition is unity of the design norms connected with the given climatic, hydrogeological and other conditions of the construction site.

In addition, it is necessary to consider not only the difference of the indexes with respect to the buildings themselves, but also the difference of the indexes with respect to the master plan of the enterprise (including by the waterline, sewerage, power supply, transport and other networks), inasmuch as on making the transition to the use of the underground space the density of building increases, and the extent of the networks is reduced.

As the calculated units of measure it is expedient to select one location (for those sheltered in the shelter) and one m^2 of useful (common) area, for these units insure comparability of the analyzed indexes: cost having the greatest comparability, natural (concrete and metal consumption) and relative (the system of coefficients K : K_1 -- ratio of the area of the basic facilities to the total area of the shelter; K_2 -- ratio of the construction volume of the shelter to the total volume of the shelter; K_3 -- ratio of the area of the basic facility to the shelter area; K_4 -- ratio of the useful area of the shelter to its capacity).

The gradual accumulation by the design organizations of technical-economic indexes for shelters will permit establishment of standard indexes which can be used to estimate the quality of shelter designs and the preliminary calculations.

The basic space-planning parameters of the shelter are its length, width, height and the ratio of its areas. The effect of these parameters on the construction expenditures can be characterized by the above-indicated relative indexes.

The ratio of the area of the basic facility to the total (useful) area of the shelter (coefficient K_1) is an important criterion of the economicalness of the planning solution. The greater the area isolated in the shelter to protect people, the more economical it is. The coefficient K_1 varies from 0.4 to 0.6 (in shelters with utility corridors along the outside walls) to 0.75-0.83. The value of K_1 increases with an increase in the capacity of the shelters, which indicates their better economic indexes by comparison with the small-capacity shelters. The coefficient K_2 characterizes the efficiency of the composition and use of the shelter space. When comparing the versions of the space-planning solutions, the smaller value of K_2 indicates that per m^2 of useful area, a smaller

FOR OFFICIAL USE ONLY

FOR OFFICIAL USE ONLY

construction volume of the shelter is required, and, consequently, the given version is more economical under other equal conditions. The volumetric coefficient can serve as the criterion of economicalness of the designs only in the case where the estimated cost of 1 m³ of the comparable shelters is identical or close. However, the estimated cost of 1 m³ of shelter with changes in the planning and design solutions can fluctuate within significant limits. Therefore even for equal volumetric coefficients, the cost of 1 m² of useful area in the compared designs can be different.

Thus, the coefficient K_2 is not a sufficiently accurate index characterizing the economicalness of the design, in spite of the fact that it reflects the effect of the height of the facilities, the wall thickness and it considers the efficiency of planning of the shelter.

The coefficient K_2 varies from 4 to 8; the larger values correspond to shelters with solid foundation slab.

The ratio of the area of the basic facilities to the basement area (the coefficient K_3) makes it possible to determine the possible capacity of the shelter beginning directly with the building (basement) dimensions. The coefficient K_3 takes into account the area of the various unprotected facilities which are provided for in basements for technological needs. In the shelters with utility corridors along the walls K_3 is equal to 0.25-0.4, increasing to 0.5-0.65 with an increase in their capacity.

The total actual consumption of usable area per man (the coefficient K_4) is 0.65 to 1.2 m², where the smaller values of K_4 are characteristic of the high-capacity shelters.

For the developed standard designs of shelters, the best indexes are the following: $K_1=0.82$, $K_2=3.8$, $K_3=0.6$ and $K_4=0.64$.

The natural indexes are also required to estimate the economicalness of the planning solutions, especially the structural designs of the shelters. The concrete consumption in the atypical designs will be the following: per man 1.3-3 m³; per m² of usable area, 1.2-3.2 m³; and in standard designs the best indexes are 0.94 and 1.05 m³, respectively.

The metal consumption in the individual designs of built-in shelters will be as follows: for 1 man 80-380 kg, for 1 m², 70-370 kg (the indexes increase with an increase in the degree of protection of the shelter). These indexes also include the concrete and metal consumption for the structural elements required by the conditions of operation and maintenance of the basement in peacetime and not designed for the effect of the shock wave loads.

The cost indexes of the individual designs of built-in shelters vary within broad limits.

FOR OFFICIAL USE ONLY

FOR OFFICIAL USE ONLY

The cost of the basement shelter is approximately 1.7 to 2 times greater than the cost of the ordinary basement. The increase in cost with respect to type of operations will be in %:

For general construction work	55-60
For water lines and sewerage	5-10
For insulation and ventilation	15-25
For electric lighting	3-6
Strong and weak current electrical equipment	2-8
For diesel electric power plants	7-15

The increase in cost of industrial buildings with a basement shelter by comparison with buildings with ordinary basement (for identical purpose of the basements in peacetime) will be 5-20%.

FOR OFFICIAL USE ONLY

CHAPTER II. DYNAMIC LOADS ON THE STRUCTURAL ELEMENTS OF CIVIL DEFENSE SHELTERS

The dynamic loads and the structural elements of the shelters are created basically under the effect of the shock wave from a nuclear blast or the explosion of chemical explosives. The maximum magnitude of this load and the law of its variation in time depend on the placement of the structure with respect to the ground surface (above ground, semiburied, completely buried), the location of it in the builtup area (built in, separately standing) and also the dimensions, shape, orientation of the investigated structural element with respect to the blast center and the parameters of the incident shock wave (the magnitude of the maximum excess pressure and the duration of its effect).

The term "incident" wave is applied to the waves moving from the blast center to the investigated surface at dip angles of 0-90°. In this case the dip angle is measured between the normal to the investigated surface and the direction of motion of the wave. With respect to magnitude it is equal to the slope angle of the shock wave front.

In addition to the loads from the shock wave, some structural elements of the shelters (for example, the ceilings in the basements of buildings) can also be subjected to the effect of short-term dynamic loads from the impact of falling fragments of the buildings on destruction of them by the shock wave. Usually the loads from the air shock wave effect are defining for the shelters.

1. Parameters of the Air Shock Wave

The shock wave has a sharply expressed front, on which the temperature, density, pressure and velocity of the medium increase discontinuously. The wave is made up of a compression phase and the rarefaction phase following directly after it (see Figure 13).

The basic characteristics of the compression phase are the excess pressure Δp_ϕ of the shock wave front and the compressure phase duration τ_+ called the time of effect of the shock wave.

FOR OFFICIAL USE ONLY

FOR OFFICIAL USE ONLY

The pressures on the air shock wave front from the nuclear blast or the explosion of chemical explosives can be defined by the formulas of V. P. Korobeynikov [29] which after simplifications, have the form:

for $0.16 < \Delta p_\phi < 100 \text{ kg/cm}^2$ or $0 < R_2 \leq$

$$\Delta p_\phi = \frac{7}{3(\sqrt{1+29.8R_2^2}-1)} \text{ kg/cm}^2; \tag{1}$$

Key: a. front

for $\Delta p_\phi < 0.16 \text{ kg/cm}^2$ or $R_2 > 2$

$$\Delta p_\phi = \frac{0.227}{R_2 \sqrt{1gR_2+0.158}} \text{ kg/cm}^2. \tag{2}$$

In these formulas R_2 is the dimensionless radius of the shock wave

$$R_2 = r_2 \sqrt[3]{\frac{p_1}{kE_0}}, \tag{3}$$

where r_2 is the distance from the blast center in meters; $p_1 \approx 10^4 \text{ kg/m}^2$ is atmospheric pressure; E_0 is the blast energy with respect to the shock wave in kg-meter; k is the coefficient equal to 2 for the ground blast and equal to one for the air blast.

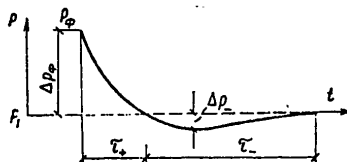


Figure 13. Variation of the pressure at a fixed point in the terrain as a function of the time t (Δp_- is the maximum rarefaction pressure).

The blast produced in the air above the ground or the water at an altitude at which the fireball does not touch the earth's surface the time of its maximum brightness is called an air blast; a ground (water) blast is a blast where the fire ball touches the surface of the earth (water) or the blast occurs at the surface of the earth (water) [21]. For high-energy air blast the dimensions of the fireball at the time of its maximum brightness are less the fireball radius L_{fireball} of the fireball, the magnitude of which according to [39] is:

FOR OFFICIAL USE ONLY

FOR OFFICIAL USE ONLY

$$L_{0.11} = 10 \sqrt[3]{q} \text{ m,} \\ \text{(a)}$$

Key: a. fireball

where q is the TNT equivalent of the blast energy in tons.

The energy E_0 communicated to the medium (air) is part of the total energy released during the blast. For a nuclear blast, approximately 50% of all of the released energy is expended on the formation of an air shock wave; for a TNT blast, 65 to 70% [7].

The power of the nuclear blast is compared with the equivalent amount of TNT with respect to energy. The heat of explosive conversion of the latter (the explosion energy) is approximately equal to 1000 kcal/kg.

For a pressure on the shock wave front with a ground blast of the nuclear material with total TNT equivalent q in tons the formulas (1), (2) are written as follows:

for

$$\bar{R} \leq 78 \text{ m/ton}^{1/3}, \\ \Delta p_{\psi} = \frac{2,333}{\sqrt{1 + 0,494 \cdot 10^{-3} \bar{R}^3 - 1}} \text{ kg/cm}^2; \quad (4)$$

for $\bar{R} > 78 \text{ m/ton}^{1/3}$

$$\Delta p_{\psi} = \frac{8,9}{\bar{R} \sqrt{1,9 \bar{R} - 1,44}} \text{ kg/cm}^2. \quad (5)$$

Here \bar{R} is the reduced distance

$$\bar{R} = \frac{r_2}{\sqrt[3]{q}} \text{ m/ton}^{1/3}. \quad (5a)$$

Formulas (4) and (5) are represented graphically in Figure 14.

For an air nuclear blast the pressure at the front of the incident shock wave is defined by the formulas:

$$\Delta p_{\psi} = \begin{cases} \frac{2,333}{\sqrt{1 + 10^{-3} \bar{R}^3 - 1}} \text{ kg/cm}^2; & 0 < \bar{R} \leq 62 \text{ m/ton}^{1/3}; \\ \frac{6,9}{\bar{R} \sqrt{1,9 \bar{R} - 1,23}} \text{ kg/cm}^2; & \bar{R} > 62 \text{ m/ton}^{1/3}. \end{cases} \quad (6)$$

The time of effect of the compression phase for a ground blast is defined by the formula of M. A. Sadovskiy [68]:

FOR OFFICIAL USE ONLY

$$\tau_+ = 3,3 \cdot 10^{-3} \sqrt[6]{q} \sqrt{r_2} \text{ sec } 15 < \bar{R} < 78 \text{ m/ton}^{1/3}, \quad (7)$$

The pressure variation $\Delta p(t)$ in time in the compression phase depends on the value of Δp_{front} is expressed by the empirical formula of Brode [70] obtained as a result of the numerical solution of the problem of a point blast:

$$\Delta p(t) = \Delta p_{\text{front}} \left(1 - \frac{t}{\tau_+}\right) e^{-\alpha \frac{t}{\tau_+}}, \quad (8)$$

where $\alpha = 0,5 + \Delta p_{\text{front}}$ for $\Delta p_{\text{front}} \leq 1 \text{ kg/cm}^2$.

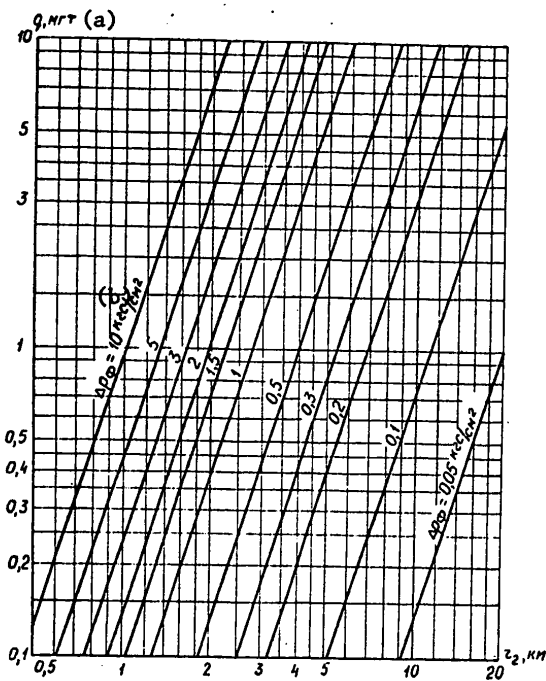


Figure 14. Excess pressure on shock wave front as a function of power and distance to the ground blast center.

Key; a. megatons b. kg/cm^2

For shock waves with $1 < \Delta p_{\text{front}} < 3 \text{ kg/cm}^2$ the coefficient α is a time function:

$$\alpha = 0,5 + \Delta p_{\text{front}} \left[1,1 - (0,13 + 0,2\Delta p_{\text{front}}) \frac{t}{\tau_+}\right]. \quad (9)$$

FOR OFFICIAL USE ONLY

FOR OFFICIAL USE ONLY

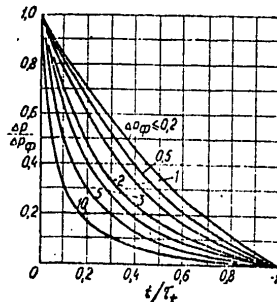


Figure 15. Variation of the pressure with time for shock waves of different intensity (at different distances from the blast center).

If Δp_{front} varies from 3 to 10 kg/cm², then

$$a = a + \frac{b}{1 + ct/\tau_+} \quad (10)$$

where

$$a = -0.231 + 0.388\Delta p_\phi - 0.0332\Delta p_\phi^2;$$

$$b = \Delta p_\phi (0.88 + 0.072\Delta p_\phi);$$

$$c = 8.71 + 0.1843\Delta p_\phi - \frac{104}{(\Delta p_\phi + 10)}.$$

The pressure variation with time at different distances characterized by the excess pressure on the shock wave front is illustrated in Figure 15.

The load on the structures depends to a great extent on the magnitude of the velocity head Q_{front} which occurs as a result of braking of the masses of air behind the shock wave front on encountering a barrier. Its value depends on the velocity and density of the air and is determined by the formula known from shock wave theory:

$$Q_\phi = \frac{1}{2} \rho_\phi u_\phi^2 = \frac{2.5\Delta p_\phi^2}{\Delta p_\phi + 7.2} \text{ kg/cm}^2. \quad (11)$$

For variation of the velocity head with time the following relations are established [70]

$$Q(t) = Q_\phi \left(1 - \frac{t}{\tau_+}\right)^2 e^{-\beta \frac{t}{\tau_+}} \text{ kg/cm}^2, \quad (12)$$

where for shock waves with $\Delta p_{\text{front}} \leq 1 \text{ kg/cm}^2$, $\beta = 0.75 + 3.2 \Delta p_{\text{front}}$.

FOR OFFICIAL USE ONLY

FOR OFFICIAL USE ONLY

For $10 > \Delta p_{\text{front}} > 1 \text{ kg/cm}^2$

$$\beta = d + \frac{f}{\left(1 + g \frac{t}{\tau_+}\right)},$$

where

$$d = -1,33\Delta p_{\phi} \text{ for } \Delta p_{\phi} \leq 3;$$

$$d = -5,6 + 0,63\Delta p_{\phi} \text{ for } 3 < \Delta p_{\phi} \leq 10;$$

$$f = 6,4\Delta p_{\phi}; \quad g = 0,725\Delta p_{\phi}.$$

The solution to the equation of motion of the structure (structural element) under the effect of the shock wave load is significantly simplified if the effective load varies in time according to linear laws. Accordingly, in the calculations frequently instead of the effective diagram $\Delta p(t)$ a line diagram (Figure 16) is used with replacement of the time of effect of the compression (rarefaction) phase by the effective time θ [40].

If the maximum deformation of the structural element comes at the end of the compression phase or after completion of the load effect, the effective time is determined from the condition of equality of the pulses:

$$(a) \quad \frac{\Delta p_{\text{max}} \theta}{2} = i = \int_0^{\tau} \Delta p(t) dt, \quad (13)$$

Key: a. max

where Δp_{max} is the maximum pressure.

Depending on Δp_{front} , the effective time of the compression phase with respect to the condition (13) is expressed by one of the approximate formulas:

$$\text{for } \Delta p_{\phi} \leq 1 \text{ kg/cm}^2 \\ \theta \approx (0,85 - 0,2\Delta p_{\phi})\tau_+ \text{ sec}; \quad (14)$$

$$\text{for } 1 < \Delta p_{\phi} \leq 3 \text{ kg/cm}^2 \\ \theta \approx (0,72 - 0,08\Delta p_{\phi})\tau_+ \text{ sec}. \quad (15)$$

For loads from the shock wave of the nuclear blast the maximum deformation of the structural element takes place during the initial period of loading in a time which in the majority of cases is two orders less than τ_+ . Therefore in the calculations it is possible to assume that the pressure varies with respect to the transient to the effective curve $\Delta p(t)$ at the point $t = 0$ (Figure 16).

FOR OFFICIAL USE ONLY

FOR OFFICIAL USE ONLY

The effective time here is determined by the formulas:

$$0_0 = \frac{\tau_+}{(1,5 + \Delta\rho_\phi)} \text{ sec for } \Delta\rho_\phi \leq 3 \text{ kg/cm}^2; \quad (16)$$

$$0_0 = \frac{\tau_+}{(0,769 + 1,268\Delta\rho_\phi + 0,0388\Delta\rho_\phi^2)} \text{ sec}$$

for $3 < \Delta\rho_\phi \leq 10 \text{ kg/cm}^2$,

and in place of formula (8) the expression

$$\Delta p(t) = \Delta\rho_\phi \left(1 - \frac{t}{\theta}\right). \quad (17)$$

is used.

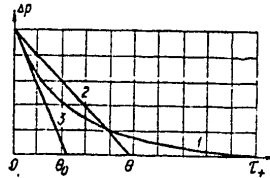


Figure 16. Shock wave pressure diagrams: 1 -- effective curve; 2 -- pulse equivalent triangle diagram; 3 -- triangle diagram formed by the tangent to the effective curve.

The shielded doors at the entrances to the shelters and the shutters (hatches) of the emergency exits are designed not only for the effect of the load in the compression phase but also for the negative (return) load in the rarefaction phase which began to operate after the compression phase. The maximum excess rarefaction pressure Δp_- and the rarefaction phase duration τ_- are well described by the Brode empirical formula [70], which for a ground blast after some substitutions are written in the form:

$$\Delta p_- = -\frac{3,28\sqrt[3]{q}}{r_s} \text{ kg/cm}^2 \text{ for } \bar{R} > 19 \text{ m/ton}^{1/3}; \quad (18)$$

$$\tau_- = 0,13\sqrt[3]{q} \text{ sec.} \quad (19)$$

The pressure variation in the rarefaction phase is approximated in the following form:

$$\Delta p_-(t) = 1,4\Delta p_- \frac{t}{\tau_-} \left(1 - \frac{t}{\tau_-}\right) e^{-4\frac{t}{\tau_-}} \text{ for } 0,1 < \Delta\rho_\phi < 200. \quad (20)$$

where t is the time measured from the end of the compression phase; Δp_- is the maximum negative excess pressure with respect to absolute magnitude.

FOR OFFICIAL USE ONLY

FOR OFFICIAL USE ONLY

The effective time θ_0 of the rarefaction phase is:

$$\theta_0 \approx 0,9\tau_-, \quad (21)$$

and the linear law of variation of the negative load (Figure 17) with build-up of it to the maximum value with respect to absolute magnitude in the time $\theta_1 \approx 0.12\tau_-$ can be represented in the form

$$\Delta p_-(t) = \begin{cases} \Delta p_- \frac{t}{\theta_1} & \text{for } 0 \leq t \leq \theta_1; \\ \Delta p_- \left(1 - \frac{t - \theta_1}{\theta_- - \theta_1}\right) & \text{for } \theta_1 \leq t \leq \theta_- \end{cases} \quad (22)$$

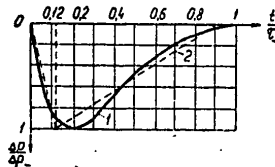


Figure 17. Variation of the negative pressure in the rarefaction phase. 1 -- curve according to equation (20); 2 -- linear law with effective operating time.

Example 1. Let us determine the parameters of the shock wave with a pressure at the front of 2 kg/cm^2 for a ground blast of a nuclear bomb with TNT equivalence of 1 million tons.

By the graph in Figure 14 we find that for $q = 10^6$ tons the excess pressure on the shockwave front of 2 kg/cm^2 will be at a distance $r_2 \approx 1960$ meters. The reduced distance according to formula (5a) is

$$\bar{R} = \frac{1960}{\sqrt[3]{10^6}} = 19,6 \text{ m/ton}^{1/3}.$$

By formula (7) let us calculate the time of effect of the compression phase

$$\tau_+ = 3,3 \cdot 10^{-3} \sqrt[3]{10^6} \cdot \sqrt{1960} = 1,46 \text{ sec.}$$

By formula (16) the effective time is:

$$\theta_0 = 1,46 / (1,5 + 2) = 0,417 \text{ sec.}$$

The pressure of the velocity head at the shock wave front by formula (11) is

$$Q_\Phi = \frac{2,5 \cdot 2^2}{2 + 7,2} = 1,09 \text{ kg/cm}^2.$$

FOR OFFICIAL USE ONLY

FOR OFFICIAL USE ONLY

The maximum excess rarefaction pressure and the rarefaction phase duration will be calculated by formulas (18) and (19):

$$\Delta p_{-} = -\frac{3.28 \sqrt{10^6}}{1960} = -0.167 \text{ kg/cm}^2, \quad \tau_{-} = 0.13 \sqrt{10^6} = 13 \text{ sec.}$$

2. Loads on the Structure from an Air Shock Wave of a Nuclear Blast

The horizontal covering of an unburied structure is subjected to the effect of a dynamic load equal to the excess pressure of the air shock wave. The law of variation of the load in time is taken by expression (17). If the shock wave moves along the span of the structure, then the loading of it will be gradual, as the shock wave advances. In the majority of practical cases the advancement of the shock wave is neglected and it is considered that the entire span is loaded simultaneously. This is admissible, for the shock wave front, moving at supersonic velocities, passes over the span of the structure in a very small time making up one to two tenths of the period of the natural oscillations of the structure.

When the shock wave arrives at an angle α_0 to the barrier, the latter expresses a pressure significantly exceeding the pressure in the incident shock wave, for on a section of it from the barrier the air particles moving in the wave are braked, and as a result of the conversion of the kinetic energy to the pressure energy, additional braking pressure is created. The reflection pressure Δp_{refl} acting on the stationary barrier can be defined by the formula [36]

$$\Delta p_{\text{orp}} = \Delta p_{\psi} (1 + \psi) + \frac{3\Delta p_{\psi}^2}{\Delta p_{\psi} + 7.2} (\eta + \psi) \text{ kg/cm}^2, \quad (23)$$

(a)

Key: a. refl

where

$$\eta = \frac{1 + \text{tg}^2 \alpha_{\text{orp}}}{1 + \text{tg}^2 \alpha_0}; \quad \psi = \sqrt{\eta} \sqrt{1 + \frac{9(\eta - 1)\Delta p_{\psi}^2}{(4\Delta p_{\psi} + 7.2)^2}},$$

α_{refl} is the angle between the front of the reflected shock wave and barrier, and $\text{tg} \alpha_{\text{refl}}$ is determined from the equation

$$\begin{aligned} M^2 (1 - \mu^2)^2 (\text{tg} \alpha_0 - \text{tg} \alpha_{\text{orp}}) + M [(1 - \mu^2)^2 - \\ - (\text{tg} \alpha_0 - \text{tg} \alpha_{\text{orp}})^2 - (\mu^2 + \text{tg} \alpha_0 \text{tg} \alpha_{\text{orp}})^2] - \\ - (\text{tg} \alpha_0 - \text{tg} \alpha_{\text{orp}}) = 0, \end{aligned} \quad (24)$$

in which

FOR OFFICIAL USE ONLY

FOR OFFICIAL USE ONLY

$$M = \frac{6\Delta p_\psi \operatorname{tg} \alpha_0}{(6\Delta p_\psi + 7,2) + (\Delta p_\psi + 7,2) \operatorname{tg}^2 \alpha_0} \quad \text{and} \quad \mu^2 = \frac{1}{6}.$$

Formula (24) is applicable only in the case where the angle of incidence (α_0) of the shock wave on the barrier does not exceed some limiting value α_{lim} , the magnitude of which as a function of the intensity of the incident shock wave is presented in reference [36, 47].

For normal reflection ($\alpha_0 = \alpha_{\text{refl}} = 0$) the coefficients η and ψ in formula (23) are equal to one, and the reflected pressure is defined by the function

$$\Delta p_{\text{refl}} = 2\Delta p_\psi + \frac{6\Delta p_\psi^2}{\Delta p_\psi + 7,2} \quad \text{kg/cm}^2. \quad (25)$$

Key: a. refl

The graphs of the variation of the reflection coefficient ($\Delta p_{\text{refl}}/\Delta p_{\text{front}}$) as a function of the angle of incidence (Figure 18) constructed by formula (23) (the solid lines), indicate that the normal or frontal reflection of the shock wave does not necessarily generate the strongest reflected shock wave. The inclined reflection of the shock wave $\Delta p_{\text{front}} \leq 2 \text{ kg/cm}^2$ can lead to the formation of a more powerful reflected shock wave and consequently, a higher peak pressure on the reflecting surface than the normal reflection. This effect was used for preliminary estimation of the optical radius of effect for the nuclear bomb blasts in Hiroshima and Nagasaki [47].

The left-hand side of the curves in Figure 18 give the value of the reflection coefficient in the regular reflection region in which the incident and reflected waves begin with one point, moving over the surface of the barrier. The right-hand sides of the curves (the dotted lines) corresponding to the angles of incidence greater than the limiting ones, belong to the region of irregular reflection in which the so-called Mach effect occurs. Its essence consists in the merging of the fronts of the reflected and the incident waves at the surface of the barrier and the formation of a third shock wave front called the head wave. All three fronts intersect at one point called the ternary point. Since in this region the reflected wave moves faster than the incident wave and overtakes it, the ternary point gradually rises above the surface of the barrier, and the height of the head wave increases on moving along the barrier.

For air nuclear blasts, the region of regular reflection on the earth's surface is called the near zone of propagation of the shock wave, and the region of irregular reflection, the far zone. The pressure on the earth's surface for air blasts can be determined by the graphs in Figure 18 with known angle of incidence and pressure at the incidence shock wave front [see formula (6)].

FOR OFFICIAL USE ONLY

FOR OFFICIAL USE ONLY

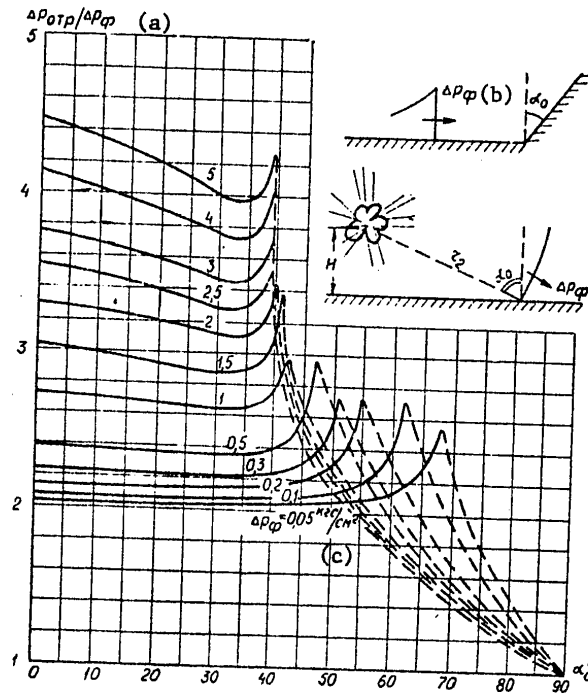


Figure 18. Reflection coefficient $k = \Delta p_{\text{refl}} / \Delta p_{\text{front}}$ as a function of the angle of incidence α_0 for different values of Δp_{front} .

Key: a. $\Delta p_{\text{refl}} / \Delta p_{\text{front}}$ b. Δp_{front} c. kg/cm^2

Under actual conditions the shock wave interacts with the barriers of limited size and, in particular, with ground structures and buildings. In this case, along with reflection, the process of movement of the shock wave around the barrier called diffraction also occurs.

The effect of the load from the shock wave on the ground structure can be divided into two phases: the diffraction phase and the braking phase [68]. The diffraction phase is the initial phase -- the reflection pressure and the pressure in the transmitted wave act on the structure.

At the time when the shock wave front reaches the wall¹ of the structure, reflection of this wave takes place, and the pressure on the wall increases

¹The wall of the structure perpendicular to the direction of the shock wave pressure will hereafter be called frontal.

FOR OFFICIAL USE ONLY

FOR OFFICIAL USE ONLY

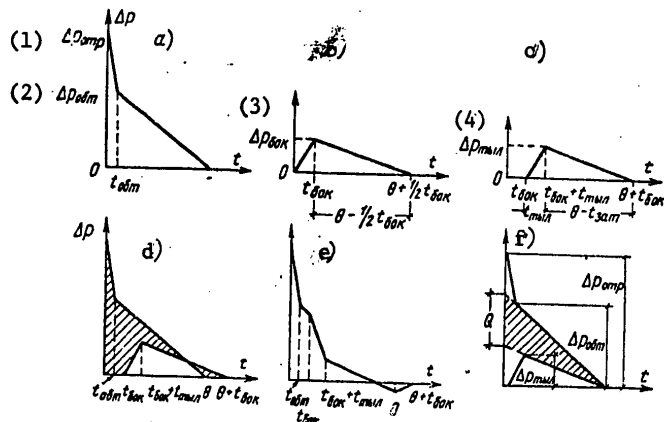


Figure 19. Diagrams of the average loads on a ground structure without openings, a -- on the front (turned toward the blast center) wall; b -- on the roof and side walls; c -- on the rear walls; d and e -- resultant horizontal load; f -- special case of the resultant horizontal load on structures of small dimensions.

Key: 1. reflected 3. side
 2. streamlined 4. rear

discontinuously from Δp_{front} to Δp_{refl} . At the same time, on the edges of the front wall as a result of the pressure difference in the incident and reflected waves, a rarefaction wave occurs, the propagation of which leads to a reduction in pressure on the wall from the value of p_{refl} to some value $p_{streamline}$ (Figure 19,a). The time from the beginning of reflection at the beginning of establishment of the streamlining conditions can be approximately [10] considered to be the least of the values.

$$t_{06r} = \frac{3h}{D_\phi} \text{ sec or } t_{06r} = \frac{3b}{2D_\phi} \text{ sec,} \tag{26}$$

(a)

Key: a. streamline

where h, b are the height and width (in meters) of the structure or part of it rising above ground level; D_ϕ is the propagation rate of the shock wave front defined by the formula

$$D_\phi = 340 \sqrt{1 + 0,83\Delta p_\phi} \text{ m/sec} \tag{27}$$

FOR OFFICIAL USE ONLY

FOR OFFICIAL USE ONLY

where Δp_ϕ is in kg/cm^2 .

Yu. B. Khariton [24] established that the streamlining pressure for $\Delta p_\phi \leq 4 \text{ kg}/\text{cm}^2$ is half the reflection pressure.

The magnitude of the maximum streamlining pressure considering the variation of the parameters of the infinite shock wave during the streamlining time can still be represented as follows:

$$\Delta p_{\text{str}} = \Delta p(t_{\text{str}}) + Q(t_{\text{str}}), \quad (28)$$

(a)

Key: a. streamlined

where $\Delta p(t_{\text{streamline}})$ and $Q(t_{\text{streamline}})$ are the excess pressure and the velocity head in the incident shock wave defined, respectively, by formulas (8) and (12) at the time $t_{\text{streamline}}$.

The sidewalls and the covering of the structure are completely loaded by the shockwave at the same time as the front travels a distance equal to the length of the structure l , that is, for $t_{\text{side}} = l/D_{\text{front}}$. The average pressure Δp_{side} on the walls and the covering at this point in time is assumed to be [21] equal to the excess pressure plus the braking load acting at the middle of the length of the structure, that is, at the distance $l/2$. The braking coefficient (resistance) for the side walls and the covering of the structure of rectangular shape is equal to 0.5; then

$$\Delta p_{\text{side}} = \Delta p_\phi(0,5t_{\text{side}}) - 0,5Q(0,5t_{\text{side}}), \quad (29)$$

(a)

Key: a. side

where the first term in the right-hand side is defined by formula (8) or (17), and the second term, by formula (12) for $t = 0,5 t_{\text{side}}$.

The average pressure on the side walls and the covering as a function of time is shown in the graph of Figure 19,b.

The load begins to act on the rear wall for the time t_{side} reaching the maximum value in the time t_{rear} (Figure 19,c) which is taken [21] equal to the least of the values:

$$t_{\text{rear}} = 4h/D_\phi \quad \text{or} \quad t_{\text{rear}} = 2b/D_\phi, \quad (30)$$

(a)

Key: a. rear

FOR OFFICIAL USE ONLY

FOR OFFICIAL USE ONLY

For the braking coefficient (resistance) on the rear wall equal to -0.5 , the maximum average pressure Δp_{rear} is determined at the time t_{rear} analogously to Δp_{side} :

$$\Delta p_{\text{TMn}} = \Delta p_{\phi}(t_{\text{TMn}}) - 0,5Q(t_{\text{TMn}}). \quad (31)$$

From investigation of the graphs in Figures 19,a and 19,b it is obvious that before complete loading of the rear wall by the shock wave, the significant pressure difference is observed on the front and rear walls of the structure. This difference in pressures creates a force which tries to shift the structure in the direction of the effect of the shock wave. This force is called the streamlining load [21]. The duration of the effect of the streamlining load is determined by the dimensions of the structure, and even for large structures it is only some proportion of the duration of the effect of the nuclear blast shock wave. After complete streamlining of the structure (barrier) by the shock wave, the braking phase begins (the steady streamlining regime). The resultant horizontal load which tries to shift the structure is represented in Figure 19,d,e in the form of a crosshatched region.

If one of the dimensions of the structure (barrier) is so small that a very short time is required for the shock wave to streamline around it, the effect of the streamlined loading can be neglected, and the shearing force defined as the load from the velocity head (the braking load). This case is presented in Figure 19,f. The resultant horizontal force F on the structure in this case will be determined by the magnitude of the velocity head $Q(t)$ and the shape of the structure characterized by the aerodynamic coefficient of frontal resistance c_x :

$$F = c_x Q(t) S; \quad (32)$$

where S is the area of the projection of the barrier on the surface normal to the direction of the velocity.

The values of the coefficient c_x are usually found experimentally.

Now let us consider the case where the shelter is built into a building.

If there are openings and holes in the enclosures of the building, the filling of which is easily destroyed and the shock wave penetrates inside, then the average loads are determined approximately [21] with the following prerequisites:

1) excess pressure inside the building increases from 0 to the maximum value in the time equal to the following: $t_{\text{zat}} = 2l/D_{\phi}$, where l is the length of the building in the direction of propagation of the wave; Δp_{zat} on the structural enclosures inside the building is defined by the formula (8) or (17) at the time t_{zat} ;

FOR OFFICIAL USE ONLY

FOR OFFICIAL USE ONLY

- 2) the velocity head inside the building is small and it can be neglected;
- 3) the effect of the openings and holes in the side walls on the pressure inside the building is not taken into account;
- 4) now it is not the value of h (or b), as in formulas (26) and (30) that is taken as the characteristic linear dimension for the front and rear walls, but the value of χ defined as the mean distance from the center of the investigated section of the wall to the edge of the opening or hole which must transmit the rarefaction wave on the front wall in order to decrease the reflected pressure to the magnitude of the streamlining pressure; then the streamlining pressure $t_{streamlining}$ and the buildup pressure $t_{background}$ of the pressure to a maximum on the rear wall are defined by the formulas:

$$\begin{aligned}
 t_{0\sigma r} &= 3\chi/D_{\phi}; & t_{\tau_{\text{вп}}} &= 4\chi/D_{\phi}. & (33) \\
 (a) & & (b) & (c) &
 \end{aligned}$$

Key: a. streamline b. front c. rear

In Figure 20 graphs are constructed for the average loads on the building with openings; it is proposed that the inside partitions are missing. The graphs of the load variation with time can be used both for inside and outside parts of the buildings. These graphs are easily approximated by the formulas and will permit determination of the load on the builtin shelters. For example, a load will act on the covering of the builtin shelter, the diagram of which is depicted by graph 2 in Figure 20, b.

The resultant horizontal load on the building is equal to the load difference on the front wall outside and inside minus the resultant load on the rear wall.

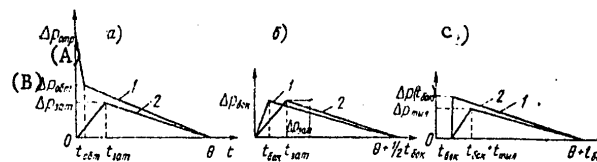


Figure 20. Average load diagrams for a building with openings. a -- on the front wall; b -- on the roof and side walls; c -- on the rear wall; 1 -- outside; 2 -- inside.

Key: A. refl B. streamline

Example 2. Let us find the excess pressure of the reflection at a distance $R = 1870$ m from the epicenter for a blast of $q = 1$ million tons at an altitude $H = 2000$ meters.

FOR OFFICIAL USE ONLY

FOR OFFICIAL USE ONLY

In accordance with the diagram in Figure 18, the distance to this blast center is

$$r_2 = \sqrt{H^2 + R^2} = \sqrt{2000^2 + 1870^2} = 2738 \text{ m.}$$

The angle of incidence will be found from the expression

$$\operatorname{tg} \alpha_0 = R/H = 1870/2000 = 0,935 \quad \alpha_0 \approx 43^\circ.$$

The pressure on the incident shock wave front will be defined by one of the formulas (6).

For the conditions of the example

$$\bar{R} = \frac{r_2}{\sqrt[3]{q}} = \frac{2738}{\sqrt[3]{10^9}} = 27,38 \text{ m/tons}^{1/3},$$

$$\Delta p_\phi = \frac{2,333}{(\sqrt{1 + 10^{-3} \cdot 27,38^3} - 1)} = 0,64 \text{ kg/cm}^2.$$

According to the graph in Figure 18 for an angle of incidence of 43° and $\Delta p_\phi = 64 \text{ kg/cm}^2$, by interpolation we find $\Delta p_{\text{refl}}/\Delta p_\phi \approx 2.8$. Hence,

$$\Delta p_{\text{отр}} = 2,8 \cdot 0,64 = 1,8 \text{ kg/cm}^2.$$

(a)

Key: a. refl

For normal reflection ($\alpha_0 = 0^\circ$) the reflection coefficient for $\Delta p_\phi = 0.64 \text{ kg/cm}^2$ is 2.5.

3. Loads on the Structures from Gas-Air Mixture Blasts

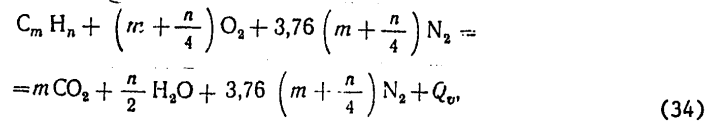
Intense evaporation of liquified gases and petroleum products takes place at oil refineries and chemical production plants as a result of destruction of the process equipment and reservoirs with the liquified hydrocarbon gases by the shock wave of a nuclear blast and the following fires. The vapor and fuel gases can form an explosive mixture with the air, the explosion of which leads to further destruction and the propagation of the fire over the territory of the enterprise. The analysis of the gas-air mixture (GVS) blasts at oil refineries [59] indicates that almost 2/3 of the blasts are accompanied by partial or complete destruction of the equipment and the structural elements. Thus, the shelters in the territory of such production facilities can be subjected to the secondary effect of dynamic loads from the GVS [gas-air mixture] blast.

The determination of the loads on the structures from the explosion of a mixture of hydrocarbon gases with air will be made with the following

FOR OFFICIAL USE ONLY

FOR OFFICIAL USE ONLY

prerequisites. Let us propose that as a result of construction of the process equipment and the reservoirs with the liquified hydrocarbon gases by the nuclear blast shock wave, a cloud of gas-air mixture was formed. The GVS concentration is assumed to be stoichiometric in accordance with the equation of the reaction of combustion (explosion) of the gas in the air which for the hydrocarbon of the type of $C_m H_n$ is expressed by the following general equation:



where Q_v is the heat of combustion at constant volume (or the heat of explosion); the procedure for calculating the heat of explosion of different materials is discussed in references [4, 7].

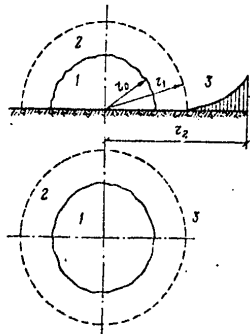


Figure 21. Diagram of an above ground explosion of gas-air mixture. 1 -- gas-air mixture cloud zone; 2 -- zone of expansion of blast products; 3 -- zone of effect of the air shock wave.

Let us take the idealized form of the GVS cloud as a hemisphere with the base on the earth's surface (see Figure 21), and let us propose that the initiation of the blast takes place at its center, from which the spherical detonation wave is propagated (the spherical detonation of the GVS is considered in references [12, 6]). In reality, the shape of the cloud can differ from the adopted shape, and the place of initiation of the blast can be quite different. Failure to consider these factors gives some reserve when estimating the effect of the blast on the structures which turn out to be in the GVS zone. For estimation of the effect of the blast beyond the limits of the GVS zone the shape of the cloud is not so significant [4, 7].

The analysis of emergencies at the oil refineries [59] shows that on destruction of the tanks not all of the products stored in the tanks in liquified state goes into the exploded gas-air mixture. Part of it (the lesser part) burns in the liquid and gaseous state. The transfer coefficient ($k_H < 1$) of the liquid product (hydrocarbon gases) from the reservoirs to the GVS

FOR OFFICIAL USE ONLY

FOR OFFICIAL USE ONLY

can be defined by the energy communicated to the air on explosion of the mixture.

The energy is determined from formulas (1) and (2) by the destructive loads (Δp_{des}) for structural designs of different types with known distances from the blast center. Then by the energy it is possible to determine the mass of the product in the GVS. The calculations show that the transfer coefficient of the liquified product to the GVS can be taken as $k_H \approx 0.8$.

For quantitative characteristic of the processes of detonation of the gas mixtures it is necessary to know the pressure on the detonation wave front ($p_D = \Delta p_D + p_1$), the detonation rate (D_D), the flow velocity (u_D), the density of the blast products (ρ_D). These values are determined by the known [7] formulas:

$$\left. \begin{aligned} \rho_D &= 2(k-1) \rho_0 q_v \cdot 10^{-4} \text{ kg/cm}^2; \\ D_D &= \sqrt{2(k^2-1)} q_v \text{ m/sec}; \\ u_D &= \frac{D_D}{k+1} \text{ m/sec}; \\ \rho_D &= \frac{(k+1)}{k} \rho_0 \text{ kg-sec}^2/\text{m}^4, \end{aligned} \right\} \quad (35)$$

where ρ_0 is the density of the exploded mixture in $\text{kg-sec}^2/\text{m}^4$; $k = c_p/c_v$ is the ratio of the heat capacities; q_v is the specific heat of the blast in units of mechanical work determined from the expression

$$q_v = \frac{Q_v \cdot 427g}{\sum n_i \mu_i} \text{ m}^2/\text{sec}^2, \quad (36)$$

in which Q_v is the heat of explosion in kcal; g is the gravitational acceleration; n_i is the number of kmoles of the i th material of the GVS; μ_i is the molecular mass of the i th material of the mixture.

In the approximate calculations of the parameters of the detonation wave front, it is admissible to take the ratio of the heat capacities for the products of explosion of the GVS $k = 1.25$ [4, 7].

The parameters of the detonation wave (D_D , u_D , Δp_D) for explosion of a stoichiometric mixture of certain hydrocarbon gases are presented in Table 4.

After the detonation wave front reaches the interface between the GVS and the medium (air), the dissipation of the detonation products begins. The

FOR OFFICIAL USE ONLY

FOR OFFICIAL USE ONLY

Table 4. Parameters of the explosion of a stoichiometric mixture of hydrocarbon gases with air

Material	Methane	Ethane	Propane	Butane	Pentane	Ethylene	Propylene	Butylene
	CH ₄	C ₂ H ₆	C ₃ H ₈	C ₄ H ₁₀	C ₅ H ₁₂	C ₂ H ₄	C ₃ H ₆	C ₄ H ₈
Chemical formula	CH ₄	C ₂ H ₆	C ₃ H ₈	C ₄ H ₁₀	C ₅ H ₁₂	C ₂ H ₄	C ₃ H ₆	C ₄ H ₈
Density of the mixture for 25° in kg-sec ² /m ⁴	0.115	0.124	0.123	0.124	0.125	0.12	0.121	0.122
Volume of the mixture for 25°C in m ³ /kg of material	16	14.3	13.8	13.4	13.25	13.3	15.2	16.2
Self-ignition temperature in °C at atmospheric pressure [58]	650	510	500	429	309	455	455	384
Specific heat of explosive conversion in kcal/kg of mixture	660	653	658	670	670	718	600	570
Blast temperature in °C [58]	2045	2100	2110	2120	2120	2285	2220	2200
Detonation rate in m/sec	1764	1754	1761	1777	1777	1839	1682	1639
Flow rate after the detonation wave front in m/sec	783	780	781	790	790	816	747	728
Speed of the GVS-air inter-face in m/sec	987	1000	1010	1020	1020	1040	960	940
Excess pressure in kg/cm ² at the detonation wave front	15.9	16.96	16.95	17.4	17.54	18.05	15.21	14.56
at the GVS-air inter-face	12.78	13.24	13.27	13.58	13.65	14.27	11.99	11.44

FOR OFFICIAL USE ONLY

FOR OFFICIAL USE ONLY

interface between the detonation products and the air will move faster than the detonation products, and from the very beginning of the process of expansion of the gas products the pressure in them will drop. The rarefaction wave travels with respect to the blast products; the shock wave travels through the air immediately entrained in the movement. The distances at which the effect of the blast products in products will not be felt on the air shock waves can be estimated by the approximate method used for condensed explosives [7]. Here it is proposed that the charge detonates simultaneously, that is, the detonation rate is not taken into account. Then in the detonation products with density equal to the initial density of the charge, there will be a mean pressure p_{ave} which is half the pressure at the detonation wave front.

On explosion of the cloud of gas-air mixture in an unlimited medium (air) the explosion products occupy some limited volume v_{∞} for sometime after the beginning of diffusion corresponding to the residual pressure of the environment p_1 . If the average initial pressure of the explosion products is equal to p_{ave} and the residual pressure $p_{\infty} = p_1$ for $v = v_{\infty}$, the limiting volume is determined from the law of expansion of the explosion products (if we consider them an ideal gas):

$$pv^k = p_1 v_1^k, \quad (37)$$

where $k = 1.25$ to 1.4 .

Hence,

$$v_{\infty}/v_0 = (p_{ave}/p_1)^{1/k}. \quad (38)$$

(a)

Key: a. ave

Here v_0 is the initial volume of the blast products equal to the volume of the GVS.

For the gas-air mixtures of propane or butane $p_{ave} = p_D/2 \approx 18/2 = 9 \text{ kg/cm}^2$ and their expressions (38), considering $p_1 = 1 \text{ kg/cm}^2$ will be obtained as follows:

$$\begin{aligned} \text{For } k = 7/5 \quad v_{\infty}/v_0 &= 9^{5/7} = 4.8; \\ \text{for } k = 5/4 \quad v_{\infty}/v_0 &= 9^{4/5} = 5.8. \end{aligned}$$

Consequently, the products of the explosion of the gas-air mixtures expand approximately 5 to 6 times, and not 800 to 1600 times as on explosion of ordinary explosives.

FOR OFFICIAL USE ONLY

FOR OFFICIAL USE ONLY

In the case of a spherical blast using GVS (see Figure 21) the maximum radius of the volume occupied by the blast products will be:

$$r^* \approx r_0 \sqrt[3]{5} = 1,7r_0,$$

where r_0 is the initial radius of the volume of the exploded gas-air mixture.

For the explosives such as TNT, the limiting radius of the volume occupied by the blast products is 10 times greater than the initial radius of the charge. The effect of the GVS blast products is limited to much smaller distances than when exploding ordinary explosives, but these distances can be expressed in hundreds of meters, for the initial radius of the GVS volume greatly exceeds the radius of the explosive charge on the basis of the fact that the GVS density is thousands of times less than the density of the standard explosives.

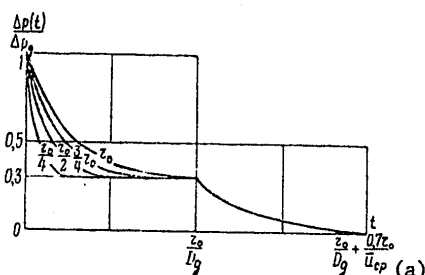


Figure 22. Variation of the excess pressure in time on different radii from the center of the hemisphere (see Figure 21) on exploding a cloud of gas-air mixture.

Key: a. ave

The surface of the base of the cloud of GVS (see Figure 21) on detonation of the mixture is under the effect of an excess pressure, the nature of the variation of which in time at different distances ($0, r_0/4, r_0/2, r_0$) from the center of the hemisphere is shown in Figure 22. The designation of u_{ave} on this figure corresponds to the mean value of the speed of the GVS-air interface when the blast products disperse. The time that the detonation wave front reaches a circle of the investigated radius is taken as the time origin.

From Figure 22 it is obvious that on approaching the outer boundary of the GVS cloud, elongation of the detonation wave in time takes place and that the duration of the effect of the effect of the loads from the detonation waves is different and depends on the radius. Consequently, the specific pulse on the base also depends on the radius of the investigated elementary area.

FOR OFFICIAL USE ONLY

FOR OFFICIAL USE ONLY

The integration of the functions presented in Figure 22 gives an approximate expression with the specific pulse

$$i = 0,43 \frac{\Delta p_n r_0}{D_n} (1 + 0,4r/r_0) \text{ kg-sec}^2/\text{m}^2 \quad (r \leq r_0)$$

or on substitution of the values of Δp_D and D_D by formulas (35) and $k = 1.25$

$$i = 0,2 r_0 \rho_0 \sqrt{q_0} (1 + 0,4r/r_0) \text{ kg-sec}^2/\text{m}^2 \quad (r \leq r_0). \quad (39)$$

On integration, the value of the average speed of the GVS-air interface was taken equal to the arithmetic mean value of the velocities at the beginning and at the end of dispersion of the blast products. Its magnitude for the mixtures of hydrocarbon gases (propane, butane, and so on) with air was approximately 0.4 of the detonation rate.

In order to simplify the solution of the equation of motion of a structural element under the effect of a load, let us take the triangle diagram for the calculations with the law of variation of the load analogous to expression (17):

$$\Delta p(t) = \Delta p_n (1 - t/\theta), \quad (40)$$

in which the effective time of effect θ is determined from the condition (13) by the expression

$$\theta \approx \frac{0,8r_0}{\sqrt{q_0}} (1 + 0,4r/r_0) \text{ sec} \quad (r \leq r_0). \quad (41)$$

For $q_v = 2.8 \cdot 10^6 \text{ m}^2/\text{sec}^2$ (GVS propane or butane), we obtain

$$\theta = 0,47 \cdot 10^{-3} r_0 (1 + 0,4r/r_0) \text{ sec} \quad (r \leq r_0). \quad (42)$$

The initial radius (r_0) of the hemisphere with gas-air mixture is determined by the formula

$$r_0 = 0,78 \sqrt[3]{w G_H} \text{ m}, \quad (43)$$

where w is the volume of the GVS of the stoichiometric composition obtained from 1 kg of the product, in m^3/kg ; the values of w are presented in Table 4;

G_H is the mass of the product in the gas-air mixture in kg.

On reflection of the detonation wave from the barrier (the structural element is arranged perpendicular to the direction of propagation of the detonation

FOR OFFICIAL USE ONLY

FOR OFFICIAL USE ONLY

wave) the pressure on the barrier exceeds Δp_D by approximately 2.5 times [7]. The law of variation of the pressure at the barrier on reflection can be represented in the form

$$\Delta p_{o,ip}(t) = 2,5\Delta p_n(1 - t/\theta), \quad (44)$$

(a)

Key: a. refl

where the effective operating time is defined by the expression

$$\theta = \frac{0,325r_0}{\sqrt{q_v}} (1 + 1,28r/r_0) \text{ sec } (r \leq r_0) \quad (45)$$

or on substitution of $q_v = 2.8 \cdot 10^6 \text{ m}^2/\text{sec}^2$,

$$\theta = 0,195 \cdot 10^{-3} r_0 (1 + 1,28r/r_0) \text{ sec } (r \leq r_0). \quad (46)$$

On expansion of the blast products after completion of the detonation process the shock wave travels from the GVS-air interface through the air. Figure 23 shows the pressure distribution shortly before arrival and immediately after arrival of the detonation wave at the GVS-air interface.

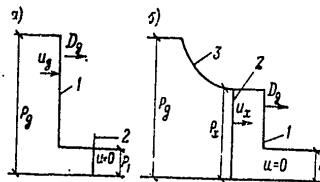


Figure 23. Wave parameters at the GVS-air interface: a -- before arrival; b -- after arrival of the detonation wave at the interface of the media; 1 -- shock wave; 2 -- interface of the media; 3 -- rarefaction wave.

Let us denote the following: p_x is the pressure at the interface of the media; u_x is the speed of the interface of the media; u_{shock} is the speed of the air after the front of the shockwave formed in it.

According to B. I. Shekhter [7], the pressure p_x is determined from the joint solution of two equations:

$$\left. \begin{aligned} u_x &= \frac{D_n}{k+1} \left\{ 1 + \frac{2k}{k-1} \left[1 - \left(\frac{p_x}{p_n} \right)^{(k-1)/(2k)} \right] \right\}; \\ u_x &= u_{yn} \approx \sqrt{\frac{2p_x}{(\gamma+1)\rho_a}} \end{aligned} \right\} \quad (47)$$

FOR OFFICIAL USE ONLY

FOR OFFICIAL USE ONLY

where γ is the isentropic index (the Poisson adiabatic curve) for air; ρ_a is the air density in front of the shock wave front.

The values of u_x and $\Delta p_x = p_x - 1$ are presented in Table 4.

In the dispersion zone of the detonation products of the gas-air explosive mixture limited to the radii $r_0 < r_1 \leq 1.7 r_0$, the pressure at the shock wave front can be determined by the formula obtained from the energy balance equation considering the natural energy of the air near the location of the blast [7]:

$$\Delta p = \frac{3(\gamma-1)\rho_0 q_v - 3p_1}{2} \left(\frac{r_0}{r_1}\right)^3 + \frac{p_1}{2} \text{ kg/m}^2 \quad (r_0 < r_1 \leq 1.7r_0), \quad (48)$$

where $\gamma = 1.25$ to 1.4 ; $p_1 = 10^4 \text{ kg/m}^2$.

For the standard GVS when $\rho_0 = 0.124 \text{ kg-sec}^2/\text{m}^4$ and $q_v = 2.8 \cdot 10^6 \text{ m}^2/\text{sec}^2$

$$\Delta p \approx 13 \left(\frac{r_0}{r_1}\right)^3 + 0.5 \text{ kg/cm}^2 \quad (r_0 < r_1 \leq 1.7r_0). \quad (49)$$

If $r_1 = r_0$, then $\Delta p = 13.5 \text{ kg/cm}^2$, which in practice coincides with the initial pressure Δp_x at the interface of two media calculated by equation (47).

Without presenting the intermediate calculations made by K. P. Stanyukovich, let us write in final form the relation determining the pulse flow for the dispersion zone of the explosion products running at a distance r_1 from the center of the GVS hemisphere:

$$i = 5.8 \cdot 10^{-3} \rho_0 r_0 \sqrt{q_v} \sqrt{\frac{r_0}{r_1}} \text{ kg-sec/m}^2 \quad (r_0 < r_1 \leq 1.7r_0). \quad (50)$$

For the calculated load diagram in the form of a triangle with maximum pressure by formula (48) the effective time is determined from the condition (13) with a pulse value with respect to the expression (50). For the standard GVS, the effective time is approximately equal to:

$$\theta \approx 1.82 \cdot 10^{-4} r_0 \sqrt{\left(\frac{r_1}{r_0}\right)^5} \text{ sec} \quad (r_0 < r_1 \leq 1.7r_0). \quad (51)$$

At distances of more than $1.7 r_0$, the shock wave is "separated" from the explosion products, the expansion of which for $r_2 = 1.7 r_0$ ends, and it begins its independent existence of them. Under these conditions the application of the point blast theory is possible [29], and, consequently, the pressure at the air shock wave front can be defined by formulas (1) and (2) or by the graph in Figure 24 for known distance r_2 from the blast center of the GVS and the amount Q of hydrocarbon gases in the storage tanks.

FOR OFFICIAL USE ONLY

FOR OFFICIAL USE ONLY

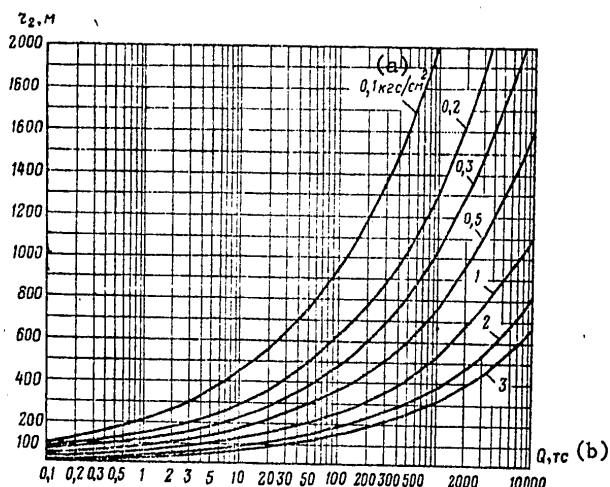


Figure 24. Graph for determining the pressure at the front of an air shock wave after the dispersion zone of the detonation products as a function of the amount of stored hydrocarbon gases (Q in tons) and a distance r_2 from the blast center of the gas-air mixture.

Key: a. kg/cm^2 b. Q, tons

The energy E_0 entering into the expression (3) for dimensionless radius of the shock wave is part of the total energy E_H released on explosion of the gas-air mixture, $E_0 = \eta E_H$ ($\eta < 1$); the rest is expended on radiation and other processes. The coefficient η is defined as follows. At the outer boundary of the dispersion zone of the blast products ($r_2 = 1.7r_0$) in accordance with (49) that the shock wave front $\Delta p_\phi \approx 3.2 \text{ kg/cm}^2$. Solving formula (1) with respect to E_0 for $\Delta p_\phi = 3.2 \text{ kg/cm}^2$ and considering $E_H = (2/3)\pi\rho_0 r_0^3 q_v$, we find that for $\rho_0 = 0.124 \text{ kg-sec}^2/\text{m}^4$ and $q_v = 2.8 \cdot 10^6 \text{ m}^2/\text{sec}^2$ the coefficient $\eta \approx 0.5$.

For the same values of ρ_0 and q_v expression (3) for the dimensionless shock wave radius assumes the form

$$R_2 = 0,24 r_2/r_0 (r_2 \geq 1,7 r_0). \tag{52}$$

The pressure pulse on the barrier arranged parallel to the direction of motion of the shock wave is defined by the approximate formula of G. Brode presented in reference [29]. Let us represent it in the form

FOR OFFICIAL USE ONLY

FOR OFFICIAL USE ONLY

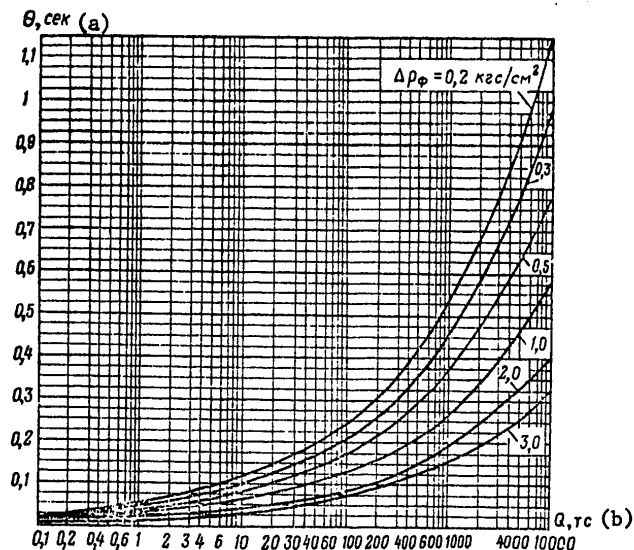


Figure 25. Effective time of effect of the air shock wave after the dispersion zone of the detonation products on explosion of the gas-air mixture.

Key: a. Q, sec b. Q, tons

$$i = 1,25 \frac{r_2}{R_2^2} \text{ kg-sec/m}^2 \quad (R_2 \geq 0,5). \tag{53}$$

Then the effective time of the effect of the shock wave will be:

$$\theta = \frac{2i}{\Delta p_\phi} 10^{-4} = \frac{2,5r_2 10^{-4}}{\Delta p_\phi R_2^2} \text{ sec}, \tag{54}$$

where Δp_ϕ in kg/cm^2 is defined by the formulas (1) and (2) as a function of the value of R_2 . This time can be determined also by the graph in Figure 25 as a function of r_2 and Q .

Thus, for the above-investigated prerequisites of the load on the structures from the explosion of a stoichiometric mixture of hydrocarbon gases with air (of the type indicated in Figure 4) depend primarily on the zone (see Figure 21) in which the structure is located and the distance r to the blast center.

Example 3. Let us determine the parameters of the dynamic loads on the structures located at different distances from the blast center of the GVS cloud formed on destruction of a tank with 1000 tons of liquid propane.

FOR OFFICIAL USE ONLY

FOR OFFICIAL USE ONLY

The radius of the GVS cloud zone by formula (43) for $w = 13.8 \text{ m}^3/\text{kg}$ (see Table 4) and $G_H = 0.8 \cdot 1000 \cdot 10^3 = 8 \cdot 10^5 \text{ kg}$ will be

$$r_0 = 0.78 \sqrt[3]{13.8 \cdot 8 \cdot 10^5} = 179 \text{ m.}$$

The limiting radius of the dispersion zone of the blast products $r_1 = 1.7 \times 179 = 304 \text{ m}$.

According to Table 4 the pressure at the detonation wave front $\Delta p_D = 16.95 \text{ kg/cm}^2$.

The effective operating time of this pressure at a distance $r = 150 \text{ m}$ will be found by the formula (42):

$$\theta = 0.47 \cdot 10^{-3} \cdot 179 (1 + 0.4 \cdot 150/179) = 0.112 \text{ sec.}$$

For normal reflection of the detonation wave from the barrier the pressure on the barrier increases by 2.5 times, that is, $\Delta p_{\text{refl.D}} = 2.5 \cdot 16.95 = 42.4 \text{ kg/cm}^2$, and the effective time of effect for $r = 150$ meters by formula (46) is: $\theta_{\text{refl}} = 0.195 \cdot 10^{-3} \cdot 179 (1 + 1.28 \cdot 150/179) = 0.072 \text{ sec}$. In the dispersion zone of the detonation products of the GVS at a distance $r = 250 \text{ m}$ the pressure at the front and the effective time of the effect of the shock wave by formulas (49) and (51) will be equal to:

$$\Delta p = 13 (179/250)^2 + 0.5 = 4.76 + 0.5 = 5.26 \text{ kg/cm}^2;$$

$$\theta = 1.82 \cdot 10^{-4} \cdot 179 \sqrt{(250/179)^3} = 0.114 \text{ sec.}$$

At the boundary of the dispersion zone of the detonation products, that is for $r = r_1 = 304 \text{ m}$, by the same formulas we find:

$$\Delta p = 13 (179/304)^2 + 0.5 = 3.2 \text{ kg/cm}^2$$

$$\theta = 1.82 \cdot 10^{-4} \cdot 179 \sqrt{(304/179)^3} = 0.123 \text{ sec.}$$

The parameters of the air shock wave at a distance from the blast center of $r_2 = 500$ meters (beyond the dispersion zone of the blast products) for the dimensionless radius of the shock wave by the formula (52) $R_2 = 0.24 \cdot 500/179 = 0.67$ will be determined from the expressions (1) and (54):

$$\Delta p_{\phi} = \frac{7}{3(\sqrt{1+29.8 \cdot 0.67^3} - 1)} = \frac{7}{3 \cdot 2.15} = 1.08 \text{ kg/cm}^2;$$

$$\theta = \frac{2.5 \cdot 500 \cdot 10^{-4}}{1.08 \cdot 0.67^2} = 0.278 \text{ sec.}$$

An analogous result was obtained by the graphs in Figures 24 and 25.

FOR OFFICIAL USE ONLY

FOR OFFICIAL USE ONLY

CHAPTER III. CALCULATION OF REINFORCED CONCRETE FLOORS, CEILINGS AND WALLS ON THE EFFECT OF AIR SHOCK WAVES

1. General Principles

The enclosing structures of the shelters must have the required strength and stability so that they can take the effect of the pressures occurring during the blasts. Usually these pressures increase in a small time interval such that the forces of inertia occurring during movement of the structures will turn out to be significant. Therefore the effect of the blast waves is considered as the effect of dynamic loads (short term), and the structural elements are calculated by the methods of structural dynamics. Here the air shock waves cause dynamic loads which usually can be considered not to depend on the deformations of the structures, and the waves traveling to the structure through the ground create loads which depend on the movement of the entire structure and deformations of its structural element.

Let us consider the basic operating requirements imposed on the shelters.

Very frequently such structures have a special operating requirement imposed on them -- the shelter structural elements must withstand the one-time effect of a load without collapsing. Large residual deformations and displacements can occur in the structures which in reinforced concrete and stone structures are accompanied by strongly developed cracks. The construction material in the most stressed cross sections is almost destroyed, as a result of which such structures can become unsuitable for further normal use, but they will save the lives of people in the shelters. At the same time the complete use of the strength characteristics of the materials will permit us to obtain the most economical structural designs of the shelters.

Similar requirements can also be imposed on ordinary structures erected in seismically dangerous areas.

In accordance with the indicated operating requirement, the specific state is formulated as follows: the achievement of the specific state leads to destruction of the structural element. This limiting state can be called the limiting state with respect to the total bearing capacity.

FOR OFFICIAL USE ONLY

FOR OFFICIAL USE ONLY

Sometimes increased strength requirements are imposed on the structural elements of the shelters; the structure must take the multiple effect of short term loads; under a single effect of a load residual deformations must not occur in the structure, and all of the cracks must be closed after the load effect ends. For such structures the special requirement consists in the fact that residual deformations and displacements should not occur in the structure, but in this case there are no restrictions on the magnitudes of the displacements. Under the effect of the load, cracks can develop in the structure (for example, in the elongated concrete zone of a reinforced concrete beam), after the closure of which the formation of insignificant residual deformations is possible; these deformations can be ignored.

In accordance with these requirements, the limiting state is determined as follows: the achievement of the limiting state is characterized by the occurrence of residual deformations in the material of the structure.

Inasmuch as insignificant residual deformations still are permitted, this limiting state can be mentioned as the limiting state with respect to absence of large residual deformations.

Later we shall use the following names for the introduced limiting states: the limiting state with respect to the total bearing capacity is state la; the limiting state with respect to absence of large residual deformations, state lb.

The dynamic methods of calculating the structural elements in the plastic stage, the principles of which were set down in the papers by A. A. Gvozdev [15] and I. M. Rabinovich [50] have been widely developed at the present time. The application of these methods to the calculation of various structures is discussed in many papers [16, 22, 43, 48, 52, 57]. The experimental data on the effect of the loading speed on the strength characteristics of the materials are presented in references [6, 9, 13, 18, 30, 31, 67].

2. Calculation of the Structural Elements in the Elastic Stage

The deformation of the elastic structures is described by linear partial differential equations which are solved considering the boundary conditions determined by the type of supporting reinforcements.

The derivation of these equations and the methods of solving them are discussed in various courses with respect to structural dynamics [5, 34, 51, 61].

When calculating the structural designs for the effect of short term loads it is expedient to solve the equations of motion by the Bubnov-Galerkin method [42]; it is possible to take the static form as the form of the bending.

Let us consider beam structures. The equation of the vibrations of a beam of constant rigidity, as is known [61], has the form

FOR OFFICIAL USE ONLY

FOR OFFICIAL USE ONLY

$$B \frac{\partial^4 w}{\partial x^4} + m \frac{\partial^2 w}{\partial t^2} = p(x, t), \quad (1)$$

where B is the bending rigidity of the beam; m is the mass of the beam per unit length; p(x, t) is the load per unit length; w(x, t) is the bending of the beam.

The bending moment and the transverse force are determined from the expressions

$$M = -B \frac{\partial^2 w}{\partial x^2}; \quad Q = -B \frac{\partial^3 w}{\partial x^3}. \quad (2)$$

Let us propose that the dynamic load can be represented in the form

$$p(x, t) = p f_1(x) f(t), \quad (3)$$

where p is a fixed (frequently the largest) value of the dynamic load; $f_1(x)$, f(t) are functions characterizing the load variation with respect to this band in time.

For bending of the beam we shall take the expression

$$w(x, t) = p F(x) T(t), \quad (4)$$

where the function F(x) (the form of the bends) is equal to the beam displacements from the effect of the static load with an intensity $f_1(x)$. The function F(x) is determined obviously from the solution of the equation

$$BF^{IV}(x) = f_1(x) \quad (5)$$

and must satisfy defined boundary conditions at the ends of the beam which depend on the type of supporting reinforcements. The function T(t) describing the variation in time of the displacement of the structure usually is called the dynamicity function. When calculating the structure in the elastic stage its largest value has the basic significance. It will be interpreted as the dynamicity coefficient in the elastic stage.

Substituting (4) in equation (1), we obtain the error

$$L(x, t) = p [T(t) f_1(x) + m \ddot{T}(t) F(x) - f_1(x) f(t)]. \quad (6)$$

From the condition $\int_0^l L(x, t) F(x) dx = 0$ we find the equation for the function T(t);

FOR OFFICIAL USE ONLY

FOR OFFICIAL USE ONLY

$$\ddot{T}(t) + \omega^2 T(t) = \omega^2 f(t), \tag{7}$$

where

$$\omega^2 = \frac{\int_0^l f_1(x) F(x) dx}{m \int_0^l F^2(x) dx} \tag{8}$$

The value of ω is a parameter similar to the angular frequency of the vibrations of the structure corresponding to the dynamic load of the type of (3). It is convenient to use equation (7) in dimensionless form. If we set

$$s = \omega t, \quad y(s) = T\left(\frac{s}{\omega}\right), \tag{9}$$

we shall have

$$\frac{d^2 y}{ds^2} + y = f\left(\frac{s}{\omega}\right). \tag{10}$$

Let us consider some examples. The load distribution with respect to the beam span will be taken as uniform, that is, $f_1(x) = 1$, and the bending function $F(x)$ is found from the equation

$$BF^{IV}(x) = 1. \tag{11}$$

For the beam with hinge-supported ends the boundary conditions will be as follows: for $x = 0$ and $x = l$, $F = 0$, $F'' = 0$. From (11) we find

$$F(x) = \frac{1}{12B} \left(\frac{x^4}{2} - lx^3 + \frac{l^2 x^2}{2} \right) \tag{12}$$

and from (8) we shall have

$$\omega = \frac{12\sqrt{21}}{\sqrt{31}l^2} \sqrt{\frac{B}{m}} = \frac{9,876}{l^2} \sqrt{\frac{B}{m}} \tag{13}$$

For the beam with rigidly clamped ends the following must occur: for $x = 0$ and $x = l$, $F = 0$, $F' = 0$. In this case we obtain:

$$F(x) = \frac{1}{12B} \left(\frac{x^4}{2} - lx^3 + \frac{l^2 x^2}{2} \right); \tag{14}$$

$$\omega = \frac{6\sqrt{14}}{l^2} \sqrt{\frac{B}{m}} = \frac{22,45}{l^2} \sqrt{\frac{B}{m}} \tag{15}$$

The forces in the beam will be equal to the product of the forces from the static load $pf_1(x)$ on the function $T(t)$. Thus, the dynamic calculation of the structure reduces to solving equation (7), the dependence of which on the

FOR OFFICIAL USE ONLY

FOR OFFICIAL USE ONLY

properties of the structure is manifested only in the magnitude of the frequency ω . In the investigated examples the frequencies of the beam oscillations (13) and (15) almost coincide with the lower frequencies of its natural vibrations corresponding with respect to boundary conditions and equal respectively to the following [61]:

$$\omega = \frac{\pi^2}{l^2} \sqrt{\frac{B}{m}}; \quad \omega = \frac{22,37}{l^2} \sqrt{\frac{B}{m}}. \quad (16)$$

This is explained by the fact that the static form of the bends is close to the form of the beam oscillation with lower frequency.

The indicated fact can be used for approximate dynamic calculations of a quite broad class of structures (continuous beams, frames, arches) and especially when calculating the structural designs for which the static form of the bends is in closed form (for example, slabs). The conditions and the displacements are determined by multiplying some of their static values assumed, for example, in accordance with the reference data, times the dynamicity function $T(t)$ determined from equation (7). The value of ω can be taken equal to the frequency of the natural vibrations corresponding to the form of the oscillations which is close to the static form of the displacement of the structure from the load distributed over the surface of the structure analogously to the dynamic load.

The values of the frequencies of the natural vibrations can be taken from various courses in oscillation theory or from the instructions [27].

It is necessary to consider that this calculation is used for the structures, the displacements of which can be represented by an expression of the type of (4). This calculation is inapplicable for structures, the deformation of which takes place as a result of the superposition of various stressed states just as, for example, the open cylindrical shells experiencing a complex stressed state.

Let us write out the values of the dynamicity function $T(t)$ for three laws of variation of load with time corresponding to different conditions of the effect of the wave on the structural element (Chapter II):

$$a) \rho(t) = \rho \left(1 - \frac{t}{\theta}\right); \quad f(t) = 1 - \frac{t}{\theta} \quad (\text{see Figure 16, the straight line 2}); \quad (17)$$

$$T(t) = 1 - \frac{t}{\theta} - \cos \omega t + \frac{\sin \omega t}{\omega \theta} \quad (0 \leq t \leq \theta). \quad (18)$$

The dynamicity coefficient will be equal to: $k_D = T(t_m)$, where t_m is the time that the function $T(t)$ reaches the largest value. The time t_m is found from the equation

FOR OFFICIAL USE ONLY

FOR OFFICIAL USE ONLY

$$\hat{T}(t) = -\frac{1}{\theta} + \omega \sin \omega t + \frac{\cos \omega t}{\theta} = 0, \quad (19)$$

from which [51]

$$\omega t_m = 2 \operatorname{arctg} \omega \theta \quad (20)$$

and

$$k_n = 2 \left(1 - \frac{\operatorname{arctg} \omega \theta}{\omega \theta} \right). \quad (21)$$

Formula (21) is valid for $\omega \theta \geq 2.33$, for then

$$\omega t_m \leq \omega \theta. \quad (22)$$

For $\omega \theta > 200$ it is possible to set $k_D = 2$.

$$6) \quad p(t) = \begin{cases} p \frac{t}{\theta_1} & 0 \leq t \leq \theta_1; \\ p \left(1 - \frac{t - \theta_1}{\theta_2} \right) & \theta_1 \leq t \leq \theta_1 + \theta_2 = \theta \quad (\text{see Figure 19, b}); \end{cases} \quad (23)$$

$$T(t) = T_1 = \frac{t}{\theta_1} - \frac{\sin \omega t}{\omega \theta_1}; \quad 0 \leq t \leq \theta_1; \quad (24)$$

$$T(t) = T_2 = 1 - \frac{t - \theta_1}{\theta_2} + \left(\frac{1}{\omega \theta_1} + \frac{1}{\omega \theta_2} \right) \sin \omega (t - \theta_1) - \frac{\sin \omega t}{\omega \theta_1}; \quad \theta_1 \leq t \leq \theta. \quad (25)$$

The dynamicity coefficient for $\theta_2 = \infty$ is:

$$k_n = 1 + \frac{2 \left| \sin \frac{\omega \theta_1}{2} \right|}{\omega \theta_1}. \quad (26)$$

$$e) \quad p(t) = \begin{cases} p \left(1 - \frac{t}{\bar{\theta}_1} \right) & 0 \leq t \leq \bar{\theta}_1, (p = p_{\text{opt}}); \\ p_{\text{opt}} \left(1 - \frac{t - \bar{\theta}_1}{\bar{\Delta}} \right) & \bar{\theta}_1 \leq t \leq \bar{\theta}_1 + \bar{\Delta} = \theta; \end{cases} \quad (27)$$

(see Figure 19, a)

$$\bar{\theta}_1 = \frac{\theta_1}{1 - \bar{\Delta}}; \quad \bar{\Delta} = \frac{(b) p_{\text{opt}}}{p_{\text{opt}}} < 1;$$

(a)

Key: a. refl
b. streamline

FOR OFFICIAL USE ONLY

FOR OFFICIAL USE ONLY

$$T(t) = T_1 = 1 - \frac{t}{\bar{\theta}_1} - \cos \omega t + \frac{\sin \omega t}{\omega \bar{\theta}_1} \quad 0 \leq t \leq \theta_1; \quad (28)$$

$$T(t) = T_2 = \left(1 - \frac{t - \theta_1}{\bar{\theta}_2}\right) \bar{\Delta} + [\alpha_1 \sin \omega(t - \theta_1) - \alpha_2 \cos \omega(t - \theta_1)]; \quad \theta_1 \leq t \leq \theta,$$

where

$$\alpha_1 = \sin \omega \theta_1 - \frac{1 - \cos \omega \theta_1}{\omega \bar{\theta}_1} + \frac{\bar{\Delta}}{\omega \theta_2};$$

$$\alpha_2 = \cos \omega \theta_1 - \frac{\sin \omega \theta_1}{\omega \bar{\theta}_1}.$$

The dynamicity coefficient will be:

for

$$\omega \theta_1 \geq 2 \operatorname{arctg} \omega \bar{\theta}_1 \quad (29)$$

$$k_x = 2 \left(1 - \frac{\operatorname{arctg} \omega \bar{\theta}_1}{\omega \bar{\theta}_1}\right); \quad (30)$$

for

$$\omega \theta_1 < 2 \operatorname{arctg} \omega \bar{\theta}_1 \quad (31)$$

$$k_x = \left(1 - \frac{t^* - \theta_1}{\bar{\theta}_2}\right) \bar{\Delta} + [\alpha_1 \sin \omega(t^* - \theta_1) - \alpha_2 \cos \omega(t^* - \theta_1)], \quad (32)$$

where the value of t^* is found from the expression

$$\operatorname{tg} \frac{\omega(t^* - \theta_1)}{2} = \frac{\alpha_2 + \sqrt{\alpha_2^2 + \alpha_1^2 - \frac{\bar{\Delta}^2}{(\omega \bar{\theta}_2)^2}}}{\alpha_1 + \frac{\bar{\Delta}}{\omega \theta_2}}. \quad (33)$$

Figure 26 shows the graphs of the dynamicity coefficients for the load of the type of (27) for $\bar{\Delta} = 0.5$.

For $\bar{\Delta} = 0.5$ the conditions (29) and (31) are equivalent, respectively, to the following:

$$\omega \theta_1 \geq 2, 785; \quad \omega \theta_1 < 2, 785. \quad (34)$$

FOR OFFICIAL USE ONLY

FOR OFFICIAL USE ONLY

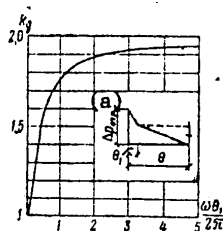


Figure 26. Dynamicity coefficient in the elastic stage (load with streamlining).

Key: a. refl

3. Dynamic Strength of Reinforcing Steel and Concrete

At the present time in the structural elements the low-carbon steel, classes A-I (St3), A-II (St5), A-III (35GS) are the most widely used. The experimental results, for example [18, 31, 67] indicate the significant effect of the deformation rate on the strength characteristics of these steels. Then when calculating the structural elements reinforced by such steel, for determination of the dynamic yield point we shall use the criterion proposed by D. Campbell [72] in the same form as it is presented in reference [32]. In it, for the case of a uniaxial stressed state for a known law of variation of the stress in the elastic stage $\sigma(t)$, the dynamic yield point will be taken equal to:

$$\sigma_d = \sigma(\tau), \tag{35}$$

where τ is the delay time of the plastic deformations (the time of the end of the elastic stage) determined from the equation

$$\int_0^{\tau} [\sigma(t)]^\alpha dt = t_0 \sigma_0^\alpha \text{ for } [\sigma(\tau) > \sigma_0] \tag{36}$$

and the condition that during some time interval $\sigma(t) > \sigma_0$. Here σ_0 is the magnitude of the static yield point of the steel, t_0 and α are certain parameters which depend on the properties of the steel and on the temperature.

The parameter t_0 is equal to the delay time for the case where the stress is applied instantaneously and is equal to the static yield point. On the basis of processing the experimental data in reference [32], the values of the parameters are obtained for the steels of classes A-I and A-II for room temperature: $\alpha = 17$, $t_0 = 0.895$ sec. For the class A-III steel, the effect of the deformation rate is somewhat less than for the class A-I and A-II steel. For practical calculations this can be considered by decreasing the magnitude of the calculated resistance for the class A-III steel (by 5-10%).

FOR OFFICIAL USE ONLY

FOR OFFICIAL USE ONLY

The expression for the stress in the reinforcing $\sigma(t)$ in the elastic stage can be represented in the form

$$\sigma(t) = \sigma_c T(t), \quad (37)$$

where σ_c is the stress from the load applied statistically and equal to some magnitude of the dynamic load;

$T(t)$ is the dynamicity function.

From (36) and (37) it follows that

$$\int_0^{\tau} [T(t)]^\alpha dt = t_0 \left(\frac{\sigma_0}{\sigma_c} \right)^\alpha. \quad (38)$$

When using the exact expression for $T(t)$ a solution of this equation is frequently difficult and possible only with the application of numerical integration. However, in many cases the procedure based on the replacement of the function $T(t)$ in the interval $(0, \tau)$ by linear functions gives sufficient accuracy.

For the case of the load of the type of (17) we set $T(t) = kt$. The coefficient k and the delay time τ are found from (38) and the condition $k\tau = T(\tau)$.

Excluding k , we obtain the following equation for determining τ :

$$[t_0(\alpha + 1)]^{\frac{1}{\alpha}} \frac{\sigma_0}{\sigma_c} = \tau^{\frac{1}{\alpha}} T(\tau). \quad (39)$$

For the steels of classes A-I, A-II, A-III we have

$$1,1776 \frac{\sigma_0}{\sigma_c} = \tau^{1/17} T(\tau). \quad (40)$$

From (39) and (40) we have the dynamic yield point $\sigma_D = \sigma_c T(\tau)$ as a function of the time it is reached:

$$\begin{aligned} \sigma_x &= [t_0(\alpha + 1)]^{\frac{1}{\alpha}} \tau^{-\frac{1}{\alpha}} \sigma_0; \\ \sigma_x &= 1,1776 \tau^{-1/17} \sigma_0 \quad (\tau \text{ in seconds}) \end{aligned} \quad (41)$$

Let us find the expression for the dynamic yield point which occurs in the structural reinforcing when the stress reaches the maximum, that is, for $\tau = t^*$, when

$$\left. \frac{d\sigma}{dt} \right|_{t=t^*} = 0.$$

For $t > t^*$ the stress decreases, as a result of which only negligibly small plastic deformations can occur in the reinforcing and it is possible to

FOR OFFICIAL USE ONLY

FOR OFFICIAL USE ONLY

consider that the structure still has not reached the elastic stage. We shall consider the stress equal to σ_* = $\sigma(t^*)$ the minimum dynamic yield point.

Let an instantaneously increasing dynamic load that is constant in time (that is, $\theta = \infty$) act on the structure. Then, as follows from (18),

$$T(t) = 1 - \cos \omega t \quad \text{and} \quad t^* = \frac{\pi}{\omega}$$

and from (38) for this case we obtain the exact solution

$$t_0 \left(\frac{\sigma_t}{\sigma_0} \right)^\alpha = \int_0^{\pi/\omega} (1 - \cos \omega t)^\alpha dt = 2 \int_0^{\pi/2} \sin^{2\alpha} \frac{\omega t}{2} dt = \frac{2}{\omega} \int_0^{\pi/2} \sin^{2\alpha} x dx. \quad (42)$$

The last integral is calculated exactly for the given value of α :

$$I = \int_0^{\pi/2} \sin^{2\alpha} x dx = \frac{(2\alpha-1)!!}{2\alpha!!} \cdot \frac{\pi}{2}.$$

From (42) we find the maximum value of σ_c (let us denote it $\bar{\sigma}_c$), for which the structure operates only in the elastic stage:

$$\bar{\sigma}_c = \frac{(\omega t_0)^{1/\alpha} \sigma_0}{2^{1/\alpha} \Gamma^{1/\alpha}}. \quad (43)$$

The minimum dynamic yield point is:

$$\sigma_* = 2\bar{\sigma}_c = (2I)^{-1/\alpha} (\omega t_0)^{-1/\alpha} \sigma_0, \quad (44)$$

from which for $\alpha = 17$ we have

$$\sigma_* = 1,0513 (\omega t_0)^{1/17} \sigma_0; \quad \bar{\sigma}_c = 0,5256 (\omega t_0)^{1/17} \sigma_0 \quad (45)$$

and for $t_0 = 0.895$ sec

$$\sigma_* = 1,0445 \omega^{1/17} \sigma_0 \quad (46)$$

(here ω is understood as the dimensionless variable $\omega \cdot 1$ sec).

In order to facilitate the use of formulas (45) and (46), the graph of the function $\omega^{1/17}$ is constructed in Figure 27.

If we set $\tau = t^* = \pi/\omega$ in formula (41), we obtain

$$\sigma_* = 1,1 \omega^{1/17} \sigma_0. \quad (47)$$

FOR OFFICIAL USE ONLY

FOR OFFICIAL USE ONLY

The comparison with (46) shows that the approximate method of determining the dynamic yield point gives an error of ~5%.

Now let us consider the effect of the load of the type of (17). For it, the function $T(t)$ and its maximum are defined by formulas (18) and (21).

If we substitute (18) in equation (38), then it is difficult to solve the equation. Therefore we replace (18) by the following expression:

$$T^*(t) = \left(1 - \frac{\text{arctg } \omega \theta}{\omega \theta}\right) (1 - \cos \omega^* t), \quad (48)$$

where ω^* is determined from the condition of the maximum $T^*(t)$, that is, $\omega^* t_{\text{max}} = \pi$, or considering (20)

$$\omega^* = \frac{\pi}{t_{\text{max}}} = \frac{\pi \omega}{2 \text{arctg } \omega \theta} = \delta \omega; \quad \delta = \frac{\pi}{2 \text{arctg } \omega \theta}. \quad (49)$$

Key: a. max

The functions (18) and (48) assume equal maximum values at the same point in time, and therefore the values of the integrals from them in (38) will be close. The values of σ_* will be found from (45) and (46), replacing ω by ω^* . We obtain:

$$\sigma_* = 1,0513 (\omega t_0)^{1/17} \delta^{1/17} \sigma_0; \quad (50)$$

$$\sigma_* = 1,0445 \omega^{1/17} \delta^{1/17} \delta_0 \quad (t_0 = 0,895 \text{ sec}). \quad (51)$$

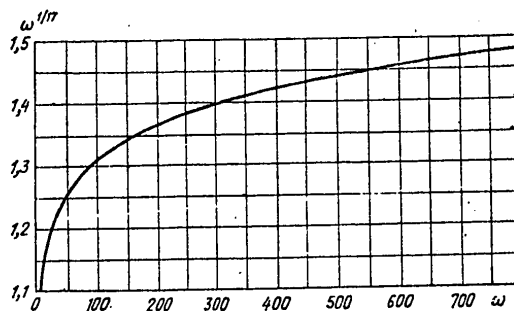


Figure 27. Graph of the function $\omega^{1/17}$

For " $\theta > 5$ " it is possible to set $\delta^{1/17} = 1$. Here the error will be less than 1%.

FOR OFFICIAL USE ONLY

FOR OFFICIAL USE ONLY

The maximum value of $\bar{\sigma}_c$ for which the structural element still operates in the elastic stage will be found from the expression

$$\sigma_* = 2 \left(1 - \frac{\text{arc tg } \omega \theta}{\omega \theta} \right) \bar{\sigma}_0.$$

Hence, considering (50) and (51) we shall have

$$\bar{\sigma}_0 = \frac{0,5256 (\omega t_0)^{1/17} \delta^{1/17} \sigma_0}{1 - \frac{\text{arc tg } \omega \theta}{\omega \theta}}; \quad (52)$$

for $\alpha = 17$, $t_0 = 895$ sec

$$\bar{\sigma}_0 = \frac{0,5222 \omega^{1/17} \delta^{1/17} \sigma_0}{1 - \frac{\text{arc tg } \omega \theta}{\omega \theta}}. \quad (53)$$

Let us consider the effect of the dynamic load of the type of (23).

The minimum dynamic ultimate strength can be reached only for $t > \theta_1$ when a decrease in the load occurs. Therefore the time of its occurrence will be equal to the time t^* at which the function $T_2(t)$ reaches the first maximum.

From expression (38) we have the following equation:

$$t_0 \left(\frac{\sigma_0}{\bar{\sigma}_0} \right)^\alpha = \int_0^{\theta_1} [T_1(t)]^\alpha dt + \int_{\theta_1}^{t^*} [T_2(t)]^\alpha dt. \quad (54)$$

In order that it be possible to obtain the analytical function from (54), let us replace the functions (24), (25) by linear functions. Let us set

$$\bar{T}_1(t) = k_1 \frac{t}{\theta_1}, \quad (55)$$

where k_1 is found from the equality $\bar{T}_1(\theta_1) = T_1(\theta_1)$, that is,

$$k_1 = 1 - \frac{\sin \omega \theta_1}{\omega \theta_1} \quad \text{and} \quad \bar{T}_1(t) = \left(1 - \frac{\sin \omega \theta_1}{\omega \theta_1} \right) \frac{t}{\theta_1}. \quad (56)$$

The function $T_2(t)$ is replaced by

$$\bar{T}_2(t) = T_1(\theta_1) + k_2 (t - \theta_1), \quad (57)$$

where k_2 will be found from the equality $\bar{T}_2(t^*) = T_2(t^*)$, that is

$$k_2 = \frac{1}{(t^* - \theta_1)} [T_2(t^*) - T_1(\theta_1)].$$

Let us substitute the linear approximations (56) and (57) in (54) in place of T_1 and T_2 , and after integration we obtain

FOR OFFICIAL USE ONLY

$$t_0 \left(\frac{\sigma_0}{\bar{\sigma}_c} \right)^\alpha = \frac{1}{(\alpha + 1)} \left\{ \theta_1 [T_1(\theta_1)]^\alpha + (t^* - \theta_1) \frac{[T_2(t^*)]^{\alpha+1} - [T_1(\theta_1)]^{\alpha+1}}{T_2(t^*) - T_1(\theta_1)} \right\}. \quad (58)$$

Hence, for $\alpha = 17$ and $t_0 = 0.895$ we find

$$\bar{\sigma}_c = \frac{1,1776 \omega^{1/17} \sigma_0}{R(\omega t^*)}, \quad (59)$$

where

$$R(\omega t^*) = \left\{ \omega \theta_1 [T_1(\theta_1)]^{17} + (\omega t^* - \omega \theta_1) \frac{[T_2(t^*)]^{18} - [T_1(\theta_1)]^{18}}{T_2(t^*) - T_1(\theta_1)} \right\}. \quad (60)$$

It is obvious that $\sigma_* = \bar{\sigma}_c T_2(t^*)$.

Let us note that the maximum "elastic" value of $\bar{\sigma}_c$ is characterized by the following conditions: for $\sigma_c > \bar{\sigma}_c$, plastic deformations occur in the reinforcing; for $\sigma_c \geq \bar{\sigma}_c$ the reinforcing operates in the elastic stage, but here the stresses can exceed the static yield point.

Inasmuch as the value of $\bar{\sigma}_c$ corresponds to stress in the reinforcing equal to the minimum dynamic yield point σ_* , this stress σ_* must be taken as the limit when calculating the structural designs by the limiting state lb).

Let us briefly touch on the problem of the effect of the deformation rate on the stress-strain state of the concrete [6, 30]. The increase in loading rate leads to an increase in the ultimate strength of the concrete and the change in its σ - ϵ deformation diagram. A characteristic feature of the dynamic σ - ϵ diagrams is their approximation to the linear diagram ($\sigma = E\epsilon$) as the deformation rate increases. This fact is explained by a decrease in the role of the plastic deformations during fast loading.

Therefore when calculating the reinforced concrete structural elements for the effect of short term dynamic loads, the determination of the moments of the internal forces will be correctly made beginning with the triangular stress diagram in the compressed zone of the concrete. This especially pertains to the calculation of the structural elements in the elastic stage (by the limiting state of lb).

The effect of the loading rate on the concrete strength can be considered with sufficient accuracy by increasing the calculated values of the stresses in the concrete by 20-30% [6].

4. Characteristic Limited States of Bent Structural Elements

The limiting state with respect to the total bearing capacity (1a) of bent and extracentrally compressed (with large eccentricity) reinforced concrete structures occurs as a result of their operation in the plastic stage, that is, when the stressed reinforcing in the cross sections most stressed

FOR OFFICIAL USE ONLY

FOR OFFICIAL USE ONLY

normal to the longitudinal axis is in the condition of plastic flow. In these cross sections a significant opening of the cracks takes place almost to the entire height of the beam. This leads to the splitting of the entire structure into individual, slightly deformed sections.

The achievement of the limiting state Ia is characterized by the beginning of destruction of the concrete in the compressed zone in the cross sections operating in the plastic stage. Here it is proposed that the reinforcing has sufficient plastic deformation reserve and does not break before complete rupture of the compressed concrete and that the cross section is not extra-reinforced, that is, the compressed concrete is not destroyed before the beginning of yield of the reinforcing.

It is known that for reinforced concrete structures the destruction with respect to inclined cross sections from a transverse force is especially dangerous. Therefore in order to prevent a large opening of the inclined crack it is expedient that the transverse reinforcing which takes the transverse force operate only in the elastic stage.

The destruction of the concrete in the compressed zone occurs at the time when the stresses in the concrete reach the ultimate compressive strength with bending. At this time the displacements of the structure must be the largest, that is, the speed of the structure is equal to zero.

The limiting state Ia is normalized by the values of the deformations which are selected in such a way that they can be found by dynamic calculation of the structure and at the same time they will be convenient for experimental determination. For bent reinforced concrete elements the most convenient normalizing value is the angle of opening of the crack at the plasticity hinge [15]. In this case the strength condition of the structure in which n plasticity hinges are formed has the form

$$\psi_i \leq \psi_{\pi i} \quad (i = 1, 2, \dots, n), \quad (61)$$

where ψ_i is the angle of opening in the i th plasticity hinge obtained from the dynamic calculation; $\psi_{\pi i}$ is the limiting angle of opening in the i th plasticity hinge.

The magnitude of the limiting angle of opening ψ_{π} essentially depends on the relative height α_p in the compressed zone of the concrete taken at the time of rupture in the p cross section with the crack and equal to the following for the rectangular cross section

$$\alpha_p = \frac{R_a}{R_u} \mu \left(\mu = \frac{F_a}{bh_0} \right), \quad (62)$$

(a) Key: a. 1

where R_a and R_u are the calculated resistances of the reinforcing and the concrete.

FOR OFFICIAL USE ONLY

FOR OFFICIAL USE ONLY

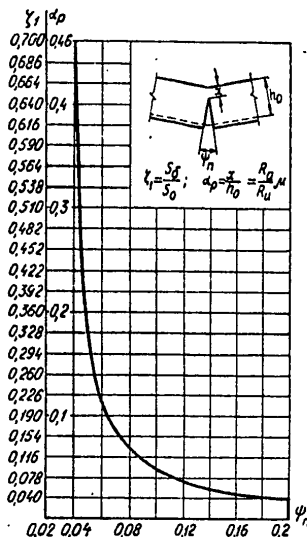


Figure 28. Graph for determining the limiting angle of opening in the plasticity hinge.

The values of ψ_n must be determined from the experiments by dynamic bending of the beam elements.

Figure 28 gives the graph of ψ_n as a function of α_p and the characteristic of the cross section S_b/S_0 constructed by the results of such numerous tests with different beam structures. When using them the values of α_p and S_b must be determined without considering the compressed reinforcing (F'), for its effect on the value of ψ_n is not investigated. The graphs in Figure 28 is well approximated by the function

$$\psi_n = 0,035 + \frac{0,003}{\alpha_p} \tag{63}$$

The calculation of the bent reinforced concrete structural elements by the limiting state lb determines the operation of the structure without residual elongations of the stressed reinforcing. The achievement of this limiting state is characterized by the beginning of the occurrence of plastic deformation in the stressed reinforcing in the most stressed cross sections.

The normalization of the limiting state lb is accomplished by the stresses; at the time the maximum displacements are reached, the stresses in the stressed reinforcing of the most stressed sections will reach the yield point (dynamic).

FOR OFFICIAL USE ONLY

FOR OFFICIAL USE ONLY

5. Calculation of a Hinge-Supported Beam in the Plastic Stage

The plastic stage occurs after the stresses in the stressed reinforcing of the most stressed cross section reached the dynamic yield point, and plastic flow begins in the reinforcing. This state of the cross section is called, as is known, the plasticity hinge. It is depicted in the form of an ordinary hinge at which a concentrated bending moment of constant magnitude is applied. When calculating the reinforced concrete structures, the position of the plasticity hinges is assumed to be constant (the stationary plasticity hinges).

The plastic stage of the entire structural element is considered to occur after the plasticity hinges form, and it is converted to geometrically variable, that is, to the mechanism. In this case all of the elements into which the structural element is broken down are assumed to be absolutely rigid.

In the case where after formation of the plasticity hinges the structural element still remains geometrically unaltered, the elastic operation of its individual elements is taken into account, and the structural element is considered to be in the elastic-plastic stage.

We shall consider that the beam is loaded uniformly under a distributed load of intensity

$$p(t) = \Delta p(t)b,$$

where b is the calculated width of the beam. When calculating the beam slabs, it is taken equal to one meter or 1 cm.

1. Calculation for an instantaneously increasing dynamic load of the type of (17)

$$p(t) = p \left(1 - \frac{t}{\theta} \right), \quad p = \Delta p b. \quad (64)$$

The bending moment in the middle of the beam span in the elastic stage in accordance with (18) is:

$$\left. \begin{aligned} M(t) &= M_p \left(1 - \frac{t}{\theta} - \cos \omega t + \frac{\sin \omega t}{\omega \theta} \right) = M_p T(t); \\ M_p &= \frac{pl^2}{8}; \quad \omega = \frac{\pi^2}{l^2} \sqrt{\frac{B}{m}}. \end{aligned} \right\} \quad (65)$$

The time at the end of the elastic stage will be found from the equations (38) or (40). In these expressions we shall replace the stress ratio in the reinforcing σ_0/σ_c by the ratio of the bending moments M_0/M_p , where M_0 is the moment of the internal forces in the middle cross section of the beam at

FOR OFFICIAL USE ONLY

FOR OFFICIAL USE ONLY

the time the stresses in the stressed reinforcing reached the static yield point σ_0 .¹

The ratio

$$k_M = \frac{M_0}{M_p} \quad (66)$$

is called the dynamicity coefficient with respect to the bending moment. For known k_M , the magnitude of M_0 is found by the formula

$$M_0 = k_M M_p. \quad (67)$$

Equation (38) is written in dimensionless form

$$k_M (\omega t_0)^{1/\alpha} = \left[\int_0^{s_y} y^\alpha(s) ds \right]^{1/\alpha}, \quad (68)$$

where $s = \omega t$ is the dimensionless time; $s_y = \omega t_0$;

$$y(s) = T\left(\frac{s}{\omega}\right); \quad (69)$$

for a load of the type of (17) we have

$$y(s) = 1 - \frac{s}{\omega\theta} - \cos s + \frac{\sin s}{\omega\theta}. \quad (70)$$

For the linear approximation of this expression from (39) we obtain

$$k_M [\omega t_0 (\alpha + 1)]^{1/\alpha} = s_y^{1/\alpha} y(s_y) \quad (71)$$

and for the special case of steels classes A-I, A-II and A-III, from (40)

$$1,1:76 \gamma = s_y^{1/17} y(s_y), \quad (72)$$

where

$$\gamma = k_M \omega^{1/17} = \frac{M_0 \omega^{1/17}}{M_p}; \quad M_p = \frac{pl^2}{8}. \quad (73)$$

The bending moment in the plasticity hinge will be equal to:

¹In the presence of a static load the value of M_0 is understood as the difference between the moment of the internal forces in the most stressed cross section and the bending moment from the static load in the same cross section.

FOR OFFICIAL USE ONLY

FOR OFFICIAL USE ONLY

$$M_{in} = M_p y(s_y) = M_p \gamma_1; \gamma_1 = y(s_y). \quad (74)$$

(a)

Key: a. hinge

If the beam is reinforced with steel, the strength of which can be considered not to depend on the deformation rate, the end of the elastic stage t_y is determined by the condition $M(t_y) = M_0$, that is,

$$k_M = y(s_y) \text{ and } M_{in} = M_0. \quad (75)$$

For $\theta = \infty$, from (75) and (70) we obtain

$$s_y = \arccos(1 - k_M). \quad (76)$$

The bending of the beam at the end of the elastic stage is:

$$\begin{aligned} \omega_0(x) &= \frac{p}{B \cdot 12} \left(\frac{x^4}{2} - lx^3 + \frac{l^3 x}{2} \right) y(s_y) = \\ &= \frac{2M_{in}}{3Bl^3} \left(\frac{x^4}{2} - lx^3 + \frac{l^3 x}{2} \right). \end{aligned} \quad (77)$$

Hence, we obtain the maximum elastic bending (for $x = l/2$)

$$\omega_0 = \frac{M_{in} l^3}{9.6 B} = \frac{5\rho l^4}{384 B} \gamma_1. \quad (78)$$

In the plastic stage the total bending of the beam is:

$$\omega_n(x, t) = \varphi(t)x + \frac{2M_{in}}{3Bl^3} \left(\frac{x^4}{2} - lx^3 + \frac{l^3 x}{2} \right) \quad \left(0 \leq x \leq \frac{l}{2} \right), \quad (79)$$

where $\varphi(t)$ is the angle of rotation of half of the beam.

The equation of motion of the beam in the plastic stage can be obtained on the basis of the principle of the possible displacements (for example, [48]) or using the Bubov-Galerkin method as was done in [22]. Let us use the second procedure: substituting expression (79) in the equation of the beam vibration (5), we obtain

$$\frac{8M_{in}}{l^3} + m\ddot{\varphi}x = \rho(t);$$

let us multiply this equation by x and integrate within the limits from 0 to $l/2$. Then

$$\frac{ml^3}{24} \ddot{\varphi} = \frac{\rho(t)l^3}{8} - M_{in}. \quad (80)$$

FOR OFFICIAL USE ONLY

The initial conditions of motion for $t = \tau$: $\phi = 0$, $\dot{\phi} = \dot{\phi}_0$.

The initial velocity $\dot{\phi}_0$ is determined from the equality of the momentum of the beam at the end of elastic and the beginning of the plastic stage:

$$\dot{\phi}_0 = \frac{4}{l^3} \int_0^l \dot{\omega}(x, \tau) dx. \quad (81)$$

Let us substitute the formulas (12) and (18) in the expression for the bending (4). Then after differentiation with respect to t and integration with respect to x we find

$$\dot{\phi}_0 = \frac{\rho l^3 \dot{\tau}(\tau)}{30B} = \frac{\rho l^3 \omega r}{30B}, \quad (82)$$

where

$$r = \sin s_y - \frac{1 - \cos s_y}{\omega \theta}. \quad (83)$$

Let us integrate the equation (80), first making the substitution $t = \bar{t} + \tau$:

$$\ddot{\phi} = \frac{3\rho}{ml} \left[1 - \frac{\tau}{\theta} - \frac{\bar{t}}{\theta} - \gamma_1 \right]; \quad (84)$$

$$\dot{\phi} = \frac{3\rho}{ml} \left[\left(1 - \frac{\tau}{\theta} - \gamma_1 \right) \bar{t} - \frac{\bar{t}^2}{2\theta} \right] + \dot{\phi}_0; \quad (85)$$

$$\phi = \frac{3\rho}{ml} \left[\left(1 - \frac{\tau}{\theta} - \gamma_1 \right) \frac{\bar{t}^2}{2} - \frac{\bar{t}^3}{6\theta} \right] + \dot{\phi}_0 \bar{t}. \quad (86)$$

The maximum angle of rotation will be reached at the time \bar{t}_m for which $\dot{\phi} = 0$. Equating the expression (85) to zero, we obtain the following formula for the dimensionless time ($s = \omega t$) of operation of the beam in the plastic stage:

$$\bar{s}_{\text{max}} = \omega \bar{t}_{\text{max}} = \omega \theta \left(\Delta + \sqrt{\Delta^2 + \frac{2.17r}{\omega \theta}} \right), \quad (87)$$

where

$$\Delta = \cos s_y - \frac{\sin s_y}{\omega \theta} = 1 - \frac{s_y}{\omega \theta} - \gamma_1. \quad (88)$$

Let us find the maximum angle of opening of the crack in the plasticity hinge. The angle of opening only in the plastic stage obviously will be:

$$\psi_n = 2\phi. \quad (89)$$

The deformation obtained during the operating time in the elastic stage where there is no sharp break of the bending curve is considered, provisionally taking the angle of opening at the end of the elastic stage equal to the angle ψ_y which would occur under the condition of deformation of the beam

FOR OFFICIAL USE ONLY

in the elastic stage by the plastic diagram.

Then

$$\psi_y = \frac{4w_0}{l}, \quad (90)$$

where w_0 is the maximum elastic bending.

From formulas (89), (90), (78), (86), we obtain the total maximum angle of opening at the plasticity hinge

$$\psi_{\text{MAKC}} = \frac{pl^3}{19,2B} k_{\Pi}, \quad (91)$$

where

$$k_{\Pi} = \gamma_1 + 0,591 \left(\Delta - \frac{\bar{s}_{\text{MAKC}}}{3\omega\theta} \right) \bar{s}_{\text{MAKC}}^2 + 1,28r \bar{s}_{\text{MAKC}}. \quad (92)$$

Here \bar{s}_{max} and r are determined by the formulas (87) and (83). The maximum bending obviously will be:

$$w_{\text{MAKC}} = \frac{l}{4} \psi_{\text{MAKC}} = \frac{5pl^4}{384B} k_{\Pi}. \quad (93)$$

Hence it is obvious that the coefficient k_{Π} is equal to the ratio of the total deflection of the beam to the elastic deflection caused by the fast loading of intensity p . Therefore k_{Π} can be called the dynamicity coefficient with respect to the displacements. From the formulas (92), (72), (74), (87) it is obvious that with a specific function $y(s)$ the coefficient k_{Π} depends only on two parameters γ and $\omega\theta$. This fact offers the possibility of easily constructing the graphs which greatly facilitate the calculation. Figure 29 also shows the graphs of the dynamicity coefficient with respect to the displacement k_{Π} as a function of γ for different values of $\omega\theta$. The function $y(s)$ was taken in the form (70), and for determination of the time s of the end of the elastic stage, the approximate equation (72) was used.

The plastic deformations in the beam occur if

$$\gamma < \gamma_0. \quad (94)$$

where γ_0 is the maximum value of γ when plastic deformations are still possible in the reinforcing. The value of γ_0 can be found from (73) and (53):

$$\gamma_0 = k_{M0} \omega^{1/17} = \frac{\sigma_0}{\sigma_0} \omega^{1/17} = 1,915 \delta^{-1/17} \left(1 - \frac{\text{arctg } \omega\theta}{\omega\theta} \right). \quad (95)$$

Here the limiting value of the dynamicity coefficient with respect to the bending moment

$$k_{M0} = \gamma_0 \omega^{-1/17} \quad (96)$$

FOR OFFICIAL USE ONLY

FOR OFFICIAL USE ONLY

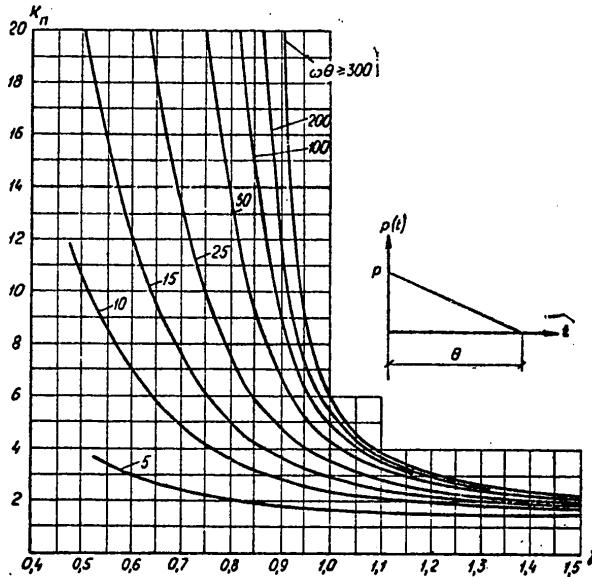


Figure 29. Dynamicity coefficient in the plastic stage for a hinge-supported beam considering the effect of the deformation rate (instantaneous increase in load).

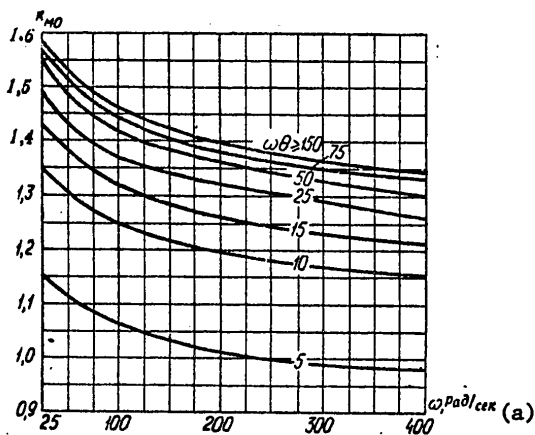


Figure 30. k_{M0} as a function of ω .

Key: rad./sec

determines the limit of elastic working of the beam, that is, for $k_M \geq k_{M0}$ the beam works only in the elastic stage. In Figure 30 we have the

FOR OFFICIAL USE ONLY

FOR OFFICIAL USE ONLY

graph of k_{MO} as a function of ω for different values of $\omega\theta$. As is obvious, the value of k_{MO} can be appreciably less than the value of

$$k_{MO} = 2 \left(1 - \frac{\text{arc tg } \omega\theta}{\omega\theta} \right). \quad (97)$$

This value determines the limit of elastic working of the structure, the mechanical properties of the material of which are not influenced by the deformation rate.

The graphs in Figure 29 show that for $\omega\theta \geq 200$ the values of the coefficients k_{II} in practice do not differ from their values of the case where $\theta = \infty$. For this case we obtain the calculation formulas using (85) and (86). The dimensionless working time of the beam in the plastic stage will be:

$$\bar{s}_{\text{MAKHO}} = \frac{1.08 \sin s_y}{\gamma_1 - 1}, \quad (98)$$

and the dynamicity coefficient with respect to displacement

$$k_n = \gamma_1 \left(1 + 0.694 \frac{2 - \gamma_1}{\gamma_1 - 1} \right). \quad (99)$$

Here $\gamma_1 = 1 - \cos s_y$ where we should have $\gamma_1 > 1$.

Let us define the transverse strength in the beam. Since in the plastic stage the beam elements are assumed to be absolutely rigid, the transverse force can be found only from the condition of equilibrium of the beam under the effect of the load and the inertial forces. For the beam cross section with the coordinate x we have:

$$\begin{aligned} Q(x, t) &= p \left(1 - \frac{t}{\theta} \right) \left(\frac{l}{2} - x \right) - \int_x^{l/2} m \ddot{\varphi} dx = \\ &= p \left(1 - \frac{t}{\theta} \right) \left(\frac{l}{2} - x \right) - \frac{m \ddot{\varphi}}{2} \left(\frac{l^2}{4} - x^2 \right). \end{aligned}$$

Substituting the value of $\ddot{\varphi}$ from (84) in this expression, we obtain

$$Q(x, t) = \frac{pl}{2} \left[\left(1 - \frac{t}{\theta} \right) \left(1 - \frac{2x}{l} \right) - \frac{3}{4} \left(1 - \frac{t}{\theta} - \gamma_1 \right) \left(1 - \frac{4x^2}{l^2} \right) \right]. \quad (100)$$

Hence, it is obvious that the transverse force has maximum value at the beginning of the plastic stage. Therefore the calculated value of the transverse force must be determined at the end of the elastic stage. In the investigated case the transverse force on the support for $t = \tau$ is:

$$Q = \frac{pl}{2} \gamma_1, \quad (101)$$

that is, the dynamicity coefficient with respect to the transverse force will be:

FOR OFFICIAL USE ONLY

$$k_Q = \gamma_1. \tag{102}$$

In Figure 31 we have the graphs of k_Q as a function of k_M for several values of ω . As is obvious, the coefficient k_Q can significantly exceed k_M . The value of k_Q for fixed ω increases to certain constant values (horizontal lines on the graph in Figure 31) which depend on $\omega\theta$.

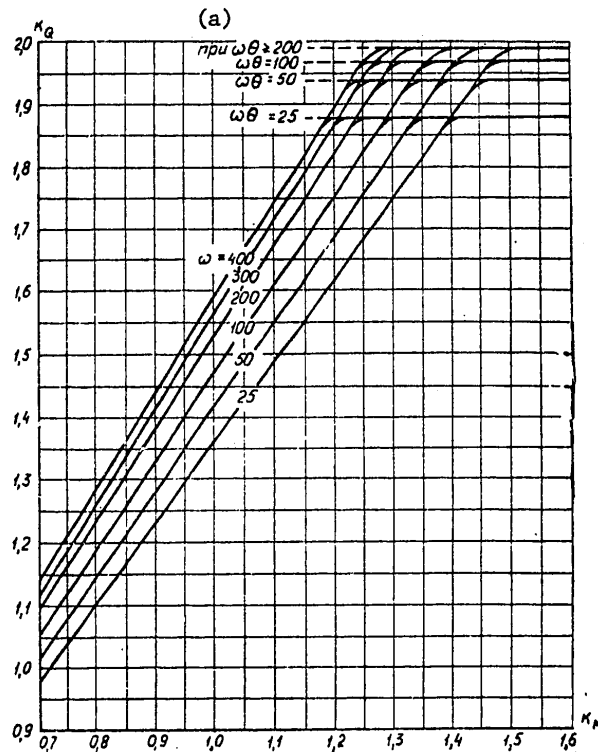


Figure 31. k_Q as a function of k_M .

Key: a. for

When calculating the strength of the inclined cross sections with respect to the transverse force it is necessary that the stresses in the transverse reinforcing not exceed the values of the minimum dynamic yield point (46).

The formulas obtained in this way can be used also when calculating beams without considering the effect of the deformation rate on the strength characteristics of the steel if we replace equation (72) by (75) and set $k_M = \gamma = \gamma_1, \gamma_0 = k_{M0}$.

FOR OFFICIAL USE ONLY

FOR OFFICIAL USE ONLY

In Figure 32 the graphs are constructed for the dynamicity coefficient with respect to displacement of k_{Π} as a function of the dynamicity coefficient with respect to bending moment k_M for different values of $\omega\theta$.

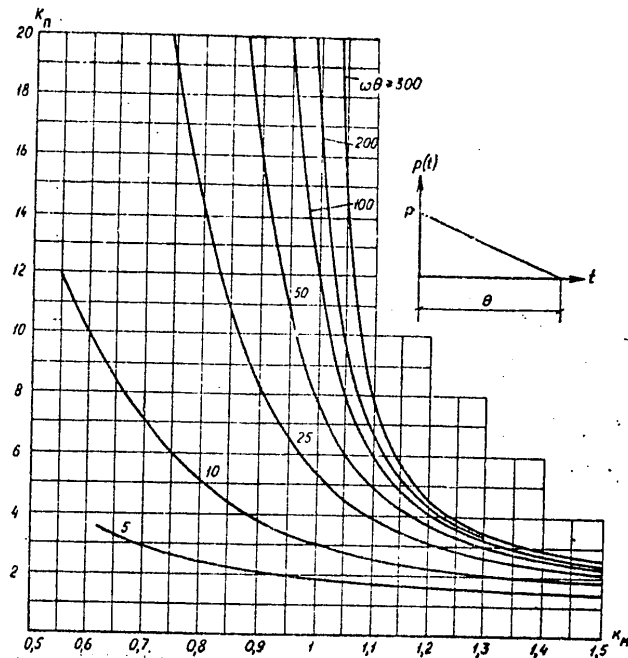


Figure 32. Dynamicity coefficient in the plastic stage for the hinge-support beam without considering the effect of the deformation rate (the instantaneously increasing load).

2. Calculation for a load with build-up of the type (23)

$$p(t) = \begin{cases} p \frac{t}{\theta_1} & 0 \leq t \leq \theta_1; \\ p \left(1 - \frac{t - \theta_1}{\theta_2}\right) & \theta_1 \leq t \leq \theta_1 + \theta_2. \end{cases}$$

In this case the function (69) of the dimensionless time $s = \omega t$ has the form

$$y(s) = \begin{cases} y_1(s) = \frac{s - \sin s}{\omega\theta_1} & (0 \leq s \leq \omega\theta_1) \\ y_2(s) = 1 - \frac{s - \theta_1(\omega)}{\omega\theta_2} + \left(\frac{1}{\omega\theta_1} + \frac{1}{\omega\theta_2}\right) \times \\ \times \sin(s - \omega\theta_1) - \frac{\sin s}{\omega\theta_1} & (\omega\theta_1 \leq s \leq (\theta_1 + \theta_2)\omega). \end{cases} \quad (103)$$

FOR OFFICIAL USE ONLY

FOR OFFICIAL USE ONLY

Let us initially find the value of γ_0 -- the maximum "plastic" value of the coefficient γ (73). From the expression (59) we obtain

$$\gamma_0 = k_{M0} \omega^{1/17} = 0,85R(s^*), \quad (104)$$

where $s^* = \omega t^*$ is the first root of the equation

$$y_2'(s) = \left(\frac{1}{\omega\theta_1} + \frac{1}{\omega\theta_2} \right) \cos(s - \omega\theta_1) - \frac{1}{\omega\theta_1} \cos s - \frac{1}{\omega\theta_2} = 0 \quad (105)$$

greater than $\omega\theta_1$, and $R(s^*)$ is defined by formula (60).

For $\gamma < \gamma_0$, the plastic stage occurs in the beam. Here the end of the elastic stage is possible for $\tau > \theta_1$ or $s_y > \omega\theta_1$ and for $\tau < \theta_1$ or $s_y < \omega\theta_1$.

It is obvious that the intermediate case will be the one where $\tau = \theta_1$ ($s_y = \omega\theta_1$). This case corresponds to the coefficient $\gamma = \bar{\gamma}$, the value of which can be determined from (40) considering the first of the expressions (103):

$$\bar{\gamma} = 0,85(\omega\theta_1)^{1/17} \left(1 - \frac{\sin \omega\theta_1}{\omega\theta_1} \right). \quad (106)$$

The displacements and the forces are also defined by the formulas (91), (93), (67), (101), (104).

1. Let the following condition be satisfied:

$$\bar{\gamma} \leq \gamma < \gamma_0. \quad (107)$$

In this case the plastic stage occurs at the time $\tau \geq \theta_1$ ($s_y \geq \omega\theta_1$). The equation for the time of the end of the elastic stage will be obtained from (59) and (60), replacing ωt^* by $s_y = \omega\tau$:

$$1,1776\gamma = R(s_y), \quad (108)$$

where

$$R(s_y) = \left\{ \omega\theta_1 [y_2(\omega\theta_1)]^{17} + (s_y - \omega\theta_1) \frac{[y_2(s_y)]^{18} - [y_1(\omega\theta_1)]^{18}}{y_2(s_y) - y_1(\omega\theta_1)} \right\}^{1/17} \quad (109)$$

Since the variation of the load with time during operation of the beam in the plastic stage is analogous to (64), the general view of the relations for the dynamicity coefficients coincides with (92), (99), (102).

FOR OFFICIAL USE ONLY

FOR OFFICIAL USE ONLY

It is easy to find that

$$k_{11} = \gamma_1 + 0,591 \left(\Delta - \frac{\bar{s}_{\text{МАКС}}}{3\omega\theta_2} \right) \bar{s}_{\text{МАКС}}^2 + 1,28r\bar{s}_{\text{МАКС}} \quad (110)$$

Here $\gamma_1 = y_2(s_y)$

$$r = \left(\frac{1}{\omega\theta_1} + \frac{1}{\omega\theta_2} \right) \cos(s_y - \omega\theta_1) - \frac{\cos s_y}{\omega\theta_1} - \frac{1}{\omega\theta_2};$$

$$\bar{s}_{\text{МАКС}} = \omega\theta_2 \left(\Delta + \sqrt{\Delta^2 + \frac{2,17r}{\omega\theta_2}} \right),$$

where

$$\Delta = 1 - \frac{s_y - \omega\theta_1}{\omega\theta_1} - \gamma_1.$$

For $\theta_2 = \infty$ we will have

$$k_n = \gamma_1 + \frac{0,694r^2}{\gamma_1 - 1} \quad (\gamma_1 > 1), \quad (111)$$

where

$$\gamma_1 = 1 + \frac{1}{\omega\theta_1} [\sin(s_y - \omega\theta_1) - \sin s_y];$$

$$r = \frac{1}{\omega\theta_1} [\cos(s_y - \omega\theta_1) - \cos s_y]. \quad (112)$$

2. If $\gamma < \bar{\gamma}$, the plastic satage occurs at the time $\tau < \theta_1$ ($s_y < \omega\theta_1$). The dimensionless time s_y of the end of the elastic stage is determined from the equation obtained from (40) for $T(\tau) = T_1(\tau)$, that is,

$$1,1776\gamma = \frac{s_y^{1/17}}{\omega\theta_1} (s_y - \sin s_y). \quad (113)$$

In the plastic stage the equation of motion of the beam in accordance with (80) and (23) has the form:

for $\tau \leq t \leq \theta_1$

$$\frac{ml^3}{24} \ddot{\varphi} = \frac{pl^2 t}{8\theta_1} - M_w; \quad (a)$$

Key: a. hinge

for $\theta_1 \leq t \leq \theta_1 + \theta_2$

$$\frac{ml^3}{24} \ddot{\varphi} = \frac{pl^2}{8} \left(1 - \frac{t - \theta_1}{\theta_2} \right) - M_w.$$

Solving these equations with insurance of continuity of ϕ and $\dot{\phi}$ for $t = \theta_1$, we obtain

FOR OFFICIAL USE ONLY

FOR OFFICIAL USE ONLY

$$k_{\pi} = \gamma_1 + 0,591 \left(\Delta - \frac{\bar{s}_{\text{maxc}}}{3\omega\theta_2} \right) \bar{s}_{\text{maxc}}^2 + 1,28 [r - 0,461 (\omega\theta_1 - s_y) \delta_1] \bar{s}_{\text{maxc}} + 0,196 (\omega\theta_1 - s_y)^2 \delta_1, \quad (114)$$

where

$$\gamma_1 = \gamma_1(s_y) = \frac{1}{\omega\theta_1} (s_y - \sin s_y); \quad (115)$$

$$r = \frac{1}{\omega\theta_1} (1 - \cos s_y); \quad (116)$$

$$\bar{s}_{\text{maxc}} = \omega\theta_2 \left[\Delta + \sqrt{\Delta^2 + \frac{2,17r - (\omega\theta_1 - s_y) \delta_1}{\omega\theta_2}} \right];$$

$$\Delta = 1 + \frac{\omega\theta_1 - s_y}{\omega\theta_2} - \gamma_1;$$

$$\delta_1 = 1 + \frac{\omega\theta_1 - s_y}{\omega\theta_2} - \frac{s_y}{\omega\theta_1}.$$

For $\theta_2 = \infty$ the formulas assume the form

$$k_{\pi} = \gamma_1 + 1,28\gamma_2 + 0,694 \frac{r_1^2}{\gamma_1 - 1} (\gamma_1 > 1), \quad (117)$$

where

$$\gamma_2 = (\omega\theta_1 - s_y) \left\{ r + 0,461 (\omega\theta_1 - s_y) \left[\frac{1}{3} \left(1 - \frac{s_y}{\omega\theta_1} \right) + \frac{s_y}{\omega\theta_1} - \gamma_1 \right] \right\};$$

$$r_1 = r + 0,923 (\omega\theta_1 - s_y) \left[0,5 \left(1 - \frac{s_y}{\omega\theta_1} \right) + 1 - \gamma_1 \right].$$

γ_1 and r are defined by formulas (115) and (116).

Figure 33 shows the graphs of k_{π} as a function of γ for several values of θ_1 and $\omega\theta_2$ constructed by the formulas (110) and (114). Part of the curve $k_{\pi}(\gamma)$ plotted by the solid line corresponds to working of the beam in the plastic stage, and the dotted line, to elastic working. These parts are adjacent to each other at the point with the x-axis γ_0 . In the plastic stage ($\gamma < \gamma_0$) the curves $k_{\pi}(\gamma)$, beginning with some value γ , go sharply upward, approaching the vertical. This section corresponds to the loss of the bearing capacity by the structural element, for an insignificant increase in load causes such large deformations (that is, k_{π}) that the structure must break.

FOR OFFICIAL USE ONLY

FOR OFFICIAL USE ONLY

As is obvious, with an increase in $\omega\theta_1$, that is, with a decrease in the dynamic effect of the load, the section corresponding to the plastic stage of the beam decreases. For $\omega\theta_1 = 2\pi$ and for $\omega\theta_2 \geq 200$ the difference in the magnitude of the load causing the limiting stage in the beam with respect to strength and with respect to absence of large residual deformations does not exceed 10%. Therefore for $\omega\theta_1 \geq 2\pi$ and $\omega\theta_2 \geq 200$ it is expedient to calculate the structural elements only in the elastic stage (limiting state 1b), for consideration of the plastic deformations provides no cost benefit. The intersection of the curves in Figure 33 is caused by a decrease in the effect of the deformation rate on the yield point of the reinforcing with an increase in the buildup time.

When calculating the structural elements without considering the effect of the deformation rate in the formulas obtained, it is necessary to replace the coefficient γ by K_M . Then the value of this coefficient which determines the limit between the elastic and plastic stages will be:

$$k_{MO} = y_s(s^*), \tag{118}$$

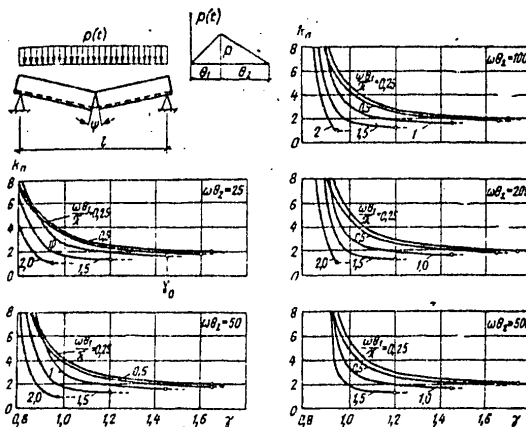


Figure 33. Dynamicity coefficient in the plastic stage for a hinge-supported beam considering the effect of deformation rate (load with buildup).

where s^* is determined from the solution of equation (105); analogously, the value of K_M for which the plastic stage occurs at the time $s_y = \omega\theta_1$ will become equal to:

$$\bar{k}_M = \gamma_i(\omega\theta_1) = 1 - \frac{\sin \omega\theta_1}{\omega\theta_1} \tag{119}$$

FOR OFFICIAL USE ONLY

FOR OFFICIAL USE ONLY

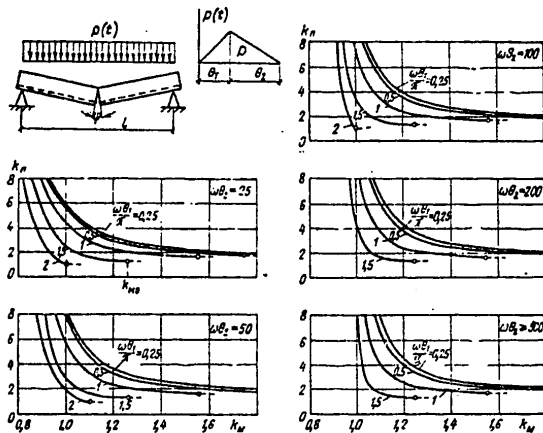


Figure 34. Dynamicity coefficient in the plastic stage for a hinge-supported beam without considering the effect of the deformation rate (loading with buildup).

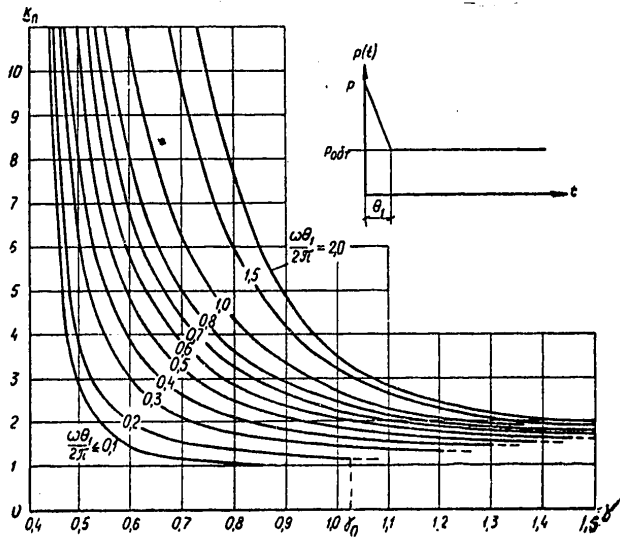


Figure 35. Dynamicity coefficient in the plastic stage for a hinge-supported beam considering the effect of the deformation rate (load during streamlining).

If $\bar{k}_M \leq k_M < k_{M0}$, the time of the end of the elastic stage is determined from the equation

FOR OFFICIAL USE ONLY

FOR OFFICIAL USE ONLY

$$k_M = y_2(s_y),$$

and the dynamicity coefficient with respect to the displacements is found from the expression (110) or (111).

If $\bar{k}_M > k_M$, then the time of the end of the elastic stage will be determined from the equation $k_M = y_1(s_y)$, and the coefficient k_π , by the formula (114).

For the cases where the effect of the deformation rate is not taken into account, the Figure 34 gives the graphs of k_π as a function of k_M for various values of $\omega\theta_1$ and $\omega\theta_2$. From these graphs it also follows that for $\omega\theta_1 \geq 2\pi$ and $\omega\theta_2 \geq 100$ it is possible not to consider the plastic stage.

The strength conditions of the structural elements permit us directly to obtain the limiting value of the dynamic load with known time characteristics which can be taken by the given structure. When performing the calculation with respect to the limiting state 1b this follows from the conditions $\gamma \geq \gamma_0$ ($k_M \geq k_{M0}$). When calculating by the limiting state 1a, using the function

$$M_p = \frac{p l^2}{8} = \frac{M_0 \omega^{1/17}}{\gamma}, \quad (120)$$

we find from (91) the equation for the coefficient γ :

$$\frac{k_\pi(\gamma)}{\gamma} = \frac{2.4 B \psi_\pi}{M_0 \omega^{1/17} l}. \quad (121)$$

After solution of it [for which it is necessary to use the graphs of the function $k_\pi(\gamma)$] (Figures 29 and 32-34) the load is found by the formula (120). If there is a relation between the load and its time of effect, then it is necessary to make several efforts, first taking, for example, $\theta = \infty$.

The selection of the cross sections of the structural element for the given dynamic load can be made only by successive approximations, for the total load on the structure depends on its characteristics. In the first approximation it is possible to set: $k_M = 0.7$ to 0.8 for the structures reinforced with class A-I, A-II, A-III steel and $k_M = 1.1$ if the effect of the deformation rate is not taken into account.

3. Calculation for the load of the type (27).

This load acts on the structural element with streamlining of it by a shock wave.

The calculations analogous to the ones presented above made it possible to obtain k_π as a function of γ or k_M for it. For $\bar{\Delta} = 0.5$ these functions are represented on graphs in Figure 35 and Figure 36 for different values of the streamlining time characterized by the value of $\omega\theta_1/(2\pi)$ and the values of $\omega\theta \geq 500$.

FOR OFFICIAL USE ONLY

FOR OFFICIAL USE ONLY

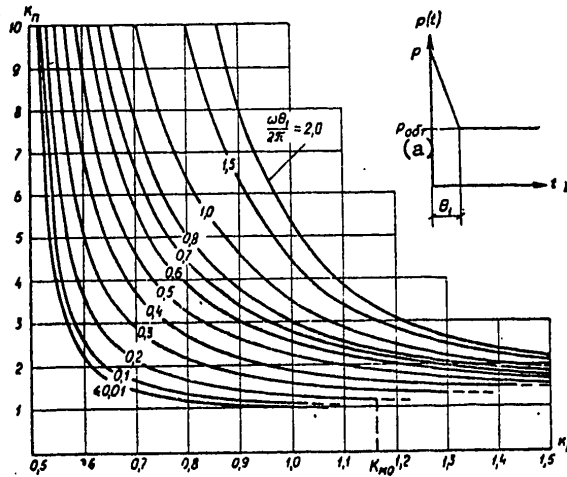


Figure 36. Dynamicity coefficient in the plastic stage for a hinge-supported beam without considering the effect of the deformation rate (loading with streamlining).

Key: a. streamlining

6. Calculation of a Beam with Clamped Ends in the Plastic Stage

When calculating beams clamped on supports it is necessary to consider the sequence of formation of the plastic hinges in the span and on the support which is determined by the relation between the effective and the limiting bending moments in these cross sections.

Let us introduce the following notation: M^{bear} , M^{span} are the bearing and spanning bending moments caused by the effective dynamical loading; M_{hinge}^{bear} , M_{hinge}^{span} are the limiting bearing and spanning moments.

Then, if

$$\beta = \frac{|M_{hinge}^{on}|}{M_{hinge}^{np}} \begin{matrix} (a) \\ > \\ (b) \end{matrix} \frac{M_{hinge}^{on}}{M_{hinge}^{np}} \begin{matrix} (c) \\ > \\ (c) \end{matrix} \quad (122)$$

Key: a. bear b. span c. hinge

then the plasticity hinges first are formed on the supports if

$$\beta < \frac{M_{hinge}^{on}}{M_{hinge}^{np}}$$

then in the span they are formed sooner than on the supports and, finally, for equality of the ratios

FOR OFFICIAL USE ONLY

FOR OFFICIAL USE ONLY

$$\frac{|M^{on}|}{M^{np}} = \frac{M_{in}^{on}}{M_{in}^{np}} \quad (123)$$

all of the hinges are formed simultaneously.

The experiments show that in the reinforced concrete clamped beams this relation (β) between the bending moments varies with variation of the load. With an increase in load, it still differs from the expression for the uniform elastic beam of constant rigidity. This "redistribution" of the forces essentially depends on the relation between the percentages of reinforcing on the supports and on the span, that is, in the final analysis, the beam rigidity determined considering the opening of the cracks in the stressed zone of the concrete.

We shall first find the values of the bearing and spanning bending moments in the clamped reinforced concrete beam under the effect of the static, uniformly distributed load p . It is proposed that the cross sections in the span and on the bearings are in stage II of the stressed state, that is, cracks occurred in the stressed zone of the concrete. Accordingly, we assume that in the sections next to the supports of length a the beam rigidity is B^{bear} , and in the central section of length $l - 2a$ it is equal to B^{span} . Here B^{bear} and B^{span} are the rigidities defined, as usual, considering the opening of the cracks in the stressed zone of the concrete, for the cross sections on the support and in the middle of the span, respectively. The value of a will be found from the condition of vanishing of the bending moment in the cross sections at a distance a from the supports.

The bearing bending moment M^{bear} can be found from the canonical equation by the force method

$$\delta_{11}M^{on} + \Delta_{1p} = 0, \quad (124)$$

where

$$\begin{aligned} \delta_{11} &= \frac{l}{B^{np}} \left[1 - 2 \frac{a}{l} \left(1 - \frac{1}{\beta_1} \right) \right]; \\ \Delta_{1p} &= \frac{pl^3}{12B^{np}} \left[1 - 2 \frac{a^2}{l^2} \left(3 - \frac{2a}{l} \right) \left(1 - \frac{1}{\beta_1} \right) \right]; \\ \beta_1 &= \frac{B^{on}}{B^{np}}. \end{aligned} \quad (125)$$

Hence, we obtain:

$$M^{on} = -\frac{pl^2}{12} k_1; \quad M^{np} = \frac{pl^2}{24} (3 - 2k_1), \quad (126)$$

where

$$k_1 = \frac{1 - 2 \frac{a^2}{l^2} \left(3 - \frac{2a}{l} \right) \left(1 - \frac{1}{\beta_1} \right)}{1 - \frac{2a}{l} \left(1 - \frac{1}{\beta_1} \right)}. \quad (127)$$

FOR OFFICIAL USE ONLY

FOR OFFICIAL USE ONLY

The value of a/l obviously itself depends on the ratio $\beta = |M^{\text{bear}}|/M^{\text{span}}$. The calculations show that for $\beta > 0.5$ it can be approximately considered to be constant and equal to $a/l = 0.23$. Then from the formula (127) we obtain

$$k_1 = \frac{0.269 + 0.731\beta_1}{0.46 + 0.54\beta_1} \quad (128)$$

From (126) it follows that

$$\beta = \frac{|M^{\text{on}}|}{M^{\text{np}}} = \frac{2k_1}{3-2k_1} \quad (129)$$

Then we shall consider that for this value the condition (122) is satisfied, that is, we assume that the plasticity hinges on the supports are formed earlier than in the span. This condition is satisfied, for example, for $\beta_1 = 2$, for then $k_1 = 1.125$, $\beta = 3$ and $\frac{M^{\text{bear}}}{M^{\text{span}}} \approx 2$. It is obvious that with a decrease in β_1 the condition (122) is all the more valid. It is violated for sufficiently large values of β_1 when the percentage reinforcing on the support exceeds by 4-5 times the percentage reinforcing in the span.

Let us now proceed to the dynamic calculation and let us obtain the calculation formulas for the load of the type $p(t) = p(1 - t/\theta)$.

In the other stage we neglect, as usual, the working of the beam concrete in the stressed zone, that is, we consider that both in the span and on the supports cracks occurred immediately which caused variation in rigidity and redistribution of forces.

The equation of the beam vibrations (1) now will have the form

$$B_i \frac{\partial^4 w}{\partial x^4} + m \frac{\partial^2 w}{\partial t^2} = p \left(1 - \frac{t}{\theta}\right) \quad (i=1, 2), \quad (130)$$

where the following is noted: $B_1 = B^{\text{bear}}$ for $0 \leq x \leq a$; $l - a \leq x \leq l$; $B_2 = B^{\text{span}}$ for $a < x < l - a$.

The expression for the dynamic bending deflection is taken in the form (4):

$$w_i(x, t) = pF(x)T_i(t). \quad (131)$$

Here, just as in item 2, $F(x)$ is the static form of the deflections from the uniformly distributed load of unit intensity satisfying the equations:

$$\left. \begin{aligned} B^{\text{bear}} F_1^{\text{IV}}(x) &= 1; 0 \leq x \leq a; l-a \leq x \leq l; \\ B^{\text{span}} F_2^{\text{IV}}(x) &= 1; a < x < l-a, \end{aligned} \right\} \quad (132)$$

Key: a. bear b. span

FOR OFFICIAL USE ONLY

FOR OFFICIAL USE ONLY

the boundary conditions $F(x) = F'(x) = 0$ for $x = 0$ and $x = l$ and the conjugation conditions for $x = a$ and $x = l - a$.

The expression for the deflection of the middle of the beam span will be obtained in the form

$$w_1\left(\frac{l}{2}, t\right) = \frac{\rho l^4 v_2}{384 B^{np}} T_1(t), \quad (133)$$

where

$$v_2 = 1 - 0,32(k_1 - 1) - 0,849(k_1 - 0,407)\left(1 - \frac{1}{\beta_1}\right) \\ \left(\text{for } \alpha_1 = \frac{a}{l} = 0,23\right); \quad (134)$$

$$T_1(t) = 1 - \frac{t}{\theta} - \cos \omega_1 t + \frac{\sin \omega_1 t}{\omega_1 \theta}. \quad (135)$$

In order to determine ω_1 , it is possible to use the formula for the oscillation frequency of the clamped beam of constant rigidity

$$\omega_1 = \frac{22,4}{l^2} \sqrt{\frac{B^{np}}{m}}. \quad (136)$$

The bending moments on the supports and in the middle of the span are equal to:

$$M_1^{on}(t) = -\frac{\rho l^2 k_1}{12} T_1(t); \quad M_1^{np}(t) = \frac{\rho l^2}{24} (3 - 2k_1) T_1(t). \quad (137)$$

The end of the elastic stage comes after the occurrence on the supports of plasticity hinges. The time (τ_1) of the end of the elastic stage is found from equation (40) in which the stress ratio σ_0/σ_c will be replaced by the ratio of the bending moment:

$$k_M^{on} = \frac{M_0^{on}}{M_{pl}^{on}}; \quad M_{pl}^{on} = \frac{\rho l^2}{12} k_1, \quad (138)$$

where M_0^{bear} is the moment of internal forces in the bearing cross section of the beam at the time the stresses in the stressed reinforcing reach the static yield point σ_0 ; the moment M_0^{span} has the same meaning for the cross section in the middle of the span.

The equation for the time of the end of the elastic stage will have the form analogous to (72):

$$1,1776\gamma = s_y^{1/17} y_1(s_y); \quad s_y = \omega_1 \tau_1, \quad (139)$$

where

FOR OFFICIAL USE ONLY

$$\gamma = k_M^{on} \omega_1^{1/17} = \frac{M_0^{on} \omega_1^{1/17}}{M_{pl}^{on}}, \quad (140)$$

$$y_1(s) = T_1\left(\frac{s}{\omega}\right) = 1 - \frac{s}{\omega_1 \theta} \cos s + \frac{\sin s}{\omega_1 \theta}. \quad (141)$$

The absolute value of the bending moments in the supporting plasticity hinges at the time $t = \tau_1$ is:

$$\left. \begin{aligned} M_w^{on} &= \frac{\rho l^2}{12} k_1 T_1(\tau_1) = M_{pl}^{on} \gamma_1; \\ \gamma_1 &= T_1(\tau_1) = y_1(s_v). \end{aligned} \right\} \quad (142)$$

The value of the coefficient γ defining the limit of elastic working of the beam is determined from the expression similar to (95):

$$\gamma_0 = k_{M0}^{on} \omega_1^{1/17} = 1.9156^{-1/17} \left(1 - \frac{\text{arctg } \omega_1 \theta}{\omega_1 \theta}\right). \quad (143)$$

where $\delta = \frac{\pi}{2 \text{arctg } \omega_1 \theta}$.

After the occurrence of plasticity on the hinge supports, the beam is converted to a hinge-supported beam, in the supporting cross sections of which concentrated bending moments are applied equal to $-M_{hinge}^{bear}$.

The working of the beam and with elastic-plastic stage will continue until the plasticity hinge occurs in the middle of the span.

The equation of the beam pressure in the elastic-plastic stage obviously is also described by the equation (130), but with boundary conditions: $x = 0$, $x = l$, $w = 0$, $B^{bear} \left(\frac{2w}{x^2}\right) = M_{hinge}^{bear}$. The Bublov-Galerkin method is also applicable for the solution of it. The beam deflection at the end of the elastic stage in accordance with (131) and (142) is:

$$w_1(x, \tau_1) = \rho F(x) \gamma_1 = \rho F(x) \frac{M_w^{on}}{M_{pl}^{on}}. \quad (144)$$

For $t > \tau_1$, the elastic-plastic stage of working of the beam begins. The expression for the deflections will be represented in the form

$$w_2(x, t) = \rho G(x) T_2(t) + \rho F(x) \gamma_1, \quad (145)$$

where $G(x)$ is the static form of the deflection of the hinged beam, and the function $T_2(t)$ is defined from the equation which was obtained from (130):

$$\ddot{T}_2 + \omega^2 T_2 = \left(1 - \frac{t}{\theta} - \gamma_1\right) \omega^2, \quad (146)$$

where

FOR OFFICIAL USE ONLY

$$\omega^2 = \frac{\int_0^l G(x) dx}{m \int_0^l G^2(x) dx} \quad (147)$$

The initial value (for $t = \tau_1$) of the function T_2 obviously is zero. The value of $\dot{T}_2(\tau_1)$ will be determined from the condition of equality of the momentum at the end of the elastic and the beginning of the elastic-plastic stage

$$\dot{T}_2(\tau_1) = \dot{T}_1(\tau_1) \frac{\int_0^l F(x) dx}{\int_0^l G(x) dx} \quad (148)$$

Then in order to simplify the calculations let us consider that the rigidity of the segments of the beam near the supports influences the deflection of the hinged girder insignificantly. Therefore as $G(x)$ let us take the form of the deflections of the hinged girder with constant rigidity with respect to the entire span equal to B^{span} , that is,

$$G(x) = \frac{1}{12B^{\text{span}}} \left(\frac{x^4}{2} - lx^3 + \frac{l^2x}{2} \right) \quad (149)$$

Then

$$\omega = \frac{\pi^2}{l^2} \sqrt{\frac{B^{\text{span}}}{m}} \quad (150)$$

$$\text{and } \dot{T}_2(\tau_1) = \omega_1 r_1 v_3, \quad (150a)$$

where

$$r_1 = \sin \omega_1 \tau_1 - \frac{1 - \cos \omega_1 \tau_1}{\omega_1 \theta}; \quad (151)$$

$$v_3 = 0,184 - 0,13k_1 + (0,184k_1 - 0,071) \frac{1}{\beta_1} \quad (152)$$

The coefficient v_3 has the following values: for $\beta_1 = 1$, $k_1 = 1$, $v_3 = 0.167$; for $\beta_1 = 2$, $k_1 = 1.125$, $v_3 = 0.105$.

Solving equation (146), we obtain

$$T_2(t) = c_1 \sin \omega(t - \tau_1) - c_2 \cos \omega(t - \tau_1) + 1 - \gamma_1 - \frac{t}{\theta}, \quad (153)$$

where

$$c_1 = \frac{\omega_1}{\omega} r_1 v_3 + \frac{1}{\omega \theta}; \quad c_2 = 1 - \gamma_1 - \frac{\tau_1}{\theta} \quad (154)$$

The bending moment in the middle of the span will be:

FOR OFFICIAL USE ONLY

APPROVED FOR RELEASE: 2007/02/08: CIA-RDP82-00850R000200090009-1

...
OF
BY

3 JUNE 1980

M. D. BODANSKIY, L. M. GORSHKOV ET AL

2 OF 3

FOR OFFICIAL USE ONLY

$$M_2^{np}(t) = -B^{np} \frac{\partial^2 w_2}{\partial x^2} \Big|_{x=\frac{l}{2}} = \frac{\rho l^3}{8} T_2(t) + \frac{\rho l^3}{24} (3-2k_1) \gamma_1 = M_{p1}^{np} T_2^*(t), \quad (155)$$

where

$$T_2^*(t) = \gamma_1 + \frac{3}{3-2k_1} T_2(t) = T_1(\tau_1) + \frac{3}{3-2k_1} T_2(t); \quad (156)$$

$$M_{p1}^{np} = \frac{\rho l^3}{24} (3-2k_1). \quad (157)$$

Let us find the angle of opening ψ_2^{bear} in the bearing plasticity hinge as the sum of such angles in the elastic ψ_y^{bear} and elastic-plastic $\psi_{y\pi}^{\text{bear}}$ stages.

According to (145) we obtain

$$\psi_{y\pi}^{\text{bear}} = \rho T_2(t) \frac{dG(x)}{dx} \Big|_{x=0} = \frac{\rho l^3}{24B^{np}} T_2(t). \quad (158)$$

The deformation on the support inclined during the time of working of the beam in the elastic stage will be considered approximately the provisional angle of opening equal to [considering (133)]:

$$\psi_y^{\text{bear}} = \frac{2}{l} w_1 \left(\frac{l}{2}; \tau_1 \right) = \frac{\rho l^3 v_2}{192B^{np}} T_1(\tau_1). \quad (159)$$

Thus, we have

$$\psi_2^{\text{bear}}(t) = \psi_y^{\text{bear}} + \psi_{y\pi}^{\text{bear}} = \frac{\rho l^3}{192B^{np}} [v_2 T_1(\tau_1) + 8T_2(t)]. \quad (160)$$

The elastic-plastic stage continues until the time τ_2 when in the middle of the beam span after the stresses in the stressed reinforcing reaches the dynamic yield point, a plasticity hinge occurs. This time is determined from equation (38) in which the stresses are replaced by the bending moments in accordance with formulas (137) and (155),

$$t_0 (k_M^{np})^\alpha = \int_0^{\tau_1} [T_1(t)]^\alpha dt + \int_{\tau_1}^{\tau_2} [T_2^*(t)]^\alpha dt, \quad (161)$$

where

$$k_M^{np} = \frac{M_0^{np}}{M_{p1}^{np}}. \quad (162)$$

In this expression let us replace the functions $T_1(t)$ and $T_2^*(t)$ by the approximate linear functions.

As a result, we obtain the equation similar to (58):

FOR OFFICIAL USE ONLY

FOR OFFICIAL USE ONLY

$$t_0 (k_M^{np})^\alpha = \frac{1}{(\alpha+1)} \left\{ \tau_1 [T_1(\tau_1)]^\alpha + \frac{(3-2k_1)(\tau_2-\tau_1)}{3T_2(\tau_2)} \times \right. \\ \left. \times ([T_2^*(\tau_2)]^{\alpha+1} - [T_1(\tau_1)]^{\alpha+1}) \right\}. \quad (163)$$

Let us take $\alpha = 17$, $t_0 = 0.895$ sec and let us write this expression in dimensionless form:

$$1,1776 \gamma' = R_1(s_{yn}); \quad s_{yn} = \omega_1 \tau_2, \quad (164)$$

where

$$R_1(s) = \left\{ s_y [y_1(s_y)]^{17} + \frac{(3-2k_1)(s-s_y)}{3y_2(s)} \times \right. \\ \left. \times ([y_2^*(s)]^{18} - [y_1(s_y)]^{18}) \right\}^{1/17}; \quad (165)$$

$$\gamma' = k_M^{np} \omega_1^{1/17}. \quad (166)$$

Here $y_1(s_y)$ is defined by the formula (141) ($s_y = \omega_1 \tau_1$);

$$y_2(s) = c_1 \sin \frac{\omega}{\omega_1} (s-s_y) - c_2 \cos \frac{\omega}{\omega_1} (s-s_y) + 1 - \gamma_1 - \frac{s}{\omega_1 \theta}, \quad (167)$$

where c_1 and c_2 are found by the formulas (154);

$$y_2^*(s) = y_1(s_y) + \frac{3}{3-2k_1} y_2(s); \quad s = \omega_1 t. \quad (168)$$

The dynamicity coefficient for the middle of the span k_M^{span} (162) will be expressed in terms of the dynamicity coefficient for the support k_M^{bear} (138):

$$k_M^{np} = k_M^{on} \frac{2k_1}{\beta_2(3-2k_1)}, \quad (169)$$

where

$$\beta_2 = \frac{M_0^{on}}{M_0^{np}}. \quad (170)$$

Then the coefficient γ' (166) in equation (164) can be expressed in terms of the coefficient γ (140) using the structural parameters β_1 and β_2 :

$$\gamma' = \gamma \frac{2k_1}{\beta_2(3-2k_1)}. \quad (171)$$

It can happen that the equation (164) has no solution.

This fact indicates that in the middle cross section of the beam the plasticity hinge does not occur, and its work is limited only by the elastic-plastic stage. Then the maximum value of the angle of opening in the bearing plasticity hinge according to (160) will be:

$$\psi_{2max}^{on} = \frac{P l^3}{192 B^{np}} k_{n2}^{on}, \quad (172)$$

FOR OFFICIAL USE ONLY

FOR OFFICIAL USE ONLY

where $k_{\pi 2}^{\text{bear}}$ is the dynamicity coefficient with respect to the displacements for the support equal to:

$$k_{\pi 2}^{\text{on}} = \nu_2 T_3(\tau_1) + 8T_2(t_{m1}). \quad (173)$$

The time t_{m1} is determined by the formula

$$\text{tg } \omega \frac{(t_{m1} - \tau_1)}{2} = \frac{c_2 + \sqrt{c_1^2 + c_2^2 - \frac{1}{(\omega\theta)^2}}}{c_1 + \frac{1}{\omega\theta}}. \quad (174)$$

The transverse force on the beam in the elastic-plastic stage will be:

$$Q_2(0, t) = \frac{pl}{2} [T_1(\tau_1) + T_2(t)]. \quad (175)$$

If the root $s_{y\pi}$ of the equation (164) is less than $s_{m1} = \omega_1 t_{m1}$, then the plasticity hinge will occur in the middle of the span, and the beam will go into the plastic stage. In this stage the beam appears in the form of a mechanism made up of absolutely rigid halfbeams joined by the plasticity hinge. In the bearing cross sections, concentrated moments are applied equal to $-M_{\text{hinge}}^{\text{bear}}$ from (142); in the middle of the plasticity hinge, a moment from (155):

$$M_{\text{w}}^{\text{np}} = M_{p1}^{\text{np}} T_2^*(\tau_2) = M_{p1}^{\text{np}} y_2^*(s_{y\pi}). \quad (176)$$

The total beam deflection for its left half in the plasticity stage is:

$$\begin{aligned} \omega_n(x, t) &= \varphi(t)x + \omega_2(x, \tau_2) = \\ &= \varphi(t)x + \rho G(x)T_2(\tau_2) + \rho F(x)T_1(\tau_1). \end{aligned} \quad (177)$$

The function $\varphi(t)$ included here will be found from the equation

$$\frac{ml^3}{24} \ddot{\varphi} = \frac{\rho l^3}{8} \left(1 - \frac{l}{\theta}\right) - M_{\text{w}}^{\text{np}} - M_{\pi 1}^{\text{on}}, \quad (178)$$

which is obtained from the equation (130) analogously to the equation (80).

Solving equation (178), let us find the total values of the deformations for the working time of the beam in all three stages:

in the bearing hinge

$$\psi_{\text{maxc}}^{\text{on}} = \psi_2^{\text{on}}(\tau_2) + \varphi(\bar{t}_{\text{maxc}}) = \frac{\rho l^3}{192B^{\text{np}}} k_{\pi 2}^{\text{on}}, \quad (179)$$

where

FOR OFFICIAL USE ONLY

FOR OFFICIAL USE ONLY

$$k_n^{on} = \nu_2 y_1(s_y) + 8y_2(s_{yn}) + 0,576 \left(1 - \frac{s_{yn}}{\omega_1 \theta} - \gamma_2 - \frac{\bar{s}_{maxc}}{3\omega_1 \theta} \right)^2 \bar{s}_{maxc}^2 + 2,82r_2 \bar{s}_{maxc} \quad (180)$$

$$\bar{s}_{maxc} = \omega_1 \bar{t}_{maxc} = \omega_1 \theta \left[1 - \frac{s_{yn}}{\omega_1 \theta} - \gamma_2 + \sqrt{\left(1 - \frac{s_{yn}}{\omega_1 \theta} - \gamma_2 \right)^2 + \frac{2,17r_2}{\omega \theta}} \right]; \quad (181)$$

$$r_2 = c_1 \cos \omega (\tau_2 - \tau_1) + c_2 \sin \omega (\tau_2 - \tau_1) - \frac{1}{\omega \theta};$$

in the middle of the beam span

$$\psi_{maxc}^{pp} = \frac{4w_2 \left(\frac{l}{2}, \tau_2 \right)}{l} + 2\varphi(\bar{t}_{maxc}) = \frac{\rho l^3}{96B^{pp}} k_n^{pp},$$

where

$$k_n^{pp} = y_1(s_y) + 5y_2(s_{yn}) + 0,576 \left(1 - \frac{s_{yn}}{\omega_1 \theta} - \gamma_2 - \frac{\bar{s}_{maxc}}{3\omega_1 \theta} \right)^2 \bar{s}_{maxc}^2 + 2,82r_2 \bar{s}_{maxc}; \quad (182)$$

$$\gamma_2 = \frac{8(M_{\bar{w}}^{pp} + M_{\bar{w}}^{on})}{\rho l^2} = T_1(\tau_1) + T_2(\tau_2).$$

The transverse force assumes the maximum value at the end of the elastic-plastic stage, and its value on the support will be:

$$Q_{maxc} = \frac{\rho l}{2} [T_1(\tau_1) + T_2(\tau_2)] = \frac{\rho l}{2} \gamma_2 = \frac{\rho l}{2} k_Q. \quad (183)$$

For $\theta = \infty$ the expressions for the dynamicity coefficients with respect to the displacements (180) and (182) have the form:

$$k_n^{on} = \nu_2 y_1(s_y) + 8y_2(s_{yn}) + \frac{3,47r_2^2}{\gamma_2 - 1}; \quad (184)$$

$$k_n^{pp} = y_1(s_y) + 5y_2(s_{yn}) + \frac{3,47r_2^2}{\gamma_2 - 1}, \quad (\gamma_2 > 1). \quad (185)$$

As is obvious from (139), (164), (171), the values of the dynamicity coefficients k_{π}^{bear} , k_{π}^{span} for the beam with given values of the parameters β_1 (125), β_2 (170) and $\omega_1 \theta$ are completely defined by the value of the coefficient (140). In Figure 37 the graphs are plotted for k_{π}^{bear} , k_{π}^{span} and k_Q for different values of the parameters β_1 , β_2 and $\omega_1 \theta$.

FOR OFFICIAL USE ONLY

FOR OFFICIAL USE ONLY

For clamped beams, the strength of the material of which is not influenced by the deformation rate, the formulas (179)-(185) are also valid if we set $\gamma = k_M^{\text{bear}}$ in them, and the equations (139) and (164) are replaced, respectively, by the equations:

$$k_M^{\text{on}} = y_1(s_y); \quad (186)$$

$$k_M^{\text{np}} = y_2^2(s_{y_n}); \quad k_M^{\text{np}} = k_M^{\text{on}} \frac{2k_1}{\beta_2(3-2k_1)}. \quad (187)$$

Figure 38 shows the graphs of the relations for k_π^{bear} , k_π^{span} and k_Q as a function of k_M^{bear} . Let us write the strength condition of a beam clamped to the supports when calculating it by the limiting state Ia:

$$\psi_{\text{max}}^{\text{on}} = \frac{pl^3}{192B^{\text{np}}} k_n^{\text{on}} \leq 0,5\psi_n^{\text{on}}; \quad \psi_{\text{max}}^{\text{np}} = \frac{pl^3}{96B^{\text{np}}} k_n^{\text{np}} \leq \psi_n^{\text{np}}, \quad (188)$$

where ψ_π^{bear} , ψ_π^{span} are the limiting angles of opening in the bearing and spanning plasticity hinges, respectively, determined by the graph in Figure 28.

The factor 0.5 on ψ_π^{bear} in (188) is taken for approximate consideration of the effect of the finishing on the strength of the section of the beam adjacent to it.

If the beam does not reach the plastic stage, that is, equation (164) has no solution, then in this case it is necessary to check its strength when working in the elastic-plastic stage from the condition

$$\psi_{2\text{max}}^{\text{on}} = \frac{pl^3}{192B^{\text{np}}} k_{n2}^{\text{on}} \leq 0,5\psi_n^{\text{on}}, \quad (189)$$

where $k_{\pi 2}^{\text{bear}}$ is found by formula (173).

If $\psi_{2\text{max}}^{\text{bear}} < 0,5\psi_\pi^{\text{bear}}$, this means that the beam can withstand a load of greater magnitude than used in the calculation. For $\psi_{2\text{max}}^{\text{bear}} > 0,5\psi_\pi^{\text{bear}}$, destruction of the beam takes place on the supports to the occurrence of plastic deformations in the reinforcing in the middle of the span. This case indicates the impossibility of redistribution of the forces as a result of the plastic deformations from inefficient reinforcing of the beam.

7. Calculation of a Beam with One Clamped End and the Other Hinged End in the Plastic Stage

When deriving the calculation functions we shall begin with the prerequisites which were adopted when calculating the beam clamped on supports. The rigidity of the beam in the section of length a adjacent to the clamped support will be denoted by B^{bear} , the rigidity on the remaining part of the

FOR OFFICIAL USE ONLY

FOR OFFICIAL USE ONLY

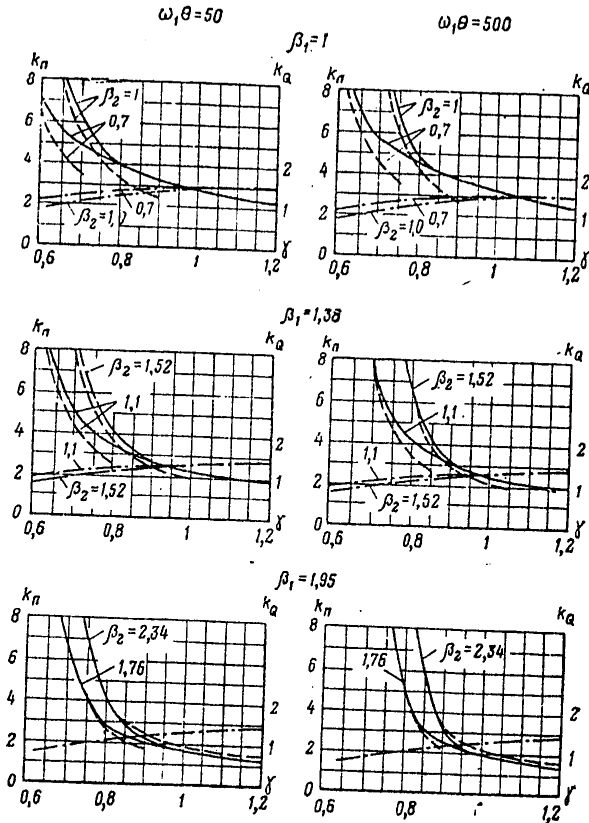


Figure 37. Dynamicity coefficients in the plastic stage for a clamped beam considering the effect of the deformation rate. Solid line -- k_n^{bear} , dotted line -- k_n^{span} , dash-dotted line -- k_Q . In Figures 37, 38 and 40-47 the left-hand scale is for the dynamicity coefficients with respect to displacements; the right-hand scale is for the dynamicity coefficients with respect to transverse force.

beam, B^{span} . The value of a will be determined from the condition of vanishing of the bending moment in the cross section with the coordinate $x = l - a$.

The magnitude of the bearing moment (M^{bear}) is found from the expression

$$M^{on} = \frac{-\rho l^2}{8} k_4, \quad (190)$$

FOR OFFICIAL USE ONLY

FOR OFFICIAL USE ONLY

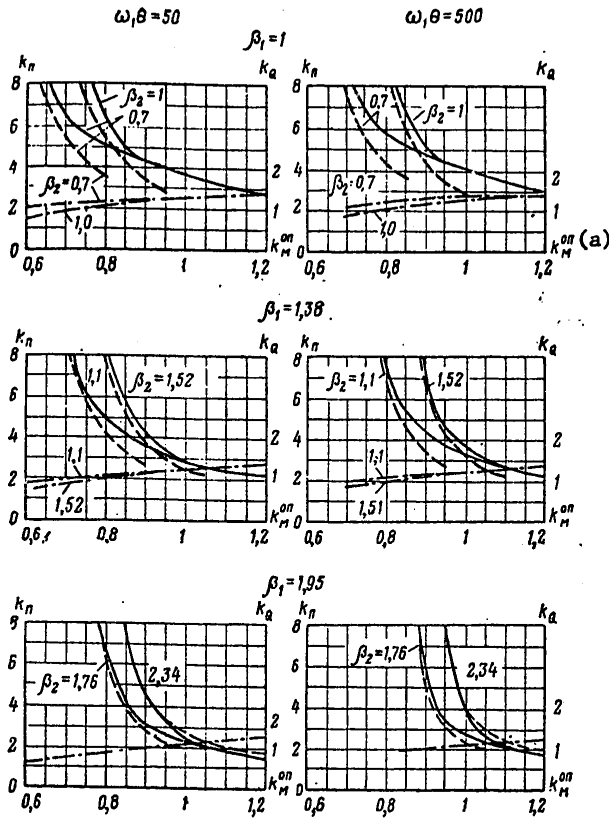


Figure 38. Dynamicity coefficients in the plastic stage for a clamped beam without considering the effect of the deformation rate. Solid line -- k_{bear} , dotted line -- k_{span} , dash-dotted line -- k_Q .

Key: a. bear

where

$$k_2 = \frac{\frac{1}{\beta_1} + (1 - \alpha_2)^3 (1 + 3\alpha_2) \left(1 - \frac{1}{\beta_1}\right)}{\frac{1}{\beta_1} + (1 - \alpha_2)^3 \left(1 - \frac{1}{\beta_1}\right)}; \quad \alpha_2 = \frac{a}{l}; \quad \beta_1 = \frac{B^{\text{on}}}{B^{\text{np}}}. \quad (191)$$

The bearing reaction on the hinged support will be:

$$A = \frac{Pl}{2} \left(1 - \frac{k_2}{4}\right) \quad (192)$$

FOR OFFICIAL USE ONLY

FOR OFFICIAL USE ONLY

The bending moment in the span will assume the maximum value in the cross section with the coordinate

$$x_0 = \frac{l}{2} \left(1 - \frac{k_2}{4} \right). \quad (193)$$

Its value will be:

$$M^{np} = \frac{p l^2}{8} \left(1 - \frac{k_2}{4} \right)^2. \quad (194)$$

If the following expression is satisfied

$$\frac{|M^{on}|}{M^{np}} = \frac{k_2}{\left(1 - \frac{k_2}{4} \right)^2} > \frac{M_{in}^{on}}{M_{in}^{np}}, \quad (195)$$

the first plasticity hinge will occur on the support. Then we shall consider the case itself. The calculations show that it is possible to set $\alpha_2 \approx 0.3$. Then

$$k_2 = \frac{0,26 + 0,74\beta_1}{0,578 + 0,422\beta_1}. \quad (196)$$

The dynamic load is assumed in the form of (17).

The expression for the elastic deflection of the beam will be represented, as before, in the form of (131), where $F(x)$ is the corresponding static for of the deflections:

$$T_1(t) = 1 - \frac{t}{\theta} - \cos \omega_2 t + \frac{\sin \omega_2 t}{\omega_2 \theta}; \quad (197)$$

$$\omega_2 \approx \frac{15,45}{l^2} \sqrt{\frac{B^{np}}{m}}. \quad (198)$$

In the elastic stage the bending moments on the support and in the span (for $x = x_0$):

$$M_1^{on}(t) = -\frac{p l^2}{8} k_2 T_1(t);$$

$$M_1^{np}(t) = \frac{p l^2}{8} \left(1 - \frac{k_2}{4} \right)^2 T_1(t). \quad (199)$$

After the occurrence of the plasticity hinge on the support, the elastic-plastic stage of working of the beam comes. The time τ_1 of the end of the elastic stage is found from the equation (139), in which:

$$\gamma = k_M^{on} \omega_2^{1/17} = \frac{M_0^{on}}{M_{p2}^{on}} \omega_2^{1/17}; \quad s_y = \omega_2 \tau_1; \quad (200)$$

$$y_1(s) = 1 - \frac{s}{\omega_2 \theta} - \cos s + \frac{\sin s}{\omega_2 \theta}; \quad M_{p2}^{on} = \frac{p l^2}{8} k_2. \quad (201)$$

FOR OFFICIAL USE ONLY

FOR OFFICIAL USE ONLY

In the elastic-plastic stage the beam is considered as a hinge-supported beam with concentrated moment on the right end equal to:

$$M_w^{on} = \frac{\rho l^2}{8} k_2 T_1(\tau_1) = M_{p2}^{on} \gamma_1; \quad \gamma_1 = T_2(\tau_1). \quad (202)$$

The angle of opening in the bearing plasticity hinge will be:

$$\psi_2^{on}(t) = \psi_y^{on} + \psi_{yn}^{on} = \frac{\rho l^2}{106,8 B^{np}} [\bar{v}_2 \gamma_1 + 4,45 T_2(t)], \quad (203)$$

where

$$\begin{aligned} T_2(t) &= \bar{c}_1 \sin \omega(t - \tau_1) - \bar{c}_2 \cos \omega(t - \tau_1) + 1 - \gamma_1 - \frac{t}{\theta}; \\ \bar{c}_1 &= \frac{\omega_2}{\omega} \bar{r}_1 \bar{v}_3 + \frac{1}{\omega \theta}; \quad \bar{c}_2 = 1 - \gamma_1 - \frac{\tau_1}{\theta}; \\ \bar{v}_2 &= 0,168 - 0,6 \left(1 - \frac{k_2}{4}\right) + 1,225 \bar{v}_1 + (0,06 k_2 - 0,018) \frac{1}{\beta_1}; \\ \bar{v}_1 &= 0,637 - 0,245 k_2 - (0,067 - 0,175 k_2) \frac{1}{\beta_1}; \\ \bar{v}_3 &= \frac{4,45}{(1 - \xi_m)} \left[\xi_m^3 - 2 \left(1 - \frac{k_2}{4}\right) \xi_m^2 + (2 - 1,5 k_2) \xi_m + k_2 - 1 \right]. \end{aligned}$$

Here $\xi_m = x_m / l$ is the relative coordinate of the cross section with maximum deflection determined from the equation

$$\begin{aligned} 4 \xi_m^3 - 6 \left(1 - \frac{k_2}{4}\right) \xi_m^2 + \bar{v}_1 &= 0; \\ 0 \leq \xi_m &\leq 1 - \alpha_2. \end{aligned}$$

The transverse forces in the elastic-plastic stage are equal to the following:

on the hinged support

$$Q_2(0, t) = \frac{\rho l}{2} \left[\left(1 - \frac{k_2}{4}\right) \gamma_1 + T_2(t) \right];$$

on the clamped support

$$Q_2(l, t) = \frac{\rho l}{2} \left[\left(1 + \frac{k_2}{4}\right) \gamma_1 + T_2(t) \right].$$

The elastic-plastic stage continues until the time of formation of the plasticity hinge in some spanning cross section of the beam in which the bending

FOR OFFICIAL USE ONLY

FOR OFFICIAL USE ONLY

moment has the greatest (with respect to this band) value. The coordinate x_0 of this cross section will be defined from the expression

$$x_0 = \frac{l \left[\left(1 - \frac{k_2}{4}\right) \gamma_1 + T_1(t) \right]}{2 \{ \gamma_1 + T_1(t) \}} \quad (204)$$

Thus, the coordinate (x_0) of the cross section in which deformation of a second plasticity hinge is possible will depend on time. Consideration of this function leads to very tedious calculations when determining the time (τ_2) of the end of the elastic-plastic stage. Therefore it is expedient to make this calculation by successive approximations: being given some value of x_0 , determine the time τ_2 and then compare the adopted value with the values calculated by formula (204) for $t = \tau_2$.

The equation for determining the time τ_2 of the end of the elastic-plastic stage has the form analogous to (164):

$$1,1776\gamma' = R_2(s_{yn}); s_{yn} = \omega_2\tau_2, \quad (205)$$

where

$$R_2(s) = \left\{ s_{yn} [(2\eta - \eta^2) \gamma_1]^{17} + \frac{\left(1 - \frac{k_2}{4}\right) (s - s_{yn}) [(y_2^*(s))^{18} - ((2\eta - \eta^2) \gamma_1)^{18}]}{2\eta \left[1 - \frac{1}{2} \left(1 - \frac{k_2}{4}\right) \eta\right] y_2(s)} \right\}^{1/17};$$

$$\gamma' = \frac{M_0^{np} \omega_2^{1/17}}{M_{p2}^{np}} = k_M^{np} \omega_2^{1/17};$$

$$M_{p2}^{np} = \frac{pl^2}{8} \left(1 - \frac{k_2}{4}\right)^2; \quad (206)$$

$$y_2(s) = T_2 \left(\frac{s}{\omega_2}\right); y_2^*(s) = (2\eta - \eta^2) \gamma_1 +$$

$$+ \frac{2\eta \left[1 - \frac{1}{2} \left(1 - \frac{k_2}{4}\right) \eta\right]}{1 - \frac{k_2}{4}} T_2 \left(\frac{s}{\omega_2}\right); \quad (207)$$

$$\eta = \frac{2x_0}{l \left(1 - \frac{k_2}{4}\right)}$$

FOR OFFICIAL USE ONLY

FOR OFFICIAL USE ONLY

Here M_0^{span} is the moment of the internal forces in the cross section in which the plasticity hinge arose;

$k_M^{np} = \frac{M_0^{np}}{M_{p2}^{np}}$ is the dynamicity coefficient with respect to the bending moment the span.

Just as when calculating the beam clamped on both ends, the case is possible where the beam works only in the elastic-plastic stage. This takes place if the equation (205) has no solution.

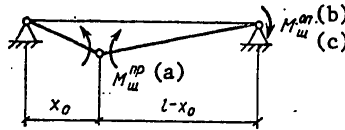


Figure 39. Calculation diagram of the beam with one clamped and the other hinged supports in the plastic stage.

Key: a. span b. bear c. hinge

The angle of opening in the bearing hinge is defined by formula (203) for $t = t_{m1}$, where t_{m1} is the time for the beam to reach the maximum elastic-plastic deflection. The time t_{m1} satisfies the equation $dT_2/dt = 0$ and is defined by the formula

$$\operatorname{tg} \frac{\omega(t_{m1} - \tau_1)}{2} = \frac{\bar{c}_2 + \sqrt{\bar{c}_1^2 + \bar{c}_2^2 - \frac{1}{(\omega\theta)^2}}}{\bar{c}_1 + \frac{1}{\omega\theta}} \quad (208)$$

The beam strength conditions in this case has the form

$$\psi_{2max}^{on} \leq 0,5\psi_n^{on} \quad (209)$$

In the plastic stage the beam is represented by a mechanism depicted in Figure 39. A moment equal to $-M_{hinge}^{bear}$ is applied to the right-hand bearing cross section. In the spanning plasticity hinge occurring in the cross section with the coordinate $x = x_0$, the moment acts equal to: $M_{hinge}^{span} = M_{p2}^{span} T_2^*(\tau_2)$.

If the angle of rotation of the left-hand side of the beam (x_0 long) it is denoted by $\phi(t)$, the angle of rotation $\phi_1(t)$ of the right-hand side of the beam will be:

$$\phi_1(t) = \phi(t) \frac{x_0}{l - x_0} = \phi(t) \frac{\xi_0}{1 - \xi_0}; \quad \xi_0 = \frac{x_0}{l}$$

FOR OFFICIAL USE ONLY

FOR OFFICIAL USE ONLY

The equation of motion of the beam in the plastic stage has the form:

$$\ddot{\varphi} = \frac{3p}{2x_0\pi} \left(1 - \frac{l}{\theta} - \gamma_2 \right), \text{ where } \gamma_2 = T_1(\tau_1) + T_2(\tau_2).$$

After the calculations we determine the angles of opening in the plasticity hinges. The angle of opening in the bearing plasticity hinge is:

$$\psi_{\text{maxc}}^{\text{on}} = \frac{pl^3}{106,8B^{\text{np}}} k_n^{\text{on}}; \quad (210)$$

where

$$k_n^{\text{on}} = \bar{v}_2 \gamma_1 + 4,45T_2(\tau_2) + \frac{0,335}{(1-\xi_0)} \left(1 - \frac{s_{yn}}{\omega_2 \theta} - \gamma_2 - \frac{\bar{s}_{\text{maxc}}}{3\omega_2 \theta} \right) \bar{s}_{\text{maxc}}^2 + \frac{1,13r_3 \bar{s}_{\text{maxc}}}{1-\xi_0};$$

$$\bar{s}_{\text{maxc}} = \omega_2 \theta \left[1 - \frac{s_{yn}}{\omega_2 \theta} - \gamma_2 + \sqrt{\left(1 - \frac{s_{yn}}{\omega_2 \theta} - \gamma_2 \right)^2 + \frac{2,17r_3}{\omega \theta}} \right]. \quad (211)$$

(212)

The angle of opening in the plasticity spanning hinge considering the provisional angle of opening in the elastic-plastic stage is:

$$\psi_{\text{maxc}}^{\text{np}} = \frac{pl^3}{43,8B^{\text{np}}} k_n^{\text{np}}, \quad (213)$$

where

$$k_n^{\text{np}} = \bar{v}_4 \gamma_1 + \bar{v}_5 T_2(\tau_2) + \frac{0,138}{\xi_0(1-\xi_0)} \left(1 - \frac{s_{yn}}{\omega_2 \theta} - \gamma_2 - \frac{\bar{s}_{\text{maxc}}}{3\omega_2 \theta} \right) \bar{s}_{\text{maxc}}^2 + \frac{0,465r_3 \bar{s}_{\text{maxc}}}{\xi_0(1-\xi_0)}; \quad (214)$$

$$\bar{v}_4 = \frac{3,65}{1-\xi_0} \left[\frac{\xi_0^3}{2} - \left(1 - \frac{\xi_2}{4} \right) \xi_0^2 + \frac{\bar{v}_1}{2} \right];$$

$$\bar{v}_5 = \frac{3,65}{1-\xi_0} \left(\frac{\xi_0^3}{2} - \xi_0^2 + \frac{1}{2} \right).$$

For $\theta = \infty$ the dynamicity coefficients with respect to displacements k_{π}^{bear} , k_{π}^{span} are calculated by the formulas:

$$k_n^{\text{on}} = \bar{v}_2 \gamma_1 + 4,45T_2(\tau_2) + \frac{0,962r_3^2}{(1-\xi_0)(\gamma_2-1)}; \quad (215)$$

$$k_n^{\text{np}} = \bar{v}_4 \gamma_1 + \bar{v}_5 T_2(\tau_2) + \frac{0,395r_3^2}{\xi_0(1-\xi_0)(\gamma_2-1)}, \quad (\gamma_2 > 1). \quad (216)$$

FOR OFFICIAL USE ONLY

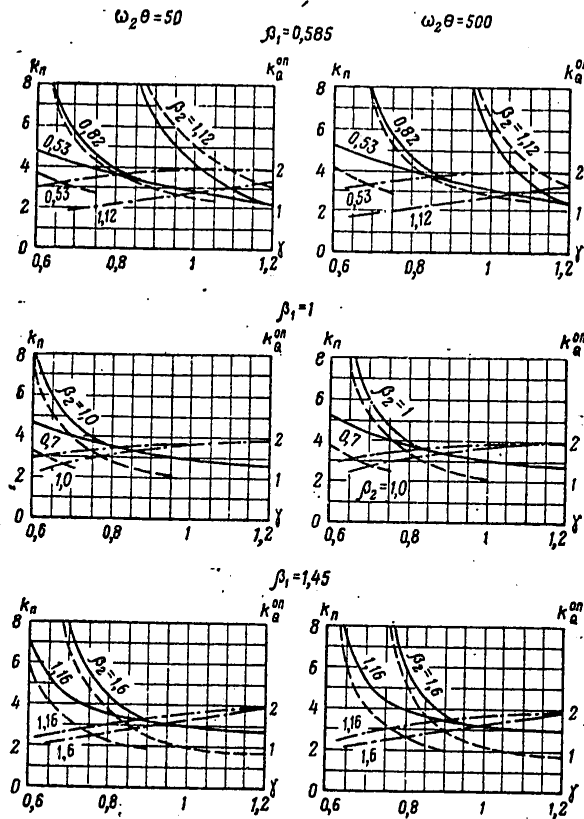


Figure 40. Dynamicity coefficients in the plastic stage for a beam with one clamp support and the other hinged support considering the effect of the deformation rate. In Figures 40-43, 46 and 47 the following are denoted: the solid line denotes k_{bear} ; the dotted line denotes k_{span} ; the dash-dotted line is k_{span}^Q on the clamped support.

The following relation exists between the dynamicity coefficients with respect to the bending moment

$$k_M^{np} = k_M^{on} \frac{k_2}{\beta_2 \left(1 - \frac{k_2}{4}\right)^2}; \quad \beta_2 = \frac{M_0^{on}}{M_0^{np}} \tag{217}$$

Then

$$\gamma' = \gamma \frac{k_2}{\beta_2 \left(1 - \frac{k_2}{4}\right)^2}$$

FOR OFFICIAL USE ONLY

FOR OFFICIAL USE ONLY

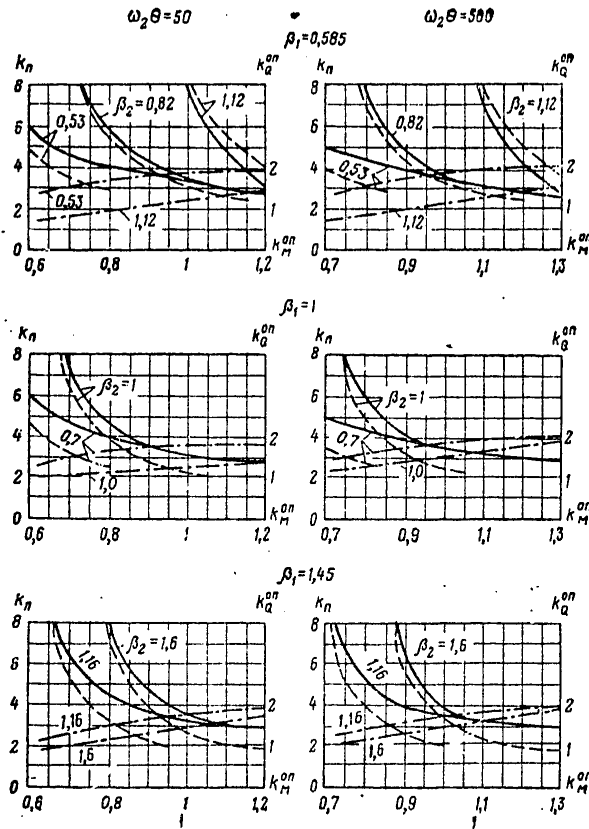


Figure 41. Dynamicity coefficients in a plastic stage for a beam with one clamped support and the other hinged support without considering the effect of the deformation rate.

and therefore the values of the dynamicity coefficients k_{π}^{bear} , k_{π}^{span} are completely determined by the values of the parameters β_1 , β_2 , $\omega_2\theta$, γ . In Figure 40 the graphs are constructed for k_{π}^{bear} , k_{π}^{span} and k_Q on a clamped support for certain values of the parameters β_1 , β_2 , $\omega_2\theta$. When calculating beams without considering the effect of the deformation rate in the expressions obtained it is necessary to set $\gamma = k_M^{bear}$, and the equations for determining s_y and $s_{y\pi}$ are taken as follows:

$$k_M^{on} = y_1(s_y); k_M^{np} = y_2(s_{y\pi}). \tag{218}$$

FOR OFFICIAL USE ONLY

FOR OFFICIAL USE ONLY

In Figure 41 graphs are presented for k^{bear} , k^{span} and k_Q on a clamp support obtained without considering the effect of the deformation rate. The checking of the beam strength when calculating it by the limiting state Ia is done just as for a beam clamped on both supports.

8. Calculation of Continuous Beams

The dynamic calculation of continuous beams is appreciably more complicated than the calculation investigated in the preceding items, especially if it is necessary to consider the nonsimultaneous loading of the spans under a dynamic load. This situation occurs in the case of movement of the shock wave front along the longitudinal axis of the beam. Later a more detailed investigation will be made only of the case where simultaneous loading of all of the spans takes place.

In the elastic stage it is possible to perform the calculation in accordance with item 2. The displacements and forces are found by multiplication of their static values from the load of intensity p (determined, for example, by the tables for calculating continuous beams) times the dynamicity function $T(t)$ which satisfies equation (7). The value of ω entering into this function is taken to coincide with the angular frequency of the natural vibrations of the continuous beam which corresponds to the shape of the vibrations closest to the elastic line from the static load p . For continuous, equal-span beams with edge hinge supports it is possible to take:

for two spans

$$\omega_B = \frac{15,45}{\rho} \sqrt{\frac{B^{np}}{m}}; \quad (219)$$

for three spans

$$\omega_B = \frac{18,3}{\rho} \sqrt{\frac{B^{np}}{m}}; \quad (220)$$

for four or more spans

$$\omega_B = \frac{22,4}{\rho} \sqrt{\frac{B^{np}}{m}}. \quad (221)$$

Here B^{span} is the bending rigidity of the beam cross sections in the spans.

After formation of the plasticity hinges on all of the supports the continuous beam is converted to a set of single-span, hinge-supported beams with concentrated bending moments in the bearing cross sections. Therefore each span can be approximately calculated by the relations obtained above for the single-span beams with different supporting conditions on the ends. Here the middle spans of the continuous beam must be calculated by the formulas for the single-span beam clamped on both supports, and the edge span with the hinge support, by the formulas for the beam with one clamped and the other hinged supports. In these formulas, the values of the coefficients (128) and (196) can be changed, taking into account the redistribution between the bending moments on the supports and in the span and the magnitude of the angular frequency of the oscillations ω_i ($i = 1, 2$).

FOR OFFICIAL USE ONLY

FOR OFFICIAL USE ONLY

The value of the coefficient k_1 must be changed in accordance with the values of the ratios between the supporting and spanning bending moments in the continuous beam. For unequal values of the moments on the supports it is possible to take their mean values. Let us obtain the values of these coefficients which will be denoted by k_1^H , for the equal-span continuous beam with edge hinge supports. From the tables for calculating the continuous beams we find that on the second supports from the ends for any number of spans greater than two, the bearing moment is: $M_1^{\text{bear}} \approx -0.1pl^2$. Therefore when calculating the edge spans it is necessary in place of k_2 from (196) to take

$$k_2^H = \frac{0.1}{1} k_2 = 0.8k_2.$$

For the two-span beam $M_1^{\text{bear}} = -0.125 pl^2$, and therefore $k_2^H = k_2$. When calculating the middle spans the value of coefficient k_1^H will depend on the number of spans:

for three spans $M_1^{\text{bear}} = -0.1pl^2$, and therefore instead of k_1 from (128) we take $k_1^H = 1.2k_1$;

for four spans $M_1^{\text{bear}} = -0.107 pl^2$; $M_2^{\text{bear}} = -0.071 pl^2$;

$$\frac{0.107+0.071}{2} = 0.089 \text{ and } k_1^H = \frac{0.089}{1} k_1 = 1.07k_1;$$

for five spans $M_1^{\text{bear}} = -0.105 pl^2$; $M_2^{\text{bear}} = M_3^{\text{bear}} = -0.079 pl^2$.

Then:

for the second span

$$k_1^H = \frac{0.105+0.079}{2 \cdot \frac{1}{12}} k_1 = 1.105k_1;$$

for the third span $k_1^H = 0.948k_1$.

The oscillation frequencies ω_i ($i = 1, 2$) are replaced by the corresponding oscillation frequencies ω_H of the continuous beam defined for the equal-span beam with edge hinged supports by the formulas (219)-(221). In the dimensionless expressions (180), (182), (211), (214) here it is necessary to multiply the third term times the ratio $(\omega_i/\omega_H)^2$ and the fourth term by ω_i/ω_H . The angles of opening in the bearing plasticity hinges ψ_1^{bear} of the continuous beam are taken equal to the sum of the angles of opening in the supporting hinges of the adjacent spans.

FOR OFFICIAL USE ONLY

FOR OFFICIAL USE ONLY

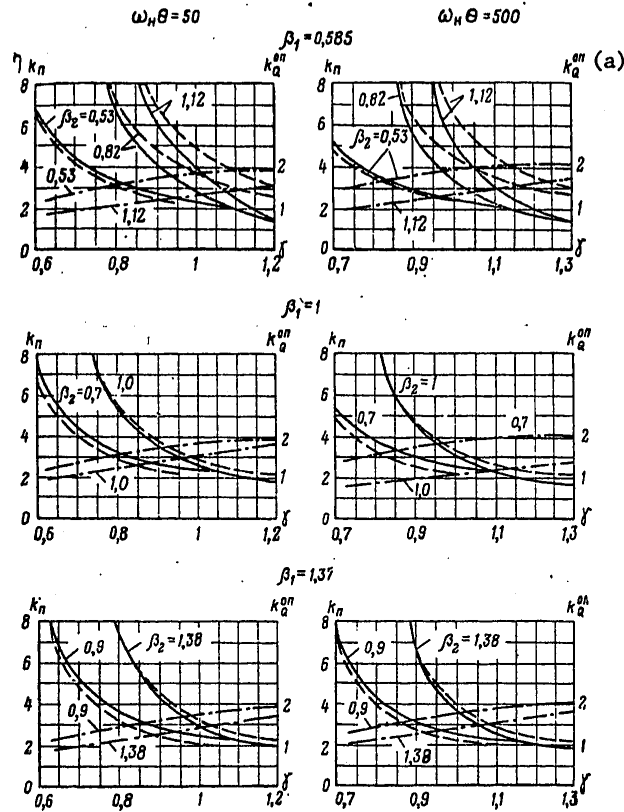


Figure 42. Dynamicity coefficients in the plastic stage for the edge span of a continuous three-span beam with edge hinge supports considering the effect of the deformation rate.

Key: a. bear

When performing the calculation with respect to the limiting state Ia the strength condition of the continuous beam is: for the spans $\psi_{\pi 1}^{span} \leq \psi_{\pi 1}^{span}$; for all of the supports, except the edge supports, $\psi_{\pi 1}^{bear} \leq \psi_{\pi 1}^{bear}$; for edge clamped supports $\psi_{\pi 1}^{bear} \leq 0.5 \psi_{\pi 1}^{bear}$.

The dynamicity coefficients k_{π}^{bear} , k_{π}^{span} , k_Q for continuous three-span beam are presented in graphs in Figures 42-45; for the edge spans of the continuous beam with more than three spans, on the graphs of Figures 46, 47. For the middle spans of continuous beams with more than three spans it is possible to use the graphs of the dynamicity coefficients for the clamped beam in Figures 37, 38.

FOR OFFICIAL USE ONLY

FOR OFFICIAL USE ONLY

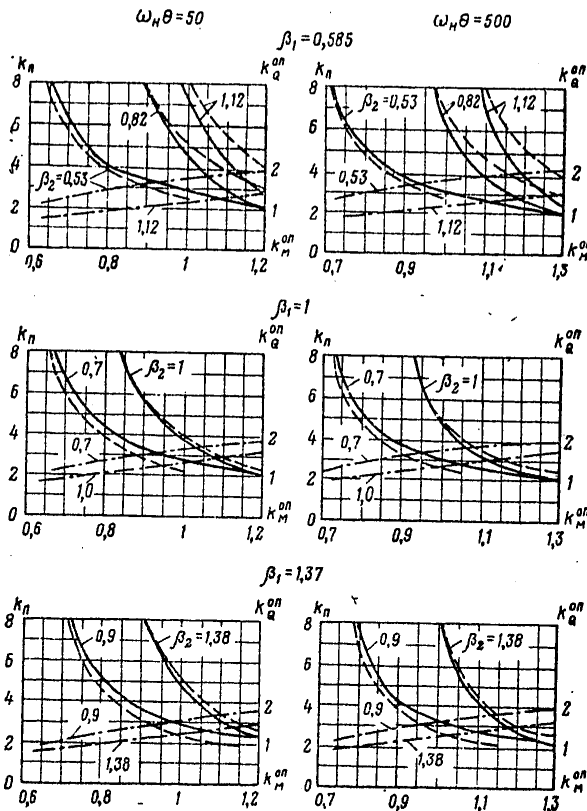


Figure 43. Dynamicity coefficients in the plastic stage for the edge span of a continuous three-span beam with edge hinge supports without considering the effect of the deformation rate.

9. Calculation of Rectangular Slabs

The rectangular slabs for which the ratio of the side lengths b and a satisfy the conditions $b/a > 2$ usually pertain to beam slabs and they are calculated by the above-discussed methods. If

$$1 \leq \frac{b}{a} \leq 2, \tag{222}$$

the calculation of the slabs must be made considering the bearing conditions with respect to all four sides.

The dynamic calculation of the slabs is much more complicated than the calculation of the beams. Even under the effect of static loads the solution

FOR OFFICIAL USE ONLY

FOR OFFICIAL USE ONLY

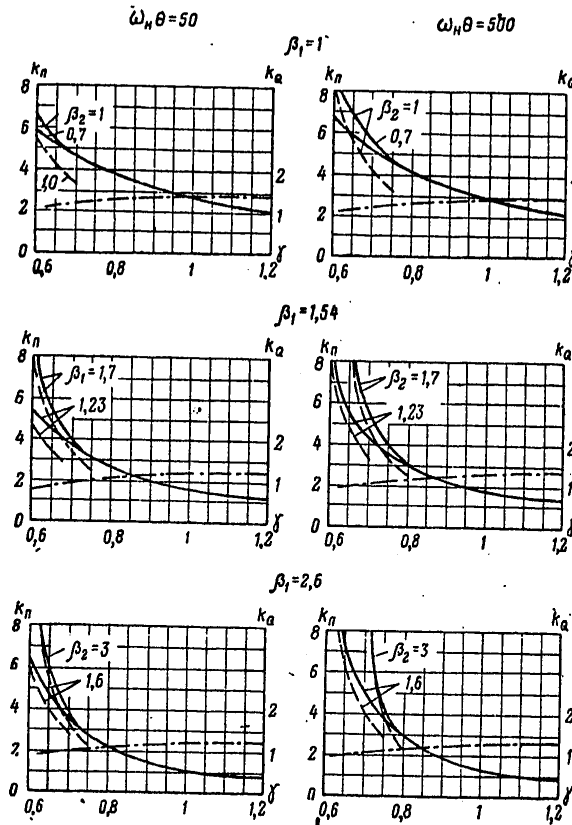


Figure 44. Dynamicity coefficients in the plastic stage for the middle spans of a continuous three-span beam with edge hinged supports considering the effect of the deformation rate (the dash-dotted line is k_Q).

of the slab equilibrium equation can be obtained only in infinite series and not for all of the support conditions along the edges [44]. Therefore the calculation of the slabs in the elastic stage for the effect of the investigated dynamic loads will be made by simplified methods discussed in item 2, as systems with one degree of freedom; the times (bending and torsional moments) and transverse forces will be found by multiplying their static values from the load with intensity $p = \Delta p$ defined by the slab calculation tables times the dynamicity coefficient $T(t)$ satisfying the equation (7). The angular solution frequency of the slab ω entering into $T(t)$ is taken equal to the lower angular frequency of the natural vibrations of the slab and is also determined by the reference data.

FOR OFFICIAL USE ONLY

FOR OFFICIAL USE ONLY

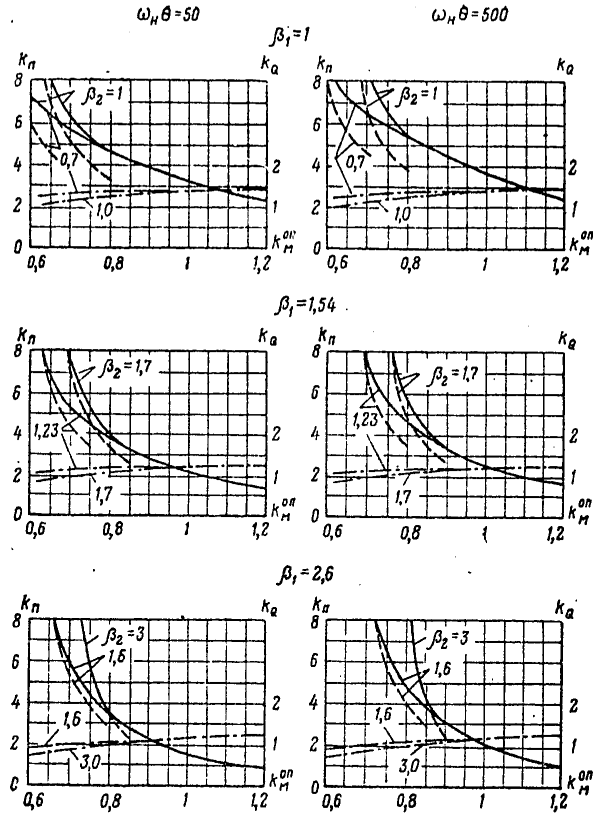


Figure 45. Dynamicity coefficients in the plastic stage for the middle spans of a continuous three-span beam with edge hinged supports without considering the effect of the deformation rate (dash-dotted line -- k_Q).

Hereafter we shall consider the calculation of a slab which is hinge supported on all four sides (see Figure 48). In this case the vibration frequency is:

$$\omega = \pi^2 \left(\frac{1}{a^2} + \frac{1}{b^2} \right) \sqrt{\frac{D}{m}}, \tag{223}$$

where m is the mass per unit area of the slab; $D = Eh^3(12(1 - \nu^2))$ is the cylindrical rigidity of the slab.

Let us denote the bending moments per unit length of cross section parallel to the sides of length b and a , respectively, by M_1 and M_2 . The largest

FOR OFFICIAL USE ONLY

FOR OFFICIAL USE ONLY

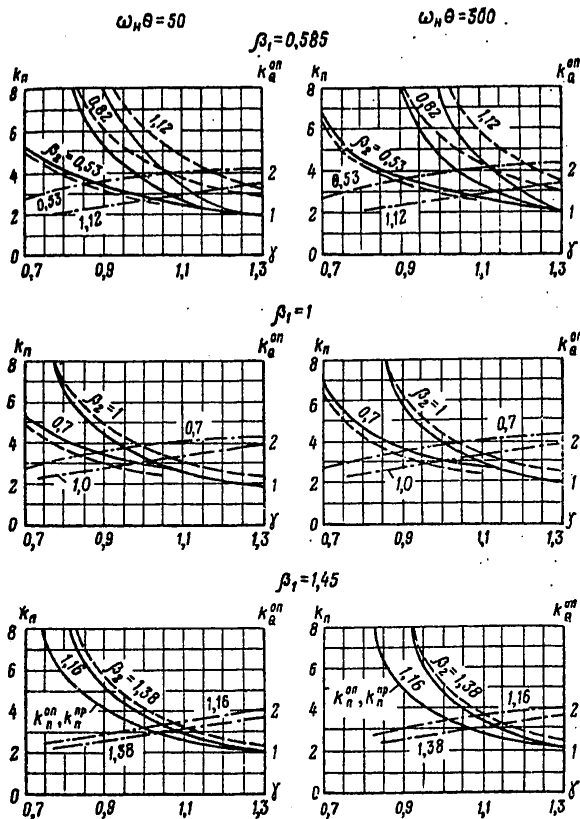


Figure 46. Dynamicity coefficients in the plastic stage for the edge span of a continuous beam with edge hinged supports with a number of spans greater than three considering the effect of the deformation rate.

values (at the center of the slab) are:

$$M_1(t) = \rho a^2 n_1 T(t); \tag{224}$$

$$M_2(t) = \rho a^2 n_2 T(t), \tag{225}$$

where the coefficients n_1, n_2 , depending on the value of the ratio b/a are assumed by Table 5.

The function $T(t)$ is defined by formulas (18), (24), (25) or (28). The deflection of the slab can be found from the expression [44]:

FOR OFFICIAL USE ONLY

FOR OFFICIAL USE ONLY

$$w(x, y, t) = \frac{16\rho a^4 \sin \frac{\pi}{b} x \sin \frac{\pi}{a} y}{\pi^6 D (1 + \chi^2)^3} T(t), \tag{226}$$

where $\chi = a/b$.

Table 5

b/a	1	1,1	1,2	1,3	1,4	1,5
n_1	0,0364	0,0438	0,0515	0,0587	0,0656	0,072
n_2	0,0364	0,0363	0,0357	0,0348	0,0336	0,032

b/a	1,6	1,7	1,8	1,9	2
n_1	0,0776	0,0829	0,0874	0,0911	0,0946
n_2	0,0303	0,0287	0,0266	0,0252	0,0236

The elastic stage of working of the slabs continues to the time τ when in certain cross sections the stresses in the reinforcing reach the yield point. Since $b > a$, the greatest bending moment will be in the cross section parallel to the side b , that is, $M_1(t)$. We shall consider that the slab is reinforced in such a way that the yield of the reinforcing is caused initially by this moment. Let us denote the dynamicity coefficient with respect to the bending moment by:

$$k_M = \frac{M_0^{(a)}}{\rho a^2 n_1} = \frac{M_0^{(a)}}{M_{p1}}; M_{p1} = \rho a^2 n_1, \tag{227}$$

where $M_0^{(a)}$ is the running moment of the internal forces in the middle of the slab in the cross section parallel to the side beam and the stresses in the reinforcing are equal to the static ultimate strength.

Then all of the relations will be valid for the end of the elastic stage obtained for a hinge-supported beam in item 5.

When calculating the slab in the plastic stage it is proposed that the slab is broken down into four rigid elements by the linear plasticity hinges (see Figure 48). Here it is important to consider the process of the development of the hinges in time and the law of variation of the stresses in the reinforcing in time, for these factors determine the magnitude of the dynamic ultimate strength in the reinforcing along the plasticity hinges. In the general case the dynamic ultimate strength will be variable along the plasticity hinges, which greatly complicates the calculation. A detailed analysis of the stressed state of the elastic slab performed on the basis of the exact solutions of the vibration equation indicates that the noted fact can be ignored for a slab loaded by a uniformly distributed load. In this case when $t > 2\pi/8\omega$ the value of the bending moment in the square slab varies little along its diagonals.

FOR OFFICIAL USE ONLY

FOR OFFICIAL USE ONLY

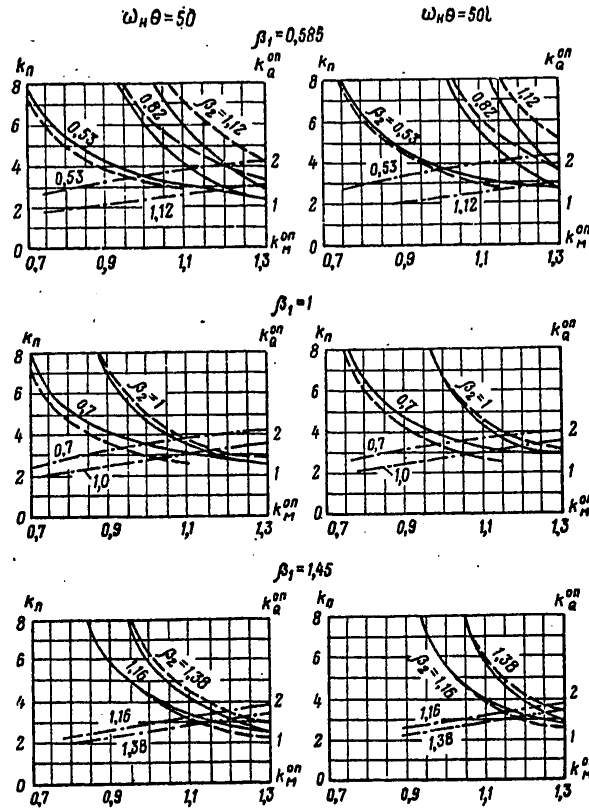


Figure 47. Dynamicity coefficient in the plastic stage for the edge span of a continuous beam with edge hinged supports with a number of spans greater than three without considering the effect of the deformation rate.

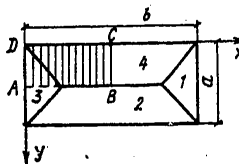


Figure 48. Calculation diagram of a rectangular hinge-supported slab. 1-4 -- rigid element.

FOR OFFICIAL USE ONLY

FOR OFFICIAL USE ONLY

In view of this fact let us assume that the stress in the reinforcing equal to the dynamic yield point occurs along all of the linear plasticity hinges simultaneously, and its value is constant along the entire length of the plasticity hinges. We shall consider that the fact is valid also for rectangular slabs under the condition (222) and sufficiently uniform reinforcing.

The equation of the vibrations of an elastic slab has the form [44]

$$D \left(\frac{\partial^4 w}{\partial x^4} + 2 \frac{\partial^4 w}{\partial x^2 \partial y^2} + \frac{\partial^4 w}{\partial y^4} \right) + m \frac{\partial^2 w}{\partial t^2} = p(t) = p f(t). \quad (228)$$

In the plastic stage the expression for the deflection will be represented in the form

$$w_a(x, y, t) = \varphi(t) \Omega(x, y) + pF(x, y) \gamma_1. \quad (229)$$

Here

$$\gamma_1 = T(\tau) = \frac{M_w^{(e)}}{\rho a^2 n_1}, \quad (230)$$

$F(x, y)$ is the static form of the deflections;

$\Omega(x, y)$ is the form of the deflections of the beam in the plastic stage.

For the segment of a slab ABCD (Figure 48) it has the form:

$$\Omega(x, y) = \begin{cases} x & \text{for } 0 \leq x \leq y, 0 \leq y \leq \frac{a}{2}; \\ y & \text{for } 0 \leq y \leq x, 0 \leq x \leq \frac{a}{2}; \\ y & \text{for } 0 \leq y \leq \frac{a}{2}, \frac{a}{2} \leq x \leq \frac{b}{2}. \end{cases} \quad (231)$$

$\phi(t)$ is the angle of rotation of the rigid discs of the slab.

Let us substitute expression (229) in equation (228), let us multiply all of the terms by $\Omega(x, y)$ and let us integrate over the area S of the slab. As a result, we obtain the equation

$$m \ddot{\varphi} \iint_S \Omega^2(x, y) dx dy = p [f(t) - \gamma_1] \iint_S \Omega(x, y) dx dy, \quad (232)$$

which after calculation of the integrals assumes the form

$$\frac{ma^3}{24} (2b-a) \ddot{\varphi} = \frac{pa^3}{12} (3b-a) [f(t) - \gamma_1]. \quad (233)$$

FOR OFFICIAL USE ONLY

FOR OFFICIAL USE ONLY

The initial velocity $\dot{\phi}_0$ will be determined from equality of the momentums of the end of the elastic and the beginning of the plastic stage:

$$\dot{\phi}_0 = \frac{64 \cdot 4 \rho a^3 T(\tau)}{\pi^2 D (1 + \chi^2)^2 \left(1 - \frac{\chi}{3}\right)} \quad (234)$$

With a load of the type of (17), $f(t) = 1 - t/\theta$, after integration of equation (233) we obtain the following expression for the angle of opening in the plasticity hinge:

$$\psi_{\text{max}} = \frac{64 \rho a^3}{\pi^2 D (1 + \chi^2)^2} k_{\pi} \quad (235)$$

where

$$k_{\pi} = \gamma_1 + \frac{0.461 (1 - 0.33\chi)}{(1 - 0.5\chi)} \left(1 - \frac{s_y}{\omega\theta} - \gamma_1 - \frac{\bar{s}_{\text{max}}}{3\omega\theta}\right) \bar{s}_{\text{max}} + \frac{0.81 r \bar{s}_{\text{max}}}{1 - 0.33\chi} \quad (236)$$

Here r is determined by the formula (83) and

$$\bar{s}_{\text{max}} = \omega\theta \left[1 - \frac{s_y}{\omega\theta} - \gamma_1 + \sqrt{\left(1 - \frac{s_y}{\omega\theta} - \gamma_1\right)^2 + \frac{1.76r (1 - 0.5\chi)}{\omega\theta (1 - 0.33\chi)^2}}\right], \quad \chi = \frac{a}{b} \quad (237)$$

When calculating the slab with respect to the limiting state Ia the strength condition will be $\psi_{\text{max}} \leq \psi_{\pi}$, where the limiting angle of opening ψ_{π} can be determined by the graph in Figure 28.

In Figures 49 and 50 the graphs are presented for k_{π} as a function of γ and k_M for two values of χ and different values of $\omega\theta$. For $\theta = \infty$ we have

$$k_{\pi} = \gamma_1 \left[1 + \frac{4.8 (2 - \chi) (2 - \gamma_1)}{(3 - \chi)^2 (\gamma_1 - 1)}\right] (\gamma_1 > 1) \quad (238)$$

Here $\chi = a/b$ (b is the length of the long side of the slab);

γ_1 is defined by the formulas:

when calculating the effect of the deformation rate $\gamma_1 = -\cos s_y$, where s_y is found from the solution of the equation

$$1.1776\gamma = s_y^{1/17} (1 - \cos s_y), \quad \gamma = \frac{M_0^2 \omega^{1/17}}{\rho a^2 n_1};$$

without considering the effect of the deformation rate

FOR OFFICIAL USE ONLY

FOR OFFICIAL USE ONLY

$$\gamma_1 = k_M = \frac{M_0^a}{\rho a^2 \alpha_1}$$

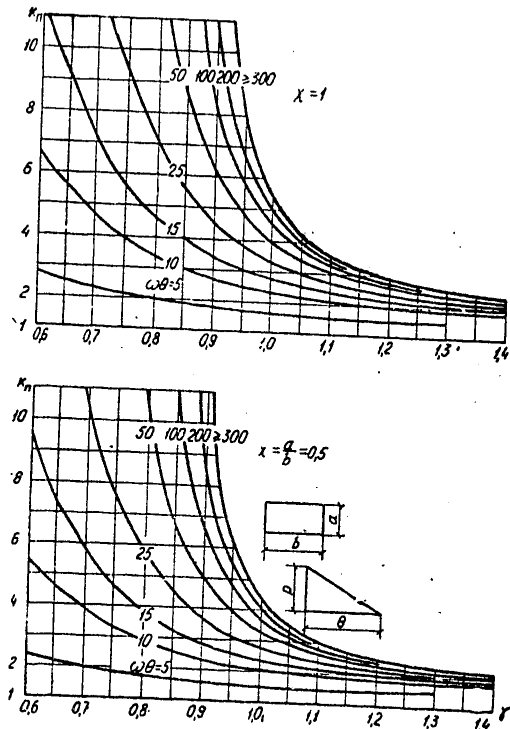


Figure 49. Dynamicity coefficient in the plastic stage for a hinge-supported plate considering the effect of the deformation rate.

10. Example Calculations

When calculating the structural elements reinforced with low-carbon steels (classes A-I, A-II, A-III) not strengthened by drawing, it is necessary to consider the effect of the deformation rate. For other reinforcing steels (for example, classes A-IV, A-IIv, A-IIIv) this effect is not taken into account.

When determining the parameters of the dynamic load (Δp , θ) we begin with the 1 Mton nuclear blast. The effective time θ of the wave effect will be determined by the formulas (16) of Chapter II -- with approximation of the law

FOR OFFICIAL USE ONLY

FOR OFFICIAL USE ONLY

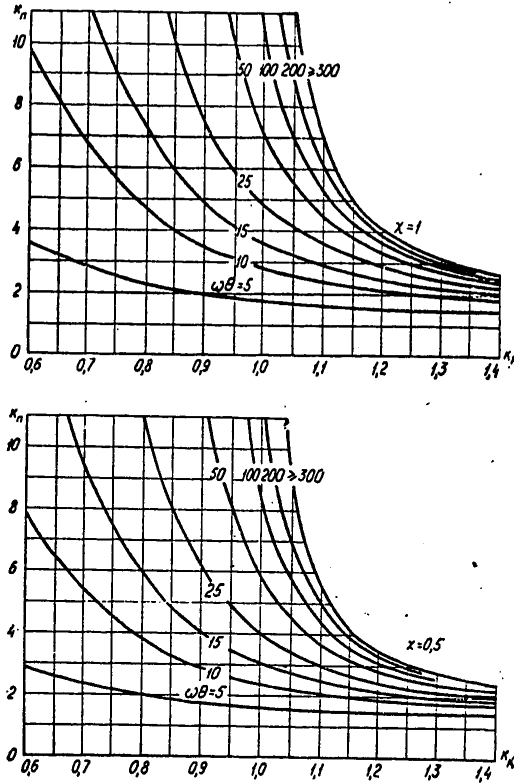


Figure 50. Dynamicity coefficient in the plastic stage for a hinge-supported plate without considering the effect of the deformation rate.

of pressure variation with time along the tangent.

Example 4. The ceiling of a separately standing shelter is made of continuous hinge-supported reinforced concrete slabs with basic characteristics: $l = 300$ cm, $b = 80$ cm, $h = 30$ cm ($h_0 = 27$ cm), $\mu = 0.012$, the operating reinforcing class A-II ($R_a = 2700$ kg/cm²), type 300 concrete ($R_1 = 160$ kg/cm²). The constant static load from the fill and natural weight $q = 0.2$ kg/cm². The calculation diagram of the slab is a hinge-supported beam.

Let us determine the limiting value of the dynamic load of the type of (17) (with instantaneous buildup) when calculating the ceiling by the limiting state 1b.

Let us find the values of M_0 and B .

FOR OFFICIAL USE ONLY

FOR OFFICIAL USE ONLY

We have:

$$M_0 = 0,18 \cdot 10^8 \text{ kg-cm};$$

$$\alpha_p = 0,012 \frac{2700}{160} = 0,202;$$

$$M_0 = 2700 \cdot 0,012 \cdot 80 \cdot 27^2 (1 - 0,5 \cdot 0,202) - 0,18 \cdot 10^8 = 1,51 \cdot 10^8 \text{ kg-cm};$$

$$B = 2,3 \cdot 10^{10} \text{ kg-cm}^2.$$

Let us define the angular oscillation frequency ω , considering that the running mass of the structural element considering the fill is:

$$m = \frac{0,2 \cdot 80}{g} = 1,63 \cdot 10^{-2}; \quad \omega = \frac{9,87}{300^2} \sqrt{\frac{2,3 \cdot 10^{10}}{1,63 \cdot 10^{-2}}} = 130 \text{ rad./sec.}$$

Let us set $\omega\theta = \infty$; then from (94), $\gamma_0 = 1,915$. By Figure 27 $\omega^{1/17} = 1,33$.

$$p = \frac{8 \cdot 1,51 \cdot 10^8 \cdot 1,33}{300^2 \cdot 1,915} = 93 \text{ kg/cm}$$

or

$$\Delta p = \frac{893}{80} = 1,16 \text{ kg/cm}^2.$$

At this pressure, according to Chapter II we have the time of effect of the wave $\tau_+ = 3$ sec. By formula (16) of Chapter II

$$\theta = \frac{3}{1,5 + 1,11} = 1,15 \text{ sec.}$$

Then $\omega\theta = 130 \cdot 1,15 = 150$ and $\gamma_0 = 1,915 (1 - 0,014) = 1,89$ and the more precise values of $p = 94,4 \text{ kg/cm}$, $\Delta p = 1,18 \text{ kg/cm}^2$. These values in practice do not differ from those which were obtained above for $\omega\theta = \infty$. Therefore, hereafter when calculating by the limiting state lb we shall consider $\omega\theta = \infty$ everywhere.

Example 5. Let us check the strength of the structural element from example 4 for the effect of a load of the type of (17) of intensity $\Delta p = 2,2 \text{ kg/cm}^2$ when calculating with respect to the limiting state la.

For this load we have $\tau_+ = 2$ sec.

$$\theta = \frac{2}{1,5 + 2,2} = 0,54 \text{ sec}$$

and $\omega\theta = 130 \cdot 0,54 = 70$.

Let us find $p = 2,2 \cdot 80 = 176 \text{ kg/cm}$; from (65) and (66) we have

FOR OFFICIAL USE ONLY

FOR OFFICIAL USE ONLY

$$M_p = \frac{176 \cdot 300^2}{8} = 1,98 \cdot 10^8 \text{ kg-cm};$$

$$k_M = \frac{1,51 \cdot 10^8}{1,98 \cdot 10^8} = 0,764;$$

$$\gamma = 0,764 \cdot 1,33 = 1,015.$$

According to the graph in Figure 29 for $\omega\theta = 70$ and $\gamma = 1.015$ we obtain $k_\pi = 4.4$. According to the graph in Figure 28 for $\alpha_p = 0.202$ we have: $\psi_\pi = 0.05$.

Then from (91)

$$\psi_{\text{mano}} = \frac{176 \cdot 300^2 \cdot 4,4}{19,2 \cdot 2,3 \cdot 10^{10}} = 0,0473 < \psi_\pi = 0,05.$$

that is, the structural element withstands the given load. A comparison of it with the limiting load of example 4 indicates that consideration of the plastic deformations permits an increase in the bearing capacity of the beam by $2.2/1.18 = 1.86$ times.

Example 6. Let the ceiling from example 4 belong to a built-in shelter. The dynamic load is taken with a gradual increase in pressure of the type of (23). The buildup time $\theta_1 = 0.02$ sec.

Let us determine the limiting value of the dynamic load for the calculation with respect to the limiting state 1b.

We have

$$\frac{\omega\theta_1}{\pi} = \frac{130 \cdot 0,02}{\pi} = 0,83.$$

Let us take $\omega\theta_2 = 200$ and by the graph in Figure 33 we find $\gamma_0 = 1.5$. Then

$$p = \frac{8 \cdot 1,51 \cdot 10^8 \cdot 1,33}{300^2 \cdot 1,5} = 119 \text{ kg/cm}$$

or

$$\Delta p = \frac{119}{80} = 1,49 \text{ kg/cm}^2$$

Example 7. Let us check the structural design of the preceding example for the effect of a load of the type of (23) with $\theta_1 = 0.02$ sec and $\Delta p = 2.3$ kg/cm² for the calculation with respect to the limiting state 1a.

For $\Delta p = 2.3$ kg/cm², $\theta_2 \approx \theta = 0.53$ sec. We have: $p = 2.3 \cdot 80 = 180$ kg/cm, $M_p = 2.06 \cdot 10^6$ kg-cm, $k_M = 0.73$, $\gamma = 0.97$.

By the graph in Figure 33 when $\omega\theta_1/\pi = 0.83$, $\omega\theta_2 = 68$ we find $k_\pi = 4.1$ and

FOR OFFICIAL USE ONLY

FOR OFFICIAL USE ONLY

$$\psi_{\text{max}} = \frac{184 \cdot 300^3 \cdot 4,1}{19,2 \cdot 2,3 \cdot 10^{10}} = 0,046 < \psi_{\text{n}} = 0,05,$$

that is, the strength condition is satisfied. The consideration of the plasticity formation permits in the given case an increase in the limiting load by 2.3/1.49 - 1.54 times.

Example 8. Let the slab from the preceding example be a wall element of a structure erected on the surface of the ground. A load acts on the wall with reflection of the type (27). Let us determine the maximum value of the dynamic load with $\theta_1 = 0.02$ sec for the calculation with respect to the limiting state Ia.

The constant horizontal load is absent; therefore $M_0 = 1.69 \cdot 10^6$ kg-cm.

The weight of the slab

$$m = \frac{2,4 \cdot 10^{-3} \cdot 30 \cdot 80}{981} = 0,585 \cdot 10^{-2} \text{ kg-sec}^2/\text{cm}^2.$$

The vibration frequency is:

$$\omega = \frac{9,87}{300^2} \sqrt{\frac{2,3 \cdot 10^{10}}{0,585 \cdot 10^{-2}}} = 218 \text{ rad./sec.}$$

Let us use the strength condition in the form of (121):

$$\frac{k_{\text{n}}(\gamma)}{\gamma} = \frac{2,4 \cdot 2,3 \cdot 10^{10} \cdot 0,05}{1,69 \cdot 10^6 \cdot 1,37 \cdot 300} = 4.$$

Using the graphs from Figure 35 for

$$\frac{\omega \theta_1}{2\pi} = \frac{218 \cdot 0,02}{2\pi} = 0,7,$$

we obtain by selection $k_{\text{n}} = 3.2$, $\gamma = 0.8$.

From formula (120) we find the dynamic load with reflection

$$p = p_{\text{отр}} = \frac{8 \cdot 1,69 \cdot 10^6 \cdot 1,37}{300^2 \cdot 0,8} = 256 \text{ kg/cm}^2$$

$$\Delta p_{\text{отр}} = \frac{256}{80} = 3,2 \text{ kg/cm}^2$$

In accordance with formula (25) of Chapter II this value corresponds to the pressure with normal reflection on the shock wave front equal to $\Delta p = 1.1$ kg/cm².

FOR OFFICIAL USE ONLY

FOR OFFICIAL USE ONLY

Example 9. The beam type reinforced concrete slab with clamped ends is an element of the ceiling of a separately standing shelter. The basic characteristics of the slab are as follows: $l = 600$ cm, $b = 100$ cm, $h_0 = 37$ cm ($h = 40$ cm), working reinforcing, class A-II, type of concrete 300. Reinforcing coefficients: on support $\mu^{\text{bear}} = 0.012$ in the span $\mu^{\text{span}} = 0.008$. The constant static load $q = 0.25$ kg/cm².

Let us determine the limiting value of the dynamic load of the type of (17) for the calculation with respect to the limiting state 1b.

Let us find the limiting moments and the rigidities on the support and in the span

$$|M_q^{\text{on}}| = \frac{0.25 \cdot 100 \cdot 600^2}{12} = 0.75 \cdot 10^6 \text{ kg-cm}, \quad \alpha_p^{\text{on}} = 0.202;$$

$$M_p^{\text{on}} = 2700 \cdot 0.012 \cdot 100 \cdot 37^2 (1 - 0.5 \cdot 0.202) - 0.75 \cdot 10^6 = 3.23 \cdot 10^6 \text{ kg-cm};$$

$$\xi^{\text{on}} = 0.33; \quad B^{\text{on}} = 7.4 \cdot 10^{10} \text{ kg/cm}^2;$$

$$M_q^{\text{np}} = 0.375 \cdot 10^6 \text{ kg-cm}; \quad \alpha_p^{\text{np}} = 0.008 \frac{2700}{160} = 0.136;$$

$$M_p^{\text{np}} = 2700 \cdot 0.008 \cdot 100 \cdot 37^2 (1 - 0.5 \cdot 0.136) - 0.375 \cdot 10^6 = 2.38 \cdot 10^6 \text{ kg-cm};$$

$$\xi^{\text{np}} = 0.272; \quad B^{\text{np}} = 5.41 \cdot 10^{10} \text{ kg-cm}^2.$$

The vibration frequency:

$$m = \frac{0.25 \cdot 100}{981} = 0.0253; \quad \omega_1 = \frac{22.4}{600^2} \sqrt{\frac{5.41 \cdot 10^{10}}{0.0253}} = 91 \text{ rad./sec}; \quad \omega^{1/17} = 1.3.$$

According to formulas (125), (128):

$$\beta_1 = \frac{7.4}{5.41} = 1.37; \quad k_1 = \frac{0.269 + 0.731 \cdot 1.37}{0.46 + 0.54 \cdot 1.37} = 1.06$$

Using formula (143) for $\omega_1 \theta = \infty$ we find:

$$\rho = \frac{12 M_0^{\text{on}} \omega_1^{1/17}}{k_1 l^3 \gamma_0} = \frac{12 \cdot 3.23 \cdot 10^6 \cdot 1.3}{1.06 \cdot 600^3 \cdot 1.915} = 68 \text{ kg/cm};$$

$$\Delta \rho = \frac{68}{100} = 0.68 \text{ kg/cm}^2.$$

Example 10. Let us check the structural design of example 9 for the effect of a load of the type of (17) with $\Delta \rho = 1.8$ kg/cm² for the calculation by the limiting state 1a. When $\Delta \rho = 1.8$ kg/cm² we have $\tau_+ = 2.2$ sec.

FOR OFFICIAL USE ONLY

FOR OFFICIAL USE ONLY

$$\theta = \frac{2,2}{1,5+1,8} = 0,665 \text{ sec and } \omega_1 \theta = 60$$

The structural strength is checked by conditions (188).

By formulas (170), (138) we have:

$$\beta_2 = \frac{3,23}{2,38} = 1,35; \quad \Lambda_{\rho_1}^{\text{on}} = \frac{180 \cdot 600^2 \cdot 1,06}{12} = 5,75 \cdot 10^6;$$

$$k_M^{\text{on}} = \frac{3,23}{5,75} = 0,561;$$

$\gamma = 0,73$ and by the graph in Figure 37 for $\omega_1 \theta = 50$, $\beta_1 = 1,38$ for $\beta_2 = 1,35$ we find by interpolation $k_{\pi}^{\text{bear}} = 5$, $k_{\pi}^{\text{span}} = 4,8$.

By the graph in Figure 28, $\psi_{\pi}^{\text{bear}} = 0,05$; $\psi_{\pi}^{\text{span}} = 0,056$ and from (188) we have:

$$\psi_{\text{max}}^{\text{on}} = \frac{180 \cdot 600^3 \cdot 5}{192 \cdot 5,41 \cdot 10^{10}} = 0,019 < 0,5 \psi_{\pi}^{\text{on}} = 0,025;$$

$$\psi_{\text{max}}^{\text{np}} = \frac{180 \cdot 600^3 \cdot 4,8}{96 \cdot 5,41 \cdot 10^{10}} = 0,036 < \psi_{\pi}^{\text{np}} = 0,056,$$

that is, the strength conditions are satisfied.

Comparison with example 9 indicates that the consideration of the plastic deformations in the beam clamped on the supports increases the bearing capacity by $1,8/0,68 = 2,65$ times.

Example 11. The beam reinforced concrete slab with one clamped end and the other hinged end is an element of the ceiling of a separately standing filter. The working reinforcing is class A-IV ($R_a = 5100 \text{ kg/cm}^2$); the remaining slab characteristics are the same as in example 9.

Let us define the limiting value of the dynamic load for the calculation with respect to the limiting state lb.

The values of the beam rigidities are the same as in example 9. Let us find the limiting elements on the support and in the span. We have:

$$|M_q^{\text{on}}| = M_q^{\text{np}} = \frac{q l^2}{8} = \frac{0,25 \cdot 100 \cdot 600^2}{8} = 1,12 \cdot 10^6 \text{ kg-cm};$$

$$\alpha_p^{\text{on}} = 0,012 \frac{5100}{160} = 0,382; \quad \alpha_p^{\text{np}} = 0,008 \frac{5100}{160} = 0,255;$$

$$M_0^{\text{on}} = 5100 \cdot 0,012 \cdot 100 \cdot 37^2 (1 - 0,5 \cdot 0,382) - 1,12 \cdot 10^6 = 5,66 \cdot 10^6 \text{ kg-cm};$$

$$M_0^{\text{np}} = 5100 \cdot 0,008 \cdot 100 \cdot 37^2 (1 - 0,5 \cdot 0,255) - 1,12 \cdot 10^6 = 3,76 \cdot 10^6 \text{ kg-cm}.$$

Oscillation frequency

FOR OFFICIAL USE ONLY

FOR OFFICIAL USE ONLY

$$\omega_2 = \frac{15,45}{600^2} \sqrt{\frac{5,41 \cdot 10^{10}}{0,0253}} = 63 \text{ rad./sec.}$$

By formulas (191), (196) we have: $k_1 = 1.37$; $k_2 = 1.1$. Let us set $\omega_2 \theta = \infty$ and let us find for $k_{MO} = 2$:

$$p = \frac{8M_0^{on}}{k_s I^2 k_{MO}} = \frac{8 \cdot 5,66 \cdot 10^6}{1,1 \cdot 600^3 \cdot 2} = 57 \text{ кгс/см}; \Delta p = 0,57 \text{ кг/см}; \Delta p = 0,57 \text{ кг/см}^2.$$

Example 12. Let us check the slab of example 11 for the effect of a load with $\Delta p = 1.3 \text{ кг/см}^2$ when calculating by the limiting state Ia. For $\Delta = 1.3 \text{ кг/см}^2$, $\tau_+ = 2.5 \text{ sec}$, $\theta = 0.83 \text{ sec}$ and $\omega_2 \theta = 52$. We have:

$$\beta_s = \frac{5,66}{3,76} = 1,51; \quad M_{p2}^{on} = \frac{130 \cdot 600^3 \cdot 1,1}{8} = 6,44 \cdot 10^6 \text{ кг-см};$$

$$k_M^{on} = \frac{5,66}{6,44} = 0,88$$

and by the graph in Figure 41 for $\omega_2 \theta = 50$ and the nearest value of $\beta_1 = 1.45$ we find $k_{\pi}^{bear} \approx 4.2$, $k_{\pi}^{span} \approx 4$.

By the graph in Figure 28, $\psi_{\pi}^{bear} = 0.042$; $\psi_{\pi}^{span} = 0.047$ and from (210), (213), we have:

$$\psi_{max}^{on} = \frac{130 \cdot 600^3 \cdot 4,2}{106,8 \cdot 5,41 \cdot 10^{10}} = 0,0204 < 0,5 \psi_{\pi}^{np} = 0,024;$$

$$\psi_{max}^{np} = \frac{130 \cdot 600^3 \cdot 4}{43,8 \cdot 5,41 \cdot 10^{10}} = 0,046 < \psi_{\pi}^{np} = 0,047,$$

that is, the strength conditions are satisfied.

Consideration of the plastic deformations for the investigated beam increases the bearing capacity by $1.3/0.57 = 2.3$ times.

Example 13. The ceiling of a separately standing shelter is made up of beam-type, three-span, continuous slabs with edge hinged supports. The basic characteristics of the ceiling: $l_1 = l_2 = l_3 = 500 \text{ cm}$, $h_0 = 37 \text{ cm}$ ($h = 40 \text{ cm}$); $b = 100 \text{ cm}$, the working reinforcing class A-IV; type of concrete 300; reinforcing coefficient for the edge spans ($i = 1$ and 3) $\mu_1^{span} = \mu_3^{span} = 0.008$; for the middle span $\mu_2^{span} = 0.006$; for the bearing cross sections $\mu_2^{bear} = \mu_3^{bear} = 0.012$. The constant static load $q = 0.25 \text{ кг/см}^2$.

Let us calculate the ceiling with respect to the limiting state Ia for the effect of a load of the type of (17) with $\Delta p = 1.4 \text{ кг/см}^2$. The rigidities and the limiting moments are equal (example 11 is used):

FOR OFFICIAL USE ONLY

FOR OFFICIAL USE ONLY

$$B_1^{np} = B_3^{np} = 5,41 \cdot 10^{10} \text{ kg/cm}^2; \quad B_2^{np} = 2,8 \cdot 10^{10} \text{ kg-cm}^2;$$

$$B_2^{on} = B_3^{on} = 7,4 \cdot 10^{10} \text{ kg-cm}^2;$$

$$M_{0,2}^{on} = M_{0,3}^{on} = 6,78 \cdot 10^8 - \frac{0,25 \cdot 100 \cdot 600^3}{10} = 5,88 \cdot 10^8 \text{ kg-cm};$$

$$M_{0,1}^{np} = M_{0,3}^{np} = 4,88 \cdot 10^8 - 0,63 \cdot 10^8 = 4,25 \cdot 10^8 \text{ kg-cm};$$

$$M_{0,2}^{np} = 3,8 \cdot 10^8 - 0,22 \cdot 10^8 = 3,58 \cdot 10^8 \text{ kg-cm}.$$

Let us find the vibration frequency of the beam by formula (220). Let us substitute the average value of the span rigidity in it:

$$B_{cp}^{np} = \frac{2 \cdot 5,41 \cdot 10^{10} + 2,8 \cdot 10^{10}}{3} = 4,55 \cdot 10^{10} \text{ kg-cm}^2;$$

$$\omega_n = \frac{18,3}{600^2} \sqrt{\frac{4,55 \cdot 10^{10}}{0,0353}} = 68 \text{ rad./sec.}$$

Let us consider the first span and let us define the angles of opening in the plasticity hinges using formulas (210), (213). For $\Delta p = 1,4 \text{ kg/cm}^2$, $\theta = 0,8 \text{ sec}$ and $\omega_H \theta = 54$.

We have:

$$\beta_1 = \frac{B_2^{on}}{B_1^{np}} = \frac{7,4}{5,41} = 1,37;$$

$$k_2^n = 0,8 \frac{0,26 + 0,74 \cdot 1,37}{0,578 + 0,422 \cdot 1,37} = 1,285;$$

$$\beta_2 = \frac{M_{0,2}^{on}}{M_{0,1}^{np}} = \frac{5,88}{4,25} = 1,38; \quad M_{p2}^{on} = \frac{140 \cdot 600^3}{8} \cdot 0,885 = 5,55 \cdot 10^8;$$

$$k_M^{on} = \frac{M_{0,2}^{on}}{M_{p2}^{on}} = \frac{5,88}{5,55} = 1,06 \text{ and by the graph in Fig. 43 we find}$$

$$k_n^{on} = 3,6, \quad k_n^{np} = 3,8. \text{ Then by Figure 8 for } \alpha_p^{np} = 0,255$$

$$\psi_{n,1}^{np} = 0,047 \text{ or } \psi_{\text{max}}^{np} = \frac{140 \cdot 600^3 \cdot 3,8}{43,8 \cdot 5,41 \cdot 10^{10}} = 0,047 = \psi_{n,1}^{np} = 0,047;$$

$$\psi_{\text{max, span}}^{on} = \frac{140 \cdot 600^3 \cdot 3,6}{106,8 \cdot 5,41 \cdot 10^{10}} = 0,0189.$$

(a)

Key. a. 2max, left

Let us proceed to the second span and let us determine $\psi_{2\text{max}}^{\text{bear}}$ and $\psi_{2\text{max}}^{\text{span}}$ using formula (188). We have:

FOR OFFICIAL USE ONLY

FOR OFFICIAL USE ONLY

$$f_1 = \frac{B_2^{on}}{B_2^{np}} = \frac{7,4}{2,8} = 2,64; \quad k_{1,2}^n = 1,4 \cdot \frac{0,769 + 0,731 \cdot 2,64}{0,46 + 0,54 \cdot 2,64} = 1,4;$$

$$\beta_2 = \frac{M_{0,2}^{on}}{M_{0,2}^{np}} = \frac{5,88}{3,53} = 1,64; \quad M_{01}^{on} = \frac{140 \cdot 600^2 \cdot 1,4}{12} = 5,88 \cdot 10^6;$$

$$k_M^{on} = \frac{5,88}{5,88} = 1$$

and by the graph in Figure 45 we find (for $\omega_H \theta = 50$ and $\beta_1 = 2.6$) $k_\pi^{bear} \approx 1.6$.
The curve for k_π^{span} is absent. This indicates that in the second span in the middle the plasticity hinge was not formed. Let us determine the angle of opening in the hinge on the support

$$\psi_{2max, прав}^{on} = \frac{140 \cdot 600^2 \cdot 1,6}{192 \cdot 2,8 \cdot 10^{10}} = 0,009.$$

(a)

Key: a. 2max, right

By figure 28 for

$$\alpha_p = 0,012 \frac{5100}{160} = 0,383$$

$$\psi_{n,2}^{on} = 0,042; \quad \psi_{2max}^{on} = 0,018 + 0,009 = 0,0279 < \psi_{n,2}^{on} = 0,042,$$

that is, the strength conditions are satisfied.

Example 14. The ceiling element of a separately standing shelter is a square slab hinge supported around the outline. The basic characteristics of the slab: $a = b = 600$ cm, $h_0 = 32$ cm ($h = 35$ cm), the working reinforcing class A-IV, concrete type 300 ($E_b = 315,000$ kg/cm²), $\mu = 0.006$. The constant static load $q = 0.2$ kg/cm².

Let us determine the limiting magnitude of the dynamic load of the type of (17) with $\theta = \infty$ when calculating by the limited state 1b.

Let us find the limiting moment (running), considering that $n_1 = 0.0364$ (Table 5):

$$\alpha_p = 0,006 \frac{5100}{160} = 0,19; \quad M_0^s = 5100 \cdot 0,006 \cdot 32^2 (1 - 0,5 \cdot 0,19) -$$

$$- 0,2 \cdot 600^2 \cdot 0,0364 = 2,57 \cdot 10^4 \text{ kg-cm.}$$

Setting $k_{MO} = 2$, we obtain

$$\Delta p = \frac{M_0^s}{k_{MO} a^2 n_1} = \frac{2,57 \cdot 10^4}{2 \cdot 600^2 \cdot 0,0364} = 1,02 \text{ kg/cm}^2.$$

FOR OFFICIAL USE ONLY

FOR OFFICIAL USE ONLY

Example 15. Let us check the slab in example 14 for the effect of the load with $\Delta p = 1.8 \text{ kg/cm}^2$, $\omega\theta = 300$ when calculating by the limiting state Ia. For

$$\alpha_p = 0,006 \frac{5100}{160} = 0,19$$

by the graph in Figure 28 we find $\psi_{\pi} = 0.05$.

We have (227):

$$k_M = \frac{2,57 \cdot 10^4}{1,8 \cdot 600^2 \cdot 0,0364} = 1,09; \quad \chi = 1.$$

By the graph in Figure 50 we find $k_{\pi} = 7$.

The cylindrical rigidity of the slab

$$D = \frac{Ek^3}{12(1-\nu^2)} = \frac{315\,000 \cdot 35^3}{12(1-0,026)} = 1,16 \cdot 10^9 \text{ kg-cm}^2/\text{cm};$$

let us check the strength conditions, using (235):

$$\psi_{\text{max}} = \frac{64 \cdot 1,8 \cdot 600^2 \cdot 7}{\pi^2 \cdot 1,16 \cdot 10^9 \cdot 4} = 0,039 < \psi_0 = 0,05,$$

that is, the strength condition is satisfied.

FOR OFFICIAL USE ONLY

FOR OFFICIAL USE ONLY

CHAPTER IV. CALCULATION OF THE STRUCTURAL DESIGNS OF CEILINGS AND FLOORS UNDER THE EFFECT OF COMPRESSION WAVES IN THE GROUND

1. Basic Prerequisites

The effect of an explosion is transmitted to the structural elements located in the ground primarily in the form of compression waves. These waves are generated by the air shock wave. During movement in the ground the basic parameters of the wave vary -- the pressure magnitude, the buildup time of the pressure and the time of effect. After the wave approaches the structure, they interact, the essence of which consists in reflection of the wave from the surface of the structure, leading to a rise in pressure, and subsequent change in pressure as a result of the movement of a structure.

In order to determine the loads on buried shelters it is necessary, consequently, to know the mechanism of propagation of a shock wave in the ground and the interaction of it with a deforming structure. These problems are the subject of many papers. They are discussed most completely in references [40] and [52] in which there is also a broad bibliography.

Let us briefly discuss the information needed hereafter on the wave processes in solid media -- the ground.

Usually, considering the relatively small dimensions of the structural elements of buried structures, it is considered that the wave front in the ground is parallel to the surface of the ground. This permits restricting the problem to studying the simplest planar one-dimensional motion. In this case all of the parameters of the wave process depends only on one spatial coordinate and time.

Let us direct the Oz axis into the ground, and let us place the origin of the coordinates at each surface. The displacement of the cross section at the time t which for t = 0 at the coordinate z will be by u(z, t). The relative deformation will be:

$$\varepsilon = \frac{\partial u}{\partial z} \quad (1)$$

FOR OFFICIAL USE ONLY

FOR OFFICIAL USE ONLY

The stress in the same cross section $\sigma(z, t)$. As is known, plane, one directional movements of the medium is described by the following equation which is valid for any solid medium independently of the magnitude of the displacement u :

$$\rho \frac{\partial^2 u}{\partial t^2} = \frac{\partial \sigma}{\partial z}, \quad (2)$$

where ρ is the initial (for $t = 0$) density of the medium.

Then we shall consider the layer of the ground of small thickness without considering the variation in density of the ground with depth, that is, we shall take $\rho = \text{const}$.

The properties of the specific medium, in the given case of the ground, are characterized by a deformation law (deformation diagram) establishing the relation between the stress and strain

$$\sigma = \sigma(\varepsilon), \quad (3)$$

which is defined experimentally.

The experiments show that the deformative properties of the nonwater-saturated soil, just as many other materials will essentially depend on the deformation rate: the deformation diagrams have a different form under the effect of the dynamic and static loads. A similar analysis of the dynamic compression diagrams of the soil based on broad experimental studies appears in references [40, 41, 53]. In the handbook for calculation of residual strains [54] a discussion is presented of the procedure for obtaining such diagrams, and a schematic of the experimental setup is given.

Let us present some of the most important information about the deformative properties of the soil. Figure 51 shows the standard compression diagrams of the soil: the dynamic curve and static curve 2. These curves have qualitatively different form in the initial section, including in practice the most important pressures (to 5-7 kg/cm²). The dynamic diagram is turned with the convexity upward, $d^2\sigma/d\varepsilon^2 < 0$. As will be obvious from what follows, this has great significance for the properties of the wave propagated in the soil.

Curves 1 and 2 correspond to the increase in pressure (that is, load). The decrease in pressure in the soil occurs in accordance with the dotted curves of 3 and 4. Here, as is obvious, after unloading in the ground large residual deformations are formed caused by packing of it.

For practical calculations usually simplified (calculation) compression diagrams are used. Figure 52 depicts such standard diagrams (see [40]): for the load the so-called Prandtl diagram with linear strengthening) (1), for unloading lines 2-4. The latter line is most frequently used corresponding to unloading occurring with constant deformation. In this case the calculation diagram of the soil deformations is characterized by three parameters: σ_s, E_0, E_1 .

FOR OFFICIAL USE ONLY

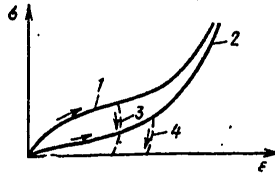


Figure 51. Diagrams of soil deformation ($\sigma - \epsilon$). 1 -- dynamic; 2 -- static; 3,4 -- on unloading.

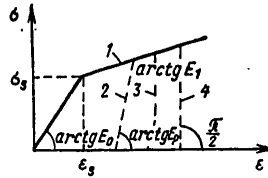


Figure 52. Calculation deformation diagrams of the ground.

Usually instead of the deformation moduli E_0 and E_1 we use the wave propagation rates: elastic $a_0 = \sqrt{\frac{E_0}{\rho}}$; elastic-plastic $a_1 = \sqrt{\frac{E_1}{\rho}}$.

The values of them are presented in Table 6 for different soils according to the data of reference [41].

Table 6

Soil	Wave propagation rates in m/sec	
	elastic a_0	elastic-plastic a_1
Sandy, disturbed structure	100	50
Sandy, undisturbed structure	200	100
Loamy	220	110
Argillaceous undisturbed structure	250	130
Packed clay	500	250
Loess	300	100

The deformative properties of the soils for the nonuniform stressed state are subjected to more complex laws which are discovered in the model proposed by S. Grigoryan [19], [20].

FOR OFFICIAL USE ONLY

FOR OFFICIAL USE ONLY

2. Loading Wave Propagation

The deformation diagram of the medium is taken in more general form in accordance with Figure 53:

for loading, the curvilinear diagram $\sigma = \Phi(\epsilon)$ with the condition

$$\frac{d^2 \Phi}{d\epsilon^2} < 0; \tag{4}$$

for unloading -- the straight line corresponding to constant deformation ($E_p = \infty$).

From condition (4) it follows that the deformation modulus $E = d\Phi/d\epsilon$ decreases with an increase in the deformation.

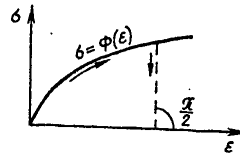


Figure 53. Deformation diagram of the medium.

Considering the expression

$$\frac{\partial \sigma}{\partial z} = \frac{\partial \sigma}{\partial \epsilon} \cdot \frac{\partial \epsilon}{\partial z} = \frac{d\Phi}{d\epsilon} \cdot \frac{\partial^2 u}{\partial z^2},$$

from (2) we obtain the following equation:

$$u_{tt} = a^2(u_z)u_{zz}, \tag{5}$$

where

$$a(u_z) = \sqrt{\frac{1}{\rho} \cdot \frac{d\Phi}{d\epsilon}} = \sqrt{\frac{E}{\rho}} \tag{6}$$

and it is denoted

$$\frac{\partial u}{\partial z} = u_z; \quad \frac{\partial u}{\partial t} = u_t. \tag{7}$$

Equation (5) is a quasilinear (since the coefficient a depends on u_z) partial differential equation. From solving the equations of this type broad use is made of the characteristic method (for example, [37]). Let us

FOR OFFICIAL USE ONLY

FOR OFFICIAL USE ONLY

briefly discuss the concepts based on physical representations here. Let the solution of equation (5) $u(z, t)$ exist, which is a wave process in the investigated medium. Let us assume that any point of the medium a new disturbance has occurred. It will be propagated with respect to the given wave in the form of a new wave. Let the new disturbance be of the type such that at its front the velocity u_0 and the deformation u_z at the medium will remain continuous, and the second derivatives u_{tt} , u_{zz} , u_{tz} will vary discontinuously (weak disturbance). Then the law of motion of the new wave front with respect to the given wave $u(z, t)$ will be the line on the surface $u(z, t)$, along which the derivatives u_{tt} , u_{zz} , u_{tz} cannot be uniquely defined by the values of u_t and u_z . In the given solution $u(z, t)$ such lines are also called characteristic curves, and their projections on the planes zt are called the characteristic projections or simply the characteristics. The characteristics and the values u_z and u_t along them are determined from the equations [37]:

$$dz = +a(u_z)dt, \quad dz = -a(u_z)dt; \quad (8)$$

$$du_t = a(u_z)du_z, \quad du_t = -a(u_z)du_z. \quad (9)$$

The entire set of characteristics is broken down into two families of lines:

The first family (C_+) - $dz = a dt$ is given by the function of the type $\alpha(z, t) = \alpha = \text{const}$; the second family (C_-) - $dz = -a dt$ is given by the function of the type $\beta(z, t) = \beta = \text{const}$.

Here α and β are constant parameters for each characteristic.

The first family of the characteristics defines the laws of motion of the fronts of all possible waves along the Oz axis in the positive directions; the second family defines the laws of motion of the fronts of the counter-waves caused, for example, by reflection of the wave $u(z, t)$ from a barrier. Important significance of the characteristics also consist in the fact that any solution of equation (5) will be made up of the characteristic curves [37].

Equations (9) can be integrated:

along the characteristics of the first family (C_+)

$$u_t - \lambda(u_z) = r_1(\alpha); \quad (10)$$

along the characteristics of the second family (C_-)

$$u_t + \lambda(u_z) = r_2(\beta), \quad (11)$$

FOR OFFICIAL USE ONLY

FOR OFFICIAL USE ONLY

where

$$\lambda(u_z) = \int_0^{u_z} a(e) de \tag{12}$$

and $r_1(\alpha)$, $r_2(\beta)$ are constant coefficients for each characteristic (the Riemann invariants).

Let the new wave front be propagated in the positive direction of the Oz axis through the medium in which the deformation and the velocity are constant (they do not depend on z and t) and area equal to the following: $u_z = \epsilon_0$, $u_t = v_0$ (steady state deformation). In this case all of the characteristics C_- began with the region with ϵ_0, v_0 (Figure 54), that is, in (11) the coefficient r_2 will have one value for all characteristics equal to:

$$r_2 = v_0 + \lambda(\epsilon_0) = \text{const.} \tag{13}$$

From (10) and (11) we have

$$\lambda(u_z) = \frac{1}{2} [r_2(\beta) - r_1(\alpha)]. \tag{14}$$

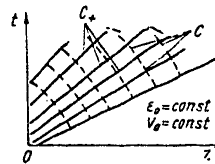


Figure 54. Wave propagation in a medium with steady state deformation.

Along the characteristic C_+ , $r_1(\alpha) = \text{const}$, then from (14) and (13) we have $\lambda(u_z) = \text{const}$, that is, the deformation u_z is constant along each characteristic of the first family. Therefore the characteristics C_+ will be straight lines and the investigated wave process which is called a simple direct wave is described by the expressions:

$$u_t = -\lambda(u_z) + v_0 + \lambda(\epsilon_0); \tag{15}$$

$$z = a(u_z)t + c(\alpha), \tag{16}$$

where $c(\alpha)$ is a constant (for each characteristic) coefficient.

FOR OFFICIAL USE ONLY

FOR OFFICIAL USE ONLY

Analogously, for the wave propagated with respect to the steady state deformation in the opposite direction (simple return wave), the following relations are valid:

$$u_t = \lambda(u_z) + v_0 - \lambda(\epsilon_0); \tag{17}$$

$$z = -a(u_z)t + c(\beta). \tag{18}$$

It is obvious along the rectilinear characteristics of simple waves the stress σ and velocity u_t are also constant.

Let us proceed with the investigation of the wave processes in the soil caused by the pressure $p(t)$ occurring on its surface. [For compression waves ($\sigma < 0$) frequently the pressure $p = -\sigma$ is given instead of the stress]. The pressure $p(t)$ is assumed to be monotonically increasing to p_{\max} (see Figure 55). It is necessary to solve equation (5) under the conditions:

$$\text{boundary -- for } z = 0, \sigma = -p(t); \tag{19}$$

$$\text{initial -- for } t = 0, u = 0, u_t = 0.$$

These problems have been investigated in detail in [52].

A simple direct wave will be propagated through the medium according to (15) and (16) for $v_0 = 0, \epsilon_0 = 0$. From each point of the axis Ot a rectilinear characteristic emerges, along which the voltage [equal to the voltage at the point $(0, t_H)$ of intersection of the characteristic with the Ot axis] and also the deformation u_z and velocity u_t are constant.

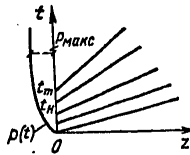


Figure 55. Wave propagation in a medium with monotonically increasing pressure on its surface.

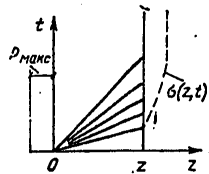


Figure 56. Propagation in a medium with suddenly applied constant pressure on its surface.

FOR OFFICIAL USE ONLY

FOR OFFICIAL USE ONLY

The equations of the characteristics from (16) will be

$$z = a(u_z(t_n))(t - t_n). \quad (20)$$

The voltage at the point (z, t) is:

$$\sigma(z, t) = -p(t_n) = -p\left(t - \frac{z}{a(u_z)}\right). \quad (21)$$

Hence, we have the equation for determining $u_z = u_z(z, t)$

$$-p\left(t - \frac{z}{a(u_z)}\right) = \Phi(u_z). \quad (22)$$

The velocity is obviously equal to:

$$u_t(z, t) = -\lambda(u_z). \quad (23)$$

In the region located above the characteristic emerging from the point $(0, t_m)$, the parameters of the medium are constant ($\sigma = -p_{\max}$). It is obvious that the value of $a(u_z)$ (6) is the propagation rate of the corresponding stress state of the medium. Under the condition (4), the velocity $a(u_z)$ decreases with an increase in pressure, as a result of which the characteristics of Figure 55 gradually diverge. Therefore in any cross sections $z > 0$ the time of increase in pressure to the maximum increases with removal of the cross section from the surface ($z = 0$). This is especially clearly manifested for a pressure on the surface that increases discontinuously to the maximum (Figure 56). In this case the characteristics form a fanlike beam, and in any cross section except $z = 0$, a gradual increase in pressure is observed. In the region of increase in pressure the relations have the form:

$$a(u_z) = \frac{z}{t}; \quad u_t = -\lambda(u_z). \quad (24)$$

The wave propagated in the ground with increasing buildup time of the pressure is also usually called the compression wave.

The conversion of the air shock wave to a compression wave is felt favorably in the strength of the structural elements, for with an increase in the pressure buildup time, the calculated value of the load on the structural elements decreases.

3. Process of Lowering the Pressure (Unloading)

Let us now assume that beginning with the time t_m the pressure on the surface decreases (Figure 57). It is obvious that in the ground, beginning with this time, the process of the decrease in pressure -- unloading -- also begins.

FOR OFFICIAL USE ONLY

FOR OFFICIAL USE ONLY

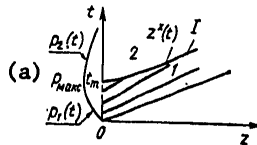


Figure 57. Propagation of waves in a medium with unloading

Key: a. max

The line that delimits the loading and unloading regions in the plane zt usually is called [52] the unloading wave (curve I on Figure 57). We shall denote all the parameters of motion of the ground in the loading region with the index 1, in the unloading region with the index 2, and in the wave itself, the index *; then the unloading wave equation will have the form $z = z^*(t)$, and the parameters of the medium on it: σ^* , ϵ^* , u_t^* . In accordance with the adopted deformation diagram of the ground during unloading (see Figure 53) the movement of the medium in the region (2) is described by the equations:

$$\rho \frac{\partial^2 u^{(2)}}{\partial t^2} = \frac{\partial \sigma^{(2)}}{\partial z}; \quad \frac{\partial u^{(2)}}{\partial z} = \epsilon^*(z). \tag{25}$$

where $\epsilon^*(z)$ is the deformation in the cross section at the time of beginning of unloading.

The boundary conditions for the system (25) are:

$$\text{for } z = 0 \quad \sigma^{(2)} = -p_s(t); \tag{26}$$

for

$$\left. \begin{aligned} z = z^*(t) \quad \sigma^{(2)} &= \sigma^{(1)}(z^*(t), t) = \sigma^*(t); \\ u_t^{(2)} &= u_t^{(1)}(z^*(t), t) = v^*(t). \end{aligned} \right\} \tag{27}$$

From (25) we have

$$u^{(2)}(z, t) = \int_0^z \epsilon^*(z) dz + u^{(2)}(0, t),$$

from which

$$\frac{\partial u^{(2)}}{\partial t} = \frac{du^{(2)}(0, t)}{dt}, \tag{28}$$

that is the velocity of the soil in the unloading region does not depend on the coordinate of the cross section remaining, just as for the absolutely solid body, constant for the entire medium of depth $z^*(t)$. From the first equation (25), the relations (28) and the conditions (26) it follows that

$$\sigma^{(2)}(z, t) = \rho \chi(t)z - p_s(t), \tag{29}$$

FOR OFFICIAL USE ONLY

FOR OFFICIAL USE ONLY

where $\chi(t) = \frac{d^2 u^{(2)}(0, t)}{dt^2}$.

Satisfying the conditions (27) considering (23), we obtain:

$$\rho \chi(t) z^*(t) - p_2(t) = \sigma^*(t); \quad (30)$$

$$u_t^{(2)}(z^*(t), t) = - \int_0^{z^*(t)} a(\varepsilon) d\varepsilon. \quad (31)$$

From (31) it follows (since $\frac{\partial u_t^{(2)}}{\partial z} = 0$)

$$\chi(t) = -a(\varepsilon^*) \frac{d\varepsilon^*}{dt},$$

and from (30) we find

$$\rho z^*(t) a(\varepsilon^*) \frac{d\varepsilon^*}{dt} + \sigma^*(t) = -p_2(t). \quad (32)$$

Let us denote by $t = \phi(p_1)$ the relation obtained by resolution of equation $p_1 = p_1(t)$. Then from expression (21)

$$\sigma^*(t) = -p_1 \left[t - \frac{z^*(t)}{a(\varepsilon^*)} \right] \quad (33)$$

we obtain

$$z^*(t) = a(\varepsilon^*) [t - \varphi(-\sigma^*)]. \quad (34)$$

Substituting (34) in (32) considering (6), we obtain

$$[t - \varphi(-\sigma^*)] \frac{d\sigma^*}{dt} + \sigma^* = -p_2(t)$$

or

$$\frac{d(t\sigma^*)}{dt} - \varphi(-\sigma^*) \frac{d\sigma^*}{dt} = -p_2(t). \quad (35)$$

Let us note that this equation does not depend on the deformation diagram $\sigma = \Phi(\varepsilon)$. Integrating (35) under the initial conditions $\sigma^*(t_m) = -p_{\max}$, we find

$$-t\sigma^*(t) + \int_{-\sigma^*}^{p_{\max}} \varphi(\xi) d\xi = + \int_{t_m}^t p_2(\tau) d\tau + t_m p_{\max}, \quad (36)$$

where ξ and τ are the integration variables.

Let us consider special cases. Let us assume that the pressure on the surface can be presented by the expressions:

FOR OFFICIAL USE ONLY

FOR OFFICIAL USE ONLY

$$\begin{aligned} p_1(t) &= p_{\text{max}} - \alpha_1 (t_m - t)^k \quad (0 \leq t \leq t_m); \\ p_2(t) &= p_{\text{max}} - \alpha_2 (t - t_m)^k; \quad (t \geq t_m); \quad \alpha_1 > 0; \quad \alpha_2 > 0, \end{aligned} \quad \begin{aligned} (37a) \\ (37b) \end{aligned}$$

where k is the integral power.

From (37a) we have

$$\begin{aligned} t &= t_m - \delta (p_{\text{max}} - p_1)^{\frac{1}{k}}, \quad \delta = \alpha_1^{-\frac{1}{k}}, \\ \text{that is,} \\ \varphi(\xi) &= t_m - \delta (p_{\text{max}} - \xi)^{\frac{1}{k}}. \end{aligned} \quad (38)$$

Substituting (38) and (37b) in (36), we obtain the following equation for determining σ^* :

$$\begin{aligned} (t - t_m) (p_{\text{max}} + \sigma^*) + \frac{\delta k}{(k+1)} (p_{\text{max}} + \sigma^*)^{\frac{k+1}{k}} - \\ - \frac{\alpha_2}{(k+1)} (t - t_m)^{k+1} = 0. \end{aligned} \quad (39)$$

This equation is satisfied by the expression

$$p_{\text{max}} + \sigma^* = c (t - t_m)^k \quad (40)$$

under the condition that the coefficient c is found from the equation

$$c + \frac{\delta k}{k+1} c^{\frac{k+1}{k}} - \frac{\alpha_2}{k+1} = 0. \quad (41)$$

Thus,

$$\sigma^*(t) = -p_{\text{max}} + c (t - t_m)^k. \quad (42)$$

The equation of the unloading wave from (34), (38) and (40) will be

$$z^*(t) = a (\varepsilon^*) (1 + \delta c^{\frac{1}{k}}) (t - t_m), \quad (43)$$

where $\varepsilon^*(t)$ is determined from the equation

$$\Phi(\varepsilon^*) = \sigma^*(t).$$

Let the compression diagram be represented by the Prandtl diagram (see Figure 52), that is,

$$\begin{aligned} \sigma &= E_0 \varepsilon \quad \text{for } |\sigma| \leq |\sigma_s|, \\ \sigma &= \sigma_s + E_1 (\varepsilon - \varepsilon_s) \quad \text{for } |\sigma| > |\sigma_s|, \\ E_1 &< E_0 \quad (\alpha_1 < \alpha_0) \quad \text{and} \quad p_{\text{max}} > |\sigma_s|. \end{aligned} \quad (44)$$

FOR OFFICIAL USE ONLY

FOR OFFICIAL USE ONLY

Then $a(e^*) = a_1 = \sqrt{\frac{E_1}{\rho}}$, and from (43) it follows that the unloading wave is a straight line

$$z^*(t) = a_1 (1 + \delta c^{\frac{1}{k}}) (t - t_m). \quad (45)$$

From (42) and (45), we find the distribution of the maximum pressures $p^* = -\sigma^*$ by the depth

$$p^*(z) = p_{\text{макс}} - c_1 z^k, \quad (46)$$

where

$$c_1 = \frac{c}{[a_1 (1 + \delta c^{\frac{1}{k}})]^k}. \quad (47)$$

Now let us consider the special case of loading (37) where $k = 1$, that is, the pressure on the surface varies according to linear laws. In this case the equation (41) has the form $c^2 + 2\alpha_1 c - \alpha_2 \alpha_1 = 0$, hence

$$c = \alpha_1 \left(-1 + \sqrt{1 + \frac{\alpha_2}{\alpha_1}} \right).$$

From the condition of vanishing of the pressure at the points $t = 0$ and $t = \theta$ we obtain

$$\alpha_1 = \frac{p_{\text{макс}}}{t_m} \quad \text{and} \quad \alpha_2 = \frac{p_{\text{макс}}}{\theta}$$

where θ is the duration of the phase of the drop in wave pressure.

The expression (46) in dimensionless variables will have the form

$$\frac{p^*}{p_{\text{макс}}} = 1 - \bar{c}_1 \frac{z}{z_0}, \quad (48)$$

where

$$\bar{c}_1 = \frac{-1 + \sqrt{1 + \frac{t_m}{\theta}}}{\sqrt{1 + \frac{t_m}{\theta}}}; \quad z_0 = a_1 t_m.$$

Let us find the depth z' on which the maximum pressure is 90% of the maximum pressure on the surface. From (48) we have

$$z' = \frac{0.1}{\bar{c}_1} z_0.$$

In Table 7 the values are presented for z'/z_0 and z' for $z_0 = 5$ m ($a_1 = 50$ m/sec, $t_m = 0.1$ sec) for several values of t_m/θ . By these data it is

FOR OFFICIAL USE ONLY

FOR OFFICIAL USE ONLY

possible to determine the degree of attenuation of the wave pressure in the ground.

Table 7

t_m/θ	1	0,2	0,1	0,05	0,025	0,01
z'/z_0	0,343	1,15	2,24	4,1	8,1	20
z' in meters for $z_0=5$ m	1,715	5,75	11,2	20,5	40,5	100

Let us consider another special case where the pressure on the surface increases discontinuously to the maximum [that is, $t_m = 0$ and $p_1(t) = 0$]. Then from (34)

$$z^*(t) = a(e^*)t, \tag{49}$$

from (32) we obtain the equation

$$\frac{d(t\sigma^*)}{dt} = -p_2(t),$$

from which

$$-t\sigma^*(t) = \int_0^t p_2(\tau) d\tau; \quad -\sigma^* = p^* = \frac{\int_0^t p_2(\tau) d\tau}{t} \tag{50}$$

For the deformation diagram corresponding to expressions (44), the unloading wave will be a straight line

$$z^* = a_1 t. \tag{51}$$

If the pressure on the surface is given by the expression (37b), then from (50) and (51) we find

$$p^* = p_{\text{max}} - \frac{\alpha_2}{(k+1)} t^k = p_{\text{max}} - \frac{\alpha_2}{(k+1)} \cdot \frac{z^k}{a_1^k}. \tag{52}$$

For $k = 1$ and $a_2 = p_{\text{max}}/\theta$, where θ is the time of the effect of the pressure on the surface, we have

$$p^*(z) = p_{\text{max}} \left(1 - 0,5 \frac{z}{\theta a_1} \right). \tag{53}$$

The maximum pressure will be 90% of p_{max} at a depth

$$z' = 0,2\theta a_1.$$

For a pressure on the surface in the form of

FOR OFFICIAL USE ONLY

FOR OFFICIAL USE ONLY

$$p_2(t) = p_{\text{max}} \left(1 - \frac{t}{\theta}\right)^2 \quad (54)$$

analogously we obtain

$$p^*(z) = p_{\text{max}} \left(1 - \frac{z}{\theta a_1} + \frac{z^2}{3(\theta a_1)^2}\right), \quad (55)$$

from which $z' = 0.1\theta a_1$.

Now let us briefly consider the unloading in medium width $E_p \neq \infty$ (line 2 on Figure 52). In this case the calculation formulas in closed form can be obtained appreciably more rarely than for $E_p = \infty$.

For the general case, therefore wide use is made of the graphoanalytical method of characteristics [8, 66]. If the diagram is presented in the form of the Prandtl diagram and the pressure on the surface assumes the maximum value discontinuously, the velocity of the unloading wave (a_p) is constant and equal to a_1 . With a pressure drop according to a linear law $p(t) = p(1 - (t/\theta))$ the maximum pressure, that is, the pressure on the unloading wave, will be found from the expression [54]

$$p^*(z) = p_{\text{max}} \left[1 - \frac{0.5z}{a_1\theta} \left(1 - \frac{a_1^2}{a_2^2}\right)\right], \quad \text{where } a_2 = \sqrt{\frac{E_p}{\rho}}. \quad (56)$$

For analytical determination of the unloading wave in the general case it is possible to use the functions presented in [52]:

$$\begin{aligned} z_1 + a_2 t_1 &= a_2 t_2 - z_2; \\ \frac{1}{2E_p} [\sigma_1(z_1, t_1) + \sigma_1(z_2, t_2)] + \frac{1}{2a_2} \{\lambda [e_1(z_2, t_2)] - \\ &- \lambda [e_1(z_1, t_1)]\} = \frac{1}{E_p} p_2 \left(t_2 - \frac{z_2}{a_2}\right), \end{aligned} \quad (57)$$

where $\sigma_1(z, t)$ and $\{e_1(z, t)\}$ are determined by the formulas (21) and (12); the values of z_1, t_1, z_2, t_2 are the coordinates of the points on the unloading wave [$z_1 = z^*(t_1), z_2 = z^*(t_2)$].

If any point of the unloading wave (z_1, t_1) is known, the expressions (57) offer the possibility of determining the other point of the unloading wave (z_2, t_2), by (z_2, t_2) it is also possible to determine (z_3, t_3) and so on. Therefore the entire unloading wave can be determined by the solution of the system (57) if some initial part of it is known.

Using expressions (57), it is possible to prove that if the Prandtl diagram is adopted, and the pressure on the surface varies according to (37), then the unloading wave will be a straight line

FOR OFFICIAL USE ONLY

FOR OFFICIAL USE ONLY

$$z^* = a_p (t - t_m). \quad (58)$$

For this purpose we shall check whether the two arbitrary points (z_1, t_1) and (z_2, t_2) of the unloading wave can lie on one straight line, that is, satisfy the equations:

$$t_1 = t_m + \frac{z_1}{a_p}; \quad t_2 = t_m + \frac{z_2}{a_p}. \quad (59)$$

Using the functions (21) and (12):

$$\sigma_1(z, t) = -p_1 \left(t - \frac{z}{a_1} \right),$$

$$\lambda(e_1) = a_0 e_2 + a_1 (e_1 - e_2) = \left(\frac{a_0}{E_0} - \frac{a_1}{E_1} \right) \sigma_1 + \frac{a_1}{E_1} \sigma_1,$$

from (57) and (37) after transformations we obtain the equation for a_p

$$\alpha_1 \left(\frac{1}{a_1} - \frac{1}{a_p} \right)^k \left[\left(\frac{a_2}{a_1} + 1 \right) \left(\frac{1}{a_p} + \frac{1}{a_2} \right)^k - \left(\frac{a_2}{a_1} - 1 \right) \left(\frac{1}{a_p} - \frac{1}{a_2} \right)^k \right] = 2\alpha_2 \left(\frac{1}{a_p} - \frac{1}{a_2} \right)^k. \quad (60)$$

As is obvious, this equation does not depend on the value of z and t ; therefore the functions (59) are valid for any z and t , that is, the unloading wave is a straight line. Taking this into account, for the unloading region we obtain:

$$\sigma^* = -p_{\text{max}} + \alpha_1 \left(\frac{a_p}{a_1} - 1 \right)^k (t - t_m)^k = -p_{\text{max}} + \alpha_1 \left(\frac{1}{a_1} - \frac{1}{a_p} \right)^k z^k;$$

$$\sigma^{(2)}(z, t) = -p_{\text{max}} + E_p r_k [z - a_2 (t - t_m)]^k + E_p s_k [z + a_2 (t - t_m)]^k;$$

$$u^{(2)}(z, t) = -a_0 e_2 + \frac{a_1}{E_1} (p_{\text{max}} + \sigma_s) - a_2 r_k [z - a_2 (t - t_m)]^k + a_2 s_k [z + a_2 (t - t_m)]^k,$$

where

$$r_k = \frac{\alpha_1 \left(\frac{1}{a_p} - \frac{1}{a_1} \right)^k \left(1 + \frac{a_2}{a_1} \right)}{2E_p \left(\frac{1}{a_p} - \frac{1}{a_2} \right)^k a_2^k};$$

$$s_k = \frac{\alpha_1 \left(\frac{1}{a_p} - \frac{1}{a_1} \right)^k \left(1 - \frac{a_2}{a_1} \right) (-1)^k}{2E_p \left(\frac{1}{a_p} + \frac{1}{a_2} \right)^k a_2^k}.$$

FOR OFFICIAL USE ONLY

FOR OFFICIAL USE ONLY

From equation (60) we have the known expressions [8]:

for $k = 1$

$$a_p = \sqrt{\frac{a_1^2 a_2^2 (\alpha_1 + \alpha_2)}{\alpha_1 a_1^2 + \alpha_2 a_2^2}}; \quad (61)$$

for $k = 2$ and $\alpha_1 = \alpha_2$ $a_p = a_2 \left[\sqrt{\frac{a_2^2}{a_1^2} + 3} - \frac{a_2}{a_1} \right].$ (62)

In the case where the deformation diagram $\sigma(\epsilon)$ is arbitrary and where the functions (37) represent the pressures $p_1(t)$ and $p_2(t)$ only near t_m , the equation (60) permits determination of the initial unloading wave velocity.

Example 16. The deformation diagram is assumed in the form of a Prandtl diagram, where $a_2/a_1 = 4$. The law of variation of the pressure for $z = 0$ will be given in the form

$$p(t) = 2\sigma_s - \frac{8\sigma_s}{\theta^2} \left(t - \frac{\theta}{2} \right)^2,$$

where θ is the time of effect of the load.

Thus,

$$p_{\text{max}} = +2\sigma_s; \quad k=2; \quad \alpha_1 = \alpha_2 = +\frac{8\sigma_s}{\theta^2}$$

and the unloading wave is a straight line. The unloading wave velocity will be determined by the formula (62) $a_p = 0.359a_2$. In dimensionless variables

$$\tau = \frac{t}{\theta}; \quad \xi = \frac{z}{a_1 \theta}$$

we obtain the following expressions for the unloading wave and the stresses in the unloading region:

$$\tau = 0,5 + 0,696\xi; \quad \frac{\sigma^*}{\sigma_s} = -2 + 0,737\xi^2;$$

$$\frac{\sigma_2(\xi, \tau)}{\sigma_s} = -2 + 0,577 [\xi - 4(\tau - 0,5)]^2 - 0,077 [\xi + 4(\tau - 0,5)]^2.$$

This problem is solved in [52] by a more complex graphoanalytical method.

4. Compression Wave Reflection from a Stationary Barrier

Let us propose that in the soil at a distance $z = H$ from its surface a stationary barrier is found, and on the surface the pressure $p(t)$ is given which increases monotonically to the maximum value of p_{max} , and then it remains constant (Figure 58). For the deformation diagram^{max} of the medium $\sigma = \Phi(\epsilon)$, let us consider the condition (4) satisfied.

FOR OFFICIAL USE ONLY

FOR OFFICIAL USE ONLY

After approach of the simple direct wave front to the barrier, the reflection process begins. As a result, the plane $z-t$ turns out to be divided into a number of regions indicated in this figure; 1 -- the region of non-steady state deformation, propagation of simple direct waves; 3 -- the region of steady state deformation with $\sigma = \sigma_m = -p_{max}$ and the corresponding ϵ_m ; 4 -- region of propagation of simple return waves with respect to steady state deformation 3; 5 -- the region of steady state deformation after reflection with $\sigma = \sigma_m^{refl}$ and σ_m^{refl} , $u_t = 0$; 2 -- region of development of reflection (the front II -- the characteristic of the second family with respect to simple direct wave). In region 2 all the characteristics are curvilinear, and therefore the determination of the parameters of the wave process in this region is the most difficult. In the majority of cases this problem is solved only by numerical integration of equation (5).

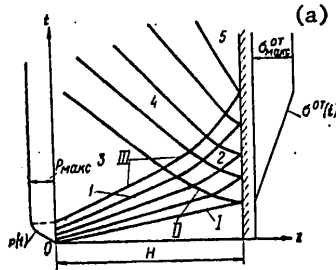


Figure 58. Wave propagation in a medium with reflection from a stationary barrier. I-III -- characteristics; 1-5 -- regions.

Key: a. σ_m^{refl}

At the same time the maximum parameters σ_m^{refl} and ϵ_m^{refl} in the reflected wave on the barrier can easily be found.

Actually, in the region 1, $r_2 = 0$, and therefore from (14) we have $r_1 = -2\lambda$ (ϵ). On the characteristic III we will then have

$$r_1^{(III)} = -2\lambda(\epsilon_m). \tag{63}$$

Since for $z = H$, $u_t = 0$, in region 2 from (10) we have $r_1 = -\lambda(\epsilon^{refl})$, where ϵ^{refl} is the deformation on the barrier at the point (H, t) , from which the corresponding characteristic of the family C_+ emerges. Then on the characteristic III $r_1^{(III)} = -\lambda(\epsilon_m^{refl})$, and comparison with (63) gives the following equation for determining the maximum deformation of the reflection on the barrier

$$\lambda(\epsilon_m^{refl}) = 2\lambda(\epsilon_m). \tag{64}$$

FOR OFFICIAL USE ONLY

FOR OFFICIAL USE ONLY

It is obvious that $\sigma_m^{\sigma r} = \phi(\epsilon_m^{\sigma r})$.

The reflection effect usually is characterized by the reflection coefficients for the stress n_H and the deformation n_D equal to:

$$n_H = \frac{\sigma_m^{\sigma r}}{\sigma_m}; \quad n_D = \frac{\epsilon_m^{\sigma r}}{\epsilon_m}. \quad (65)$$

For a linearly elastic medium ($\sigma = E\epsilon$) from (64)

$$n_H = n_D = 2. \quad (66)$$

Let us consider the medium with deformation diagram in the form of (44). It is obvious that:

$$\lambda(\epsilon) = \begin{cases} a_0 \epsilon & \text{for } |\sigma| \leq |\sigma_s|; \\ a_0 \epsilon_s + a_1(\epsilon - \epsilon_s) & \text{for } |\sigma| > |\sigma_s|. \end{cases} \quad (67)$$

Then from equation (64) we obtain:

a) for $\frac{|\sigma_s|}{2} < |\sigma_m| < |\sigma_s|$

$$\begin{aligned} \epsilon_m^{\sigma r} &= \frac{2a_0}{a_1} \epsilon_m - \left(\frac{a_0}{a_1} - 1 \right) \epsilon_s; \\ n_H &= \frac{2a_0}{a_1} - \left(\frac{a_0}{a_1} - 1 \right) \frac{\epsilon_s}{\epsilon_m} = \\ &= \frac{2a_0}{a_1} - \left(\frac{a_0}{a_1} - 1 \right) \frac{\sigma_s}{\sigma_m}; \end{aligned} \quad (68)$$

$$\begin{aligned} \sigma_m^{\sigma r} &= \frac{2a_1}{a_0} \sigma_m + \left(1 - \frac{a_1}{a_0} \right) \sigma_s; \\ n_H &= \frac{2a_1}{a_0} + \left(1 - \frac{a_1}{a_0} \right) \frac{\sigma_s}{\sigma_m}. \end{aligned} \quad (69)$$

b) for $|\sigma_m| > |\sigma_s|$

$$\epsilon_m^{\sigma r} = 2\epsilon_m + \left(\frac{a_0}{a_1} - 1 \right) \epsilon_s;$$

$$n_H = 2 + \left(\frac{a_0}{a_1} - 1 \right) \frac{\epsilon_s}{\epsilon_m} = 2 + \frac{\frac{a_0}{a_1} - 1}{1 + \frac{a_0^2}{a_1^2} \left(\frac{\sigma_m}{\sigma_s} - 1 \right)}; \quad (70)$$

$$\begin{aligned} \sigma_m^{\sigma r} &= 2\sigma_m - \left(1 - \frac{a_1}{a_0} \right) \sigma_s; \\ n_H &= 2 - \left(1 - \frac{a_1}{a_0} \right) \frac{\sigma_s}{\sigma_m}. \end{aligned} \quad (71)$$

FOR OFFICIAL USE ONLY

FOR OFFICIAL USE ONLY

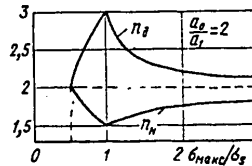


Figure 59. Graphs of the reflection coefficient for the stress (n_H) and strains (n_D) for interaction of the wave with a stationary barrier.

As is obvious from the expressions obtained, for $|\sigma_m| > |\sigma_s|/2$ the following expressions are valid:

$$n_H > 2, n_D < 2; \tag{72}$$

for $|\sigma_m| \leq |\sigma_s|/2$ the conditions (66) are satisfied.

For $\sigma_m = \sigma_s$ the reflection coefficients assume their extremal value:

$$\begin{matrix} \text{(a)} & & \text{(b)} \\ n_H^{\text{min}} = 1 + \frac{a_1}{a_0}; & n_D^{\text{max}} = 1 + \frac{a_0}{a_1} \end{matrix} \tag{73}$$

Key: a. min b. max

The graphs of the coefficients n_H and n_D are constructed in Figure 59 for $a_1 = 0.5a_0$. With an increase in σ_m/σ_s the coefficients n_H and n_D approach 2, which is explained by a decrease in the effect of the initial section of the deformation diagram (for $|\epsilon| \leq |\epsilon_s|$).

5. Interaction of Compression Waves in the Ground with Flexible Structures

The calculation of the structures buried in the ground is connected with investigation of the processes influencing each other: the deformation of the structural element and wave propagation in the ground, that is, with the solution of the problem interaction of the wave with the structural element.

This problem can be solved using the above-investigated methods of investigating the wave processes in the ground and the movement of the structural elements.

Results are presented below from studying the motion in the elastic stage of a beam structure located in the ground at shallow depth when the effect of a free surface is felt.

The pressure with a density Δp , instantaneously increasing and constant in time, acts on the surface of the ground. The compression diagram of the

FOR OFFICIAL USE ONLY

FOR OFFICIAL USE ONLY

ground under load is assumed to be linear; for unloading, with constant deformation ($E_p = \infty$). Here the reflection coefficient will be 2. The variation of the buildup time of the compression wave with depth is taken into account by the fact that on the surface of the ground a buildup of the pressure to a maximum with time equal to

$$t_n = H \left(\frac{1}{a_1} - \frac{1}{a_0} \right), \quad (74)$$

is provisionally assumed, where H is the thickness of the ground above the structure.

As a result of the calculations, the generalized dynamicity coefficients k_D^{gen} were defined taking into account the entire process of interaction of the wave with the structure and with the free surface of the ground.

In Figure 60 graphs of k_D^{gen} are constructed as a function of the dimensionless parameters

$$s_a = \frac{\omega H}{a_1}; \quad \mu_1 = \frac{\rho a_1}{2m_1 \omega}, \quad (75)$$

where ω is the lower frequency of the vibrations of the structure in the air; ρ is the soil density; m_1 is the mass of the structure per unit area of buried surface.

The dotted line plots the function for k_D^{gen} obtained for the ground of the linearly elastic medium without considering the effect of the free surface of the ground which we shall call "approximate."

For any μ_1 curves k_D^{gen} increase from 2 for $s_a = 0$ to some maximum value and then decrease to a value also close to two.

For small s_a the value of k_D^{gen} is close to the dynamicity coefficient for the structure in the air, and for large s_a , it approaches the reflection coefficient of the wave from a stationary barrier, which indicates the static effect of the compression wave on the structure when it is buried deep in the ground.

The points $s_a^{(m)}$ corresponding to the maxima k_D^{gen} determine two calculated cases. For $s_a < s_a^{(m)}$ the effect of the free surface and consideration of the unloading in the layer of soil are significant. For $s_a \geq s_a^{(m)}$ these facts almost have no effect on k_D^{gen} , and the layer of soil can be considered as an infinite linearly elastic medium.

FOR OFFICIAL USE ONLY

FOR OFFICIAL USE ONLY

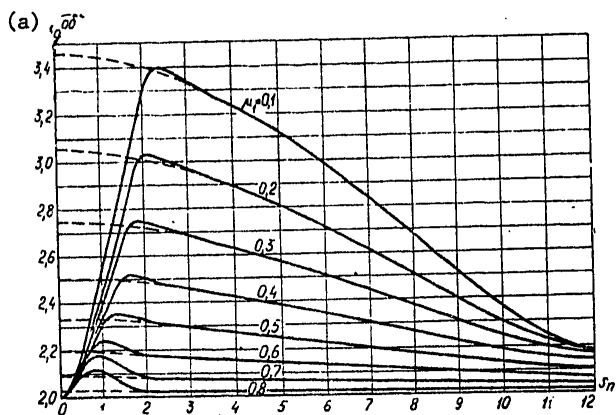


Figure 60. Generalized dynamicity coefficient in the elastic stage for structural elements with soil fill.

Key: a. k_D^{gen}

For each of these cases defined wave processes in the ground layer are characteristic. Figure 61 depicts the unloading waves $\xi_1(s)$ (from the structure), $\xi_2(s)$ from the free surface), the relative pressure q^* on the surface of the beam and the relative deflection $y(s)$ for certain values of s_{π} and μ_1 . The crosses and dotted lines depict the values of the deflections $y^*(s)$ defined approximately. As is obvious, $s_{\pi} < s_{\pi}^{(m)}$ (Figure 61,a,b) intersection of the unloading waves running from the structural element and from the surface of the ground takes place. Here, all of the ground over the structure is converted as if into a solid state and remains such until the maximum deflection is reached. This is connected with the fact that the pressure on the surface of the structural element does not exceed its first maximum value (for $s = s_{\pi} + s_0$, where $s_0 = \omega t_H$). The magnitude of the deflection determined "approximately" has in this case large values beginning with the time of conversion of all of the soil to an associated mass. In these cases the soil layer can be defined as a "thin" layer. The primary role in the conversion of the "thin" layer of soil to a solid state is played by the unloading process not from the surface of the ground, but from the structural element, for the unloading wave from the structure begins earlier and is propagated with greater velocity than from the surface of the soil.

For $s_{\pi} > s_{\pi}^{(m)}$ (Figure 61,c,d) the unloading process caused by the wave from the structural element ceases before encounter of this wave with the unloading wave running from the surface of the ground. Beginning with some time $s_H^{(I)}$ less than the time the deflection reaches a maximum, the pressure on the surface of the structure exceeds its value of $s = s_{\pi} + s_0$, that is, the

FOR OFFICIAL USE ONLY

FOR OFFICIAL USE ONLY

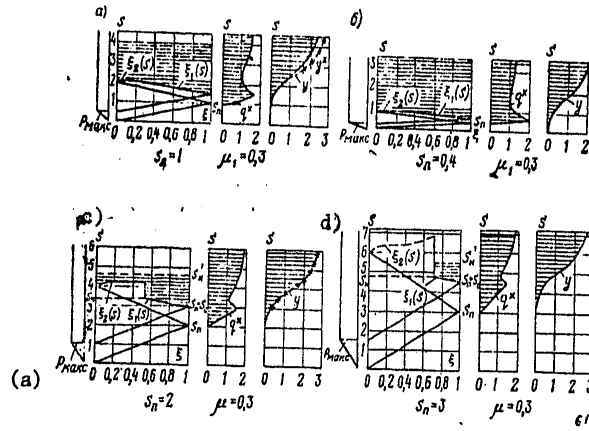


Figure 61. Processes of the interaction of a compression wave with a flexible structure from various values of the parameters s_{π} ($s = wt$).

Key: a. max

weight associated with the structural element is again converted to a deformable medium. The deflection of the beam $y^*(s)$ calculated approximately, as is obvious, in practice coincides with $y(s)$ at the times when there is an associated mass on the beam with a thickness less than the total thickness of the soil layer. The noted circumstances explain the cause of the fact that when $s_{\pi} > s_{\pi}^{(m)}$ the layer of soil when calculating the structural element can be considered as an infinite linearly elastic medium.

In reference [40] a similar conclusion regarding the possibility of considering the soil as a linearly elastic medium in the problems of the interaction of waves with structural elements was drawn on the basis of experimental data.

Using the graphs of k_D^{gen} (Figure 60), we obtain the condition of correctness of each of the two noted cases of calculating the buried structural elements. For this purpose we assume that these cases are delimited by the values of s_{π} , μ_1 corresponding to the points of intersection of the solid and dotted lines. Applying the coordinates s_{π} , μ_1 of these points in the coordinate plane s_{π} , μ_1 , we find that the "boundary" values of s_{π} , μ_1 lie on a straight line

$$s_{\pi} + 3\mu_1 = 2.5. \quad (76)$$

Therefore when calculating the buried structures in the elastic stage for the effect of a shock wave of sufficiently great duration applied to the surface of the ground, it is possible to consider the soil as an infinite linearly

FOR OFFICIAL USE ONLY

FOR OFFICIAL USE ONLY

elastic medium if

$$s_n + 3\mu_1 \geq 2,5. \quad (77)$$

In the case where

$$s_n + 3\mu_1 < 2,5, \quad (78)$$

it is necessary to consider the effect of the free surface of the ground and the propagation of the unloading processes in the soil layer.

From Figure 60 it is also possible to find that the buried structure can be calculated without considering its interaction with the ground which is taken into account only as the associated mass, if

$$s_n \leq 0,25. \quad (79)$$

Here the error in determining the dynamicity coefficient does not exceed 2.5%.

FOR OFFICIAL USE ONLY

FOR OFFICIAL USE ONLY

CHAPTER V. CALCULATION OF ROCK WALLS AND COLUMNS FOR THE EFFECT OF SHOCK WAVE LOADS

Depending on the location in the structure the walls of the shelters are divided into outside and inside walls. The operating conditions of these walls under the effect of external loads on the structure from a shock wave differ significantly, for the outside walls take the vertical and horizontal external loads, and the inside walls, only the vertical (mass forces occurring during horizontal displacement of the structure are not considered here). In addition, the working conditions of the outside walls under the effect of a horizontal external load depend in turn on their location with respect to the other bearing structures of the shelter -- the floors and ceilings, columns, inside walls, and so on. Accordingly, the schematics of the operation of the outside walls in the horizontal direction can be different -- the schematics of beams structures or slabs with different supporting conditions around the outline.

From this chapter a discussion is presented of the method of calculating the outside unreinforced rock walls working by the beam structural schematic. For calculation of the outside stone wall with longitudinal reinforcing, the methods of calculating reinforced concrete structures investigated in Chapter III can be used. The calculation of the inside walls and columns is presented in the case of the effect of only vertical forces causing central compression or extracentral compression with small eccentricities.

The calculated resistances of the column and wall materials made from concrete and rock masonry are taken with a hardening coefficient equal to 1.2 [6, 30], and the calculated pressures for nonrocky soil in the foundation, equal to the normative pressures of the soils of the foundations in accordance with the main SNiP II-B. 1-62*, augmented by several times if by the operating conditions of the structure its settling under the effect of the dynamic load is permitted.

For shallow laying of the foundations having relatively small dimensions, it is necessary to consider the possibility of squeezing of the soil from under their footings under the effect of the load. In order to prevent this phenomenon, the calculated pressures for soft ground must not be designated as more than 15-kg/cm².

FOR OFFICIAL USE ONLY

FOR OFFICIAL USE ONLY

The static loads are taken into account with a coefficient of 1.2.

The strength calculations of the inside walls and columns are performed by the static methods with respect to the corresponding chapters of the SNiP by the general formula

$$N_n \leq N_B,$$

where N_B is the maximum value of the large general force, N_n is the reduced longitudinal force from the external force effects determined from the expression

$$N_n = N_{\text{maxc}} + 1,2N_{\text{ст}}, \quad (\text{a})$$

Key: a. static

in which N_{max} is the maximum value of the longitudinal force from the effect from the dynamic load; $N_{\text{ст}}$ is an arbitrary force from the static loads.

1. Loads

All the loads are divided into horizontal and vertical. The vertical (or longitudinal) forces are transferred to the walls from the floors and ceilings. These forces are taken to be equal to the support reactions of the ceiling from the dynamic load acting on it which is variable with respect to the law (17) of Chapter II and applied only within the limits of the ceiling span purely. Here the effect of the deformation of the ceiling is not taken into account, which can be permitted when calculating the walls of structures on soft ground.

When determining the cost of vertical load on the walls of the builtin shelters the mass of the walls of the building supported on the walls of the structure is not taken into account for $\Delta p \geq 1 \text{ kg/cm}^2$, where Δp is the pressure on the shock wave front, for under such loads the building is entirely destroyed [14]. For $\Delta p < 1 \text{ kg/cm}^2$, the weight of the part of the building walls resting on the calculated wall can be taken into account.

The basis load causing the bending of the outside wall is horizontal. The magnitude of the horizontal dynamic load $p_2(t)$ is determined without considering the nonsteady state transient processes occurring during the buildup time of the load to the maximum value and the time of loading of the wall by the compression wave with respect to the entire height (the arrival time). This load is therefore taken to be uniformly distributed with respect to the height of the wall and equal to the following:

$$p_2(t) = \xi p \left(1 - \frac{t}{0} \right), \quad (1)$$

FOR OFFICIAL USE ONLY

FOR OFFICIAL USE ONLY

where p is the maximum pressure determined by the formulas in Chapter II, and ξ is the coefficient, the magnitude of which is determined by the conditions of the interaction of the compression wave in the ground or the transmitted shock wave with the structural elements of the wall.

For the walls which take the load through the ground, the value of ξ depends on the fill diagram and the type of soil. For complete burial of the wall ξ is equal to the coefficient of the lateral pressure k_b , the value of which varies from 1 to 0.3 [35, 40]. In the calculations it is possible to set $k_b = 1$ for water saturated soil and $k_b = 0.5$ for soil with natural humidity.

For the walls enclosing the shelter from the facilities not protected from the shock wave it is approximately possible to set $\xi = 1$.

For the elements of the walls erected above the level of the ground and taking the load from the air shock wave directly, the value of the coefficient ξ is taken according to the data of Chapter II in accordance with the conditions of reflection of the air shock wave from the surface of the walls and flow over the structure.

2. Characteristic of the Limiting States

Under the effect of the calculated forces, deformation of the walls and the soil in the foundation takes place as a result of which the points of the wall take the vertical and horizontal displacements.

Depending on the relation between the bending moment and the longitudinal force the wall can work with respect to two different diagrams: either under the conditions of compression of all of the cross sections or on the occurrence in some of the cross sections of the tensile stresses leading to the occurrence of horizontal cracks.

The first case is extended to walls centrally and extracentrally compressed with small eccentricities of application of the longitudinal force, and the second case, is extended to the extracentrally compressed walls with large eccentricities of the force. In the general case for any cross sections the boundary between the regions of small and large eccentricities under static loading is the ratio $s_k/s_0 = 0.8$, where s_k is the static moment of the compressed zone of the cross section with respect to its stressed face and s_0 is the static moment of the entire cross section with respect to the same face.

Let us consider the conclusions obtained during static loading for the case of dynamic loading. Then for $s_k/s_0 \geq 0.8$ we shall have a region of small eccentricities. For a rectangular cross section of height d , this inequality is equivalent to the following:

$$e_0 \leq 0,225d, \quad (2)$$

FOR OFFICIAL USE ONLY

where e_0 is the eccentricity of the longitudinal force with respect to the center of gravity of the cross section,

On satisfaction of this inequality the calculation of the wall for strength can be made by the methods discussed in item 4 of this chapter.

Great eccentricity will occur under the condition $s_k/s_0 < 0.8$ or rectangular cross section

$$e_0 > 0,225d. \quad (3)$$

When calculating the walls extracentrally compressed with large eccentricities for dynamic load, the magnitude of the eccentricity is not limited.

The numerical value of the eccentricity of the longitudinal force is determined by dividing the moment of all of the forces with respect to the wall axis by their resultant. During the process of displacement of the points of the wall under the effect of external dynamic loads the magnitude of the eccentricity of the longitudinal force changes. For the beginning of loading, the relative eccentricity of the longitudinal forces can be approximately determined (without considering the static loads) by the formula

$$\frac{2e_0}{d} = \frac{\xi H^2}{4d^2} \cdot \frac{(2-\alpha)^2}{1+0,5 \frac{l}{d}}, \quad (4)$$

where H is the wall height; l is the span of the ceiling; α is the dimensionless level defined from the expression

$$\alpha = 1 + \frac{l(0,5d-e)}{\xi H^2}, \quad (5)$$

in which e is the distance from the axis of application of the bearing reaction of the ceiling to the inside face of the wall.

The cross section for which the eccentricity is defined by formula (4) will be found at a distance $H\alpha/2$ from the lower plane of the ceiling. For the values of $\alpha < 1.172$ the maximum bending moment will in practice be in the cross section of the middle of the height of the wall, for α differs insignificantly from one. For $\alpha > 1.172$ the maximum moment with respect to the absolute value will occur in the cross section on the level of the ceiling, and the eccentricity of the longitudinal force in this cross section will be defined by the formula

$$\frac{2e_0}{d} = \frac{0,5 l (1-2e/d)}{d(1+0,5 l/d)}. \quad (6)$$

This case requires special investigation. In the first approximation for $\alpha > 1.172$ the wall can be calculated by static methods. Then we shall consider the bearing outside walls with a magnitude of the dimensionless parameter $\alpha < 1.172$.

FOR OFFICIAL USE ONLY

FOR OFFICIAL USE ONLY

For self-bearing outside walls the maximum bending moment will be in the middle of the height of the wall, and the magnitude of the relative eccentricity of the longitudinal force in this cross section will be defined by the formula

$$\frac{2e_0}{d} = \frac{\xi H^3}{4d^3} \cdot \frac{\left(1 - \frac{k_T d}{2H}\right)}{\left(1 + \frac{\xi k_T H}{2d}\right)}, \quad (7)$$

where k_T is the friction coefficient of the wall material with respect to the ceiling material. Formula (7) was obtained considering the longitudinal forces occurring in the self-bearing outside walls as a result of friction of the upper end of the wall against the bearing structures (the ceiling).

The first limiting state of stone walls with large eccentricities is reached as a result of the appearance in the most stressed cross sections of horizontal cracks opening with an increase in the displacement of the wall and decreasing the working part of the compressed cross section. These cracks divide up the wall into individual blocks which rotate relative to each other which are deformed at the points of contacts with each other, with the foundation and the ceiling. The horizontal cracks occur in the masonry after destruction of the mortar from tension. As a result of low tensile strength of the mortar, the elastic deformations of the wall turn out to be negligibly small by comparison with the residual, and when calculating walls by the first limiting state the elastic stage can be neglected.

The achievement of the first limiting state is characterized by the beginning of destruction of the masonry material of the compressed zone in the cross section with open horizontal cracks at the time the wall receives the greatest displacements.

The first limiting state (state Ia) is normalized by the magnitude of the total angle of opening of the horizontal cracks. The strength condition of the wall is

$$\varphi_{\text{max}} \leq \varphi_{\pi}, \quad (8)$$

where φ_{max} is the angle of rotation of the blocks obtained from the dynamic calculation;

φ_{π} is half the limiting angle of opening of the crack (the seam), the magnitude of which is determined from the experimental data or by the formula

$$\varphi_{\pi} = \frac{1,2 R \sqrt{d/y_0} H'}{E_h y_0}, \quad (9)$$

in which R is the calculated resistance to compression of the masonry; H' is the height of the row of masonry; y_0 is the height of the compressed zone of

FOR OFFICIAL USE ONLY

masonry in the cross section with the crack; E_k is the modulus of deformation of the masonry determined by the formula $E_k = 0.5 E_0$, where E_0 is the modulus of elasticity (the initial modulus of deformation) of the masonry defined by the chapter SNiP II-B. 2-62*. The value of y_0 is determined by the formulas (37), (38).

The calculation of the stone walls with respect to absence of large residual deformations (state lb) insures preservation of the initial seal of the walls. The achievement of this limiting state is characterized by the beginning of reduction in seal of the walls as a result of the appearance of cracks in the stressed zone of the most stressed cross section of the masonry at the time the wall receives the greatest displacements.

The condition of calculation of the walls with respect to absence of large residual deformations is the following: at the time the wall reaches the maximum displacement, the height of the opening of the seam must not exceed the admissible values. This condition is reduced to the following:

$$\phi_{\text{max}} \leq \phi_{\pi}^* = \frac{\eta}{d - y_0} \quad (10)$$

where ϕ_{max} is the angle of rotation of the block obtained from the dynamic calculation; ϕ_{π}^* is half the angle of opening of the crack from the condition of preserving the seal of the wall; η is the maximum width of opening of the crack.

According to the experimental data, for a value of $\eta = 0.4$ mm the seal of the walls with stucco is maintained. When it is necessary to maintain the initial seal of the wall the calculation with respect to absence of large residual deformations is made in the case where $\phi_{\pi}^* < \phi_{\pi}$, where ϕ_{π} is determined by the formula (9). If $\phi_{\pi}^* \geq \phi_{\pi}$, then this indicates that the width of opening of the cracks from the strength condition is less than (or equal to) that permitted with respect to absence of large residual deformations, that is, the initial seal of the wall is maintained for the calculation by the first limiting state.

3. Calculation of Outside Stone Walls

The wall is assumed to be broken up by the horizontal crack into two identical blocks 1 and 2 which rotate relative to each other (Figure 62). The angle of rotation of the longitudinal axis of the block with respect to the vertical is denoted by ϕ . The height of the compressed zone, the crushing zones at the point of supporting the wall on the foundation and the point of supporting the ceiling elements on the wall is denoted by y_0 , y_1 and y_2 respectively. The value of y_1 can be taken equal to y_0 ; the values of y_2 is defined by the formula

$$y_2 = \frac{pl}{R^{n/2}} \quad (11)$$

FOR OFFICIAL USE ONLY

where R^h is the normative resistance to compression of the masonry; l is the ceiling span.

It is possible to take y_2 approximately equal to the length of the finishing of the ceiling elements which usually does not exceed 12 cm. For the walls filling the frames, $y_2 = y_0$.

The lumped masses m_b and m_* are equal to the mass of part of the ceiling with which the load is transferred to the wall and the mass of part of the wall located above considered in the calculation, respectively. By $Q(t)$ the load from the ceiling is denoted:

$$Q(t) = p_1(t) \frac{l}{2}, \quad (12)$$

where $p_1(t)$ is the dynamic load acting on the ceiling;

$$R(t) = R_1 + p(t)d, \quad (13)$$

where R_1 is the weight of part of the walls located above considered in the calculation.

The horizontal load $p_2(t)$ is taken by the formula (1). The pressure diagrams obtained in the experiments at various points in time with respect to height of the wall indicates the significant effect of the interaction of the compression wave with the wall blocks rotating with respect to the direction of effect of the load on the magnitude of the horizontal load. In the central part of the wall the pressure can be half the pressure at the upper and lower points of the wall (after loading of the wall by the compression wave with respect to the entire height). This interaction on derivation of the calculation formulas was taken into account by the generally accepted procedure: by subtraction of the term $\rho a_0 (\partial u / \partial t)$ from the horizontal load where u is the horizontal displacements of the points of the wall, ρ is the soil density, a_0 is the propagation rate of the elastic waves in the soil (see Table 6).

The displacement of each point of the wall (for example, A and B) is expanded into the horizontal u and vertical w displacements. The displacements of the points of the lower disc of the wall caused only by rotation of the discs by a small angle ϕ (Figure 63) are defined by the formulas

$$u = -z\phi; \quad w = x\phi. \quad (14)$$

Analogously, for the points of the upper disc (Figure 63)

$$u = -(H - z)\phi; \quad w = -x\phi. \quad (15)$$

FOR OFFICIAL USE ONLY

FOR OFFICIAL USE ONLY

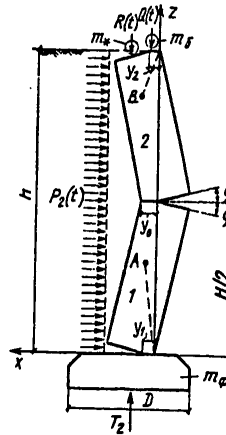


Figure 62. Calculated diagram of a stone unreinforced wall.

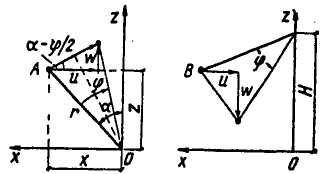


Figure 63. Displacements of the points of the wall in the lower and upper disc.

The total displacements of the points of the discs will be:

a) for the lower disc

$$u_1 = -2\varphi; \tag{16}$$

$$w_1 = W_\phi - \omega_c^{(1)} + x\varphi = W_\phi + (x - y_1)\varphi, \tag{17}$$

where W_ϕ are the vertical displacement of the foundation (without rotation);

$\omega_c^{(1)} = y_1 \sin \varphi \cos \varphi \approx y_1 \varphi$ is the vertical displacement of the disc caused by crushing at the point of supporting the wall on the foundation;

b) for the upper disc

$$u_2 = -(H - z)\varphi; \tag{18}$$

$$w_2 = W_\phi + \omega_c^{(2)} - x\varphi = W_\phi + (y_2 - x)\varphi. \tag{19}$$

FOR OFFICIAL USE ONLY

FOR OFFICIAL USE ONLY

where W_b is the vertical displacement of the ceiling element;

$$w'_c \approx y_2 \varphi.$$

The value of W_b can be expressed in terms of W_ϕ and ϕ from the condition that $w_1 = w_2$ for $x = d - y_0$, $z = H/2$. Hence:

$$W_0 = W_\phi + (2d - 2y_0 - y_1 - y_2)\varphi; \quad (20)$$

$$w_2 = W_\phi + (2d - 2y_0 - y_1 - x)\varphi. \quad (21)$$

The equations of motion of the wall will be obtained beginning with the principle of the possible displacements. As the possible displacements let us take the displacements caused by small variations of ϕ and W_ϕ , that is, the values of $\Delta\phi$ and ΔW_ϕ .

Then in accordance with the principle of possible displacements we write

$$\Delta A_i + \Delta A_p + \Delta A_B = 0, \quad (22)$$

Key: $\overset{(a)}{d} \cdot i$

where the indexes for operation of the forces (ΔA) on the adopted displacements denote the following: i -- force of inertia; p -- external and B -- internal forces.

The work of the internal forces on the possible displacements will be determined under the assumption of the rectangular compressive stress diagram. We shall assume that at the point where the wall is supported on the foundation this work is half the work of the stresses at the point of contact of two blocks. Let us also assume that the vertical displacement of the wall foundation W_ϕ has little influence on its horizontal displacements.

Then considering the assumptions made by formula (22) we obtain the desired equations of motion:

a) for bearing walls

$$A_1 \ddot{\varphi} + A_2 \dot{\varphi} + A_3 \varphi = p A_b \left(1 - \frac{t}{\theta}\right) - R_1 (1.5d - 3y_0) \quad (23)$$

where

$$A_1 = m_0 d^2 \left[\frac{H^3}{12d^3} + \frac{4}{3} - 5 \frac{y_0}{d} \left(1 - \frac{y_0}{d}\right) + 4 \frac{m_0}{m_0} \left(1 - 1.5 \frac{y_0}{d} - \frac{y_2}{d}\right)^2 + 2.25 \frac{m_*}{m_0} \left(1 - 2 \frac{y_0}{d}\right)^2 \right]; \quad (24)$$

$m_0 = \rho_c dH$ is the small mass; $m_* = R_1/g$, where g is the gravitational acceleration;

FOR OFFICIAL USE ONLY

FOR OFFICIAL USE ONLY

$$A_3 = \rho a_0 \frac{H^3}{12}; \tag{25}$$

ρ, a_0 are the soil characteristics of the wall;

$$A_4 = \frac{1.5 E_H y_0}{H}; \tag{26}$$

$$A_5 = d^3 \left[\frac{\xi H^3}{4d^3} - \frac{l}{d} \left(1 - 1.5 \frac{y_0}{d} - 0.5 \frac{y_2}{d} \right) - 1.5 \left(1 - 2 \frac{y_0}{d} \right) \right]; \tag{27}$$

b) for self-bearing walls

$$\bar{A}_1 \ddot{\varphi} + \bar{A}_3 \dot{\varphi} + \bar{A}_4 \varphi = \rho \bar{A}_5 \left(1 - \frac{l}{\theta} \right) - R_1 (1.5d - 3y_0), \tag{28}$$

where

$$\bar{A}_1 = A_1 - k_r m_c \frac{dH}{4} \left(1 - 1.5 \frac{y_0}{d} \right) \left[1 + \frac{4d^2}{H^2} \left(1 - 2 \frac{y_0}{d} \right) \right]; \tag{29}$$

$$\bar{A}_3 = \frac{\rho a_0 H^2 d}{4} \left[\frac{1}{3} \cdot \frac{H}{d} - k_r \left(1 - 1.5 \frac{y_0}{d} \right) \right]; \tag{30}$$

$$\bar{A}_5 = d^3 \left[\frac{\xi H^3}{4d^3} - k_r \frac{d}{H} \left(1 - 1.5 \frac{y_0}{d} \right) \left(\frac{\xi H^2}{d^2} + 1 \right) - 1.5 \left(1 - 2 \frac{y_0}{d} \right) \right]; \tag{31}$$

$\bar{A}_4 = A_4$, where A_4 is defined by formula (26).

The equations of motion of the walls (23) and (28) are also valid for walls that are not banked with soil. It is only necessary to assume that $\rho a_0 = 0$ in them and the value of the coefficient ξ from formula (1) in accordance with the indications of item 1 is taken. The presented equations are applicable for $\phi \leq 0.1$ rad. For large angles of rotation it is necessary to introduce the term $[R(t) - Q(t)] H\phi$ into the left-hand side of the equations (23) and (28).

In the equations (23) and (28), A_1, A_3 and A_4 are the inertia, resistance and rigidity coefficients respectively.

The equations (23) and (28) are nonuniform second-order differential equations with constant coefficients.

The solution of equation (23) as a function of the type of roots of the characteristic equation

$$A_1 s^2 + A_3 s + A_4 = 0 \tag{32}$$

FOR OFFICIAL USE ONLY

FOR OFFICIAL USE ONLY

will be:

a) for the effective roots s_1 and s_2

$$\varphi = \frac{\rho A_3}{A_4} \left(1 - \frac{t}{\theta} + D_1 e^{s_1 t} + D_2 e^{s_2 t} + \frac{A_3}{A_4 \theta} \right) - \frac{R_1}{A_4} (1,5d - 3y_0), \quad (33)$$

where

$$D_1 = \frac{1}{s_2 - s_1} \left[s_2 \left(1 + \frac{A_3}{A_4 \theta} \right) + \frac{1}{\theta} \right];$$

$$D_2 = \frac{1}{s_2 - s_1} \left[s_1 \left(1 + \frac{A_3}{A_4 \theta} \right) + \frac{1}{\theta} \right];$$

b) for the complex roots

$$\varphi = \frac{\rho A_3}{A_4} \left(1 - \frac{t}{\theta} + \frac{A_3}{A_4 \theta} - e^{s_1 t} \left[\left(1 + \frac{A_3}{A_4 \theta} \right) \cos s_2 t - \bar{D}_2 \sin s_2 t \right] \right) - \frac{R_1}{A_4} (1,5d - 3y_0), \quad (34)$$

where

$$\bar{D}_2 = \frac{1}{s_2} \left[s_1 \left(1 + \frac{A_3}{A_4 \theta} \right) + \frac{1}{\theta} \right];$$

For the walls not banked with soil $A_3 = 0$; therefore the solution of equation (23) has the form

$$\varphi = \frac{\rho A_3}{A_4} \left(1 - \frac{t}{\theta} - \cos \lambda t + \frac{\sin \lambda t}{\lambda \theta} \right) - \frac{R_1}{A_4} (1,5d - 3y_0), \quad (35)$$

where

$$\lambda = \sqrt{\frac{A_4}{A_1}}.$$

The solution of equation (28) is determined from the expressions (33)-(35) in which the coefficients A_1 are replaced by \bar{A}_1 .

The strength condition of the wall when calculating by the first limiting state will be the expression (8); for the calculation with respect to absence of large residual deformations, expression (10).

The limiting magnitude of the load on the walls is determined in accordance with the expression (8) from the equality $\phi_{\max} = \phi_{\pi}$, where ϕ_{π} is determined by the formula (9) and ϕ_{\max} is determined by the formulas (33)-(35) for $t = t_{\max}$, the magnitude of which is determined from the equation $\dot{\phi}(t) = 0$.

Hence the limiting value of the load for $R_1 = 0$

FOR OFFICIAL USE ONLY

FOR OFFICIAL USE ONLY

$$p_{II} = \frac{\varphi_{II}(y_0)}{g(y_0) f(t_{\max})}, \quad (36)$$

where $\varphi_{II}(y_0)$ is defined by formula (9); $g(y_0) = A_5/A_4$; $f(t_{\max})$ is the maximum value of the time function from the right-hand side of the expressions (33)-(35).

From formula (36) it is obvious that p_{II} depends on the value of y_0 . Let us take the value of y_0 to be that for which p_{II} has the least value. Then from the condition of the minimum limiting loads

$$\left(\frac{dp_{II}}{dy_0}\right)_{t=t_{\max}} = 0,$$

the height of the compressed zone is:

a) for self-bearing walls

$$\left. \begin{aligned} y_0 &= 1,25 d \left[1 - \frac{2}{3} \left(\frac{2e_0}{d} \right) \right] \quad \text{for } \frac{2e_0}{d} < 1,35; \\ y_0 &= 0,125 d \quad \text{for } \frac{2e_0}{d} \geq 1,35; \end{aligned} \right\} \quad (37)$$

b) for the bearing walls

$$\left. \begin{aligned} y_0 &= 1,25 d \frac{\left[1 + \frac{2}{3} \left(\frac{l}{d} - \frac{\xi H^2}{4d^2} \right) \right]}{1 + 0,5 \frac{l}{d} + 0,925 \frac{l}{d}} \quad \text{for } \frac{\xi H^2}{4d^2} < 1,35 + \\ & \quad + 0,925 \frac{l}{d}; \\ y_0 &= 0,125 d \quad \text{for } \frac{\xi H^2}{4d^2} \geq 1,35 + 0,925 \frac{l}{d}. \end{aligned} \right\} \quad (38)$$

For the walls filling the frames including quite rigid bars, between which the masonry is located, the height of the compressed zone is determined from the equation (20) for $W_b = W_\phi = 0$ and $y_1 = y_2 = y_0$:

$$y_0 = 0,5 d - \frac{H}{8} \varphi \approx 0,5 d.$$

In the solutions of (33)-(35) for these walls $R_1 = 0$,

$$A_1^* = \frac{m_0 d^2}{12} \left(1 + \frac{H^2}{d^2} \right), \quad A_6^* = \frac{\xi H^2}{4}.$$

the remaining coefficients, just as in formula (23).

FOR OFFICIAL USE ONLY

FOR OFFICIAL USE ONLY

4. Calculation of Columns and Inside Walls

The formulas presented below for determining the longitudinal forces in the column and wall cross sections and under the footing of their foundations are obtained considering the vertical displacements of the structure investigated as a rigid body.

Let us consider the frame of the structure made up of columns (walls) with foundations and part of the ceiling from which the load is collected which is transmitted to the column (the wall) through the span supported on it. Under the effect on the structure of the dynamic loading, vertical shifting of the columns (walls) and the foundations takes place. The equation of motion of the entire structure as a rigid body will be

$$P(t) + N_{\phi}(t) - M\ddot{u} = 0, \quad (39)$$

where $P(t)$ is the total dynamic load acting on the covering of the structure; $N_{\phi}(t)$ is the total longitudinal force under the footing of the foundation caused by the resistance of the soil to the movement of the structure; M is the mass of the entire structure; u is the vertical displacement of the structure.

The expression $N_{\phi}(t)$ can be represented in the form

$$N_{\phi}(t) = -\rho a_1 F_{\phi} \dot{u} - \frac{\rho a_1^2 F_{\phi}}{2D} u, \quad (40)$$

where ρ is the density of the soil in the base; a_1 is the propagation rate of the elastic-plastic wave in the foundation soil taken by Table 6 from Chapter IV; F_{ϕ} is the area of the foundation footing under the column (wall); D is the large side of the foundation footing of the column or the width of the footing of a strip wall foundation.

When calculating the wall the area of the foundation footing is defined by the formula

$$F_{\phi} = bD, \quad (41)$$

where b is the distance between the axes of the beams (slabs) resting on the walls.

As a result of solving equation (39), the displacement, the velocity, the acceleration, the force under the foundation footing are found, and from the condition of dynamic equilibrium, the force in any cross section of the column (wall).

The longitudinal force in any cross section of the column (wall) at the time t is:

FOR OFFICIAL USE ONLY

FOR OFFICIAL USE ONLY

$$N(t) = N_p \Phi(t), \quad (42)$$

where N_p is the longitudinal force caused by the load p applied statically, and $\Phi(t)$ is the function which depends on the time and is defined by the formula

$$\Phi(t) = S(t) - \frac{m_1}{M} \left[S(t) - 1 + \frac{t}{\theta} \right], \quad (43)$$

in which $m_1 = m_\phi + m_{1k}$, $M = m_\phi + m_k + m_\pi$, m_k , m_ϕ , m_π are the mass of the column (wall), the foundation under the column (wall) and part of the ceiling respectively, from which the load is collected on the column (wall); m_{1k} is the mass of part of the column (wall) from the foundation to the investigated cross section;

$$S(t) = 1 - \frac{t}{\theta} e^{-\bar{q}_1 t} \left[\cos \bar{q}_2 t - \frac{1}{r} \left(1 + \frac{1}{\theta \bar{q}_1} \right) \sin \bar{q}_2 t \right], \quad (44)$$

where \bar{q}_1 , \bar{q}_2 and r are defined by the formulas respectively:

$$\bar{q}_1 = \frac{a_1}{\mu_0 D}; \quad \bar{q}_2 = r \bar{q}_1; \quad r = \sqrt{\mu_0 - 1}; \quad \mu_0 = \frac{kM}{\rho F_\phi D},$$

where k is the coefficient equal to 2 for columns and 1 for walls.

As is obvious from formula (43), with an increase in m_1 , that is, with an increase in the distance from the foundation to the investigated cross section, the dynamicity coefficient decreases.

The maximum value of the longitudinal force in the column (wall) is:

$$N_{\max} = N_p \Phi_{\max}, \quad (45)$$

where Φ_{\max} is the dynamicity coefficient which respect to the force in the column (the wall) determined by the formula (43) on substitution in it of $t = t_{\max}$ found from the solution of the equation

$$\frac{d\Phi(t)}{dt} = -\frac{1}{\bar{q}_1 \theta} + \left(1 - \frac{m_1}{M} \right) e^{-\bar{q}_1 t} \left[\left(2 + \frac{1}{\theta \bar{q}_1} \right) \cos \bar{q}_2 t + \left(r - \frac{1}{r} - \frac{1}{\theta \bar{q}_1} \right) \sin \bar{q}_2 t \right] = 0. \quad (46)$$

For $\theta = \infty$, the time t_{\max} is defined from the expression

$$\operatorname{tg} \bar{q}_2 t = -\frac{2}{r - \frac{1}{r}}. \quad (47)$$

FOR OFFICIAL USE ONLY

FOR OFFICIAL USE ONLY

The longitudinal force under the foundation footing is:

$$N_{\phi}(t) = N_p^{(\phi)} S(t), \quad (48)$$

where $N_p^{(\phi)}$ is the longitudinal force caused by the load P applied statically, and $S(t)$ is defined by the formula (44).

The maximum value of the longitudinal force under the foundation footing is:

$$N_{\phi \text{ max}} = N_p^{(\phi)} S_{\text{max}}, \quad (49)$$

where S_{max} is the dynamicity coefficient with respect to the force defined by formula (44) on substitution in it of $t = t_{\text{max}}$, which we find from the solution of the equation

$$\begin{aligned} \frac{dS(t)}{dt} = & -\frac{1}{\theta \bar{q}_1} + e^{-\bar{q}_1 t} \left[\left(2 + \frac{1}{\theta \bar{q}_1} \right) \cos \bar{q}_2 t + \right. \\ & \left. + \left(r - \frac{1}{r} - \frac{1}{r \theta \bar{q}_1} \right) \sin \bar{q}_2 t \right] = 0. \end{aligned} \quad (50)$$

For $\theta = \infty$ the time t_{max} is determined from the expression (47).

In Figure 64 the graph is presented for S_{max} as a function of r for various values of $\theta \bar{q}_1$ constructed by the formula (44).

The longitudinal forces can be defined more exactly by comparison with the investigated method if the column (wall) with the foundation is considered a rigid body loaded by the longitudinal force from the ceiling elements, which is found considering the deformation of these elements under the effect of dynamic loads. When calculating the deformation of the ceiling elements the equation of motion of the column (wall) with the foundation of the rigid body has the form

$$T(t) + N_{\phi}(t) - m\ddot{u} = 0, \quad (51)$$

where $T(t)$ is the longitudinal force from the ceiling elements:

$$m = m_n + m_{\phi}.$$

The longitudinal force for the column on which two spans are supported with identical rigidity B is:

$$T(t) = -2B \frac{\partial^2 y}{\partial x^2},$$

where y are the deflections of the span.

FOR OFFICIAL USE ONLY

FOR OFFICIAL USE ONLY

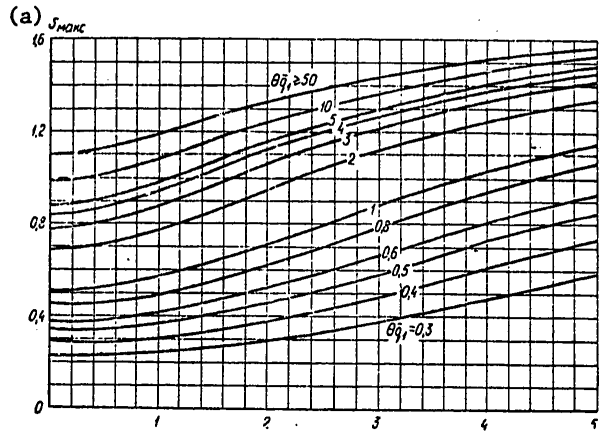


Figure 64. Graphs of the dynamicity coefficient with respect to force in the centrally compressed and extracentrally compressed columns and walls with small eccentricities considering the vertical displacement of the entire structure as a rigid body.

Key: a. max

The forces in the column (wall) cross sections and under the foundation footing are defined by the formulas (42), (43) and (45) in which the form of the function $S(t)$ depends on the investigated stage of operation of the ceiling elements.

The expression for $S(t)$ is complex and awkward and is not presented here. The consideration of the deformation of the ceiling is recommended for use in structures located on foundations made of sufficiently dense soil, with ceilings that have low frequency of natural oscillations, with a magnitude of the dimensionless parameter $n_2 \geq 1.7$ defined by the expression:

$$n_2 = \frac{2\Omega(1+n_3)}{\mu_0}; \quad \Omega = \frac{a_1}{\omega D}; \quad n_3 = \frac{m_{\pi}}{m_{\pi} + m_{\phi}},$$

where ω is the angular frequency of the natural vibrations of the beam on stationary support.

In Table 8 for three values of $n_1^{(1)}$ the values of the dynamicity coefficients are presented for the force under the foundation footing calculated as the maximum values of the function $S(t)$ for working of the ceiling elements in the elastic stage for a suddenly applied load with $\theta = \infty$ for the following values of the dimensionless parameters:

$$n_3 = 2; \quad n_2^{(i)} = \frac{\Omega_i}{\Omega_1} n_2^{(1)}; \quad n_1^{(i)} = \left(\frac{\Omega_i}{\Omega_1}\right)^2 n_1^{(1)},$$

FOR OFFICIAL USE ONLY

FOR OFFICIAL USE ONLY

where the value of $n_2^{(1)}$ is assumed to be equal to 0.57.

Table 8

Number t	$\frac{a_1}{a_2}$	Values of S_{\max} for values of parameter $n_1^{(1)}$		
		0,095	0,076	0,063
1	1	1,237	1,208	1,182
2	1,5	1,248	1,222	1,2
3	2,25	1,296	1,259	1,23
4	3	1,336	1,278	1,241
5	4,5	1,586	1,528	1,486
6	6	1,736	1,686	1,646
7	12	1,938	1,916	1,835

For the values of $n_2 < 0.57$ the dynamicity coefficient S_{\max} varies little, remaining close to 1.1-1.2.

From Table 8 it is also obvious that on variation of the value of $n_2(\Omega)$ the dynamicity coefficient varies within the limits from 1.2 to 1.94.

5. Example Calculations

Example 17. Let us determine the magnitude of the limiting load which the self-supporting wall withstands ($d = 0.5$ m, $H = 3$ m) laid from concrete blocks using type 25 mortar ($R = 430$ tons/m², $E_k = 705,000$ tons/m², $\rho_c = 0.184$ ton-sec²/m⁴). The wall is completely buried in the ground ($\rho = 0.124$ ton/sec²/m⁴, $a_0 = 100$ m/sec, $\xi = 0.35$). The friction coefficient of the wall material against the ceiling $k_m = 0.6$. The height of the masonry row $H' = 0.6$ m.

The relative eccentricity according to formula (7) $2e_0/d = 1.83 > 1.35$; therefore by formula (37) $y_0/d = 0.125$ or $y_0 = 0.0625$ m. When calculating by the first limiting state ϕ_n according to formula (9) is:

$$\phi_n = \frac{1,2 \cdot 430 \cdot 2 \cdot 0,6}{705 \cdot 10^3 (62,5 \cdot 10^{-3})} = 14 \cdot 10^{-3} \text{ rad};$$

for calculation with respect to absence of large residual deformations from formula (10)

$$\phi_n^0 = \frac{0,4}{500 - 62,5} = 0,915 \cdot 10^{-3} \text{ rad.}$$

Calculation by the first limiting state. Let us determine the mass of the wall $m_c = 0.184 \cdot 0.5 \cdot 3 = 0.276$ ton-sec²/m. Let us find the coefficient A_1 of the equation (28):

FOR OFFICIAL USE ONLY

FOR OFFICIAL USE ONLY

$$\begin{aligned} \bar{A}_1 &= 0,276 \cdot 0,5^2 \left(\frac{36}{12} + 1,33 - 0,546 \right) - 0,6 \cdot 0,276 \frac{0,5 \cdot 3}{4} \times \\ &\times (0,8125) \left(1 + \frac{4}{36} \cdot 0,75 \right) = 0,242 - 0,05 = 0,237 \text{ ton-m-sec}^2; \\ \bar{A}_2 &= \frac{0,124 \cdot 100 \cdot 3^2 \cdot 0,5}{4} \left(\frac{6}{3} - 0,6 \cdot 0,8125 \right) = 21,1 \text{ ton-m-sec}; \\ \bar{A}_3 &= \frac{1,5 \cdot 705 \cdot 10^3 (6,25 \cdot 10^{-3})^3}{0,6} = 430 \cdot \text{ton-m}; \\ \bar{A}_4 &= 0,5^2 \left[\frac{0,35 \cdot 36}{4} - \frac{0,6}{6} (0,8125)(0,33 \cdot 36 + 1) - 1,125 \right] = 0,206 \text{ m}^3. \end{aligned}$$

The characteristic equation (32) $0.237s^2 + 21.1s + 430 - 0$ gives the real roots $s_1 \approx -32$ and $s_2 \approx -57$.

The maximum value of ϕ_{\max} from (33) for $\theta = 1$ sec will occur for $t = 0.135$ sec (the term with $e^{s_2 t}$ will be neglected in view of its smallness)

$$\varphi_{\max} = 0,48 \cdot 10^{-3} \rho (0,882).$$

From the condition (8)

$$\rho < \frac{14 \cdot 10^{-3}}{0,48 \cdot 10^{-3} \cdot 0,882} = 33 \text{ ton/m}^3 \text{ or } \Delta p = 3.3 \text{ kg/cm}^2.$$

For the calculation with respect to absence of large residual deformations the limiting load will be:

$$\rho < \frac{0,915 \cdot 10^{-3}}{0,48 \cdot 10^{-3} \cdot 0,882} = 2,6 \text{ tons/m}^2 \text{ or } \Delta p \leq 0.26 \text{ kg/cm}^2.$$

In this case it is possible to consider the mass of the masonry located above. Here the value of \bar{A}_1 is more precisely defined, the roots s_1 and s_2 are defined, and the further calculation is performed by the formulas (33), (34).

Example 18. The structure is given with the basic characteristics: column good 6×6 meters; coating made of reinforced concrete slabs 40 cm thick over bars with a cross section of 40×85 cm ($\omega = 50$ radians/sec); the constant load on the covering without considering the natural weight $q = 0.128$ kg/cm²; reinforced concrete columns 240 cm high, 40×40 cm in cross section made of type 300 concrete ($R_{\text{limb}} = 130$ kg/cm²), with longitudinal reinforcing made of class A-II steel ($R_{a,c} = 3000$ kg/cm²); $\mu = 0.02$; the foundation 40 cm high, $240 \times 240 = 57,600$ cm² in area; subcolumn $40 \times 120 \times 120$ cm; foundation soil sandy ($\rho = 1.6 \cdot 10^{-6}$ kg-sec²/cm⁴; $a_1 = 5 \cdot 10^3$ cm/sec).

Let us determine the limiting magnitude of the dynamic load on the column of the structure.

FOR OFFICIAL USE ONLY

In accordance with the above-presented data we find the values of the masses (the dimensionality $[m] = \text{kg}\cdot\text{sec}^2/\text{cm}$); $m_k = 0,92$; $m_\phi = 7,6$; $m_\pi = 85,53$;
 $M = 0,92 + 7,6 + 85,53 = 94,05$.

Let us determine the dimensionless parameter

$$n_2 = \frac{2\Omega}{\mu_0} \left(1 + \frac{m_\pi}{m_k + m_\phi} \right) = \frac{2 \cdot 0,416}{8,5} \left(1 + \frac{85,53}{8,52} \right) = 1,08.$$

where

$$\Omega = \frac{a_1}{\omega D} = 0,416; \quad \mu_0 = \frac{2M}{\rho F_\phi D} = \frac{2 \cdot 94,05}{1,6 \cdot 10^{-8} \cdot 240^2 \cdot 240} = 8,5.$$

Since $n_2 = 1,08 < 1,7$, the calculation is performed by the formulas (43)-(49).

Let us find the parameters

$$r = \sqrt{\mu_0 - 1} = 2,74;$$

$$\bar{q}_1 = \frac{a_1}{\mu_0 D} = 2,45 \text{ l/sec}; \quad \bar{q}_2 = r \cdot \bar{q}_1 = 6,7 \text{ l/sec}.$$

By formula (43) let us determine the dynamicity coefficient with respect to the force for the lower cross section of the column. For this cross section $m_1 = m_\phi = 7,6 \text{ kg}\cdot\text{sec}^2/\text{cm}$.

For simplification of the calculations let us take $\theta = \infty$. Then by formula (47)

$$\lg \bar{q} t_{\text{MARC}} = \frac{2}{r - 1/r} = -0,842; \quad \bar{q}_2 t_{\text{MARC}} \approx 2,44$$

or

$$t_{\text{MARC}} = \frac{2,44}{6,7} = 0,364 \text{ sec}.$$

By formula (44)

$$S_{\text{MARC}} = 1 - e^{-0,89} \left(\cos 2,44 - \frac{1}{2,74} \sin 2,44 \right) = \\ = 1 - 0,41 (-0,999) = 1,41.$$

The same result will be obtained by the graph in Figure 64 for $\bar{\Theta}q_1 > 50$ and $r = 2,74$.

The dynamicity coefficient Φ_{max} is;

$$\Phi_{\text{MARC}} = 1,41 - \frac{7,6}{94,06} (1,41 - 1) \approx 1,38$$

FOR OFFICIAL USE ONLY

FOR OFFICIAL USE ONLY

and the maximum value of the longitudinal force

$$N_{\max} = (\Delta p \cdot 600^2) 1,38 = 496 \cdot 10^3 \Delta p \text{ kg.}$$

The limiting magnitude of the longitudinal force for the coefficient of longitudinal bending $\phi = 1$ in accordance with the chapter SNiP II-V. 1-62* is:

$$N_B = 1,2R_{np} F_R + R_{a,c} \mu F_R = 1,2 \cdot 130 \cdot 40 \cdot 40 + 3000 \cdot 0,02 \cdot 40 \cdot 40 = 346 \cdot 10^3 \text{ kg.}$$

The longitudinal force from the static loads

$$N_{cr} = (m_n + m_R) g = (85,53 + 0,92) 981 = 84,8 \cdot 10^3 \text{ kg.}$$

then from the condition $N_{\max} + 1,2 N_{st} \leq N_B$ the limiting magnitude of the dynamic load on the ceiling which can be taken by the column is:

$$\Delta p < \frac{N_B - 1,2 N_{cr}}{496 \cdot 10^3} = \frac{(346 - 1,2 \cdot 84,8) 10^3}{496 \cdot 10^3} \approx 0,5 \text{ kg/cm}^2.$$

The maximum value of the longitudinal force under the foundation footing from the dynamic load by formula (49)

$$N_{\phi, \max} = (0,5 \cdot 600^2) 1,41 = 254 \cdot 10^3 \text{ kg.}$$

The maximum stress in the ground under the foundation footing considering the static loads will be:

$$\sigma_{r, \max} = \frac{N_{\phi, \max} + Mg}{F_{\phi}} = \frac{254 \cdot 10^3 + 94,05 \cdot 981}{240^2} = 6 \text{ kg/cm}^2 \leq R_g,$$

where R_g is the calculated pressure on the foundation soil under the effect of the dynamic loads.

FOR OFFICIAL USE ONLY

CHAPTER VI. CALCULATION OF THE ENCLOSING STRUCTURES FOR THE THERMAL EFFECTS OF MASS FIRES

1. Calculated Thermal Effects

The effect of fires on the enclosing structures of shelters is connected with the variation of the temperature of the environment with time depending on the type of fire. Inasmuch as the temperature conditions of mass fires have been discussed little [3, 11, 45], it is expedient to take the standard temperature as the initial curve for determining the calculated thermal effects of mass fires. In contrast to the temperature regime represented by this curve, for any single fire the temperature distribution is more complicated. If measures are not taken with respect to extinguishing or localizing it, four periods are distinguished: the initial period of ignition, the period of complete combustion, the period of afterburning and the cooling off period. In the case of the occurrence of fires in buildings subjected to the effect of a nuclear blast shock wave or damaged after ordinary air bombing, the duration of the initial fire period does not exceed 10 to 15 minutes [11, 45].

At the end of the initial period, as a result of the combustion of the volatile products the temperature at the center of the fire reaches 500 to 600°C.

During the second period combustion of the basic mass of the combustible materials takes place. Under the effect of high temperatures, the structural elements of the building -- the ceilings and floors, the supports, the partitions -- are heated up, deformed and collapse. A charred heap is formed at the place where the building stood in which the charred remains burn completely up.

The third period is characterized by the afterburning of the solid carbon residue in the pile of incandescent fragments of building materials.

The fourth period -- the cooling off of the charred pile -- is characterized by the fact that the combustion is in practice absent in the body of the pile.

FOR OFFICIAL USE ONLY

FOR OFFICIAL USE ONLY

The curves for the temperature regimes of mass fires of the first three types (see Table 2) without considering the duration of the cooling off period of the charred piles are presented in Fig 65. Curves (1, 2, 3) were calculated under the following prerequisites: 1) the duration of the initial period of the fire was taken equal to 15 minutes; 2) the burned load for 1 m² of projection of a floor of the building will be 50 kg; 3) the nature of the temperature variation during the first and second periods of the fire corresponds to the standard temperature curve; 4) the temperature at the end of the third period of the fire drops to the initial temperature.

The temperature drop in the burned piles to 100-70°C can continue for several days [69, 71, 73].

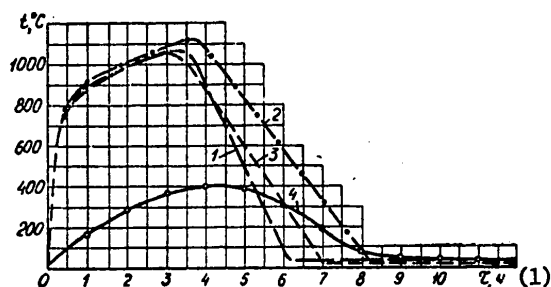


Figure 65. Variation of temperatures at the center of the fire.

1 -- type I (see Table 2); 2 -- type II; 3 -- type III;
4 -- type IV (KV-III)

Key:

1. hours

The specially performed studies made it possible to establish that the temperature regime of the fires considering the cooling off period of the charred piles can be represented in the form of a curve made up of three sections (Fig 66).

The first of them is limited with respect to time to 1 hour -- from the time of beginning of the fire to collapse of the structures (basically, the ceilings and floors). The calculations show that at the time of collapse the surface temperature of the unburned structural elements can reach 700 to 800°C at the same time as the average temperature of the fragments does not exceed 250°C.

During the second period as a result of redistribution of the temperatures with respect to the thickness of the fragments, the total temperature drop in the pile is from 700 to 250°C. The duration of this period defined by calculation does not exceed 8 hours and depends on the thickness of the fragments and their thermal physical characteristics.

FOR OFFICIAL USE ONLY

The third section of the curve is characteristically the cooling off period of the pile. Its duration is affected by the significant effect of the hollowness of the pile, its height and the temperature of the fragments at the beginning of this period. However, the convective air temperatures formed in the piles as a result of the temperature difference of the pile (to 250°C and the environment (less than 50°C) have a decisive effect on the shortening of the time of the third period. The intensity of the convective currents of the pile increases significantly if unobstructed through channels -- passages -- are created under them in advance.



Figure 66. Graphs of the temperature variation
 1 -- in the center of the fire; 2 -- fragments of the structural elements after collapse; 3 -- surfaces of the structural elements before reaching the limit of their fireproofness

Key:

1. hours

The temperature variation of the lower surface of the pile in time considering the effect of the convective currents can be determined using the expression

$$t = t_{\text{init}} + 230 e^{-\left[(0.21 + e^{0.125}) \frac{\tau}{n} - 0.25 \right]}, \tag{1}$$

Key: 1. init

where t is the desired temperature of the lower surface of the pile in °C; t_{init} is the temperature of the collapsed structures before the fire in °C; ϵ is the hollowness of the pile in fractions of a unit; τ is the time from the beginning of the fire in days; n is the number of floors.

In contrast to the charred piles, the temperature regime of the obstructions formed as a result of the destruction of buildings and other above-ground structures by a nuclear blast shock wave is significantly more favorable for the shelter enclosures (Fig 65, curve 4). At the same time the duration of the fires in the piles (type IV) can exceed by 2 or 3 times the duration of other types of mass fires. The combustion in such piles will be center type combustion. On the average, no more than a third of the combustion materials which also support the high temperatures for 10 to 12 hours, burn actively in the pile.

FOR OFFICIAL USE ONLY

FOR OFFICIAL USE ONLY

During the process of development of mass fires, the air temperature also varies, which reaches 800, 500 and 200°C for type I, II and III fires, respectively [69, 73]. The maximum increase in the air temperature in the territory where the type IV fires occurred does not exceed 10°C.

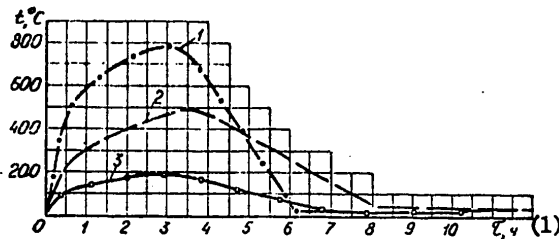


Figure 67. Variation of the air temperature during the fires.
1 -- type I (KV-I); 2 -- type II (KV-II); 3 -- type III (KV-IV)

Key:

1. hours

The actual temperature conditions in each individual case can differ somewhat from those presented in Figures 65 and 67. However, before taking the field measurements, the proposed temperature curves with small margin can be used when calculating the enclosing structures of shelters and designing the internal equipment.

From what has been stated it follows that the enclosing structures of the shelters during mass fires occurring as a result of nuclear blast can experience the following thermal effects:

Short-term effect lasting up to 12 hours directly from the center of the fire and the heated air;

Prolonged effect lasting more than 12 hours from the charred pile formed in the building as a result of collapse of the ceilings and floors, and the partitions when the limit of their fireproofness comes.

The floors and ceilings not in contact with the ground or unburied outside walls and the entrances of the built-in (under an above-ground structure) and separately standing shelters can be subjected to the short term thermal effects.

Only the floors and ceilings of the built-in shelters can be subjected to long-term thermal effects.

The short-term thermal effects, depending on the type of mass fire and the temperatures occurring in it can be of five types: KV-I, KV-II, KV-III, KV-IV and KV-V.¹

¹[Translator's note: KV stands for short term.]

FOR OFFICIAL USE ONLY

FOR OFFICIAL USE ONLY

The calculated thermal effect on the enclosing structures of shelters is defined according to Table 9 depending on the expected type of fire, the type of construction (built-in or separately standing) and the calculated structural design. For mass fires of the first three types the calculated thermal effects presented in the second column of the table are realistic only for calculating the floors and ceilings of the shelters located under two-story or higher buildings of I, II and III degree of fireproofness. If there are passages in the floors and ceilings of such shelters, the prolonged thermal effect (DV) must be replaced by the short-term type KV-V during the calculation (see Fig 68), and in all remaining cases (other degrees of fireproofness of the above-ground buildings, the one-story residential or industrial structures) the DV is replaced by the KV-I type effect. When the separately standing shelters are located in the zone of the formed piles their enclosures are designed for the short-term thermal effect type KV-III.

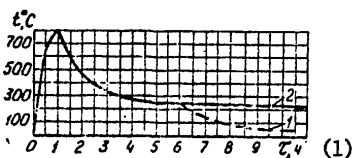


Figure 68. Variation of the temperature of the outer surface of the ceiling of a shelter.

1 -- with passages (KV-V); 2 -- without passages

Key:

1. hours

Table 9

Calculated Thermal Effects

Type of fire	Thermal effects on the structures		
	Built in		Separately standing
	Floors and ceilings	Walls and entrances	Floors and ceilings, walls and entrances
I	DV	KV-I	KV-I
II	DV	KV-II	KV-II
III	DV	KV-IV	-
IV	KV-III	-	-

2. Protection of the Enclosing Structures of Shelters from Heating

The admissible heat and humidity parameters of the air in the shelters in the case of limited air supply are basically maintained as a result of the accumulation of heat released by people and equipment and the enclosing structures [14].

FOR OFFICIAL USE ONLY

FOR OFFICIAL USE ONLY

Under the conditions of the thermal effect of a mass fire the removal of heat from the structures becomes worse, and with insufficient thickness of the enclosures, an inflow of heat from the outside will be observed which undoubtedly will worsen the protective properties of the shelter. Accordingly, the enclosures and the entrances of the shelters must be thermally insulated in the corresponding fashion, which is achieved by increasing the thickness of the bearing structure or the structure of the thermal insulation layer, the shields and ducts.

The thermal insulating layer can be built both on the outside and on the inside surface of the enclosure. The outside thermal insulation is made from incombustible materials with low coefficient of thermal diffusivity (slag, sand, crushed claydite, pumice, slag concrete and so on).

In order to construct the internal thermal insulation, special heat insulating wadding, slabs, panels, and sheet thermal insulating materials are used [55].

The shields designed to protect people against radiant heat emitting from the heated inside surface of the enclosure are made of sheet building materials (metal, asbestos, plywood, and so on), and they are installed on the inside surface of the enclosing structures at the points where people are constantly present. The greatest effect is achieved with double shields installed at a distance of 10-15 mm from the inside surface of the enclosure and from each other.

The ducts can be constructed to lower the thermal load acting on the floors and ceilings of the shelter and decrease the required shielding. They are channels that are open at the top (or closed by any burned structural element) arranged perpendicularly to the length of the building. The width and spacing of the ducts (the distance between their axes) must be no more than 0.4 meters, and the depth, no less than 0.3 meters. In the buildings, the floors and ceilings of which are made of reinforced concrete panels, the width of the ducts can be increased to 1 meter. It is expedient to construct the ducts in the floors and ceilings of built-in shelters located in buildings, the floors and ceilings between floors of which will collapse when the limit of fireproofness arrives.

3. Designing Enclosing Structures of Shelters for Heating During Fires

The problem of designing the enclosures for heating consists in determining the temperature of their inside surfaces.

The desired temperature in general form can be represented as a function of many parameters:

$$t = f(t_{\text{PB.B.}}^{(1)}; h, a; B; H; t_{\text{HAY}}^{\text{OP.}}^{(2)}; t_{\text{HAY}}^{\text{CP.}}^{(2)}; \alpha_{\text{H.}}^{(3)}; \alpha_{\text{BH.}}^{(4)}; \dots), \quad (2)$$

Key: 1. external effect; 2. init; 3. enclosure; 4. soil; 5. outside;
6. inside

FOR OFFICIAL USE ONLY

where t_{external} effect is the external thermal effect; h is the thickness of the calculated structural element; a is the coefficient of thermal diffusivity of the enclosing material; B is the width of the shelter; H is the height of the shelter; $t_{\text{enc}}^{\text{init}}$ is the initial temperature of the calculated enclosure; $t_{\text{soil}}^{\text{init}}$ is the initial soil temperature surrounding the shelter; α_{ext} is the heat exchange coefficient for the outside surface of the enclosure; α_{int} is the coefficient of heat exchange for the inside surface of the enclosure.

It is extremely difficult to obtain this function using the Fourier equation of thermal conductivity. The calculation formulas that are presented below were found after mathematical processing of the results of the numerical solution of a series of problems on a hydrointegrator.

The experimental checking of the proposed calculation formulas demonstrated that they insure a precision of calculating the enclosures for heating with- in the limits of $\pm 10\%$.

Design for Short-Term Thermal Effect

The design of the enclosing structures for short-term thermal effect is carried out from the condition

$$t_{\text{max}}^{(1)} \leq t_{\text{pred}}^{(2)} \tag{3}$$

Key: 1. max; 2. lim

where t_{lim} is the limiting temperature ($^{\circ}\text{C}$) on the inside surface of the structure, the magnitude of which for the shelters is taken at 30°C [14, 55] (when constructing double shields on the inside surfaces of the enclosures the value of t_{lim} increases by 10°C); t_{max} is the maximum temperature ($^{\circ}\text{C}$) on the inside surface of the structure defined by the formula

$$t_{\text{max}}^{(1)} = A \frac{a^{1,3}}{h^2} \cdot \frac{1}{\varphi\psi} + t_{\text{soil}}^{\text{init}} \tag{4}$$

Key; 1. max; 2. init

A is the coefficient characterizing the total amount of heat acting on the enclosure taken according to Table 10 as a function of the type of calculated thermal effects;

Table 10
Table of Coefficients A and K...

Thermal effect	KV-I	KV-II	KV-III	KV-IV	KV-V
$A \cdot 10^{-3}$	16.7	11.8	11	7.2	13.9
$K \cdot 10^{-3}$	13	17.2	17.8	21	15.4

FOR OFFICIAL USE ONLY

h is the total thickness of the calculated structure in meters;

$$h = \sum_{i=1}^m h_i, \quad (5)$$

where h_i is the thickness of the individual layers of the multilayered structure in meters; m is the number of layers;

a is the coefficient of thermal diffusivity of the structure in m^2/hr

$$a = \frac{\left(\sum_{i=1}^m h_i\right)^2}{\sum_{i=1}^m \frac{h_i}{\lambda_i} \sum_{i=1}^m c_i \gamma_i h_i}, \quad (6)$$

where λ_i , γ_i , c_i are the coefficients of thermal conductivity, the specific mass and the heat capacity of the i -th layer taken in accordance with SNiP II-A.7-62 [56];

ϕ is the coefficient taking into account the effect of the size of the structure on the temperature of the inside surface of the structural element; when calculating the walls of a shelter the coefficient ϕ in all cases is taken equal to one, and when calculating the floors and ceilings, it is determined by the formula

$$\phi = 1 + \frac{5,46 - B/H}{\tau_{\max}^{1,45} (1)}, \quad (7)$$

Key: 1. max

where B is the width of the facility (the spacing between the outside wall adjacent to the ground or the inside concrete walls no less than 0.4 meters thick) in meters;

H is the height of the facility (the distance from the surface of the floor to the upper point of the inside surface of the ceiling) in meters;

τ_{\max} is the time of occurrence (days) of the maximum temperature on the inside surface of the structure during the short-term thermal effect taken equal to:

$$\tau_{\max} = 0.15 \text{ days for } \tau \leq 0.15; \quad (8)$$

$$\tau_{\max} = \tau \text{ days for } \tau > 0.15.$$

Here

$$\tau = K \frac{h^2}{a^{0,5}} \text{ days} \quad (8a)$$

FOR OFFICIAL USE ONLY

K is the coefficient characterizing the total amount of heat acting on the enclosure; it is taken according to Table 10 as a function of the type of calculated thermal effect;

ψ is the coefficient taking into account the effect of the amount of heat exchange on the temperature of the inside surface of the enclosure defined by the formula

$$\psi = 1 - \frac{(1)_{0.182}^{0.182}}{3.31} (1 - 0.1\alpha), \quad (9)$$

Key: 1. max

α is the heat exchange coefficient on the inside surface of the enclosure in kcal/m²-hr-deg;

t_{init} is the initial temperature of the calculated structure taken equal to the maximum calculated temperature of the soil for the given terrain, but no less than 15°C.

When calculating the enclosure with internal thermal insulation, the maximum temperature of application of the thermally insulating material [55] must be above the temperature of the inside surface of the enclosure in contact with the heat insulating layer defined by the formula (4) under the condition that $\alpha=0$ and $\phi=1$.

The calculation of the heat insulation of the outside door of the shelter (for example, in the lock chamber) is made in accordance with the discussed method of thermal calculation of the floors and ceilings; the difference only consists in the fact when determining the coefficient ϕ it is not the height of the facility that is taken as H, as when calculating the floors and ceilings, but the length of the lock chamber; correspondingly B is equal to the height of the lock chamber.

In the structures where it is possible to neglect the heat influx through the entrances, the calculation of the thermal insulation of the outside door is not made.

In order to facilitate the calculations by formulas (4)-(9), a nomogram (Fig 69) is constructed which makes it possible to determine the maximum temperature on the inside surface of the enclosure t_{max} and the time of its onset τ_{max} depending on the type of short-term thermal effect KV. In addition, the nomogram permits calculation of the enclosures under the thermal effects differing from the KV type effects. For this purpose the nomogram has the scales S, the divisions of which correspond to the areas (deg-hr) included between the x-axis and the curve for the temperature variation on the outside surface of the enclosure. When calculating the enclosures for the effect of the thermal load similar with respect to outline but different with respect to absolute magnitude from the calculated

FOR OFFICIAL USE ONLY

loads, from the corresponding points of the scales S straight lines are drawn at an angle of 45° to the horizontal axis. These straight lines will also be calculated for the given thermal load.

It is possible also to use the nomogram when determining the values of ϕ and ψ used in the formulas (4) and (11).

The determination by the nomogram of the maximum increase in temperatures on the inside surface of the enclosure is made in the following procedure.

On the a -axis, from the point corresponding to the thermal diffusivity of the calculated structural element (point 1) a perpendicular is drawn to the intersection with the curve h corresponding to the thickness of the enclosure (point 2). From point 2 a horizontal line is drawn until it meets the given calculated thermal load of the KV type (point 3), from which a vertical is dropped to the intersection with the curves α (point 4) and b/H (point 7). In addition, on the τ_{\max} axis at the point of intersection of it by the vertical, we determine the time of occurrence of the temperature maximum on the inside surface of the enclosure. Drawing horizontal straight lines from the points 4 and 7, on the lefthand scales when necessary [for calculation by formulas (4) and (11)] we determine the values of ϕ and ψ . On the right of point 4 we find the point 5 from which in the given sector we draw the straight line to the intersection with continuation of the τ_{\max} axis (point 6), and then the inclined straight line to the intersection of point 8 with the horizontal straight line drawn from the point 7. We find the point 9 at the point of intersection of the perpendicular dropped from the point 8 in the horizontal axis of the nomogram. Drawing the ray of the process (X) from the point 9, we return to the point 1 from which we now drop the perpendicular to the intersection at the point 10 with the curve h , just as when finding point corresponding to the thickness of the calculated enclosure. From point 10 we draw the horizontal line to the intersection with the inclined straight line X drawn from point 9. Reproducing or dropping (depending on the location of point 11) the perpendicular to the given thermal load of the KV type and drawing the horizontal straight line from the point of their intersection (point 12), on the lefthand scale we determine the desired increase in temperature (Δt_{\max}). Summing the value of Δt_{\max} obtained with t_{init} , we determine the maximum temperature on the inside surface of the enclosure during the time of the fire.

When using the nomogram it is necessary to consider two peculiarities.

First, the straight line drawn from point 2 does not always intersect the straight lines of calculated thermal loads. This case is possible when calculating the enclosing structure, the thickness of which is equal to or less than 0.5 meters. In this case the horizontal straight line drawn from point 2 intersects with the vertical straight line bounding the straight lines KV on the right; the points 4 and 7 are shifted to the same vertical straight line, and the point 5 merges with point 4. The time of

FOR OFFICIAL USE ONLY

occurrence of the maximum temperatures with an enclosure thickness to 0.5 m and a coefficient of thermal diffusivity of the enclosure material is no less than $1.0 \cdot 10^{-3} \text{ m}^2/\text{hr}$ will always be equal to or less than 0.15 days.

Secondly, when calculating the heating of the shelter walls in connection with the fact that ϕ is taken equal to one, the point 7 is shifted to the τ_{max} axis, and the point 8 merges with point 6. For the rest, with the exception of the indicated peculiarities, the procedure for performing the calculations by the nomogram in both cases does not change.

Simplified Method of Calculating the Floors and Ceilings of Shelters for the KV-III type Thermal Effect

For designers the fires in the piles (IV type mass fires) are unconditionally of the greatest interest. Therefore, along with the investigated method of calculating the enclosures for thermal effect of the KV type, let us present a simplified version of it.

The minimum thickness of the single-layer reinforced concrete structure providing protection from heating during type IV fires must not be less than 0.6 m^* . The thickness of the two-layer structures can be taken according to Table 11.

Table 11
Thickness of the Heat Insulating Layer Providing Protection
from Heating of Two-Layer Structures

Material of the heat insulating layer	Thickness of the heat insulating layer in m for a thickness of the bearing layer of reinforced concrete in meters					
	0.4	0.35	0.3	0.25	0.2	0.15
Sheet asbestos	0.05	0.06	0.08	0.09	0.1	0.11
Asbestos cement slabs	0.09	0.11	0.13	0.16	0.18	0.2
Concrete with gravel	0.21	0.26	0.31	0.35	0.4	0.45
Concrete with brick rubble	0.17	0.21	0.25	0.29	0.33	0.37
Planted ground	0.23	0.28	0.34	0.39	0.45	0.5
Sandy clay (wet)	0.3	0.38	0.45	0.52	0.59	0.67
Brick masonry and crushed claydite	0.12	0.14	0.17	0.2	0.23	0.25
Claydite concrete, dry sand and slag concrete	0.13	0.16	0.19	0.23	0.26	0.29
Boiler slag	0.11	0.13	0.16	0.19	0.21	0.24
Blast furnace slag	0.1	0.12	0.14	0.17	0.19	0.21

*In accordance with the norms adopted in the Federal Republic of Germany, the thickness of the reinforced concrete ceiling preventing its heating during fires in piles also must be equal to or greater than 0.6 meters [74].

FOR OFFICIAL USE ONLY

When making the heat insulation from material not presented in Table 11, the thickness of the layer can be determined by the formula

Key: 1. ins

where h_{ins} is the desired thickness of the heat insulating layer in meters; A_1 is the coefficient determined by Table 12 as a function of the actual thickness of the bearing reinforced concrete structure; a_{ins} is the coefficient of thermal diffusivity of the heat insulating material in m^2/hr .

Table 12

Values of the Coefficient A_1

Structure	Values of A_1 for the thickness of the reinforced concrete structures in meters					
	0.4	0.35	0.3	0.25	0.2	0.15
Without shield	82.5	102.5	122	141	160	180
With shield	27.5	47	66.7	86.3	106	125

Calculation for the Long-Term Heating Effect

The calculation of the ceilings for long-term heating is also made from the condition of satisfaction of the inequality (3) in which t_{max} is the highest temperature ($^{\circ}C$) of the lower surface of the ceiling reached while people are in the structure equal to:

$$\left. \begin{aligned} t_{max}^{(1)} &= f(\tau_{max}^{(2)}) \text{ for } \tau_{max} \leq \tau_{pred}^{(3)} \\ t_{max}^{(1)} &= f(\tau_{pred}^{(3)}) \text{ for } \tau_{max} > \tau_{pred}^{(3)} \end{aligned} \right\} \quad (10)$$

Key: 1. max; 2. ext; 3. lim

where τ_{lim} is the limiting time people will be in the structure, days; τ_{ext} is the time (in days) for the lower surface of the ceiling to reach the maximum (extremal) value of the temperature determined by the graph of function $f(\tau)$; $f(\tau)$ is the function of the temperature variation on the lower surface of the ceiling as a function of the time τ ;

$$t = f(\tau) = \frac{230e^{-\xi\tau^\delta}}{\varphi\psi} + t_{init}^{(1)} \quad (0,5 \leq \tau \leq 10 \text{ days}); \quad (11)$$

Key: 1. init

τ is the time from the beginning of the fire in days; ξ , δ are the empirical coefficients equal to:

FOR OFFICIAL USE ONLY

$$\delta = \frac{0,112h}{a^{0,41}}; \quad (12)$$

$$\xi = 1,1 \frac{\tau}{n} + \frac{\delta h}{\tau} + 0,05 \frac{h}{a^{0,60}} - 0,25, \quad (13)$$

where n is the number of floors in the building above the shelter; h , a are calculated by the formulas (5) and (6); ϕ , ψ are the coefficients determined by formulas (7) and (9) for any time within the limits from 0.5 to 10 days; t_{init} is the initial temperature of the calculated structure defined just as when calculating for a short term thermal effect.

When constructing the inside thermal insulation, the surface temperature of the enclosure in contact with the heat insulating layer, just as during the short term thermal effect, must not exceed the limiting temperature of the application of the selected heat insulating material in accordance with the SNiP [55].

The temperature of the inside surface of the enclosure in contact with the heat insulating layer is defined by the formula (11) under the condition that $\alpha=0$, and $\phi=1$.

4. Effect of Heating on the Bearing Capacity of the Ceilings and Floors and Seal of the Structure

The thermal effect of mass fires is not only the cause of heating the enclosing structures, but in a number of cases leads to a significant reduction of their calculated bearing capacity and to destruction of the seal of the structure.

The heating is of special danger for the ceiling of a shelter as the most outer structural element. Therefore the bearing capacity of the ceiling must be determined not only by the force effect but also by the thermal load.

When calculating ceilings it is assumed that:

The bearing capacity of the ceiling before heating (q_1) corresponds to the calculated equivalent static load for the given shelter;

The bearing capacity of the ceiling after the calculated thermal effect of fires (q_2) must not be less than $0,15 \text{ kg/cm}^2$ in buildings up to 3 stories, and $0,3 \text{ kg/cm}^2$ in buildings over 3 stories high inasmuch as the basic load on the ceiling of the built-in shelters in the case of a mass fire is the load from the collapsed structure;

The effect of the shock wave when determining the value of q_2 is not taken into account, for the occurrence of the mass fires is possible only with

FOR OFFICIAL USE ONLY

FOR OFFICIAL USE ONLY

a pressure on the shock wave front of no more than 0.5 kg/cm² for which the enclosing structures of the shelter do not reach the calculated limiting state.

The value of q_2 within the limits of accuracy of the engineering calculations can be determined from the condition that the compressed concrete layer h_1 , the temperature of which reached 500°C and higher does not participate in the working of the cross section [60].

Therefore the calculation of the bearing capacity of the ceilings considering the thermal load must be made for thermal effects type KV-I, KV-II, KV-V, and DV for which the outside temperature can exceed 500°C (see Fig 65 and 68). In other cases (thermal effects of the KV-III and KV-IV type) the effect of heating on the bearing capacity of the ceilings can be neglected.

The procedure for calculating the ceiling considering its heating during a fire can be considered in the example of a single-span beam.

For a single-span reinforced concrete structure q_2 is defined by the formula

$$q_2 = \frac{8F_a R_a h'_0 \left(1 - \mu \frac{R_a}{R_n}\right)}{bl^2}, \quad (14)$$

where F_a is the area of the transverse cross section of the reinforcing in cm²; R_a is the calculated resistance of the reinforcing in kg/cm²; R_n is the calculated resistance of the concrete compressed with bending in kg/cm²; l is the calculated span of the structure in cm; b is the width of the cross section in cm; μ is the reinforcing coefficient

$$\mu = \frac{F_a}{bh'_0}; \quad h'_0 = h_0 - h_1, \quad (15)$$

where h'_0 is the working height of the cross section after heating of the structure in cm; h_0 is the working height of the cross section before heating of the structure in cm; h_1 is the height of the concrete layer in cm with a temperature of 500°C or more. It is determined by the formula obtained from expression (4):

$$h_1 = 652 a^{0.65} \text{ cm}. \quad (16)$$

In the presence of heat insulation over the ceiling h_1^{ins} the magnitude of the layer h_1^{ins} heated to 500°C will be found by the formula (16) after substitution of the coefficient of thermal diffusivity of the heat insulation in it in place of the coefficient of thermal diffusivity of the reinforced concrete.

If $h_1^{\text{ins}} < h_1^{\text{ins}}$, the bearing capacity of the ceiling is not checked.

FOR OFFICIAL USE ONLY

If $h_1^{ins} > h_2^{ins}$, the value of h_1^{ins} is calculated again with the coefficient of thermal diffusivity found by formula (6), after which q_2 is determined by formula (14), the magnitude of which must not be less than that indicated in the present item.

In order to prevent loss of seal of the structure, it is necessary to provide for protection of the sealing materials by the heat insulating layer insuring maintenance of their properties during heating of the enclosures during fires. The thickness of such a layer can be determined by the nomogram in Fig 69 under the condition that $\alpha=0$, and $\phi=1$. The surface temperature of the heat insulating layer bordering with the sealing insert is taken equal to the limiting temperature of application of the sealing material for the calculation.

In connection with the fact that the limiting temperature for the sealing material, as a rule, is appreciably below 500°C, the calculation of the protective heat insulation layer must be made in practice under the effect of any (from KV-1 to DV) thermal load.

In cases where the protective heat insulating layer was calculated from the condition of maintenance of the temperature below 500°C on the surface of the sealing material, the additional checking of the bearing capacity of the enclosures with respect to thermal load can be omitted.

The heating of the entrances and, in particular, their rubber seals can have a significant effect on the overall seal of the structure. In particular, this pertains to the outside door of the structure, the seals of which burn under the thermal effect of mass fires. The seals of the inside sealed door are maintained in this case, inasmuch as for the normative dimensions of the lock the temperature of the inside door does not exceed 100°C during a fire.

The application of heat resistant rubber or other materials suitable for this purpose (for example, asbestos cork) to make the seals will permit prevention of the loss of seal of the structure in the presence of mass fires.

5. Example Calculations

Example 19. Let us calculate a ceiling of a separately standing shelter located in the vicinity of a formed pile for the thermal effect of type IV fires.

The structural design of the ceiling is as follows: asphalt 5 cm, concrete foundation 15 cm, sand base 10 cm, protective layer from mortar with metal screen 3 m, two layers of hydraulic insulation based on bituminous mastic, a layer of claydite concrete 10 cm, reinforced concrete 40 m. The height of the facility is 2.2 meters, it is 6 meters wide. The limiting time for people to be in the shelter is 1 24-hour period.

FOR OFFICIAL USE ONLY

In accordance with Table 9 and the explanation to it, the calculated thermal effect is taken for the KV-III ceiling.

Let us calculate the ceiling. By Table 10 $A=11 \cdot 10^3$; $K=17.8 \cdot 10^{-3}$. Let us take $t_{init}=15^\circ\text{C}$.

By formula (6) we find the magnitude of the coefficient of thermal diffusivity for the ceiling (the fifth layer is not considered):

$$a = \frac{(0,05+0,15+0,1+0,03+0,1+0,4)^2}{\frac{0,05}{0,6} + \frac{0,15}{1,1} + \frac{0,1}{0,5} + \frac{0,03}{1,2} + \frac{0,1}{0,46} + \frac{0,4}{1,2}} \times$$

$$\times \frac{1}{0,5 \cdot 2110 \cdot 0,05 + 0,2 \cdot 2200 \cdot 0,15 + 0,5 \cdot 1600 \cdot 0,1 + 0,2 \cdot 2350 \cdot 0,03 + 0,18 \cdot 1600 \cdot 0,1 + 0,2 \cdot 2350 \cdot 0,4} =$$

$$= 1,615 \cdot 10^{-8} \text{ m}^2/\text{s};$$

$$h = 0,05 + 0,15 + 0,1 + 0,03 + 0,1 + 0,4 = 0,83 \text{ m};$$

$$\tau_{\text{MAHC}} = 17,8 \cdot 10^{-3} \frac{0,83^2}{\sqrt{1,615 \cdot 10^{-8}}} = 0,306 \text{ day.}$$

(1)

Key: 1. max

Let us take $\alpha=5 \text{ kcal/m}^2\text{-hr-deg}$; $B/H=2.73$;

$$\varphi = 1 + \frac{5,46 - 2,73}{0,306^{1,45}} = 16,15;$$

$$\psi = 1 - \frac{0,306^{0,182}}{3,31} \cdot 0,5 = 0,878;$$

$$t_{\text{MAHC}} = 11 \cdot 10^3 \frac{(1,615 \cdot 10^{-8})^{1,3}}{0,83^2} \cdot \frac{1}{16,15 \cdot 0,878} + 15 =$$

(1) $= 15,26 < t_{\text{DPOH}} = 30^\circ\text{C}$. (2)

Key: 1. max; 2. lim

The ceiling satisfies the condition (3).

Example 20. Let us calculate the ceiling and walls not adjacent to the ground of a built-in shelter in the presence of type II fires for thermal effect. The limiting time for people to be in the shelter is 2 days. The structural design of the ceiling is 0.3 meters of reinforced concrete; the walls are brick, 0.51 meters thick. The dimensions of the facility are as follows: $B=12$ meters; $H=2.2$ meters. The number of floors of the building above the shelter is equal to 5. The ceilings and floors of the building between floors collapse when they reach the limit on their fireproofness.

FOR OFFICIAL USE ONLY

In accordance with Table 9, the calculated thermal effect on the DV ceiling and the KV-II walls is as follows. Let us take $t_{init}=15^{\circ}\text{C}$, $\alpha=5 \text{ kcal/m}^2\text{-hr-deg}$. The ceiling is calculated from the conditions (3) and (10) by formula (11). According to the calculation result, the lower face of the ceiling, already by the 12th hour after the beginning of the fire, is heated to 100°C , which is appreciably greater than the limiting temperature equal to 30°C . Consequently, it is necessary to thermally insulate the ceiling.

Let us calculate a ceiling with a heat insulating layer made of slag fill 0.3 meters thick

$$\mu = \frac{(0,3+0,3)^2}{\left(\frac{0,3}{0,25} + \frac{0,3}{1,2}\right)(0,17 \cdot 1000 \cdot 0,3 + 0,2 \cdot 2350 \cdot 0,3)} = 1,29 \cdot 10^{-3} \text{ m}^2/\text{hr};$$

$$h = 0,3 + 0,3 = 0,6 \text{ m.}$$

The results of the calculations of the ceiling by formula (11) are presented in the table, from which it is obvious that the temperature on the lower face of the ceiling reinforced with a 30-cm layer of slag in practice will become equal to $t_{lim}=30^{\circ}\text{C}$ on the second day.

τ , сутки (1)	δ	ξ	τ^{δ}	\bar{z}^{ξ}	φ	ψ	$\frac{230z^{\delta}\tau^{\delta}}{\varphi\psi}$	$t^{\circ}\text{C}$
0,5	1,027	3,514	0,49	0,0299	1	0,867	3,89	18,85
1	1,027	3,006	1	0,04979	1	0,849	13,5	28,5
1,5	1,027	2,911	1,52	0,05448	1	0,837	14,95	29,95
2	1,027	2,918	2,035	0,0544	1	0,828	15,12	30,12

Key:

1. t , days

The calculation of the walls will be made for a short-term thermal effect of the KV-II type. By Table 9, $A=11,8 \cdot 10^3$; $K=17,2 \cdot 10^{-3}$.

$$\tau = 17,2 \cdot 10^{-3} \frac{0,51^2}{\sqrt{1,4 \cdot 10^{-3}}} = 0,120 \text{ day.}$$

In accordance with formula (8) let us take τ_{max} equal to 0.15 days; then

$$t_{max} = 11,8 \cdot 10^3 \frac{(1,4 \cdot 10^{-3})^{1,3}}{0,51^2} \cdot \frac{1}{1 \cdot 0,893} + 15 = 24,92 < t_{преж} = 30^{\circ}\text{C.} \quad (2)$$

Key: 1. max; 2. lim

FOR OFFICIAL USE ONLY

The walls satisfy the requirements of condition (3).

Example 21. Let us calculate the bearing capacity of the ceiling built into a five-story shelter building with type II fires. The shelter ceiling is reinforced concrete without heat insulation:

$$h_0=30 \text{ cm}; a=2.55 \cdot 10^{-3} \text{ m}^2/\text{hr}; F_a=30 \text{ cm}^2; R_a=3000 \text{ kg/cm}^2;$$

$$R_1=200 \text{ kg/cm}^2; l=600 \text{ cm}; b=100 \text{ cm}; q_1=0.51 \text{ kg/cm}^2.$$

By formula (16) $h_1=652 (2.55 \cdot 10^{-3})^{0.65}=13.4 \text{ cm}$. Then

$$h'_0=30-13.4=16.6 \text{ cm}; \mu=\frac{30}{100 \cdot 16.6}=0.0181$$

and by formula (14)

$$q_2=\frac{8 \cdot 30 \cdot 3000 \cdot 16.6 \left(1 - 0.0181 \frac{3000}{200}\right)}{100 \cdot 600^2}=0.243 \text{ kg/cm}^2 < 0.3 \text{ kg/cm}^2.$$

From example 20 it is obvious that the temperature of the lower face of this ceiling during fires significantly exceeds the maximum admissible temperature equal to 30°C.

Considering that the construction of the inside thermal insulation does not prevent reduction of the bearing capacity of the ceiling, let us consider the case with outside heat insulating layer. Just as in example 20, let us take the 30-cm layer of slag. The height of the slag layer heated to 500°C for $a=1.47 \cdot 10^{-3} \text{ m}^2/\text{hr}$ will be determined by formula (16):

$$h_1^{(1)}=652 (1.47 \cdot 10^{-3})^{0.65}=9.4 < h_0^{(1)}=30 \text{ cm}.$$

Key: 1. ins

Consequently, the 30-cm layer of slag fill not only improves the heat engineering properties of the ceiling, but it also insures invariability of its calculated bearing capacity ($q_1=0.57 \text{ kg/cm}^2$) even after the thermal effect of mass fires.

APPROVED FOR RELEASE: 2007/02/08: CIA-RDP82-00850R000200090009-1

ST - - - - -
OF
BY
3 JUNE 1980 M. D. BODANSKIY, L. M. GORSHKOV ET AL 3 OF 3

FOR OFFICIAL USE ONLY

BIBLIOGRAPHY

1. Akimov, N. I.; Vasilevskiy, M. L.; Makarov, I. D.; Rusman, L. P.; Umnov, M. P. GRAZHDANSKAYA OBORONA [Civil Defense], Kolos, 1969.
2. Aleksandrov, V. N. OTRAVLYAYUSHCHIYE VESHCHESTVA [Poisons], Voenizdat, 1969.
3. Ammosov, F. A.; Roytman, M. Ya.; Tarasov-Agalakov, N. A. PROTIVOPOZHARNAYA ZASHCHITA BEZFONARNYKH ZDANIY [Fire Protection of Unfaced Buildings], Stroyizdat, 1965.
4. Andreyev, K. K.; Belyayev, A. F. TEORIYA VZRYVCHATYKH VESHCHESTV [Theory of Explosives], Obcrongiz, 1960.
5. Babakov, I. M. TEORIYA KOLEBANIY [Oscillation Theory], Gos. izd. tekhn.-teoret. lit-ry, 1958.
6. Bazhenov, Yu. M. BETON PRI DINAMICHESKOM NAGRUZHENII [Concrete Under Dynamic Load], Stroyizdat, 1970.
7. Baum, F. A.; Stanyukovich, K. P.; Shekhter, B. I. FIZIKA VZRYVA [Explosion Physics], Fizmatgiz, 1959.
8. Biderman, V. P. "Calculations for Shock Load," OSNOVY SOVREMENNYKH METODOV RASCHETA NA PROCHNOST' V MASHINOSTROYENII [Principles of Modern Methods of Strength Calculation in Machine Building], Mashgiz, 1952.
9. Bodner, S.; Symonds, P. "Plastic Deformations under Shock and Pulsed Loading of Beams," MEKHANIKA [Mechanics], No 4 (68), IL, 1961.
10. Brode, G. L. "Effect of a Nuclear Blast," DEYSTVIYE YADERNOGO VZRYVA [Effect of a Nuclear Blast], Mir, 1971.
11. Bushev, V. P.; Pchelintsev, V. A.; Fedorenko, V. S.; Yakovlev, A. I. OGNESTOYKOST' ZDANIY [Fireproofness of Buildings], Moscow, 1970.
12. VZRYVOBEZOPASNOST' I OGNESTOYKOST' V STROITEL'STVE [Explosion Safety and Fireproofness in Construction], edited by N. A. Strel'chuk, Stroyizdat, 1970.
13. Voloshenko-Klimovitskiy, Yu. Ya. DINAMICHESKIY PREDEL TEKUCHESTI [Dynamic Yield Point], Nauka, 1965.
14. Ganushkin, V. I.; Morozov, V. I.; Nikonov, B. I.; Orlov, G. I. PRISPOBLENIIYE PODVALOV SUSHCHESTVUYUSHCHIKH ZDANIY POD UBEZHISHCHA [Adaptation of the Basements of Existing Buildings for Shelters], Stroyizdat, 1971.

FOR OFFICIAL USE ONLY

FOR OFFICIAL USE ONLY

15. Gvozdev, A. A. "Calculating Structural Elements for the Effect of a Blast Wave," STROITEL'NAYA PROMYSHLENNOST' [Construction Industry], Nos 1-2, 1943.
16. Gol'denblat, I. I.; Nikolayenko, I. L. RASCHET KONSTRUKTSIY NA DEYSTVIYE SEYSMICHESKIKH I IMPUL'SIVNYKH SIL [Calculation of Structural Elements for the Effect of Seismic and Pulse Forces], Gosstroyizdat, 1961.
17. Gorshkov, L. M. SPOSOBY I SREDSTVA ZASHCHITY NASELENIYA OT YADERNOGO ORUZHIIYA [Methods and Means of Protecting the Population from Nuclear Weapons], Znaniye, 1964.
18. Gressel', P. M.; Kuyevda, A. V. "Earthquakeproofness of Prestressed Reinforced Concrete Structures," PROMYSHLENNOYE STROITEL'STVO [Industrial Construction], No 4, 1969.
19. Grigoryan, S. S. "General Equations of Soil Dynamics," DAN SSSR [Reports of the USSR Academy of Sciences], Col 124, No 2, 1959.
20. Grigoryan, S. S. "Basic Concepts of Soil Dynamics," PMM [Applied Mathematics and Mechanics], Vol 24, No 6, 1960.
21. DEYSTVIYE YADERNOGO ORUZHIIYA [Effect of Nuclear Weapons], translated from the English, Voenizdat, 1960.
22. Dikovich, I. A. DINAMIKA UPUGOPLASTICHESKIKH BALOK [Dynamics of Elastic-Plastic Means], Sudpromgiz, 1962.
23. Yegorov, P. T.; Shlyakhov, I. A.; Alabin, N. I. GRAZHDANSKAYA OBORONA [Civil Defense], Vysshaya shkola, 1970.
24. Zakharova, T. V.; Khariton, Yu. B. "Flow of a Shock Wave Around Obstacles," FIZIKA VZRYVA [Explosion Physics], No 1, Izd-vo AN SSSR, 1952.
25. Ivanov, A. I.; Naumenko, I. A.; Pavlov, M. I. RAKETNO-YADERNOYE ORUZHIIYE I YEGO PORAZHAYUSHCHEYE DEYSTVIYE [Nuclear Rocket Weapons and Their Destructive Effect], Voenizdat, 1971.
26. INSTRUKTSIYA PO RASCHETU NESUSHCHIKH KONSTRUKTSIY PROMYSHLENNYKH ZDANIY I SOORUZHENIY NA DINAMICHESKIYE NAGRUZKI [Instructions for Calculating the Bearing Structures of Industrial Buildings under Dynamic Loads], Stroyizdat, 1970.
27. INSTRUKTSIYA PO RASCHETU PEREKRYTIY NA IMPUL'SIVNYE NA GRUZKI [Instructions for Calculating Ceilings and Floors for Pulsed Loads], Stroyizdat, 1966.
28. Kimel', L. R.; Mashkovich, V. P. ZASHCHITA OT IONIZIRUYUSHCHIKH IZLUCHENIY (SPRAVOCHNIK) [Protection from Ionizing Radiation (Reference)], Atomizdat, 1972.

FOR OFFICIAL USE ONLY

29. Korobeynikov, V. P.; Mel'nikova, N. S.; Ryazanov, Ye. V. TEORIYA TOCHECHNOGO VZRYVA [Point Blast Theory], Fizmatgiz, 1961.
30. Korchinskiy, I. L.; Becheneva, G. V. PROCHNOST' STROITEL'NYKH MATERIALOV PRI DINAMICHESKIKH NAGRUZHENIYAKH [Strength of Building Materials Under Dynamic Loads], Stroyizdat, 1966.
31. Korchinskiy, I. L.; Rzhhevskiy, V. A.; Tsipenyuk, I. F. "Calculating Reinforced Concrete Frame Buildings for Seismic Effects Considering Plastic Deformations," BETON I ZHELEZOVETON [Concrete and Reinforced Concrete], No 1, 1970.
32. Kotlyarevskiy, V. A. "Mechanical Characteristics of Low-Carbon Steel under Pulse Loading Considering the Delaying Yield and Viscous-Plastic Properties," PRIKLADNAYA MEKHANIKA I TEKHNICHESKAYA FIZIKA [Applied Mechanics and Technical Physics], No 6, 1961.
33. Kotlyarevskiy, V. A. "Elastic-Viscous Plastic Waves in a Material with Delaying Yield," PRIKLADNAYA MEKHANIKA I TEKHNICHESKAYA FIZIKA, No 3, 1962.
34. Krylov, A. N. VIBRATSII SUDOV [Vibration of Ships], Vol X, Izd. AN SSSR, 1948.
35. Kul'chitskiy, G. B. "Side Pressure Coefficient as a Function of Density and Granulometric Composition of Consolidated Soils," OSNOVANIYA, FUNDAMENTY I MEKHANIKA GRUNTOV [Bases, Foundations and Soil Mechanics], No 2, 1967.
36. Gourant, G.; Friedrichs, K. SVERKHZVUKOVOYE TECHENIYE I UDARNYYE VOLNY [Supersonic Flow and Shock Waves], IL, 1955.
37. Courant, R.; Gilbert, D. METODY MATEMATICHESKOY FIZIKI [Methods of Mathematical Physics], GTTL, Vol 2, 1934.
38. Kukhtevich, V. I.; Goryachev, I. V.; Trykov, L. A. ZASHCHITA OT PRONIKAYUSHCHEY RADIATSII YADERNOGO VZRYVA [Protection from the Penetrating Radiation of a Nuclear Blast], Atomizdat, 1970.
39. Leypunskiy, O. I. GAMMA-IZLUCHENIYE ATOMNOGO VZRYVA [Gamma Radiation of a Nuclear Blast], Atomizdat, 1959.
40. Lyakhov, G. M.; Polyakova, N. I. VOLNY V PLOTNYKH SREDAKH I NAGRUZKI NA SOORUZHENIYA [Waves in Dense Media and Loads on Structures], Nedra, 1967.
41. Lyakhov, G. M. OSNOVY DINAMIKI VZRYVA V GRUNTAKH I ZHIDKIKH SREDAKH [Fundamentals of the Dynamics of a Blast in Soils and Liquid Media], Nedra, 1964.

FOR OFFICIAL USE ONLY

42. Mikhlin, S. G. VARIATSIONNYE METODY V MATEMATICHESKOY FIZIKE [Variation Methods in Mathematical Physics], Gos. izd. tekhn.-teoret. lit-ry, 1957.
43. Ovechkin, A. M. RASCHET ZHELEZOBETONNYKH OSESIMMETRICHNYKH KONSTRUKTSIY [Calculation of Reinforced Concrete Axisymmetric Structures], Gosstroyizdat, 1960.
44. Ogibalov, P. M. IZGIB, USTOYCHIVOST' I KOLEBANIYA PLASTINOK [Bending, Stability and Vibrations of Plates], Izd-vo Mos. universiteta, 1958.
45. OGNESTOYKOST' ZDANIY. NAUCHNO-TEKHNICHESKIY TSENTR PO STROITEL'STVU [Fireproofness of Buildings. Scientific-Technical Center on Construction], translated from the English, Gosstroyizdat, 1963.
46. Petrov, R. V.; Pravetskiy, V. N.; Stepanov, Yu. S.; Shal'nov, M. I. ZASHCHITA OT RADIOAKTIVNYKH OSADKOV [Protection Against Radioactive Fallout], Medgiz, 1963.
47. Polachek, Kh.; Ziger, R. I. VZAIMODEYSTVIYE UDARNYKH VOLN. OSNOVY GAZOVOY DINAMIKI [Interaction of Shock Waves. Principles of Gas Dynamics], translated from the English, IL, 1963.
48. Popov, N. N.; Rastorguyev, B. S. RASCHET ZHELEZOBETONNYKH KONSTRUKTSIY NA DEYSTVIYE KRATKOVREMENNYKH DINAMICHESKIKH NAGRUZOK [Calculation of Reinforced Concrete Structures for the Effect of Short-Term Dynamic Loads], Stroyizdat, 1964.
49. POSLEDSTVIYA VOZMOZHNOGO PRIMENENIYA YADERNOGO ORUZHIIYA, A TAKZHE POSLEDSTVIYA PRIOBRETIENIYA I DAL'NEYSHEGO RAZVITIYA YADERNOGO ORUZHIIYA DLYA BEZOPASNOSTI I EKONOMIKA GOSUDARSTV [Consequences of the Possible Application of Nuclear Weapons and Also Consequences of the Acquisition and Further Development of Nuclear Weapons for the Safety and Economy of Governments], report of the Secretary General of the United Nations U. Tant, Izd-vo Mezhdunarodnyye otnosheniya, Moscow, 1970.
50. Rabinovich, I. M. "Dynamic Calculation of Structures for the Elasticity Method," ISSLEDOVANIYA PO DINAMIKE SOORUZHENIY [Studies of the Dynamics of Structures], Stroyizdat, 1947.
51. Rabinovich, I. M.; Sinitsyn, A. P.; Luzhin, O. V.; Terenin, B. M. RASCHET SOORUZHENIY NA IMPUL'SIVNYE VOZDEYSTVIYA [Calculating Structures for Pulse Effects], Stroyizdat, 1970.
52. Rakhmatulin, Kh. A.; Dem'yanov, Yu. A. PROCHNOST' PRI INTENSIVNYKH KRATKOVREMENNYKH NAGRUZKAKH [Strength Under Intense Short-Term Loads], Fizmatgiz, 1961.

FOR OFFICIAL USE ONLY

FOR OFFICIAL USE ONLY

53. Rakhmatulin, Kh. A.; Sagomonyan, A. Ya.; Alekseyev, N. A. VOPROSY DINAMIKI GRUNTOV [Problems of Soil Dynamics], Izd-vo MGU, 1964.
54. RUKOVODSTVO PO RASCHETU OSTATOCHNYKH DEFORMATSIY GRUNTOV PRI DINAMICHESKIKH NAGRUZKAKH [Handbook for Calculating Residual Deformations of Soils Under Dynamic Loads], Stroyizdat, 1967.
55. SnIP I-V. 26-62. TEPLOIZOLYATSIONNYYE I AKUSTICHESKIYE MATERIALY I IZDELIYA [SNIP I-V. 26-62. Heat Insulating and Acoustic Materials and Problems], Stroyizdat, 1962.
56. SNIP II-A. 7-71. STROITEL'NAYA TEPLOTEKHNIKA. NORMY PROYEKTIROVANIYA [SNIP II-A. 7-71. Construction Heat Engineering. Design Norms], Stroyizdat, 1973.
57. SPRAVOCHNIK PO DINAMIKE SOORUZHENIY [Handbook on Structural Dynamics], Stroyizdat, 1972.
58. Staskevich, N. L.; Mayzel's, P. B.; Vigdorichik, D. Ya. SPRAVOCHNIK PO SZHIZHENNYM UGLEVODORODNYM GAZAM [Reference on Liquefied Hydrocarbon Gases], Nedra, 1964.
59. Strel'chuk, N.; Imaykin, G. "Analysis of Explosions of Gas-Air Mixtures," POZHARNOYE DELO [Fire Affairs], No 10, 1969.
60. Strel'chuk, N. A.; Yakovlev, A. I.; Bubyr', N. F. "Calculated Determination of the Fireproofness of Statically Defined Reinforced Concrete Girders," BETON I ZHELEZOBETON [Concrete and Reinforced Concrete], No 5, 1965.
61. Timoshenko, S. P. KOLEBANIYA V INZHENERNOM DELE. [Vibrations in Engineering], Gizmatgiz, 1959.
62. Taylor, D.; Tenkin, R. "Gas Dynamic Aspects of the Deonation Problem," OSNOVY GAZOVOY DINAMIKI [Fundamentals of Gas Dynamics], translated from the English, IL, 1963.
63. Hodge, F. G. RASCHET KONSTRUKTSIY S UCHETOM PLASTICHESKIKH DEFORMATSIY [Calculation of Structural Elements Considering Plastic Deformations], Mashgiz, 1963.
64. Tsvilev, M. P.; Nikanorov, A. A.; Osadchenko, I. M.; Kudryavtsev, V. M. INZHENERNYYE RABOTY V OCHAGE YADERNOGO PORAZHENIYA [Engineering Operations in a Center of Nuclear Destruction], Voenizdat, 1968.
65. Chuykov, V. I. GRAZHDANSKAYA OBORONA V RAKETNO-YADERNOY VOYNE [Civil Defense in Nuclear Missile Warfare], Atomizdat, 1969.
66. Shapiro, G. S. "Longitudinal Vibrations of Rods," PMM, Vol 10, No 5 and 6, 1946.

FOR OFFICIAL USE ONLY

67. Shcherbina, V. I. "Study of the Working of Reinforced Concrete Flexible Elements under the Effect of Short-Term Dynamic Loads," NAUCHNO-TEKHNICHESKAYA INFORMATSIYA, MEZHOTRASLEVIYYE VOPROSY STROITEL'STVA (OTECHESTVENNYY OPYT) [Scientific and Technical Information, Interbranch Problems of Construction (Soviet Experience)], No 6, TsINIS, Gosstroya, SSSR, 1967.
68. Yakovlev, Yu. S. GIDRODINAMIKA VZRYVA [Hydrodynamics of Explosions], Moscow, Sudpromgiz, 1961.
69. Besson, P. "Der Feuersturm," VFDB-ZEITSCHRIFT, Vol 9, No 1, February 1960.
70. Brode, H. L. "Numerical Solutions of Spherical Blast Waves," I, APPL. PHYS, 26, No 6, 1955.
71. Brunswig, H. "Flachenbrände und Feuerstürme," VFDB-ZEITSCHRIFT, No 11, 1952.
72. Campbell, I. D. "The Dynamic Yielding of Mild Steel," ACTA METALLURGICA, Vol 1, No 6, 1953.
73. FIRE EFFECTS OF BOMBING ATTACKS, United States Civil Defense, Technical Manual, 1958.
74. Michel, R. "Schutzbaupflicht für Neubauten-Hausschutzräume (Grundsatz)," STRASSENBAU-TECHN., Vol 818, No 24, 1965, pp 1888-1891.

COPYRIGHT: Stroyizdat-1974

10845
CSO: 8144/1038

END